Experimental Determination of Drying Capacity of Wood-Frame Envelope Systems for Comparative Studies and Limit State Verification

Qian Mao

A Thesis

in the

Department

of

Building, Civil and Environmental Engineering

Presented in Partial Fulfillment of the Requirements
for the Degree of Doctor of Philosophy at
Concordia University
Montréal, Québec, Canada

July, 2008

Your file Votre référence
ISBN: 978-0-494-45672-9
Our file Notre référence
ISBN: 978-0-494-45672-9

Abstract

Experimental Determination of Drying Capacity of Wood-Frame Envelope Systems for Comparative Studies and Limit State Verification

Qian Mao, PhD
Concordia University, 2008

The building envelope protects the occupants against outdoor weather and contains the indoor environment to provide comfort for the occupants. As demonstrated through field observations and large-scale experimental tests, wind-driving rain can penetrate the building envelope through design defects or through defects which may develop during its lifetime operation. The rate at which the penetrated water can be evacuated, which is a function of the drying capacity of the envelope, can affect significantly the durability of building envelope systems. However, adequate methods for quantifying the relative drying capacity of building envelope systems do not exist. The objective of this research is to develop a methodology to evaluate the relative drying capacity of building envelope systems of different compositions and thereby to assist the performance evaluation and design of envelope systems.

An innovative experimental procedure has been introduced to apply uniform in-cavity moisture loading by placing a water tray at the bottom of the stud cavity to represent the penetrated water. After a preliminary test for verification and improvement, an experimental program was carried out to monitor the processes of water evaporation from the tray, moisture absorption by envelope materials and moisture evacuation from the envelope. Thirty-one full-size wall specimens of various configurations formed the enclosures of a two-story test hut, located in a large environmental chamber. Tests were carried out over five test periods in 283 days under steady-state "outdoor" conditions that

were selected from 10% worst-drying months of Montreal based on 31-year weather data. Over 1,000 electronic sensors and 750 gravimetric samples were installed. By implementing the water tray, a quantitative relationship between in-cavity moisture loading and the moisture responses in the envelope systems was established experimentally for the first time for each wall specimen.

A drying capacity indicator has been developed to *quantitatively* characterize and compare the relative drying capacity of wood-framed building envelope systems. First, load-response profiles are developed by monitoring the evaporation from the water trays as the moisture source in the stud cavity and by monitoring the moisture absorbed in the gravimetric samples in the sheathings. Second, an allowable moisture limit of wood-framed envelopes is set at 20% MC by weight. Third the region from this 20% MC to the fiber saturation point (FSP), about 28% MC depending on wood species, is deemed as a safety margin against fungal decay. Fourth, the loading at which the 20% MC limit is reached in the moisture response of sheathing was determined from the load-response profiles and was defined as the In-Cavity Evaporation Allowance (ICEA). By comparing the ICEA values obtained from the experimental data for the 31 specimens, the drying performances of these wall configurations were characterized and compared; and ICEA has shown to be a good indicator for evaluating drying capacity of envelopes.

To demonstrate the potential of the newly proposed experimental method and the ICEA concept, a procedure is presented to verify *quantitatively* the acceptability of a wall configuration by matching potential moisture penetration of the wall against its drying capacity. This verification procedure adopts the concept of the LSD (limit state design) principle used in structural engineering. A case study applying this procedure to 12 testing wall assemblies is presented.

This thesis research on experimental and analytical investigation on the drying performance of building envelope systems has explored innovative concepts, validated them with quantitative testing procedures, advanced the current understanding and design of building envelope systems, and posed new challenges for future research.

Acknowledgements

This thesis research would never have been accomplished without the enormous assistance from colleagues in the CRD (Collaborate Research & Development) project. It is a great pleasure to express my sincere gratitude to everybody who contributed to the research.

I would like to acknowledge the support of my thesis supervisor, Dr. Paul Fazio. He inspired and challenged me in every aspect of my research, and he kindly provided financial support and constant encouragement to me. He always reminded me to keep in mind the needs of the industry. His attitude towards research, the enthusiasm and the inspiration, has been and will be of great benefit to me.

I would like to express my gratitude to Dr. Jiwu Rao for his crucial support to the experimental program, and invaluable reviews and comments. Also, I would like to thank Mr. Luc Demers who not only provided great support for the experimental facility but also taught me the essence of instrumentation and techniques in measurements. My sincere appreciation is also due to Dr. Hua Ge for providing invaluable, timely comments. Special thanks are due to our department staff — Jacques Payer, Joe Hrib, Sylvain Bélanger, Olga Soares, Sheila Anderson, Linda Swinden, and Betty Bondo — for providing unfailing services and creating a supportive atmosphere.

I would like to express my gratitude to my colleagues and friends: Arslan Abed-Alturkistani, Shan Huang, Sergio Vera, Ying Ye, Yang Wu, Xiangjing Yang, Qinru Li,

Huasheng He, Teasdale-St-Hilaire Anik, and Luis Candanedo; I could not ask for a finer group of colleagues. I also want to acknowledge the hard work of several undergraduate students--Jiejun Zhao, Jonation St-Pierre, Nazmi Boran, and Bruno Lee — in the installation and operation of the experiment during their summer internships. Many thanks go to my friend Jian Zhang and Liang Zhou for their support, entertainment and care.

Finally, and most importantly, I wish to express my warmest appreciation and love for my family. My family has provided me with unconditional encouragement and support at all times. So I wish to dedicate my thesis to my mother (Yanqin Zhang), my father (Weizhao Mao), my brother (Wen Mao), and my little sister (Hua Mao). Thanks for your love, patience, and understanding. I know you are all proud of my achievement!

Table of Contents

List of Figures

List of Tables

Abbreviations

AAMA:	America Aluminum Manufacturers Association
ASD:	Allowable Stress Design
ASHRAE:	American Society of Heating, Refrigerating and Air-Conditioning Engineers
ASTM:	American Society for Testing and Materials
CFD:	Computational Fluid Dynamics
CI:	Climate Index
CMC:	Canadian Meteorological Centre
CMHC:	Canada Mortgage and Housing Corporation
CRD:	Collaborative Research & Development
CSA:	Canadian Standards Association
CWC:	Canadian Wood Council
DAS:	Data Acquisition System
DI:	Drying Index
DRI:	Driven Rain Index
DRY:	Design Reference Year
DWTF:	Dynamic Wall Testing Facilities
EDRA:	Envelope Drying Rates Analysis
EIFS:	Exterior Insulation and Finish System
EMC:	Equilibrium Moisture Content
FEM:	Finite Element Method
FIB:	Fiberboard
FSP	Fiber Saturation Point
HAM:	Heat, Air and Moisture
HAM-BE:	Heat, Air, and Moisture transport in the Building Envelope
HAMSTAD:	Heat, Air, and Moisture STAndards Development
HVAC:	Heating, Ventilation & Air Conditioning
ICEA:	In-Cavity Evaporation Allowance
IEA:	International Energy Agency
IRC:	Institute for Research in Construction
ISO:	International Standards Organization
LSD:	Limiting States Design
LRFD:	Load and Resistance Factor Design
MC:	Moisture Content
MEWS:	Moisture Management for Exterior Wall Systems
MI:	Moisture Index
MRY:	Moisture Reference Year
NRC:	National Research Council of Canada
OSB:	Oriented Strand Board

PIV:	Particle Image Velocimetry
PLW:	Plywood
RH:	Relative Humidity
RHT:	Relative Humidity and Temperature
SLS:	Serviceable Limit States
ST:	Stucco
TA:	Thermo Anemometer
TG:	Tracer Gas technique
TMY:	Typical Meteorological Year
TRY:	Test Reference Year
NBCC:	National Building Code of Canada
SBPO:	Spun bonded polyolefin
ULS:	Ultimate Limit States
VB:	Vapor Barrier
WDR:	Wind Driven Rain
WI:	Wetting Index
WRB:	Weather Resistant Barrier
WS:	Wood Siding

Nomenclature

Greek letters

α	load factors corresponding to different attributes of loads
β	load importance factor
γ	various kinds of load factors
ε	strain, *%*
θ	angle of the wind to the wall normal
ρ	density of materials, kg/m^3
μ	permeability of material, $ng/s{\cdot}m{\cdot}Pa$
σ	stress, *Pa*
τ	time elapse of testing, *day*
ψ	load combination factor
ϕ	orientation angle of façade
κ	resistance reduction factor

Latin letters

b	distance between the water surface and a specific point above water, *m*
d	thickness of the sheathing board, *mm*
$f(\,)$	proportionality factor of rainscreen, $L/(L/m^2)$
h	height, *m*
l	thickness of a layer of component, *mm*
n	number of hours of driving rain considered during a specific period of time (day, week, month or year)
p	vapor pressure, *Pa*
q_v	mass flow rate of vapor flow, $ng/s{\cdot}m^2$
r_v	vapor resistance, $s{\cdot}m^2{\cdot}Pa/ng$
t	duration, *s/hr/day* (base on formula)
Δp	vapor pressure difference across the flow path, *Pa*
x, y	coordinates of the location at the sheathing where moisture content is measured
A	area of the cross section of the vapor flow, m^2
Aw	free water evaporation area, m^2
B	characteristic length, *m*
C_ϕ	attenuation coefficient
D	number of days, *day*
DEI	drying by evaporation index, *g/day*
DRF	driving rain factor, *s/m*
DRI	drying rain index
Dv	diffusivity of water vapor, m^2/s
E	accumulative evaporation, *g*
$\dot{E}$	transient evaporation rate, *kg/s*
$\overline{E}$	daily average evaporation rate, *g/day*
$F(\,)$	load-response function
Fs	full scale of load cell, *g*
$\overline{H}$	average or general roof-top level, *m*
ICEA	in-cavity evaporation allowance, *g*
L	load
MC	moisture content of the material, *%* by weight
MCL	moisture content limit of material
ΔMC	moisture content variation, *%* by weight
ΔM_S^T	total mass of moisture storage increase for entire wall specimen, *g*
M_d	dry mass of material, *g*

M_E^B	mass of moisture evaporated from the bottom plate of the stud cavity, *g*
M_E^T	total mass of moisture evacuated in vapor form, *g*
M_P	mass of rain penetration, *g*
$\dot{M}_v$	vapor permeance coefficient, $ng/Pa \cdot s \cdot m^2$
$\dot{M}_v^e$	effective vapor permeance coefficient, $ng/Pa \cdot s \cdot m^2$
N	number of layers
P	precipitation, *mm*
ΔPw	wind-induced pressure difference across the wall
Q	mass flow rate of rain penetration into the cavity, mm/hr or $L/m^2 \cdot hr$
R	rainfall intensity (rate of rainfall), mm/hr or $L/m^2 \cdot hr$
RAF	rain admittance factor
RH	relative humidity, %
Re	Reynolds number
Rn	nominal resistance (ultimate strength)
Rw	rainfall intensity on the wall, mm/hr or $L/m^2 \cdot hr$
S	sensitivity of load cell, *mV/V*
Sc	Schmidt number
T	temperature, *°C/°F*
V	wind speed, *m/s*
U	voltage, *V*
W	weight support by load cell, *g*
X, *Y*	for minimum levels of relative humidity and temperature respectively for growth of mold
Z	zero balance of load cell, $\mu V/V$

Superscripts

e	effects or effective
B	at the bottom plate
T	in total

Subscripts

1	start point
2	end point
a	air
ave	average
d	dry
hor	horizontal
i	*i*th
in	indoor or inside
m	meteorological
mea	measured
min	minimum
out	outdoor
p	pressure
r	rain
ref	reference
s	specific location
v	vapor
w	water
D	dead load
E	evaporation
L	live load
P	penetration
S	storage
T	temperature caused load
W	wind load

Chapter 1
Introduction

1.1. Moisture in the building envelope

The primary function of the building envelope is to separate the comfortable interior climate from its natural surrounding which can sometimes be harsh for the habitants. The building envelope, as the separator, is subjected to various elements such as wind, rainfall, snow, frost, solar radiation, and biological degradation. These elements can be seen as different kinds of loads that make the envelope the most vulnerable part in the entire building. Mismanagement of them can affect the performance and durability of the entire building envelope.

Among various causes of deterioration of the building envelope, moisture often plays a crucial role (Pel 1995). Trechsel (1994) estimated that about 75% to 90% of all damages in building envelopes were caused by moisture. Many reports and surveys, e.g. Desjarlais et al. (2001), Chouinard and Lawton (2001), Tsongas et al. (1998), and Morrison Hershfield Limited (1996, 1999, and 2000), showed that most envelope failures were caused by moisture accumulation. Another conclusion from these studies is that no practical wall system can completely prevent moisture penetration at all times. Therefore, certain amount of moisture accumulation in walls due to rain penetration, condensation,

and initial moisture storage has to be taken into account when the building envelope is designed and constructed.

Moisture performance of the building envelope depends on the wetting and drying processes and moisture storage. In other words, just as important as the wetting process, the drying process also plays a critical role in determining the overall hygrothermal performance of the building envelope. Drying greatly affects the durability of an envelope system. Therefore, understanding the mechanism of the drying process and evaluating the drying performance of different wall types are necessary for the design of the building envelope (Fazio et al. 2006a).

1.2. Research scope

1.2.1. Moisture transport mechanisms: wetting and drying

Moisture is the term used to describe water in all its three phases — liquid, vapor and ice. There is much literature published on the presence and transportation of moisture inside the building envelope. Moisture transport can make the envelope either wetter or drier. It can be grouped into two processes: wetting and drying. Each process includes several sub-processes or mechanisms. Straube and Burnett (2005) summarized wetting and drying processes, as adopted in Fig. 1.1.

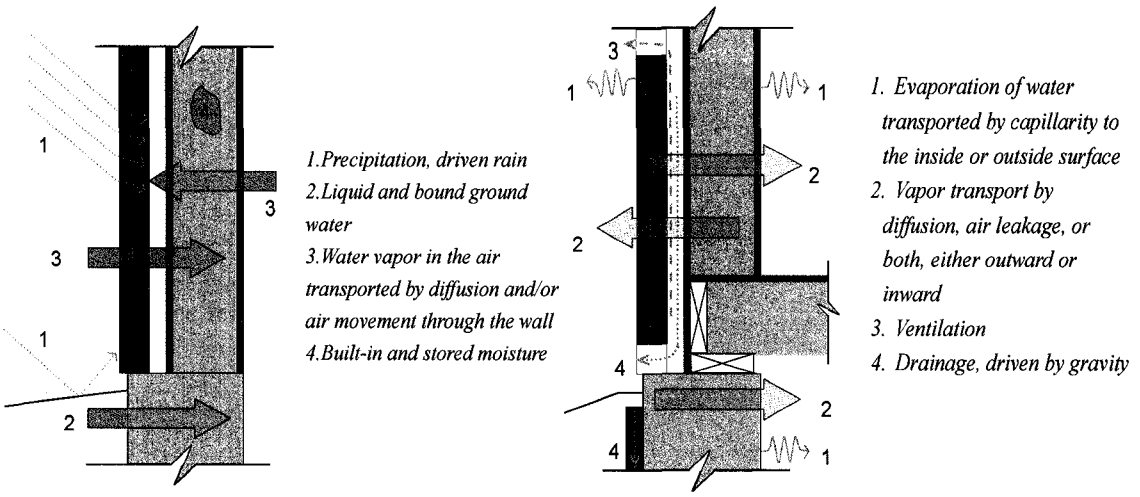

(a) Paths of wetting (b) Paths of drying

Figure 1.1. Wetting and drying moisture transport paths
(Adopted from Straube and Burnett 2005)

ASTM standard E241-04 (ASTM 2004) classified the wetting of building assemblies by three sources: (1) exterior, (2) interior, and (3) built-in moisture; three mechanisms: (i) liquid flow by gravity, air pressure, surface tension, momentum, and capillary suction, (ii) movement of water vapor by air movement, and (iii) water vapor diffusion by vapor pressure differences. Mechanism (i) usually happens from exterior side by rain penetration. Both mechanisms (ii) and (iii) are related to water vapor; they can happen from either the exterior or the interior. Mechanisms for removing (drying of) moisture are also divided into three groups: (1) liquid flow by gravity (drainage) or capillary suction, (2) movement of water vapor by air movement (ventilation), and (3) water vapor diffusion by vapor pressure differences.

1.2.2. Research topics in hygrothermal performance of building envelope

Studies in hygrothermal performance of wood-frame walls focus on several specific research subjects or categories, as listed in Table 1.1. These subjects are both interdependent and specific to wetting/drying processes. In many cases, the topics in the wetting process have their counterparts in the drying process, e.g. material hygrothermal properties; in others, topics under the two processes are quite different, e.g. transport mechanisms.

Table 1.1. Grouping of topics in hygrothermal performance of building envelope

<table>
<tr><th>Main research subjects / categories</th><th>Wetting process</th><th>Drying process</th></tr>
<tr><td rowspan="2">Transport mechanisms</td><td colspan="2">• Vapor
- vapor diffusion
- air transport</td></tr>
<tr><td>• Liquid water
- rain penetration
- rising damp
.....</td><td>• Liquid water
- drain
- water diffusion
- capillary action
.....</td></tr>
<tr><td rowspan="2">Material properties</td><td colspan="2">• Permeance properties
- vapor permeance
- water permeance
- air permeance
• Thermal properties for
- conduction
- convection
- radiation
• Water diffusivity
• Moisture failure
- criteria
- moisture limit
.....</td></tr>
<tr><td>• Retention property (Sorption)</td><td>• Retention property (Desorption)</td></tr>
<tr><td rowspan="2">Characterization of loads</td><td colspan="2">• Outdoor environment
- air conditions (temperature & relative humidity)
- driven rain index (rainfall & wind)
- moisture reference year
.....
• Indoor environment
- controlled indoor air condition
- non-controlled indoor air condition
.....</td></tr>
<tr><td>None of specific</td><td>• Penetration load (In-cavity load)</td></tr>
</table>

Characterization of wall responses	• Moisture performance - moisture content profiles - mold growth	
	• Evaluation method/index - penetration resistance - penetration rate	• Evaluation method/index - drying rate - drying capacity
Roles/functions of wall components	• Functions and effectiveness of - vapor barrier - cladding - air gap - air barrier - weather resistance barrier - sheathing	
Influences of different wall configurations	• Influences of different - claddings - air gaps (vented/unvented/ventilated) - sheathing materials - vapor barriers	
Influences of climate	• Climate types and classifications • Moisture response of wall under different type of climates	
Experimental & analytical techniques	• Laboratory testing - full scale test - small scale test • Numerical simulation - FEM model - CFD model	
Application in design	• Design method - design criteria - limit state design	

1.3. Problems and solution

According to a report from the Urban Development Institute (UDI) (Urban Development Institute 2000) and field observation by Brown et al. (2003), water may occasionally penetrate deeply into the stud cavity. Mao et al. (2004) analyzed the scenarios when rainwater driven by capillarity and air pressure passes across the air gap behind the cladding and gets into the stud cavity. Water ingress into stud cavities due to rain

penetration has been identified as the most severe moisture loading that leads to moisture problems (Morrison Hershfield Limited 1996) and has been the focus of recent research. To defend against this water intrusion, the building envelope should have four important characteristics, 4D (Hazleden and Morris 1999): deflection, drainage, drying, and durability. Deflection and drainage are effective means to reduce the amount of rainwater passing through the envelope's second line of defense; however, it is unrealistic to assume a perfect wall without any leakage. Moisture may also accumulate in the stud cavity due to condensation, presence of wet material during construction, or/and accidental water intrusion such as flooding.

Once moisture is trapped in the stud cavity, it cannot be evacuated easily and in many cases it may remain there long enough to do damage. Ironically, sometimes the better the performance of the building envelope against WDR (Wind Driven Rain) and/or vapor is, the lower the drying potential of the stud cavity. Therefore, practices that only focus on improving the WDR and/or vapor defense aspect, without considering the drying characteristics of the wall system, may lead to poor performance.

It may be stated that failure of the building envelope can be avoided if the rain penetration remains within a range which does not exceed the drying capacity of the wall system. In order to determine this range, quantification of potential moisture penetration and corresponding drying capacity are necessary. In other words, the building envelope should be designed with drying capacity to tolerate some level of rain penetration.

Engineering design involves the application of scientific knowledge to the design of products and systems to make them economical, functional, and reliable within the users'

expectations. In wood-frame wall design, there are currently many approaches to measure or calculate moisture penetration but there is a lack of methods to quantify the drying capacity of different wall systems. Due to such a lack of methods, an engineering design approach for hygrothermal performance has yet to be developed.

Successful methodologies developed in other engineering fields, such as the principle of limit state design, may be adapted to building envelope systems to aid the evaluation of hygrothermal performance. The quantification of drying capacity in this thesis research may also present a new way for evaluating drying performance of exterior walls.

1.4. Research objectives

The primary objective of this thesis research is to develop an approach to evaluate the relative drying capacities of wall systems. Moisture content level in the wall components was deployed as a limiting condition. The secondary objective is to evaluate quantitatively the acceptability of a wall configuration by matching the potential moisture penetration of the wall against its drying capacity.

To achieve these objectives, a large-scale experiment was devised and conducted in the environmental chamber at Concordia University. A test hut that was made up of wall specimens with wall assemblies of different compositions was constructed. The study was carried out within the context of a Collaborative Research & Development (CRD) project sponsored by NSERC (Natural Sciences and Engineering Research Council of Canada), the wood industry, University of British Columbia, Laval University, and Concordia University.

1.5. Structure of thesis

The rest of the chapters of the thesis contain the following:

Chapter 2 focuses on the literature review on

- The basic knowledge about design philosophy;
- The previous studies on moisture responses or moisture status of wall systems;
- The existing approaches for quantification of moisture loadings as well as the techniques for applying moisture loadings;
- The existing methods for evaluating the drying performance of wall systems.

Chapter 3 explores the experimental design through preliminary tests in order to

- Devise a suitable load method for the CRD experiment;
- Monitor both the moisture loadings and the corresponding moisture responses.

Chapter 4 presents the development of the methodology proposed in this thesis research to

- Define the criteria for identifying the moisture status of frame wall system;
- Develop an indicator for evaluating the drying performance of the entire wall system.

Chapter 5 describes the experimental setup that included 31 full size wall assemblies and tests lasting more than 200 days.

Chapter 6 presents the experimental results and application of the In Cavity Evaporation Allowance (ICEA) indicator including

- Comparison of the performance of different wall assemblies based on the developed drying evaluation indicator — ICEA;
- Comparison of the newly developed indicator with other existing evaluation

methods;

- Potential application of ICEA for quantitative verification of wall configurations by comparing predicted penetration water to ICEA.

The last chapter summarizes the contribution of this thesis research and points out the future research directions.

Chapter 2
Literature Review

Due to construction tradition and advantages such as cost-effectiveness and renewability of resources, wood-frame building is one of the most popular construction types in the North American housing industry. Every year, over 90% of residences in North America are built in wood-frame construction (Canadian Wood Council 2000a). The review in this chapter refers only to moisture performance studies of wood-frame wall system.

One aspect of this thesis is based on the notion that successful methodologies in other engineering fields may be deployed for building envelope systems to aid in the evaluation of hygrothermal performances. The design philosophies of structural engineering as well as the concepts such as the limit state and the design allowable capacity are borrowed with the goal of developing a new way for evaluating drying performance of exterior walls. The approach used in structural engineering that is based on load-response relationship analysis, is reviewed in the first part of this chapter. In the latter part of this chapter, methods commonly used for evaluating the drying performance in the building envelope community are reviewed in terms of both the experiment setup and the evaluation method.

2.1. Moisture loading on building envelope

Experimental as well as numerical studies on moisture transfer in building envelopes require setting appropriate boundary conditions or loadings to which enclosure systems are exposed. Any relevant factor that may cause responses in building envelopes can be defined as loading. *Moisture loading* is therefore identified as those loads that can cause moisture responses in wall systems.

Moisture loads can be categorized based on the characteristics of the loads or the positions where the loads are applied. According to the former, moisture loads can be classified into three subcategories: mass factors, energy factors, and biological factors. To be more specific, rain, snow, hail, vapor and ground water are identified as mass factors; temperature (e.g. difference, frozen, and fire), radiation (e.g. solar, long-wave), and mechanical forces (e.g. kinetic, hydrostatic pressure, capillarity) belong to energy factors; mold, fungi, termite, and human behavior fall into the group of biological factors. Regarding the positions, many previous research studies have focused on two types of moisture loads, one from the outdoor environment and the other from the indoor environment. Examples were IEA-Annex24 (Sanders 1996), IRC's WeatherSmart (Djebbar et al. 2001) and ASHRAE SPC 160P-Design Criteria for Moisture Control in Buildings (TenWolde and Walker 2001). In recent years, there has been a trend towards distinguishing the rain penetration from other outdoor sources and recognizing it as an independent moisture source. The current study adopts the third factor in the position category based on where the moisture loads occur in envelope system and considers three types of moisture loadings namely the external, internal, and in-cavity.

2.1.1. External moisture loading

External moisture loading refers to all the moisture loads coming from the outdoor environment that are mostly related to the weather factors.

2.1.1.1. Parameter Identification

In the field of building envelope research, the components of external moisture loading are identified by climatic parametric studies. Many professional organizations, such as ASHRAE (American Society of Heating, Refrigerating and Air-Conditioning Engineers), National Oceanic and Atmospheric Administration (NOAA) and Canadian Meteorological Centre (CMC), publish weather data. Researchers such as Sanders (1996) and Kragh (1998) proposed different parameter associated with external moisture loading, as shown in Table 2.1. Most of the parameters in these two lists are weather parameters, e.g. air temperature, relative humidity, etc. Driving rain in Kragh's list is represented by DRI (Driven Rain Index); though it is not a regular parameter of weather data, rather it integrates several metrological parameters including wind speed and direction as well as rainfall intensity. Air velocity in Kragh's list is equivalent to the total pressure and pressure difference in Sanders' list. Therefore, parameters in these two lists do not have significant differences.

DRI is defined as the product of the hourly average wind speed and the average rainfall intensity by Lacy (1962). It can be calculated by the following equation:

$$\mathrm{DRI} = V_m R_m \tag{2.1}$$

where V_m [m/s] is the average wind speed during rain at the meteorological station, R_m [mm/hr] is the rate of rainfall corresponding to the time of the wind at the meteorological station.

Table 2.1. Lists of parameters identified by Sanders (1996) and Kragh (1998)

Sanders (1996) / Annex 24	Kragh (1998)
• Temperature • Humidity • Solar radiation • Long-wave radiation • Wind speed and direction • Total pressure • Total pressure difference • Rainfall	• Temperature • Humidity • Solar radiation • Long-wave radiation • Driving rain • Air velocity

2.1.1.2. Characterization

The characteristics of the local weather of a building can be reflected by two aspects: the climate zone and the reference year.

Climate zone

Climate classification can facilitate the quantification, comparison, and ranking of climates at different geographic locations. Different approaches have been used to define climatic types and zones. Some simple approaches directly use a single meteorology parameter. For example, annual rainfall is usually used for identifying rain exposure zones and the heating or cooling degree-day is based on daily temperatures. Fig. 2.1 and Fig. 2.2 are maps based on these two different parameters in North America.

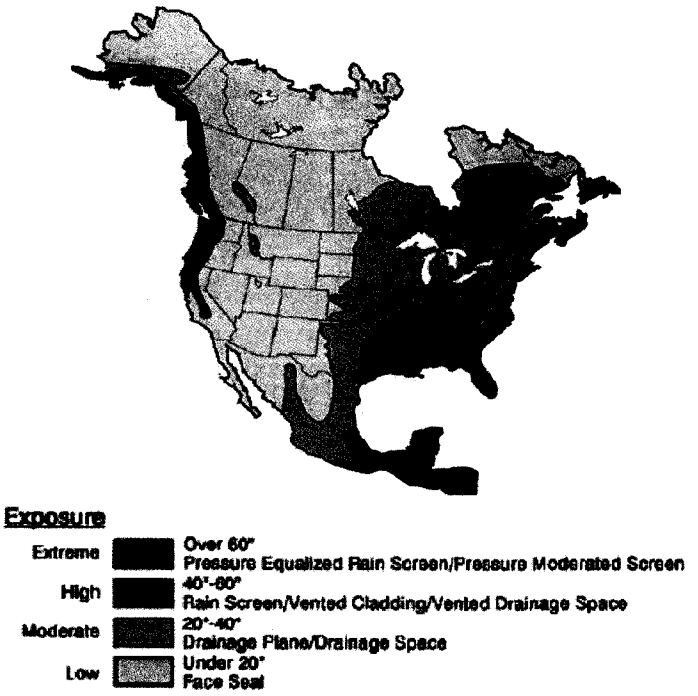

Figure 2.1. Annual precipitation map of North Americas

(Adopted from Lstiburek 2002)

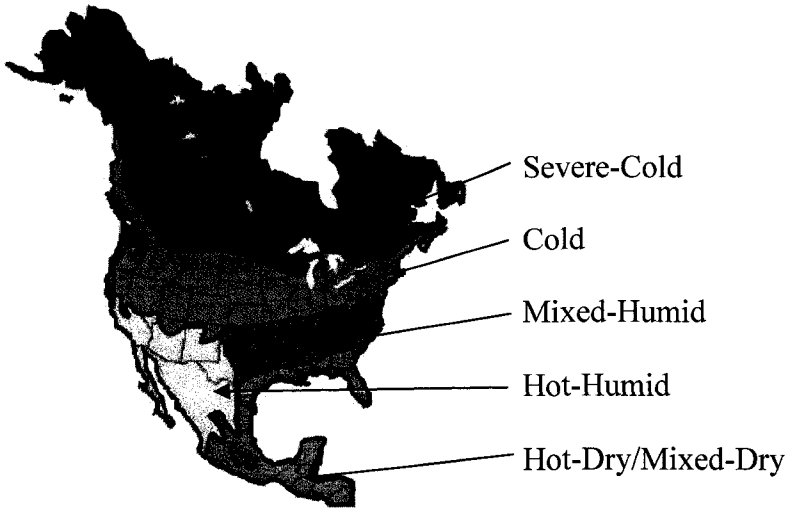

Figure 2.2. Hygrothermal regions map of North Americas

(Adopted from Lstiburek, 2002)

More sophisticated classifications employ parameters such as driving rain index (DRI) (e.g. Hoppestad 1955, Lacy 1965, and Zhu et al. 1995a), Wetting Index (WI), Drying Index (DI), and Moisture Index (MI) (e.g. Beaulieu et al. 2002 and Cornick et al. 2002).

Moisture Reference Year (MRY)

The selection of a typical reference year is intended to find the representative pattern of climate over time distribution. Many professional organizations and associations provide their weather data in suitable formats for energy calculations. In North America, the energy reference year is called TMY (Typical Meteorological Year); while in Europe it is referred to as TRY (Test Reference Year) or DRY (Design Reference Year) (Argiriou et al. 1999, Sanders 1996). In the area of building envelope design/research, Djebbar et al. (2001) named the year when weather data were specifically used for moisture analysis as Moisture Reference Year (MRY). As a reference year specifically used for building envelope analysis, MRY is defined as the year possibly with critical moisture performance of the building envelope.

There are two approaches for selecting or generating MRY: the construction independent method and the construction dependent method. The former generates the MRY by creating an artificial year consisting of "long-term average months" (Hensen 1999), which is only based on the analysis of meteorological data. The latter, on the other hand, selects the MRY according to building specifications and wall characteristics. Based on the prediction of the construction performance, this method uses different MRY with the variation in constructions (assemblies). The construction dependent method requires the use of HAM models to predict the performance of assemblies (Geving 2000).

2.1.1.3. Quantification of rain load on building façade

The rate of rainfall impinging onto a vertical building façade Rw [L/m^2·hr] is a commonly used parameter for quantification of a building exposure to wind driving rain. Lacy (1965) measures the vertical rainfall intensity and correlated the rate of water deposition on the

vertical plane with that on the horizontal plane, as specified by Eq. 2.2.

$$Rw = \frac{2}{9} V_m R_{hor}^{8/9} \tag{2.2}$$

where Rw [mm/hr] is the rainfall intensity on a vertical surface; V_m [m/s] is the wind velocity measured by meteorological station at a reference level, 10 m above the ground; R_{hor} [mm/hr] is the rainfall intensity on a horizontal surface.

Straube and Burnett (2000) uses Eq. 2.3 for calculating Rw [L/m^2·hr] in respect to the predominant direction of rain:

$$Rw = \mathrm{RAF} \cdot \mathrm{DRF}(R_{hor}) \cdot \cos\theta \cdot V \cdot R_{hor} \tag{2.3}$$

where RAF is the rain admittance factor; DRF [s/m] is the driving rain factor (depending on raindrop size and its terminal velocity, which equals 0.222 according to Lacy's statement; R_{hor} [mm/h = L/m^2·hr] is the horizontal rainfall intensity; V [m/s] is the wind speed at the height of interest, i.e. 1.8 m; and θ is the incident angle of the wind to the normal plane of the wall façade.

Fazio et al. (1995) and Zhu et al. (1995b) studied the driving rain exposure for 15 Canadian cities in terms of frequency, precipitation, intensity on vertical surface, and duration. Their method is based on Lacy's formula as well as the work done by Prior (1985). Eq. 2.4 is the formula they used for calculating the total precipitation of driving rain impinging on the vertical façade.

$$P_{\phi ver}^{T} = \frac{2}{9} \cdot C_{\phi} \cdot \sum_{i=1}^{n} R_{i\,hor}^{\frac{8}{9}} \cdot V_i \cdot \cos\theta_i, \qquad -90° \le \theta \le +90° \tag{2.4}$$

where P_{ϕ}^{T} [mm] is the total amount of driving rain passing a vertical plane; subscript ϕ indicates the building façade orientation; θ_i is the direction of the hourly mean wind normal to the vertical wall during a specific hour i (see Fig. 2.3); $R_{i\,hor}$ [mm/hr] is the

hourly rainfall on a horizontal surface during a specific hour i; V_i [m/s] is the hourly mean wind speed during specific hour i; n is the number of hours when driving rain is calculated during a specific period of time (day, week, month or year). Topographical features in urban region were considered by multiplying an attenuation coefficient C_ϕ (Zhu, Mallidi, and Fazio 1995b). This coefficient at the height of $\overline{H} + h$ was determined from Table 2.2 (see Fig. 2.4).

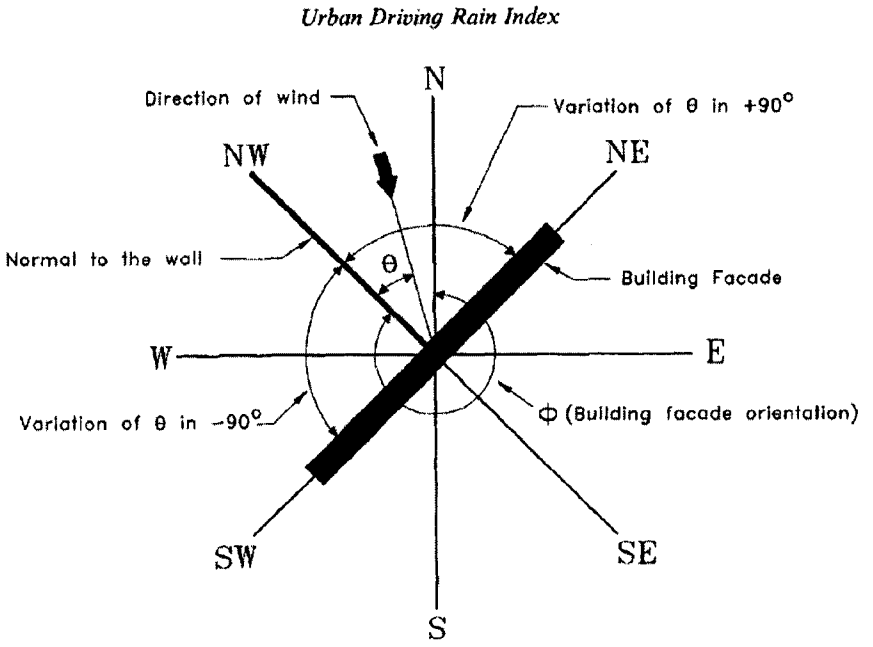

Figure 2.3. Building façade orientation and direction of wind
(Adopted from Zhu, Mallidi, and Fazio 1995a)

Table 2.2. Values of C_ϕ for various topographical categories

(Adopted from Zhu, Mallidi, and Fazio 1995b)

Location	Largely urbanized area centre of large city, high rise building district Z_0=2.5 m	Topographical categories moderately urbanized area centre of small town, low building district Z_0=1 m	Slightly urbanized area outskirts, park in city Z_0=0.3 m
$\overline{H} + 5m$	0.347	0.434	0.587
$\overline{H} + 10m$	0.432	0.547	0.712
$\overline{H} + 15m$	0.494	0.620	0.788

*z_0 is the roughness length; $\overline{H}$ is the average or general roof-top level.

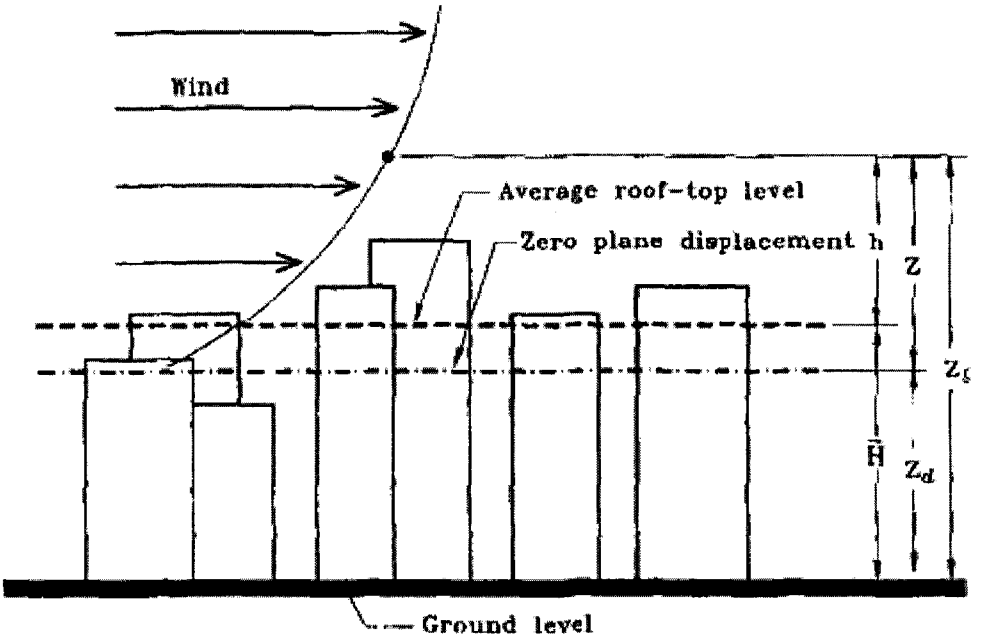

Figure 2.4. Position of average roof-top level in an urban environment

(Adopted from Zhu, Mallidi, and Fazio. 1995a)

2.1.2. Internal moisture loading

Compared with external loading, internal loading involves less parameters, usually only temperature and relative humidity. The indoor condition can be either controlled or non-controlled.

A standard for estimating moisture design loads is under development within ASHRAE SPC 160P-Design Criteria for Moisture Control in Buildings. According to TenWolde and Walker (2001), ASHRAE SPC 160P includes interior design loads (temperature, humidity, and air pressure) as well as exterior design loads (temperature, humidity, and rain), appropriate design assumptions for moisture design analysis, and criteria for evaluating acceptable performance. It will include criteria for moisture design weather data instead of the actual weather data. Before such design weather data are available, a moisture analysis has to be conducted using currently available weather data or design weather data generated by the user.

Table 2.3 summarizes the internal conditions used in several experimental projects and the corresponding methods for the determination of indoor conditions.

Table 2.3. Summary of methods for determination of indoor conditions

Literatures / Projects	Season	Indoor conditions		Method	Suit for
		T_{in} °C	RH_{in}%		
TenWolde et al. 1995 (ASHRAE Standard 55-1993R)	Winter	21°C	28%~77%	Thermal comfortable (controlled model)	Everywhere
	Summer	24 °C	50%~65%		
Beaulieu et al. 2002 (IRC MEWS)	Winter	21°C	30%	Thermal comfortable (controlled model)	Everywhere
	Summer	24°C	50%		
Djebbar et al. 2001 (ISO standard)	N/A	21°C (when outdoor at 8 °C; 76%)	46%	Five class models (non-controlled model)	Everywhere (Medium humidity building)
Sanders 1996 (IEA Annex 24)	Winter	21°C	30%~55%	Statistical summary (Questionnaire data)	Canada
	Summer	24°C	30%~80%		
	Winter	N/A	52%	Worst case	Montreal
Jenssen et al. 2002	Winter	21.4± 2.3°C	28.7±6%	Statistical summary from monitored data	Living room Trondheim,

					Norway
Lawton et al. 1999	Winter	23°C	Control the pressure difference constant	Local experience	BC, Canada
Hazleden and Morris 2001 (EDRA)	Winter	20°C	40%	Lab condition	Vancouver, Canada

2.1.3. In-cavity moisture loading

As previously mentioned, there is a trend to consider the penetrated water as the third independent moisture source in recent years. By adding an in-cavity moisture source, the consequence of different wall configurations, different workmanship, and process of wall deterioration was mimicked.

In previous experimental studies, there have been several different methods for applying in-cavity moisture source, e.g. injecting water directly into stud cavity (Lawton et al. 1999); soaking components into water up to a certain level moisture content before running of the test (Hazleden and Morris 2001); inserting a piece of wetted wood on the bottom plate of the wall (Teasdale-St-Hilaire et al. 2004); and putting a water tray on the bottom plate (Fazio 2004).

2.1.3.1. Parameter for characterization of in-cavity loading

In-cavity moisture is mainly originated by rain penetration that is driven by rainfall and wind. The moisture transported by water vapor, for example due to condensation, is regarded as a result of indoor and outdoor conditions. Under certain external and internal loadings, condensation is not considered part of the in-cavity loading. Other sources such as construction moisture and accidental flooding are deemed irregular. Therefore, rain

penetration is the only major source for in-cavity loading for wood-frame wall systems. For study purpose, rain that penetrates the stud cavity is replaced by a moisture source within the cavity.

Methods for implementing in-cavity loading vary from one experiment to another, and there is no consensus on the magnitudes and locations of inserted water. Further research on characterizing in-cavity moisture loading is necessary. The parameters for characterization of in-cavity moisture loading vary depending on the loading methods. For example,

- with direct injection, the total amount of water is used to characterize the loading (Lawton et al. 1999);
- with soaking components, the moisture content of a component is used for measuring loading potential (Hazleden and Morris 2001);
- with the wetted wood block at the bottom plate of the stud cavity (Teasdale-St-Hilaire et al. 2004), the weight reduction during drying; and,
- in cases of a water tray on top of the bottom plate in the stud cavity, the evaporation rate from the moisture source represents the intensity of the in-cavity loading (Fazio 2004).

The last loading method has been employed in this thesis research and will be thoroughly analyzed throughout this thesis.

2.1.3.2. Quantification of rain penetration

There have been some research efforts on the rain penetration prediction. The amount of

intrusion caused by rain penetration is related to the degree of "leakiness" and the severity of the driving rain impinging over the façade of a building. Brown et al. (1997) first measured the quantity of rain penetration by carrying out a full scale test at the National Research Council of Canada (NRC). However, their test concentrated on the performance of cladding systems and on the rainwater penetrating through the air gap behind the cladding. The formula below was developed during the MEWS project (Beaulieu et al. 2002) (see Eq. 2.5) to calculate the hourly rate of rain penetration into stud cavity.

$$Q = Rw \cdot f(\Delta Pw) \tag{2.5}$$

where Q [L/hr] is the hourly rate of rain penetration into stud cavity; Rw [L/m^2·hr] is the hourly rainfall impinging on the wall obtained from Eq. 2.2 or Eq. 2.3; the term f ( ) is called the proportionality factor of a rainscreen system [L/(L/m^2)], ΔPw [Pa] is the wind-induced pressure on the exterior surface of the wall. The function f ( ) consists of empirical correlations estimated through testing. Eqs. 2.6 through 2.9 are the proportionality factors for four types of wall assemblies that based on representative specimens with 2,400 mm × 2,400 mm exposure area and some conventional openings/defects (Beaulieu et al. 2002).

Stucco-clad walls:

$$f(\Delta Pw) = 0.0314 + 7.74\times10^{-5} \cdot \Delta Pw - 8.14\times10^{-8} \cdot (\Delta Pw)^2 \tag{2.6}$$

EIFS-clad walls:

$$f(\Delta Pw) = 0.0418 + 0.0243 \cdot \Delta Pw/(110.3359 + \Delta Pw) \tag{2.7}$$

Masonry-clad walls:

$$f(\Delta Pw) = 0.0115 + 1.722\times10^{-4} \cdot \Delta Pw - 1.471\times10^{-7} \cdot (\Delta Pw)^2 \tag{2.8}$$

Hardboard and vinyl siding-clad walls:

$$f(\Delta Pw) = 0.0422 + 1.618\times10^{-5}\cdot\Delta Pw - 3.88\times10^{-8}\cdot(\Delta Pw)^2 + 1.115\cdot10^{-10}\cdot(\Delta Pw)^3 \quad (2.9)$$

In the above 4 equations, ΔPw is obtained from:

$$\Delta Pw = \left(\rho_a \cdot V^2\right)/2 \quad (2.10)$$

where ρ_a [kg/m^3] is the density of air; V [m/s] is the wind speed at the location of interest.

2.2. Drying capacity and moisture responses

In structural engineering, bearing capacity is the maximum load that a system can support before failing. Capacity is usually expressed in terms of the ultimate load, but the judgment of failure is based on the response, e.g. certain strain or deformation; therefore, the determination of capacity should be based on the load-response relationship. In addition, a methodology for judging the failure and maintaining a certain margin of safety is important as well.

In the past two decades, several studies, such as Bomberg and Allen (1996), Carll (2000), and Lstiburek (2002), have started to introduce a few concepts of structural engineering, for example limit state, to the hygrothermal analysis and design of building envelopes. When developing an engineering approach for aiding the design of a wall system with the goal of avoiding damage from water penetration, Carll (2000) pointed out that four related aspects need to be addressed and/or to be agreed upon:

1. Method to quantitatively describe moisture loads;
2. Means to describe and predict the response of the envelope to the moisture loads;
3. Criteria on the limit of the response (i.e. the "limit states"); and
4. Extent of the safety margin.

These four aspects can be summarized into four concise terms: Load(s), Response(s)/ Resistance(s), Limit, and Margin. The knowledge of moisture load(s) has been review in section 2.2. Drying can be seen as a process during which the wall components endure and resist moisture load(s). In this section the review focuses on the drying capacity which the author believed is a concept that associates moisture load(s) to the rest three factors above.

2.2.1. Drying capacity

Within the last decade, the terms like "drying capacity" or "drying capability" or "drying efficiency" have gained more and more attention (Salonvaara et al. 1998). However, existing studies have yet to be agreed upon the definition of drying capacity, not to mention a method for quantifying it. For the system of wood-frame wall, the drying process is a comprehensive concept that describes the process of moisture going from the inner section of a wall to the external environment. In many cases, both wetting and drying processes take place in a wall system simultaneously.

As analogical principles from structural engineering, this thesis considers that factors affecting drying capacity include i) responses to moisture loads; ii) moisture failure criterion; and iii) margin of safety. In addition, drying capacity should serve as an index to compare different envelope systems; and thus measuring drying capacity requires a uniform baseline for assessment and an identical boundary condition for all tested wall specimens. Accordingly, specimen wetting techniques and environment condition maintenance are critical issues. There have been plenty of studies on these topics, and the subsequent section summarizes the related literatures.

2.2.2. Moisture responses

The responses of wall systems to moisture loading can be physical changes, chemical processes, and/or biological degradation. Sometimes these changes are reversible, but sometimes not. Some of these changes affect only the appearance of the systems under consideration while some others may seriously affect the health of the occupants (e.g. growth of molds and fungi) and even affect the integrity of the envelope and structure. Plenty of literature, such as Brundrett (1990), Zabel and Morrell (1992), Wood Handbook by FPL (Forest Products Laboratory 1999), Viitanen and Salonvaara (2001), Morris and Winandy (2002), and Nofal and Morris (2003), provided detailed descriptions of moisture responses of buildings. More sophisticated approaches for characterizing moisture responses of wall systems include a RHT indicator (Lacasse et al. 2003) and the Mold Index (Viitanen and Salonvaara 2001). RHT is a moisture response indicator that reflects the mold growth potential at a certain location of a wall system.

Most of the previous experimental studies measured the moisture contents at specific locations in wall assemblies by using relative humidity or moisture content probes, or gravimetric samples (e.g. Salonvaara et al. 1998, Hazleden and Morris 2001, Lawton et al. 1999, van Straaten 2003, Teasdale-St-Hilaire et al. 2005, and Fazio et al. 2006a). Moisture contents were often plotted versus time in those studies.

In many cases, moisture responses are shown as time-dependent variables, e.g. MC vs. time, Mold Index vs. time. Another option is to plot the response with respect to load, for example, RHT vs. Q (as shown in Fig. 2.5). Here, the rain penetration rate Q characterizes the severity of rain penetration (Kumaran et al. 2003), while RHT is a

moisture response indicator proposed by the MEWS project. RHT is essentially a mold growth index, and is defined based on the duration of the coexistence of moisture and thermal conditions above a set of minimum levels during an exposure over two years. RHT index can be computed from the following equation (Beaulieu et al. 2002):

$$\mathrm{RHT}(X) = \sum (\mathrm{RH} - X) \cdot (T - Y) \tag{2.11}$$

where X and Y are the minimum levels of relative humidity and temperature respectively, the summation is applied only when both the differences in the two parenthesis are positive over a 10-day period. Two X values used in MEWS were 80% for corrosion (e.g. for metal fasteners) and 95% for the growth of wood decay fungi. A temperature threshold of 5°C was considered appropriate for both damage processes. RHT quantitatively represents the corrosion or mold growth (potential) response of the wall system to moisture loads (Lacasse et al. 2003).

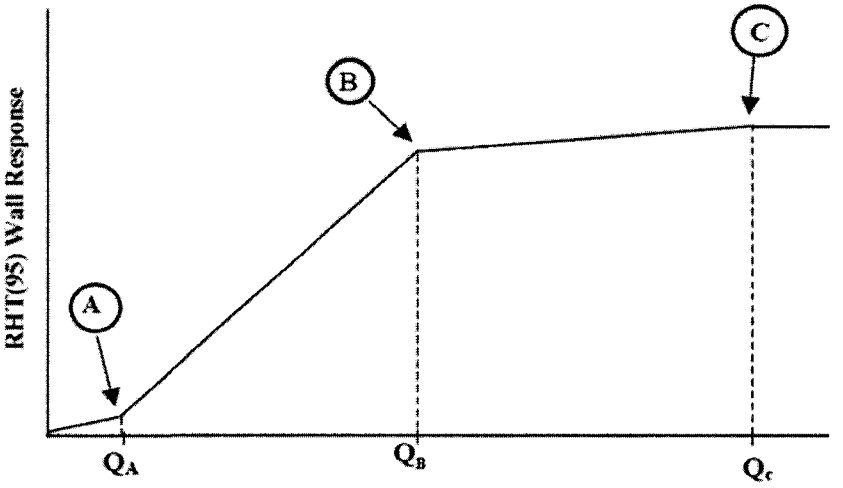

Figure 2.5. RHT vs. moisture loading Q
(Adopted from MEWS final report, Beaulieu et al. 2002)

2.3. Limit states and safety margin for moisture performance

In structural engineering, Limit State Design (LSD) is a design method for checking the performance of a structure by studying various limit states corresponding to different load levels. LSD has been used with great success for decades in the design of concrete and steel structures. For the wood frame construction before the 1980s, the only authoritative design method by the Canadian Standards Association (CSA) was the Working Stress Design (WSD), or Allowable Stress Design (ASD). Later in the CSA Standard 086.1-94 (CSA 1986), LSD was modified for the design of wood structures by introducing reliability analysis of loadings and material properties to obtain relative factors (Keenan 1986).

Two types of limit states are prominently distinguished: the Ultimate Limit States (ULS) and the Serviceable Limit States (SLS). ULS deals with the safety of the structures, while SLS deals with the functionality during the normal use and occupancy of the building.

Moisture related failure is generally characterized as a durability failure, which belongs to the category of SLS. In CSA Standard O86.1-94 (for engineering design in wood using the limit states design concept), the moisture relevant limit has not yet been included.

2.3.1. Limit states

In structural engineering, a limit state is defined as a set of performance criteria (e.g. vibration levels, deflection, and strength) that ensure stability (buckling, twisting, and collapse) when the structure is subjected to certain loads. In other words, the limit state is the critical state at which failure is about to occur.

Failures in buildings may result in direct changes in the properties of materials or even the strength of the structures. The definition of failure, as given by Viitanen and Salonvaara (2001), is the "termination of the ability of an item to perform a specified function". To know if a building envelope system performs properly, care should be taken to define the criteria for judging failure. Wang et al. (1992) provide a list of criteria related to environment, structure, cost, esthetics, erection, and maintenance respectively. Determining the load-carrying capacity of a structure involves one of the criteria, while identifying moisture limitation for mold growth in building envelope involves another.

In studies on moisture performance of a building envelope, the concepts of limit state and failure are interpreted as moisture limit state and moisture failure. To defining the moisture limit state, moisture failure criteria should be determined first. There are different types of criteria for deciding the failure due to moisture, such as metal corrosion, (board) edge swelling, nail holding strength reduction (due to wetting of materials), etc. One of the frequently used criteria is based on the level of microbiological activity, i.e. mold growth and fungi decay, which is reviewed in the subsequent subsection.

2.3.2. Failure criteria based on mycology

Criterion for deciding moisture failure plays a very important role in building envelope study. According to the National Building Code of Canada, if changes caused by moisture do not result in any unacceptable consequence, the envelope is deemed to be in a tolerable state (Morris and Winandy 2002). Here, the term "unacceptable consequence" means any damage that is caused by loss of structural strength or that affects the occupant health (Nofal and Morris 2003). Failure as a consequence of excessive moisture in the

envelope can be caused by physical, chemical, or biological factors (Viitanen and Salonvaara 2001). For wood frame buildings, the most prominent moisture-related biological consequence is mold growth and fungal decay. Studies at both material level and system level had been conducted to determine the limit state in terms of molds and decays. Studies at the material level considered the decay-caused limit state from a wood microbiological perspective, e.g. the appropriate conditions for mold germination, growth, and survival (Zabel and Morrell 1992). Studies at the system-level correlated the definition of limit state with the moisture performance of the entire wall system. Usually, system-level topics focused on analysis or judgment whether the performance of wall system could result in mold growth and fungal decay in any part of the wall system, e.g. Morris and Winandy (2002).

From the material perspective, the occurrence of mold or decay fungi is affected by many factors. Sedlbauer et al. (2001) indicated that such factors as humidity (moisture), temperature, time, substrate, ph-value, light, oxygen, spore dissemination, roughness of the surface, and biotic interactions should be taken into consideration. Other research provided a slightly different list, for example, Zabel and Morrell (1992) included water, oxygen, temperature, substrate, ph-value, and chemical environment in their list. Among all these parameters, moisture and temperature are the most important ones in the context of the building envelope. If one must select a single factor as the most essential one to mycological process, the answer should be moisture; more importantly, moisture can be more easily controlled during microorganism growth compared to other parameters, e.g. temperature. Previous studies have indicated that mold growth would stop if temperature fell out of a certain range. Drastic diurnal and seasonal variations in the outdoor

temperature and wide tolerable range of molds to temperature make the temperature to be a less predictable and controllable factor than moisture for establishing a mold growth criterion.

Therefore, the moisture content (MC) level is the most appropriate parameter for diagnosing the limit state of material failure caused by molds and decays. The most favorable moisture condition for the majority of the decay fungi in wood is above the fiber saturation (that is, all the wood fibers are fully saturated) but below the completely soaked condition (Zabel and Morrell 1992). The fiber saturation point for wood is around 25% to 30% MC (by weight), and some researchers even narrowed the range down to 28% to 30% (Griffin 1977, Morris and Winandy 2002, and Canadian Wood Council 2000b). Hence, 28% MC can be taken as the moisture level at which failure due to fungal decay may occur.

Studies at the envelope-system level are targeted at the entire building envelope in order to predict moisture transportation within the components of the building envelope and to improve the overall performance of the envelope system. Some studies have introduced mold growth analysis to predict mold occurrences or growth rates on the surfaces of layers in building envelope (Moon and Augenbroe 2004). Mold growth limitation curves were estimated from long-term material tests in some of the studies, e.g. critical relative humidity (Karagiozis and Salonvaara 1995) in LATENITE and the Lowest Isopleth for Mold (LIM) in the biohygrothermal model (Krus et al. 2001). But most of these models were multi-factor models considering parameters such as relative humidity, exposure

time, material properties, fluctuating of conditions all together. These models were not available, thus difficult to be applied in engineering design.

2.3.3. Margin of safety

In the field of moisture performance, the design allowable moisture level for wood or wooden material has been discussed for a long time. Hunt and Garratt (1938) prescribed a 20% rule as early as the 1930s. This rule is still in use by the industry today, e.g. the FPL's Wood Handbook (Forest Products Laboratory 1999) and ASHRAE Fundamentals (ASHRAE 2001), because it does not contradict any range proposed in recent research (Carll and Highley 1999). Another reason for this 20% rule is based on observations in more recent research studies, which indicated that mold growth and fungal decay occur only after the moisture content breaks through the FSP (at about 28% MC by weight); and on the premise that, once molds and fungi are established, it is difficult to stop them until the moisture content in the wood is dropped below 20% during the drying process (Morris and Winandy 2002). Apparently, MC range between 20% and 28% provides a margin of safety against fungus damage (Nofal and Morris 2003). It should be noted that moisture is not the only factor that may sustain and limit microbiological degradation; therefore, other factors such as suitable temperature and long time duration should be included into safety margin as well.

CWC (Canadian Wood Council 2000a) recommends a moisture limit of 19% MC by weight on all wood materials (mainly for dimensional lumber) in construction. Such a 19% MC limit is also required by NBCC (NRC 1995) and ASTM standard E241-04

(ASTM 2004) for the purpose of preventing not only decay but also shrinkage during construction.

In summary, 20% MC appear to be a reasonable moisture level limit in wood-frame wall design to reduce the risk of degradation.

2.4. Full scale experiments on envelope systems

Many experimental studies have been carried out worldwide to investigate the hygrothermal performance of building envelope components and systems. There have been several notable and relevant full scale experimental studies on the drying process of exterior wall systems, such as: 1) as possibly the first full-scale lab test on drying performance, the EDRA project (Envelope Drying Rates Analysis) (Hazleden and Morris 2001) was carried out by BERC (Building Envelope Research Consortium, an industry/government consortium led by CMHC-Canada Mortgage and Housing Corporation); 2) IRC's MEWS program included experimental tasks to evaluate wetting intensity due to rain penetration, though the program mainly focused on computer simulations with the numerical tool hygIRC (Beaulieu et al. 2002 and Kumaran et al., 2002); and 3) the pre-CRD test was carried out in an environmental chamber at Concordia University (Fazio 2004, Teasdale-St-Hilaire et al. 2004). Other experimental testing included the drying experiment of stucco-clad wall by Lawton et al. (1999) and the tests carried out in the BEGHUT (Building Engineering Group's HUT) at Waterloo University (van Straaten 2003). In Europe, a program of Finnish Wood Building Technology in VTT (the Technical Research Centre of Finland) carried out a test to

measure the drying capability of wood-frame walls (Salonvaara et al. 1998); and Ojanen et al. (2002) designed a method to evaluate the drying efficiency of wall structures.

In envelopes under different moisture loads such as described above, the hygrothermal processes involved can be divided into two groups: wetting and the drying processes. Many investigations studied both process groups, while others focused on only one of them.

To carry out moisture performance evaluation, the processes of moisture transport in building envelope are divided into two groups: wetting and drying processes. Though most researches investigate the entire process of moisture transport and cover both the wetting and the drying processes at the same time, a number of experimental studies have focused on only one of them. In these cases, wetting and drying are tested separately.

Because drying comes after wetting, specimens need to be wetted before running of any drying test. Wetting technique has to be considered even in studies focusing on the drying aspect. In previous studies, diverse wetting methods have been applied to building envelope assemblies before the specimens were subjected to drying, whether in the field test or in the mock-up labs. These experimental studies are reviewed in the section below.

2.4.1. Existing techniques for applying wetting loads in experiments

For testing of a single material, a specimen can be simply sprayed with water over its surfaces, or directly placed in contact with water, or even completely soaked in water. Wetting a multi-component wall assembly is much more complicated since wall specimens cannot be directly soaked. Previous experimental studies, such as TenWolde et

al. (1995), Salonvaara et al. (1998) and Hansen et al. (2002) studied moisture introduced by vapor diffusion only. This method, however, just simulates one of the pathways of moisture transfer. Rain penetration, a more critical pathway in terms of magnitude, was neglected.

There are miscellaneous wetting techniques for simulating the process of rain penetration, e.g. spraying water over the exterior cladding (Brown et al. 1997), directly inserting water into the stud cavity, or soaking wall components (Tsongas et al. 1998, Hazleden and Morris 2001) in water. There is no standard protocol yet and no consensus has been reached either on the water-adding method or on the quantity of water added. Though standard testing methods such as ASTM standard E-331, E-514, E-547, E-1105 (ASTM 1996a, b, c, d) or AAMA standard 501.1, 501.2, and 501.3 (AAMA 1994a, b, c) specify methods for simulating the wind driving rain, these protocols are focused exclusively on estimating the quantity of intruding water. Direct wind driving rain was rarely employed together with experimental investigations of the hygrothermal responses of envelopes. It is understandable that a faster wetting is needed when a research focuses on the drying process. As a result, direct insertion and component soaking were used frequently in the last decade. The difference between the methods by direct inserting water into stud cavity and by spraying water onto the cladding is that the former is applying in-cavity moisture loading and the latter is not. Table 2.4 shows available methods of adding water to specimens in the full-scale experiments reviewed.

Table 2.4. Summary of wetting methods and moisture source types

Literatures	Institution /Program	Environmental Conditions		Wetting methods	Moisture sources*
		Outdoor	Indoor		
TenWolde et al. (1995)	USDA/ Forest Service	Natural climate	21°C; 35%; 21°C ; 45%	Vapor diffusion	1,2
Salonvaara et al. (1998)	CMHC/ EDRA	Winter: -10°C; 60%	Winter: 20°C; 25%	Vapor diffusion	1,2
		Spring: 5°C; 60%	Spring: 20°C; 50%		
Hazleden and Morris (2001)	CMHC/ EDRA	5°C; 70%	20°C; 40%	1.Immersing wood members into water 2.Vapor diffusion	1,2,3
Kumaran et al. (2002) Beaulieu et al. (2002)	IRC/ MEWS**	MRY (hourly)	Winter: 22°C; 25% Summer: 25°C; 55%	1.Estimated amount of penetrated water were applied in numerical model 2.Vapor diffusion	1,2,3
Lawton et al. (1999)	CMHC	5~14°C; 45~85%	19°C ~25°C; 35~60%	1.Inject same amount of water into cavity 2.Vapor diffusion	1,2,3
Ojanen et al. (2002)	VTT	-10°C 3°C	20°C; 100%	Vapor diffusion	1,2
van Straaten (2003)	Waterloo University/ BEGHUT	Natural climate	20°C; 50%	Inject water to highly absorbent paper located at vulnerable positions	1,2,3
Teasdale-St-Hilaire et al. (2004, 2005)	Concordia University/ Pre-CRD	1.6~10.9°C; 64% 8.6~18.7°C; 63%	21°C; 40% 21°C; 43%	1.Inject water by peristaltic pump 2.Insert a piece of wetted wood 3.Vapor diffusion	1,2,3

* 1:Outdoor climatic source; 2: Indoor environmental source; 3:In-cavity evaporation source.

** The drying process of MEWS project was studied using a computer simulation program, hygIRC.

It can be noticed that many studies have applied in-cavity moisture loading in their tests, but the methods used for adding moisture were diverse and without a consensus on principles and magnitude. For example, Lawton et al. (1999) injected certain amount of water into all tested panels, while Teasdale-St-Hilaire et al. (2003) used different quantities to mimic rain penetration. Hazleden and Morris (2001) wetted specimens by

immersing the entire wood members into water before testing, while van Straaten (2003) injected water to highly absorbent paper that was inserted at vulnerable positions of the wall assembly.

In recent studies, efforts have been made to assess the sizes of flaws in walls and to correlate water penetration through the flaws with wind-driven rain. The correlations were used for determining the amount of water added into wall assemblies in simulation scenarios to predict the hygrothermal response of walls with different cladding types. In the precursor project for the experimental program presented in this thesis research, this approach was employed to investigate flaws and amount of water penetration for wall segments under windows using a rain-penetration chamber following the ASTM E-331 standard (ASTM 2000) (Teasdale-St-Hilaire et al. 2004); and, in the full scale experiment testing, water was injected by a multi-channel peristaltic pump at the top of the four-foot-high frame-wall specimens to mimic the water penetrating through the flaws. In comparison with other methods in literature, this project added a new element: adjusting the amount, duration, and frequency of water injection so as to mimic wind-driven rain penetration through envelope defects. This method does represent a realistic situation of rainwater after penetrating through typical discrete holes/cracks under a window, and it may quantify moisture distribution differences between sheathing materials (i.e. lateral diffusion vs. transmission of moisture across the sheathing thickness). However, this method cannot make comparative studies of the drying performance when wall assemblies are subjected to the random tracks of water flow.

For comparative study, another method, initially suggested by Fazio (2004), was devised

to establish uniform wetting conditions for all the specimens at the beginning of the drying process. This method involved partially immersing segments of 2 × 6 wood studs in water, weighing the moisture content in these segments, and then placing one piece between the two studs above the original bottom plate of each wall specimen through an access door that cut out from the drywall. The insert pieces were of approximately the same weight and were cut from the same piece of spruce wood stud. The immersion took 31 days, and it allowed the stud pieces to reach a moisture content of around 55% by weight. The method showed promise in establishing correlations that would be useful as a yardstick in comparing the performance of different envelope configurations (as shown in Fig. 2.6), however, the limited total amount of water in the inserts subjected to the walls to only limited moisture loads.

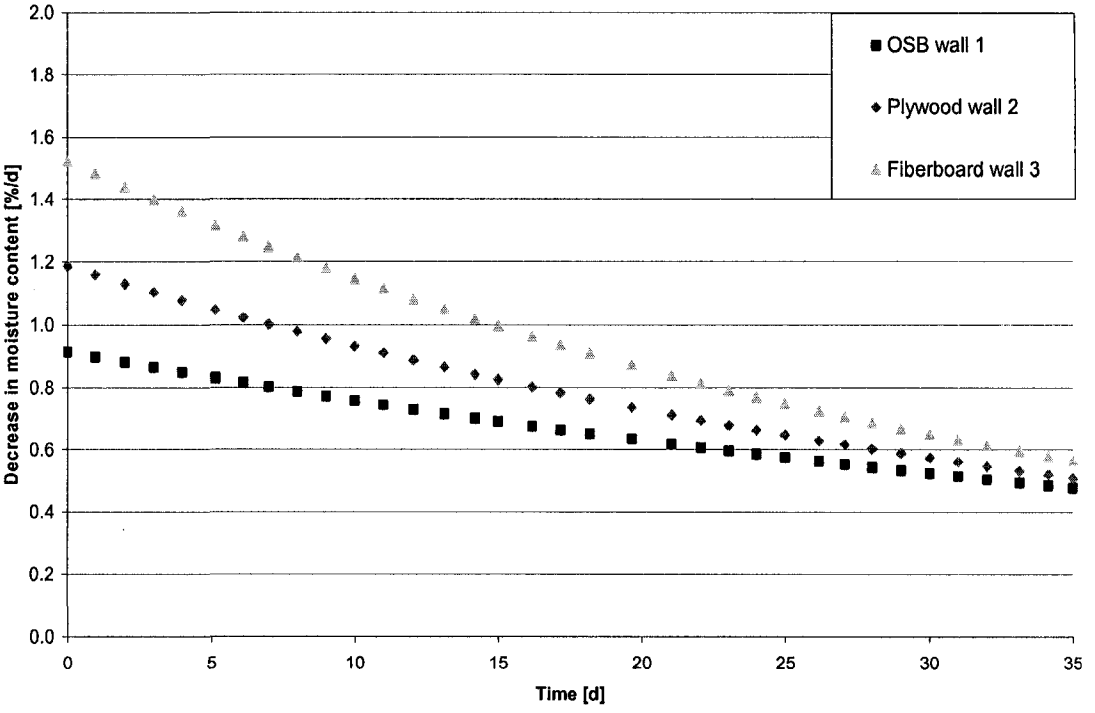

Walls 1, 2, and 3 sheathed with OSB, plywood, and fiberboard respectively

Figure 2.6. Change in moisture content in an inserted bottom-plate with time
(Adopted from Teasdale-St-Hilaire et al. 2004)

2.4.2. Indicator of drying performance

For any evaluation method, two essential factors that may affect the evaluation results are evaluation index and comparison baseline. In structural engineering, load-carrying capacity not only sets a design allowance, but also serves as the indicator for comparative study of different materials or structures. In moisture performance studies, an analogue term is needed to evaluate and compare different wall systems. Such an indicator would describe the performance of a wall in overcoming various moisture loads without damage, and generally contains the modifying or attribute word "drying". In previous studies, indicators have been proposed for evaluating drying performance. This "drying performance" indicator had various descriptions and/or definitions, such as vapor permeance, evaporation rate at bottom plate, moisture content variation at specific location, and wood decay observation. However, there has not yet been a consensus on the definition.

The rest of this section is a review of a few examples of these "drying performance" indicators. They have been grouped into three categories according to the speed of moisture transport and the rate of moisture content variation. The Type I approach reflects the total moisture evacuation from the entire wall system, the Type II approach focuses on the change of the moisture content of a wetted insert at the bottom plate, and the Type III approach represents a specific criteria (e.g. moisture content or mold growth) at certain locations in the wall components. Fig. 2.7 illustrates these three types of drying evaluation approaches. Table 2.5 presents the frequently used parameters or indexes for quantifying loadings and responses.

Type I: Total moisture evacuation rate

Drying performance is indicated by the total rate of moisture evacuation from the entire specimen (e.g. work by Hazleden and Morris 2001). It is evaluated by the effective moisture (vapor) permeance coefficient $\dot{M}_v^e$ [ng/P_a·s·m^2]. This permeance coefficient can be expressed as:

$$\dot{M}_v^e = M_E^T /(A \cdot t \cdot (p_{\text{in}} - p_{out})) \tag{2.2}$$

In the above equation, M_E^T [g] is the total mass of moisture evacuated from the entire wall panel over a specific duration of time t [s]; A [m^2] is the cross section area of the vapor path, i.e. the panel area; p_{in} and p_{out} [Pa] are the partial water vapor pressures inside and outside the stud cavity, respectively. Some other indicators such as net vapor diffusive flux (TenWolde and Carll 1992) and drying efficiency (Ojanen et al. 2002) are the same as $\dot{M}_v^e$ in nature.

The value M_E^T is normally difficult to measure. Compared to the total weight of the wall, the mass of dissipated moisture is relatively small and cannot be monitored easily. Direct electronic measurements have been attempted only in a few existing studies, such as experimental work by Maref et al. (2002). Lawton et al. (1999) and Hazleden and Morris (2001) obtained the total weight of the test panel by weighting its components piece by piece at the beginning and end of the test.

Usually the total vapor permeance coefficient $\dot{M}_v$ [ng/P_a·s·m^2] is calculated as the reciprocal of the sum of vapor resistances associated with every component layer in an assembly (see Eq. 2.3).

$$\dot{M}_v = 1/\sum_{i=1}^{N} r_{vi} \tag{2.3}$$

where r_{vi} [s·m^2·P$_a$/ng] is the vapor resistance of each layer of material, and it equals to $1/\dot{M}_{vi}$ or l_i/μ_i, here $\dot{M}_{vi}$ [ng/Pa·s·m^2] is the vapor permeance of the ith layer of material; l_i is the thickness of the ith layer of material; μ_i [ng/Pa·s·m] is the permeability of the ith layer of material; N is the number of layers (Hutcheon and Handegord 1995, TenWolde and Carll 1992). The vapor resistance of common envelope materials can be obtained from Table 7 in Chapter 22 of ASHRAE Handbook (ASHRAE 2001).

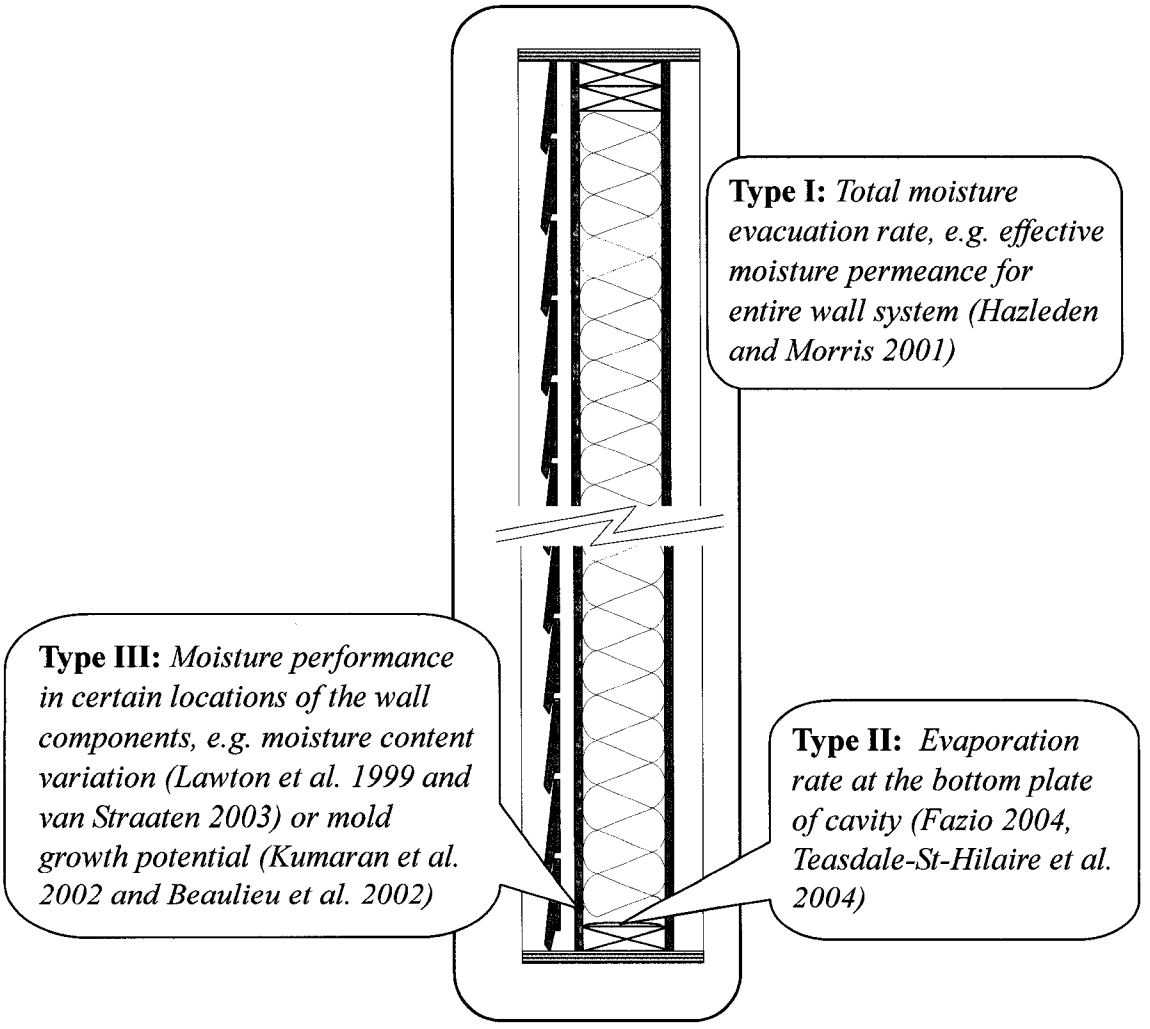

Figure 2.7. Three types of approaches for wall drying performance evaluation

Table 2.5. Summary of drying evaluation approaches

Literatures	Institution/Program	Drying evaluation approaches	Type*
TenWolde and Carll (1992)	USDA/ Forest Service	Net vapor diffusive flux [kg/m^2·s]	I
TenWolde et al. (1995)	USDA/ Forest Service	Moisture conditions (RH) inside cavity as well as condensation and mold growth observations	III
Salonvaara et al. (1998)	CMHC/ EDRA	Moisture contents vs. time	III
Hazleden and Morris (2001)	CMHC/ EDRA	Effective moisture permeance of the whole specimen	I
Kumaran et al. (2002) Beaulieu et al. (2002)	IRC/ MEWS	RHT(80) or RHT(95)	III
Lawton et al. (1999)	CMHC	Moisture content at relative locations	III
Ojanen et al. (2002)	VTT	Mass loss from specimen and its water source (drying efficiency)	I
van Straaten (2003)	Waterloo University/ BEGHUT	Moisture content variation along with time	III
Teasdale-St-Hilaire et al. (2004, 2005)	Concordia University/ Pre-CRD	Moisture content variation along with time at bottom plate and sheathing board	II

*I: Effective moisture (vapor) permeance coefficient; II: Evaporation rate at the bottom plate of stud cavity; III: moisture performance (e.g. moisture content or mold growth) at certain locations of the wall components.

Type II: Evaporation rate at bottom of stud cavity

Fazio (2004) proposed to use the moisture evaporation rate at the bottom plate of stud cavity $\dot{E}_v^B$ [kg/s] as an indicator to assess the building envelope capacity to evacuate moisture. The evaporation rate at the bottom plate of the cavity can be calculated by:

$$\dot{E}_v^B = M_E^B / 1000t \tag{2.24}$$

where M_E^B [g] is the amount of water evaporated from the bottom plate of the stud cavity; t [s] is the duration of test period; and the constant 1,000 converts the mass unit from

kilograms to grams. The cumulative evaporation of water during a day from the bottom plate of the stud cavity, $\overline{E}$ [g/day], is defined as:

$$\overline{E} = M_E^B / D \tag{2.25}$$

where D is the number of days during the test period. In an experiment (Teasdale-St-Hilaire et al. 2004), this approach was implemented to study the evaporation rate from a wetted insert at the bottom of the stud cavity when wall specimens were subjected to various exterior and interior conditions. The indicator, evaporation rate, was calculated from:

$$\dot{E}_v^B = (\Delta \mathrm{MC}/t) \cdot M_d \tag{2.26}$$

where ΔMC [%] is the moisture content variation in the inserted wood block which placed on the top of the bottom plate, and M_d [g] is the dry mass of the wood insert.

Type III: Moisture content variations in wall components

The variation rate of moisture contents at some specific locations (e.g. sheathing board) of the wall components is frequently used to evaluate the drying performance. Most of the time this variation rate was observed and explained in profile of MC with respect to t. Examples can be found in tests conducted by Lawton et al. (1999) and Teasdale-St-Hilaire et al. (2004). Occasionally such a rate was expressed in the form of the MC change during a certain period (days), for example by van Straaten (2003).

In many other cases, mold growth observation or mold related index is used to evaluate drying performance, e.g. Kumaran et al. (2002) and Beaulieu et al. (2002). These mold growth evaluation tests can be regarded as an indirect investigation of moisture content variation at particular locations of wall systems.

2.4.3. Baseline and boundary condition

Any comparative analysis of moisture performance of walls should have a uniform baseline and uniform boundary conditions for all objects to be compared. The baseline and boundary conditions in the majority of existing experiments were conducted under steady-state, which were realized by pre-conditioning and controlling HVAC (Heating, Ventilation & Air Conditioning) system. Pre-conditioning could produce equilibrium moisture content (EMC) for specimens and therefore result in uniform initial moisture state (Zarr et al. 1995).

The selection of a baseline depends upon which section of the process a test is aimed at. For example, if a test focuses on the whole process of moisture movement, including both wetting and drying processes, the baseline is the start point of the wetting process. The quantities of water insertion can be decided either from measurements or from estimation of moisture penetration. For example, Teasdale-St-Hilaire et al. (2004) determined the amount of water injection based on estimated rain penetration into stud cavity based on tests.

When a test concentrates only on the drying process, the baseline should be at the onset of the drying process and a uniform in-cavity moisture source is required. However, a few drying tests neglected the baseline. The magnitudes of moisture source in these tests are arbitrary and the quantities and locations of water insertion vary from one experiment to another (Fazio 2004). For example, Lawton et al. (1999) injected uniform amount of water into all test panels for comparative study; Hazleden and Morris (2001) wetted specimens by immersing the entire wood members into water before testing, while van

Straaten (2003) injected water to highly absorbent paper that was embedded at vulnerable positions of wall assembly. Without a common baseline quantitative comparisons are difficult to carry out. Up to this point, there has been little agreement on the methods for water insertion as well as on the quantities and locations of water insertion.

2.4.4. Evaluation of the role of wall components

There have been many publications that focused on the roles of wall components during the drying process. These researches covered many components of a wall system, such as vapor barrier (VB), vented/ventilated air gap behind cladding, weather resistance barrier, and so on. Table 2.6 lists ten wall configurations used in the experiments reviewed in the current research. Because the drying performance evaluation results often led to contradictory conclusions in previous studies, e.g. conflicting effects of vented/ventilated air gap on drying performance were reported, further investigation through either experiment or simulation work is still necessary.

Table 2.6. Summary of wall configurations in literature

Publication	Specimen configurations							
	Cladding	Vent	Air gap	WRB	Sheathing	Insulation	Vapor barrier	Dry wall
TenWolde and Carll (1992)	Painted Waferboard	Vented/ ventilated	None / 6mm (1/4″)	None	none	Glass fiber (R19)	Vinyl finish	Gypsum board
TenWolde et al. (1995)	Waferboard / steel	Vented/ ventilated	None when none of sheathing/ 6mm(1/4″)	None	None/ foamcore/ fiberboard	Glass fiber (R19)	Vinyl finish	Gypsum board
Salonvaara et al. (1998)	Wood siding/ Steel plate	Vented/ ventilated	22mm for wood siding/ none for steel plate	None	Porous wood fiberboard/ spun-bonded polyolefin	Mineral wool/ loose-fill cellulose fiber	Polyethylene / Building paper	Gypsum board

Hazleden and Morris (2001)	Stucco/ wood siding	Vented/ ventilated	0mm(0″), 10mm(3/8″), 19mm(3/4″)	2 layers 30 minute HAL Building paper / 1 layer Tyvek Homewrap (SBPO)	OSB/ plywood	Glass fiber (R14)	6 mil polyethylene	Plywood
Kumaran et al. (2002)	3 types of Stucco	Vented/ ventilated	0mm(0″), 2mm(1/16″), 10mm(3/8″)	Three types in terms of vapor transport property	OSB/ plywood/ fiber board	Applied	3 types of vapor barrier	Gypsum board
Lawton et al. (1999)	Stucco	Vented/ ventilated	0mm(0″), 10mm(3/8″), 19mm(3/4″)	60 minute building paper	plywood	Glass fiber (R12)	10 mil polyethylene	Gypsum board
Ojanen et al. (2002)	Typical wind barrier materials, including Four types of Plywood/ Five types of OSB					Glass wool	Not clear	
Hansen et al. (2002)	Wood siding /Stucco	Vented/ ventilated	0mm(0″), 25mm(1″)	None/ four types of wind barrier	Gypsum board	Stone wool	Polyethylene	Gypsum board
van Straaten (2003)	Vinyl siding/ Brick veneer	Vented/ ventilated	0mm, 20mm, 50mm	#15 asphalt impregnated felt (AIF)/ spun bonded polyolefin (SBPO)	Homasote sheathing	Glass fiber (R20)	medium density particle board coated with a vapor barrier plastic coating on both sides (Melamine)	
Teasdale-St-Hilaire et al. (2004, 2005)	none	Vented/ ventilated	none	Spun-bonded polyolefin membrane	OSB/ plywood/ fiber board	Glass fiber	6 mil polyethylene	Gypsum board

2.5. Summary

From the literature review, the lessons learnt and possible advancements are summarized below:

In terms of design approach

- Load and capacity are two parameters that have to be quantified when applying limit state design in structural engineering. Applying the analogy to moisture analysis of an exterior wall system, moisture load has to be controlled within the drying capacity of a wall in order to prevent damage introduced by moisture intrusion;
- There have been abundant methods for the quantification of moisture load in previous studies but method for quantification of drying capacity is still absent. The absence of drying capacity leads to the absence of a practical design method. Therefore, a reasonable criterion to determine the drying capacity for design purpose is essential;
- The wood construction community has reached a consensus on the failure criterion for wood products against microbiological degradation. FSP (28% MC) is regarded as ultimate limit of moisture content to prevent the formation of decay and fungi. 20% MC is regarded as the allowable limit recommended by several institutes in the wood industry. The gap between fiber saturation and 20% line is considered a safety margin.

With respect to the moisture loading

- There has been a series of methods to quantify moisture loading. These methods covered such issues as parametric study, climatic classification, and selection of reference year;
- In some recent studies, the in-cavity loading has been isolated from the indoor and outdoor loadings; the relationship between in-cavity loading and moisture

responses was examined to evaluate the drying performance of wall system in the MEWS project;

- In some recent researches, various methods for applying in-cavity loading have been developed, though the uniformity of wetting conditions was not assured by most of them.

With respect to the drying capacity evaluation

- At least three types of parameters have been used as indicators for the evaluation of the drying performance of wall systems, including total moisture evacuation, evaporation at the bottom plate, and moisture performance at specific locations of the wall assembly. The current study proposes a comprehensive indicator that can take all these three aspects into consideration;
- To simulate penetrated rainwater, a water source was inserted directly into the stud cavity in several previous experiments. However, there has been no consensus on the amount of water or the location of insertion. Uniform moisture loading cannot be guaranteed for different panels tested by these existing methods. To compare the drying capacities of different panels, a new loading protocol is required to provide uniform in-cavity moisture loads.

Chapter 3

Preliminary Test — Development of a In-Cavity Moisture Source

The main objective of this research is to study the relative drying capacity for different wood-frame wall systems subjected to in-cavity moisture loads. Drying of an exterior wall involves complex processes and some of the involved mechanisms are still not fully understood. Experimental investigations still serve as a critical mean to understand the mechanisms, to evaluate alternative envelope systems, and to provide data to develop and validate numerical simulation tools. To overcome the limitations in existing experimental programs surveyed in Chapter 2, especially the lack of a uniform moisture loading method, a new testing approach was proposed that utilizes an innovative in-cavity moisture load (Fazio 2004). A preliminary test was been carried out to fully develop the new loading method and to finalize the test setup and procedure.

3.1. Purpose of preliminary test

The drying process is driven by different mechanisms, such as drainage, capillary action in redistributing the moisture within materials, evaporation and diffusion through materials, and transport through air leakage. Drainage within the stud cavity is not common in practice even though it may occur sometimes; therefore, it was excluded from

the current study. Capillary action redistributes water from a concentrated source (e.g. a wetted bottom plate) to the surrounding regions or components of the envelope system. It can thus increase the chances of moisture evaporation within the stud cavity or even moisture transportation to outside the stud cavity. The major mechanism of moisture evacuation examined in this research is the evaporation in conjunction with vapor diffusion.

Rainwater can penetrate into the stud cavities of envelopes. When climatic loading conditions, deflection and drainage characteristics of building envelope systems remain equal, the envelope system with a greater capacity to remove the intruding water from the stud cavity through evaporation and diffusion would be less susceptible to moisture damage. This drying capacity is referred to in this thesis research as the Drying by Evaporation Index (DEI) of the envelope system. DEI belongs to the Type II drying indicator discussed in Section 2.5.2.

For a comparative study, it is essential to create a uniform baseline of identical boundary conditions and a uniform loading intensity for all the specimens tested. Therefore, it is necessary to keep a uniform evaporation exposure area in the stud cavities of tested specimens. An innovative loading method was proposed (Fazio 2004) to provide the required uniformity of in-cavity moisture loading.

This loading method employs a water tray on the bottom plate of the stud cavity. The advantages of this method include:

i) The equal water evaporation areas provided by the water trays ensure the uniformity of in-cavity moisture loading for all tested specimens;

ii) The large free water exposure provides an efficient in-cavity loading; and

iii) An electronic weight sensor, load cell, can be placed under the tray system to monitor the water evacuation rate during testing.

As a new method, the mechanism and the feasibility need to be explored. Accordingly, a preliminary test was carried out for this purpose. This preliminary test was also expected to provide some critical information and lessons for the main test, such as the specimen configurations, sensor positions and installation, and relationship between moisture loading and moisture response.

In the test setup of this preliminary test, the wall specimens were equipped with thermocouples, humidity meters, electronic moisture content probes, and gravimetric samples. Extensive data were collected from these sensors over 186 days. The data and analysis would help:

i) To better understand the mechanisms of moisture dissipation from the stud cavity;

ii) To observe the moisture accumulation and its subsequent responses and damage;

iii) To establish the relationship between moisture dissipation rate and moisture accumulation at any location of the wall assembly; and

iv) To develop a new loading method.

3.2. Drying by Evaporation Index (DEI) and related factors

The proposed concept DEI — drying by evaporation index — in effect is a measure of the rate of the moisture transported out from the stud cavity. It is envelope specific; DEI depends on the configuration of the wall and the materials used in the wall. It also varies with the climatic load applied; DEI is a complex function of the indoor and outdoor temperature (T_{in}, T_{out}), indoor and outdoor relative humidity (RH_{in}, RH_{out}), pressure difference across the envelope (ΔPw), initial moisture content (IMC) distribution within the components of wall specimens, and the potential of the in-cavity moisture load from the water tray. In addition, a few other factors may also affect the DEI, including air leakage characteristics of the wall assembly.

In designing the experiment to evaluate the relative impacts of envelope configurations, some of these factors and parameters were held constant while others were changed. When the uniform baseline was achieved and test conditions were maintained the same for all tested wall specimens, the DEI values can be estimated and be compared to indicate the relative performance. This relative ranking can help develop an engineering approach aiding the future design of building envelope systems whereby the performance of a given envelope system can be predicted at the design stage.

Since identical climatic load was applied to all of the specimens, a relative ranking can be established between the wall configuration and its drying capacity, which is independent of the wetting method but influenced by the Initial Moisture Content (IMC). For example, from Fig. 2.13 of the test with inserting wet wood (Teasdale-St-Hilaire et al. 2004), DEIs could be characterized by the decreasing slopes of the curves and would be equivalent to

the average daily evaporation rate of the water contained in the wood insert. A similar analysis using the rate of moisture loss under specific climatic loads was carried out by Ojanen (1998). In that case, DEI could also be considered as the tolerance level of a given envelope configuration. The DEI at the onset of condensation on the sheathing could be increased if necessary by revising the configuration. For example, the integration of smart vapor barriers, the permeance of which increases significantly at high RH levels (Kuenzel 1998), would increase the capacity of the wall to evacuate moisture from the stud cavity to the indoor.

3.3. Test setup

Half-height wall specimens were used in a previous experimental project to investigate the hygrothermal behavior of different wall designs and with rain penetration under the window sills (Teasdale-St-Hilaire et al. 2004). Six of the wall specimens were modified and were implemented with the new water tray testing method. The main objective was to verify and improve the proposed water tray loading techniques and to develop the test setup and procedure that employs the new loading method. The overall approach was to subject wall specimens to typical indoor conditions and typical outdoor climatic loads derived from 30-year local weather data and to implement the constant moisture source inside the stud cavity. Both the evaporation from the in-cavity moisture source (loading) and the moisture contents at specific locations on sheathing and studs (hygrothermal response) are monitored.

3.3.1. Considerations and implementation approach

To obtain the DEI, the preliminary test should be designed with the following

considerations:

- The moisture source should be uniform for all the specimens;
- The moisture source should be refillable so as to provide enough moisture to establish moisture equilibrium in the components of the specimen, and to feed the drying mechanisms through diffusion and air leakage, if any;
- The testing should be continuous;
- The drying rate or evaporation rate should be monitored continually along with all the other parameters (T_{in}, T_{out}, RH_{in}, RH_{out}, ΔPw) associated with climatic loading and hygrothermal response;
- Other specimen characteristics such as air leakage should be monitored or minimized.

In response to the above requirements, the experimental design had the following characteristics:

- A moisture source in a container was placed at the bottom plate of the specimen between the two studs;
- The water source could be replenished;
- The evaporation rate could be weighed on a continuous basis by sitting the moisture source on a load cell and connecting the load cell to the data acquisition system without having to open the stud cavity.
- Because of the difficulty in monitoring air leakage the effect of air leakage was minimized by caulking all the gaps at the joints of the drywall and sheathing to the frame of the specimen.

During the tests described above, the specimens were subjected to various loading

conditions including:

- Indoor and outdoor conditions were applied. The selection was based on weather data and state-of-the-art approach to select representative weather year and seasonally adjusted indoor temperature and relative humidity; and
- Pressure differentials across the specimens due to stack effect.

Strategic sampling points monitored for responses were laid out. Gravimetric samples on sheathing and studs provided the main response but other sensors were used to map out moisture and thermal conditions in the specimen.

3.3.2. Test facility — the environmental chamber

The environmental chamber at Concordia University is a unique facility for studying heat and moisture transfers (including air infiltration, rain penetration, and condensation) in building envelope systems. The chamber consists of two parts named cold box and hot box according to the controllable temperature ranges. Both cold and hot box are 7.5m in height and 4.4m in width, while cold box is 3.6m in depth and the hot box is 6.1m in depth (Fazio et al. 1997). The cold box is fixed on the floor and the hot box can be moved closer to and away from the cold box by using a set of four air pads.

There are two major modes of operation of the chamber. In the guarded hot-box mode, the large wall specimen, up to 7.2 m high by 4.1 m wide, can be installed in a specimen frame between the hot box and the cold box (Fig. 3.1). The temperature and relative humidity inside these two boxes can be controlled to recreate indoor and outdoor conditions. The cold box is equipped with a 5 ton cooling unit with a screw compressor, a 12,000 ft^3/min (CFM) recirculation fan, and a 25 kW re-heating unit for subtle

environment adjustment. The hot box is equipped with a 600 CFM air recirculation system, a fresh air supply/return damper, and a humidifier. The design temperatures of the cold box and the hot box range from -40°C to 50°C and from 4°C to 60°C, respectively; the design relative humidity for both boxes ranges from 10 to 90%. More information about this facility can be found in Fazio et al. (1997).

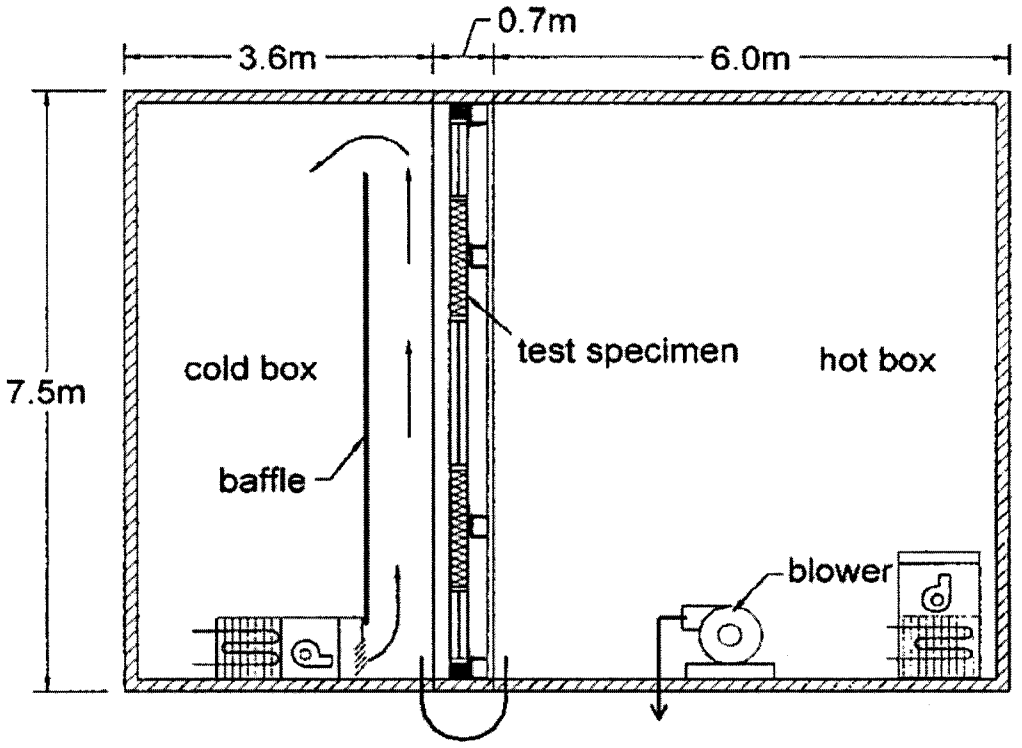

Figure 3.1. Guard mode of the environmental chamber
(Adopted from Ge and Fazio 2004)

The other mode of operation of the facility is the climatic chamber mode, as shown in Fig. 3.2. The hot and cold boxes are joined together and form a 7.5 m high by 4.4 m wide by 9.3 m long climatic chamber. Such a large space can host inside a two-story test hut. This is also the operation mode in which this preliminary test was carried out, albeit with a one-story test hut.

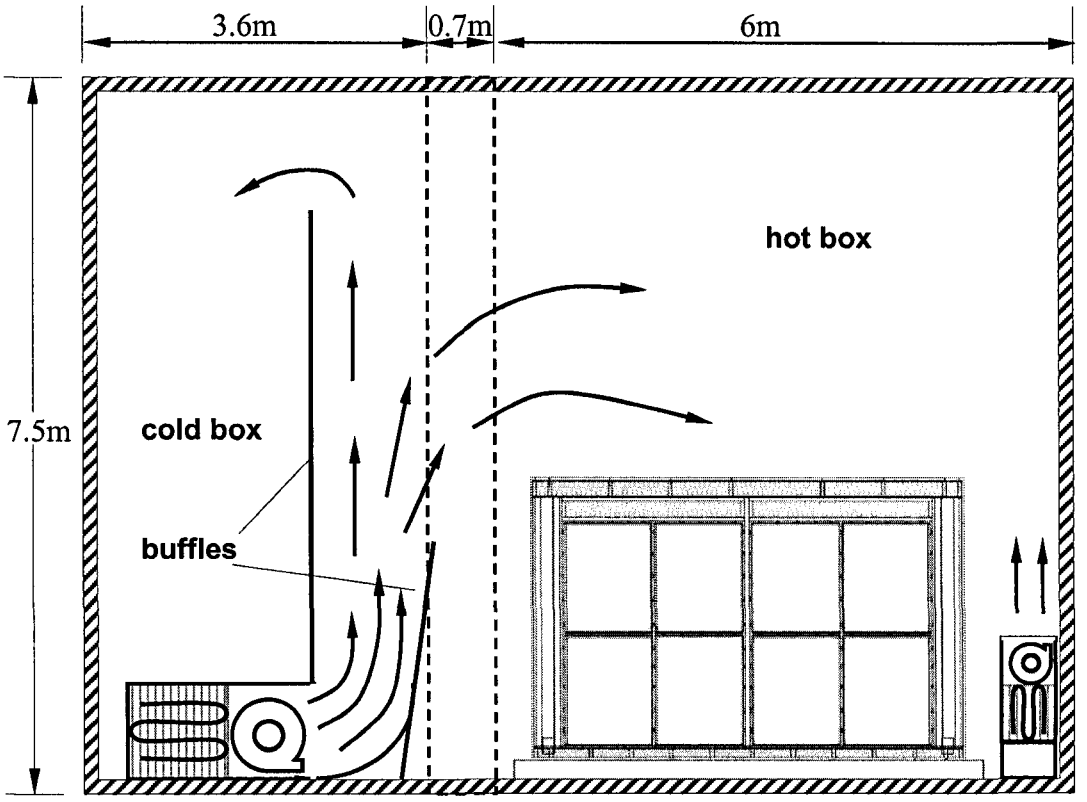

Figure 3.2. Climatic chamber mode of the environmental chamber

3.3.3. Test hut and wall specimens

Fig. 3.2 shows the overall setup with the test hut inside the climatic chamber. Six wall specimens located on one sidewall of the hut. The test hut and the original wall specimens were built for a previous testing program (Teasdale-St-Hilaire et al. 2004). Fig. 3.3 shows the layout of the hut and Fig. 3.4 shows the cross-section elevation of all the wall specimens from the exterior view.

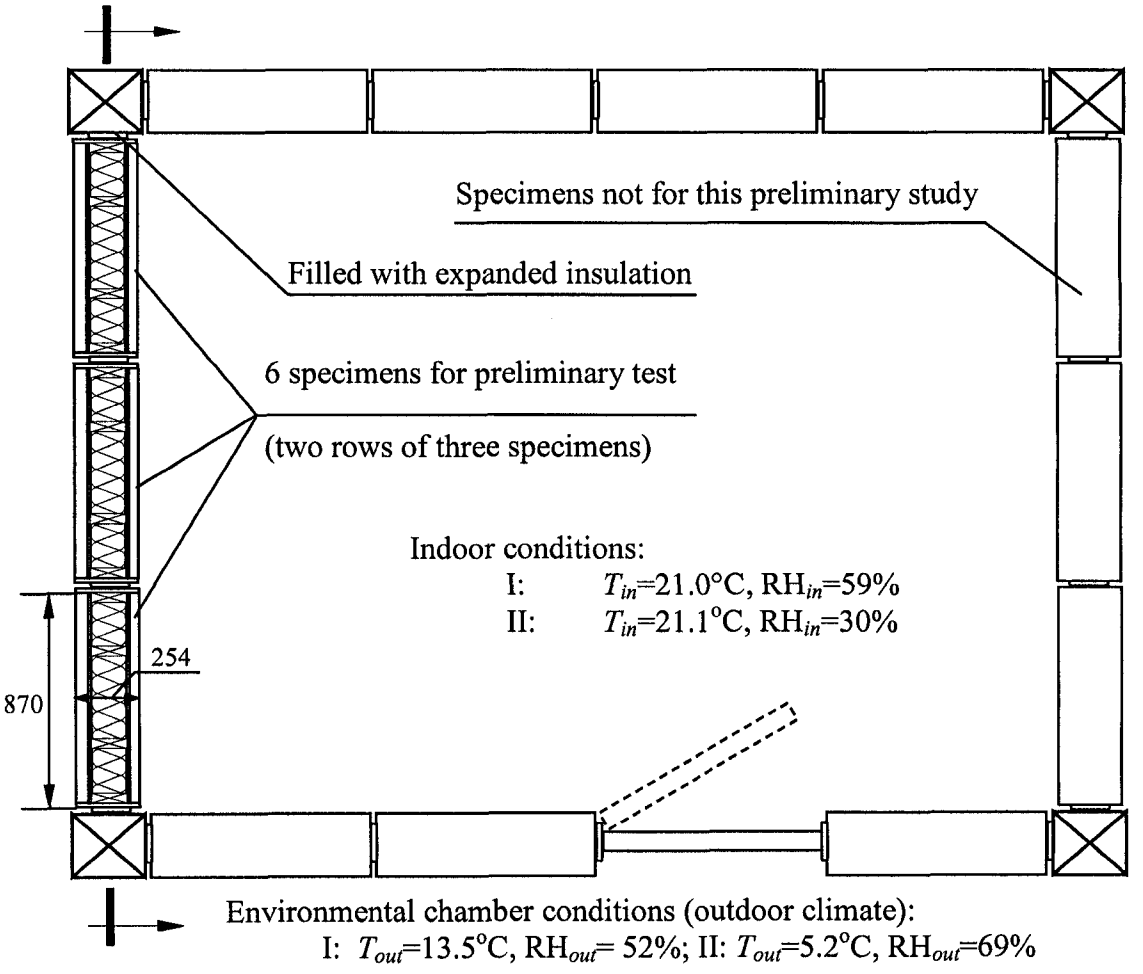

Figure 3.3. Layout of the hut for preliminary test

The composition of the 6 wall specimens is listed in Table 3.1 and material properties of all the components of the specimens are shown in Table 3.2. Fig. 3.5 presents a photo of the specimens installed wall in the test hut from the room interior. It should be noted that the cladding was excluded from the wall configuration parameters, since the main purpose of this preliminary study was to validate the test method.

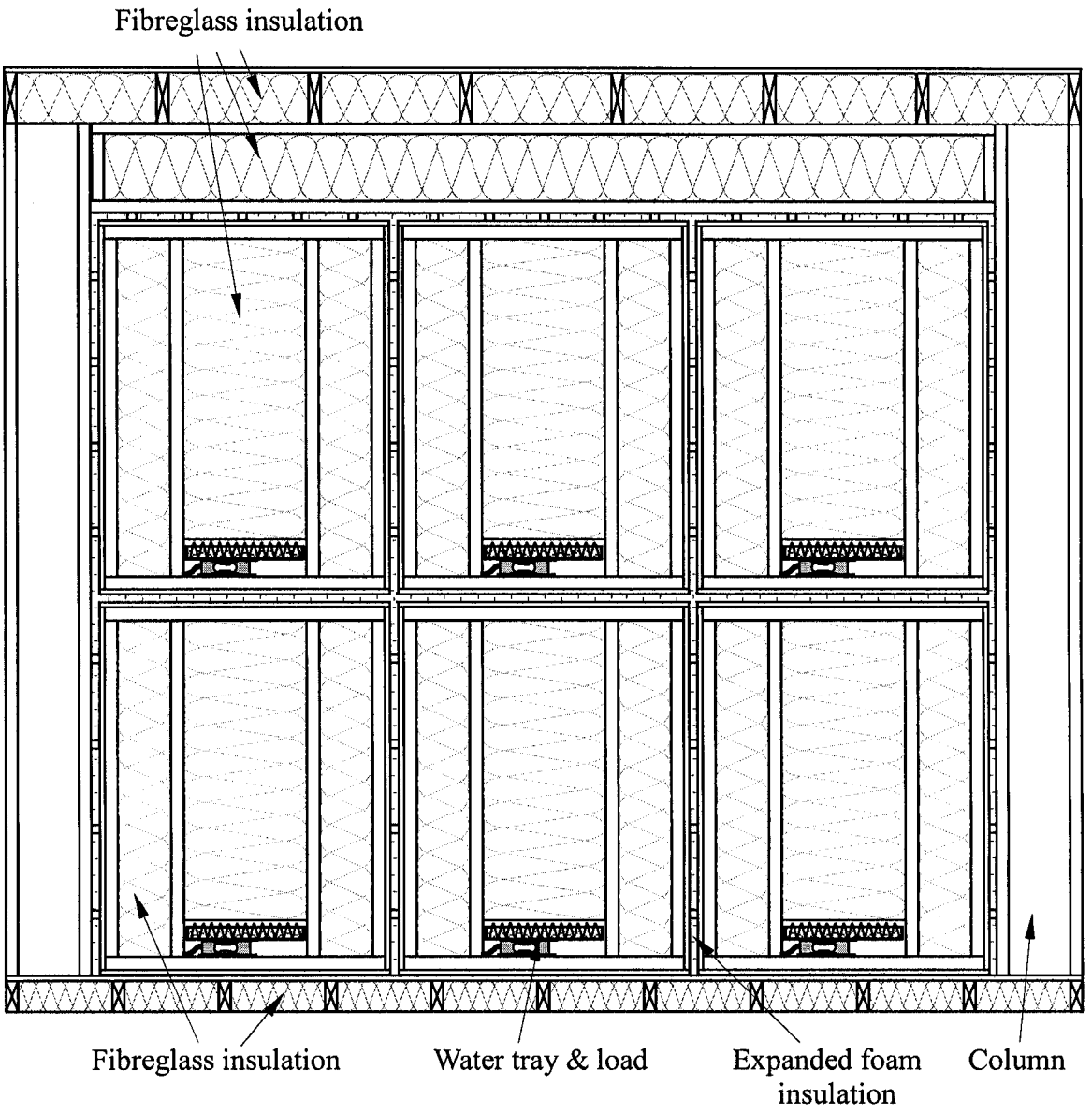

Figure 3.4. Cross-section elevation of the test wall (from exterior side view)

Table 3.1. Composition of specimens

No.	Weather resistant barrier	Sheathing board	Insulation	Vapor barrier	Drywall
1	Spun-bonded polyolefin membrane (@Tyvek), stapled	OSB	Fiberglass batt	Polyethylene	Unpainted gypsum board
2		Plywood		Polyethylene	
3		Wood Fiberboard		Polyethylene	
4		OSB		None	
5		Plywood		None	
6		Wood fiberboard		None	

Table 3.2. Properties of wall assembly components members*

Property	Material	Nominal thickness [mm]	Typical density [kg/m^3]	Typical vapor permeability [kg/s·m·Pa]
Weather resistant barrier	Spun-bonded polyolefin membrane (@Tyvek), stapled	0.15		6.56E-13
Sheathing	OSB	13	664	2.78E-12
	Plywood		456	6.18E-12
	Fiberboard		279	1.89E-11
Insulation	Fiberglass batt	140		
Vapor barrier	Polyethylene	0.15		4.84E-15
Drywall	Unpainted gypsum board	13		

Notes: Data for typical density and vapor permeability are adapted from Wu et al. (2008).
The permeability value of Tyvek is taken from ASHRAE 1018-RP (Kumaran et al. 2002).
The permeability values are based on 80% relative humidity.

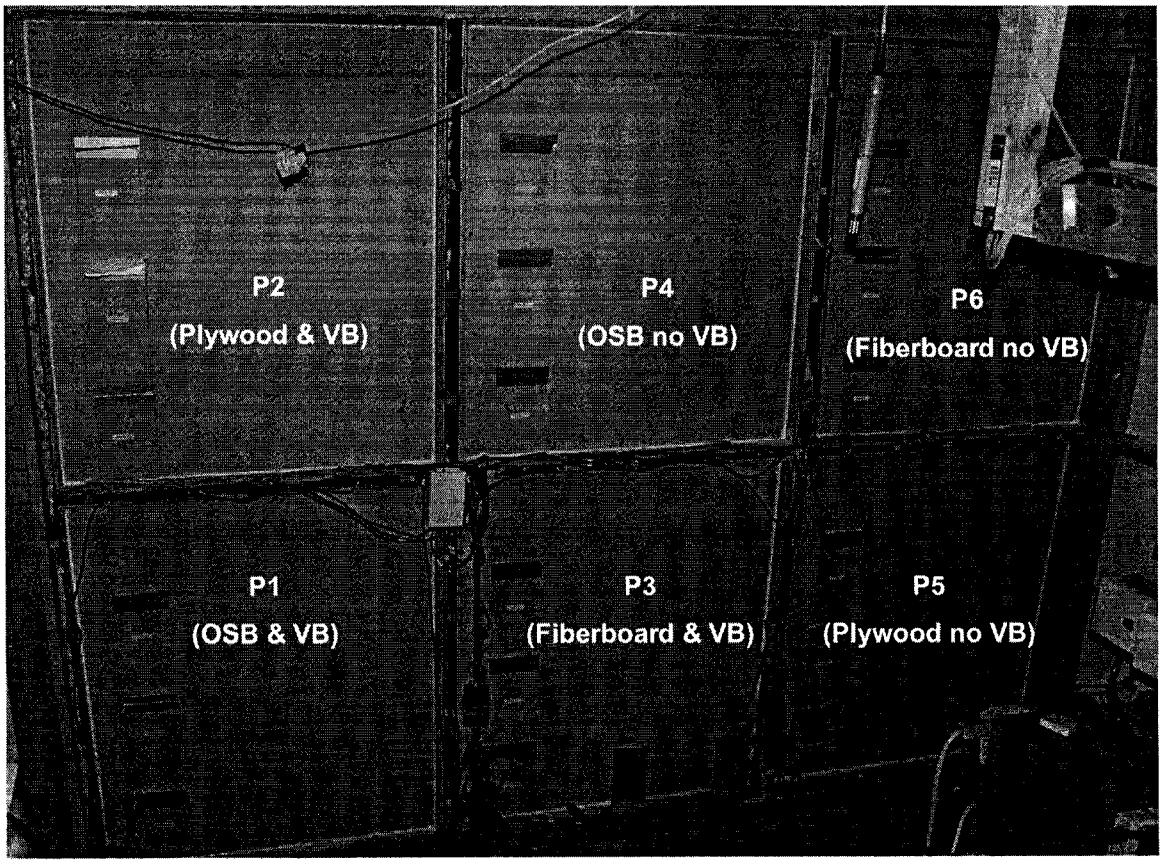

Figure 3.5. Photo of six specimens installed in test hut, taken from drywall side

3.3.4. Water tray and load cell system

For providing the in-cavity moisture loading, a tray containing water was placed at the bottom of each stud cavity where penetrating rain would typically be trapped to serve as the moisture source. A precision load cell was placed under the water tray to measure the total mass of the tray and water inside.

The tray was made of 3 mm (1/8") thick acrylic sheets that were bonded and sealed by silicon caulking compounds. The outside dimension of the tray was 356 mm in length, 127 mm in width, and 38mm in height (14" × 5" × 1½"). The water (from bottled spring water bottles) was injected periodically into the tray through a thin (1/8" in diameter)

plastic tube; a hole for housing a gravimetric sample on the sheathing board was used to pass the plastic tube through the sheathing, as shown in Fig. 3.6).

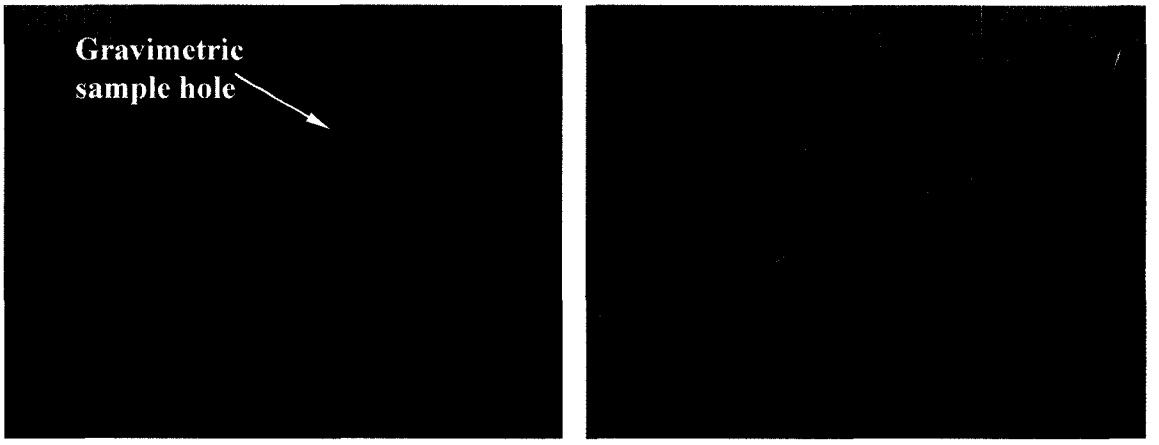

(a) (b)

Figure 3.6. Plastic hose for replenishing of water tray

Wick cloths were hung into the water in a zigzag pattern to promote the evaporation of water as shown in Fig. 3.8. Wick cloths were made of fast-absorbing wiper (by Kimberly-Clark) and were hung from equally spaced cross pins that rested on the top of the water tray walls.

The weight of the tray was monitored continually by a load cell (Fig. 3.7 and Fig. 3.8). The evaporation rate from the water tray depended on the conditions over the water surface, which during the test was influenced by the material properties surrounding the stud cavity as well as the indoor/outdoor conditions. By monitoring the evaporation rate, the drying capacity of each wall assembly could be acquired.

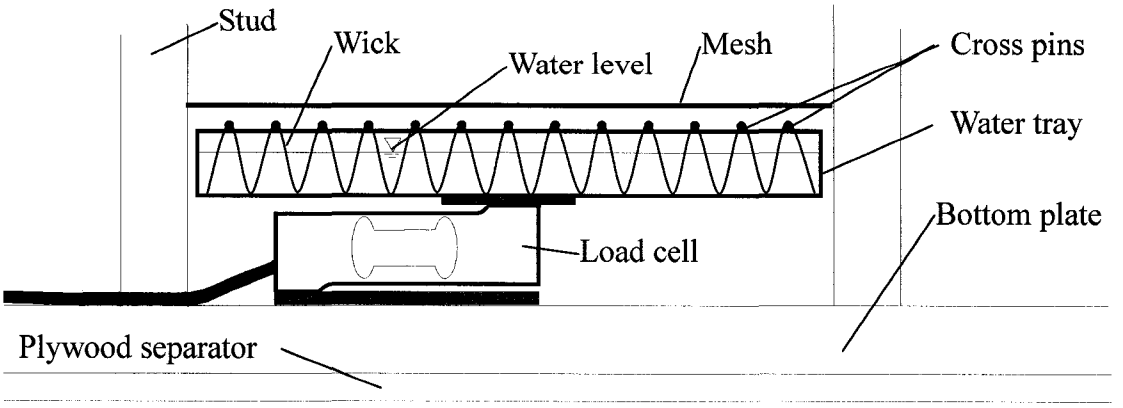

Figure 3.7. Setup of water tray and load cell inside a stud cavity

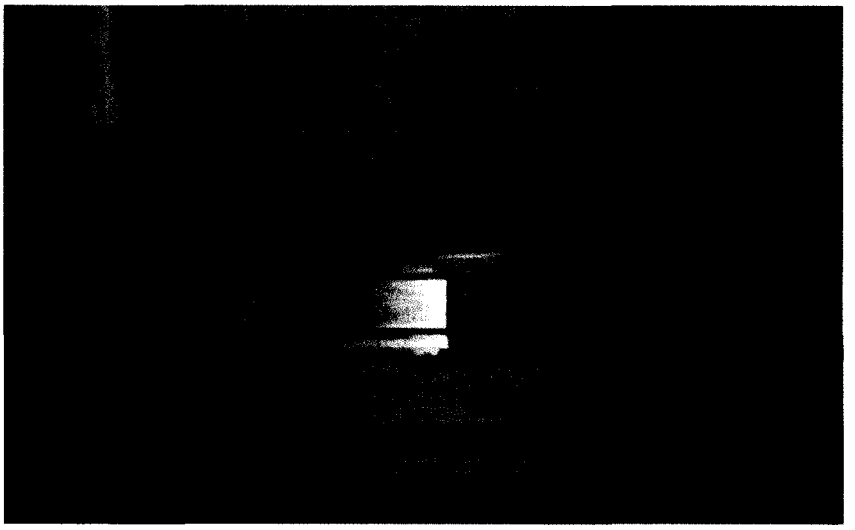

Figure 3.8. Photo of load cell and water tray system

The load cells were the single-point mounting, model AG by SCAIME (Fig. 3.9), with a nominal rated capacity of 1 kg and accuracy of ±0.25 g. Each load cell was calibrated at the factory. Only negligible differences were observed between the measured sensitivity values (by calibration with precision weight standards) and those provided by the manufacturer, therefore the sensitivity values by the manufacturer were used.

The output of the load cell was a voltage in mini-volt range. Eq. 3.1 was used to convert the measured voltage into the actual weight.

$$W = \frac{\left(U_{mea} - 0.001 \cdot Z \cdot U_{ref}\right) \cdot Fs}{S \cdot U_{ref}} \tag{3.1}$$

where W [g] is the weight supported by the load cell; U_{mea} [mV] is the measured output voltage; U_{ref} [V] is the reference voltage that is actually applied at the terminals on the load cell; Z [μV/V] is the zero balance of the load cell; S [mV/V] is the sensitivity of the load cell; and Fs is the full scale capacity of the load cell (1,000 g). For each load cell, both the output voltage and the reference voltage were monitored by the data acquisition system.

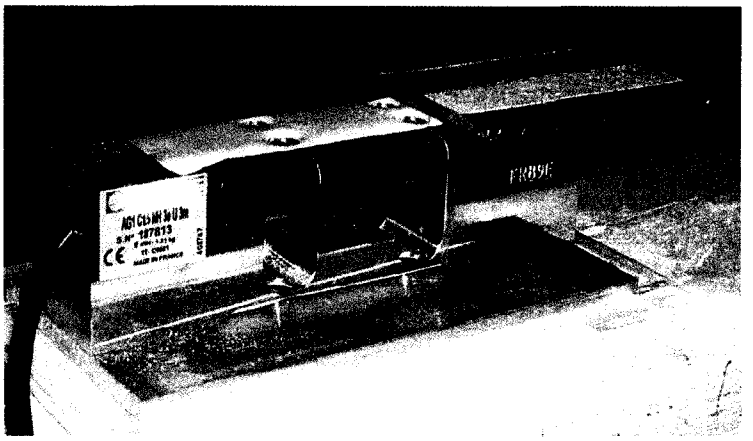

Figure 3.9. Load cell with single-point mounting under water tray

3.3.5. Electronic sensors and gravimetric samples

Temperature, relative humidity, and moisture content across the wall assemblies were monitored as well during the preliminary test. Both electronic moisture probes and gravimetric samples were used to monitor the moisture content in the sheathing panel and in the wood studs (Fig. 3.10). The relative humidity in the stud cavity was measured at three elevations: low (102 mm), middle (476 mm) and high (843 mm) from the top surface of the bottom plate. Each RH sensor was fixed at the center between the two studs by a tout nylon string. A thermocouple was installed with each RH sensor to

measure the temperature at the same spot.

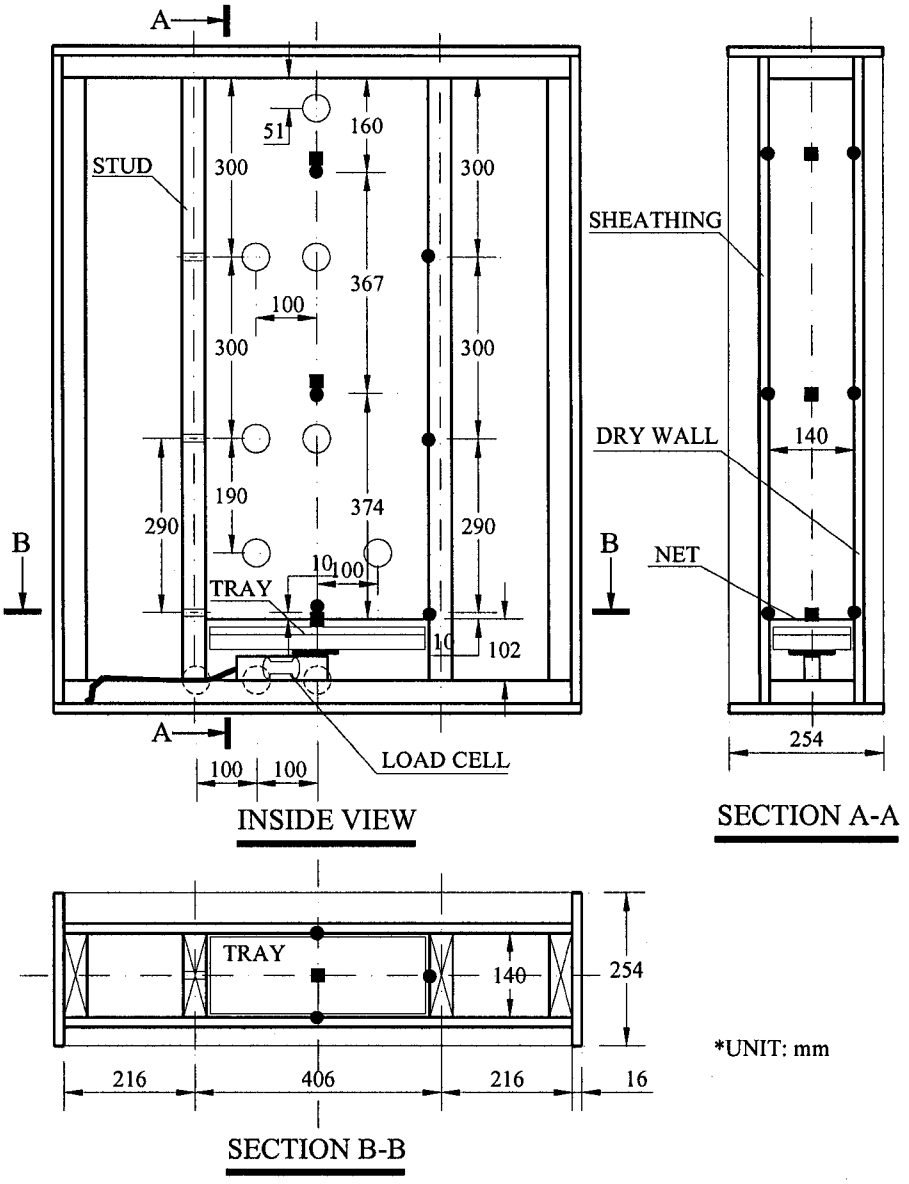

○ : Gravimetric samples in sheathing panel;

▭ : Gravimetric samples in stud;

● : Thermocouples on drywall and sheathing;

■ : Relative humidity sensor.

Figure 3.10. Sensor locations

3.4. Results of preliminary test

The test was carried out under two sets of steady-state conditions:

I. T_{in}=21.0°C, RH_{in}=59%, and T_{out}=13.5°C, RH_{out}= 52%;

II. T_{in}=21.1°C, RH_{in}=30%, and T_{out}=5.2°C, RH_{out}= 69%.

The total test duration was 148 days. The test with the first set conditions lasted 83 days. The test conditions were then switched to the second set and the test lasted for another 65 days.

Fig. 3.11 shows the cumulative evaporation from the water trays inside the 6 wall assemblies. The time axis starts from day 35 when assemblies had reached equilibrium indicated by the moisture content of gravimetric samples. The curves divide the six walls into two groups; the first group has higher average daily evaporation rate of about 12.5 g/day, and the second group in the range of 6.7-8.2 g/day. Since the areas of the water surfaces in the 6 trays were the same and the boundary conditions were identical, the differences between the water evaporation rates were governed by the characteristics of the specimens. These characteristics include the material properties of the specimens around the stud cavity and the air leakage that may be introduced in the construction.

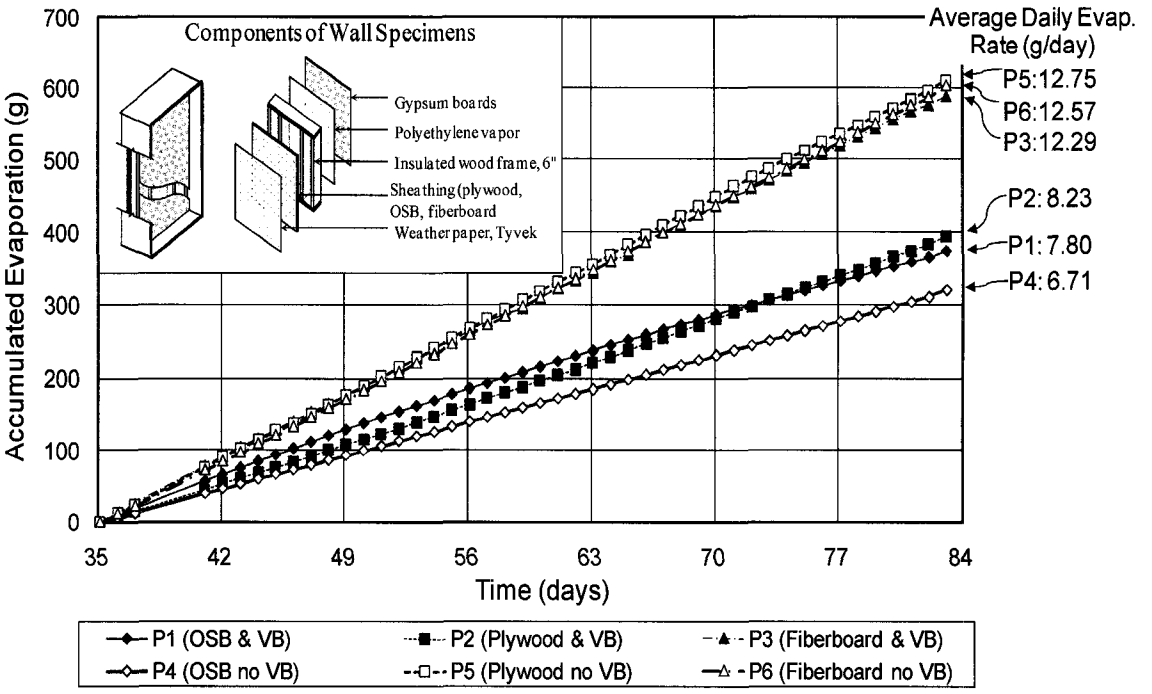

* The plots represent data collected between day 35, when all samples had reached equilibrium moisture content, and day 82, when test conditions were changed to condition II.

Figure 3.11. Evaporation profiles of different wall assemblies under test conditions I: (T_{in}=21.0°C, RH_{in}=59%, and T_{out}=13.5°C, RH_{out}= 52%)

The total amount of water evaporated from the tray included i) the moisture added to the stud cavity, ii) the moisture absorbed and retained by the materials surrounding the stud cavity during the diffusion process, iii) the water vapor transferred either to the indoor or to the outdoor environment, and, in some cases, iv) the water vapor that condensed on the interior surface of the sheathing board within the stud cavity. At the beginning of the evaporation test, the surrounding materials were relatively dry, their absorption rate was high, and there were rapid increases in the moisture contents in the sheathing and studs. This transient process was indicated by the change of moisture content in the gravimetric samples on the sheathing panels during the first 28 days as indicated in Fig. 3.12. The moisture contents in the gravimetric samples increased during the first three weeks, remained relatively unchanged after day 35, and thus reached their equilibrium. Therefore,

the evaporation rates recorded by the load cell after day 35 can be considered as the rates of moisture transported to the outside of the stud cavity. These exiting moistures can be employed as an indicator of the drying rate of the stud cavity and is a function of the wall system characteristics. Since the drying in this experiment started with evaporation of water in the water trays, this drying capacity is termed as Drying by Evaporation Index or DEI.

The major differences in the configurations of the six tested wall panels can be found in the types of sheathing boards and the presence of vapor barrier. When a vapor barrier, polyethylene sheet, was installed on the indoor side of the stud cavity, the vapor resistance to the indoors was much greater than that toward the outdoors. Hence, it may be expected that, in the cases of negligible or low leakage rates, the majority of vapor was transported to outdoors through the sheathing board and was thus influenced by the vapor permeability of the board. As shown in Fig. 3.12 and Table 3.3, wall panels sheathed with fiberboard had a higher evaporation rate, which is followed by plywood and OSB (Oriented Strand Board). It is worth noting that although fiberboard is about 5 to 10 times and plywood about 2.5 times more permeable than OSB (when RH was in the range of 60-90%) (Kumaran et al. 2002), the differences between the drying rates of the wall specimens with such sheathing materials, as shown in Table 3.3, were much less pronounced. This phenomenon can be attributed to other characteristics of the wall specimens. It also indicates that the drying performance of sheathing is not linear or solely related to the water vapor permeability of sheathing, but it should be assessed in the context of the wall configuration and design.

Table 3.3. Daily average evaporation rates [g/day] of wall panels under condition I:

(T_{in}=21.0°C, RH_{in}=59%, and T_{out}=13.5°C, RH_{out}=52%)

	OSB	Plywood	Fiberboard
Vapor barrier present	7.80 (Panel 1)	8.23 (Panel 2)	12.29 (Panel 3)
Vapor barrier absent	6.71 (Panel 4)	12.75* (Panel 5)	12.57 (Panel 6)

*The result for panel 5 is not consistent with others. Further analysis is required to make viable explanation.

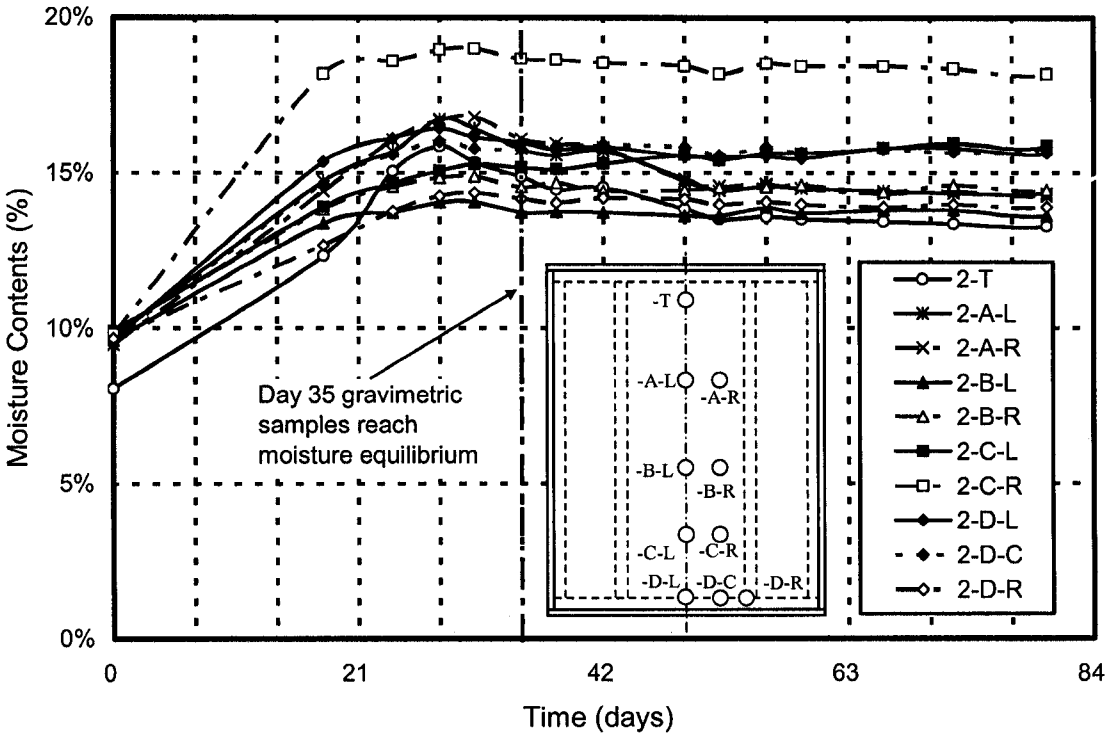

Figure 3.12. Moisture content of gravimetric samples on plywood sheathing of panel 2

The evaporation rate was also influenced by the vapor pressure gradients along the height of the stud cavity, and different vapor pressures occurred in indoor and outdoor. The values of measured partial vapor pressure, relative humidity (RH) and moisture flow across all the 6 wall assemblies at three heights, at which RH probes were located in the stud cavities, are graphically displayed in Fig. 3.13. Some patterns can be observed from these diagrams between the moisture content or vapor pressure and the permeability of the sheathing. In case of plywood and OSB sheathed walls, the RH varied from 90 to

100% at the bottom of the cavity (just above the water tray), to 61% (in the case of OSB) and 72% (in the case of plywood) at the top of the cavity. In case of the fiberboard sheathed wall with a vapor barrier, the RH varied from 100% at the bottom to 41% at mid-height and to 46% at the top of the cavity; whereas in case of the fiberboard wall without the vapor barrier, the RH varied from 100% at the bottom to 55% at mid-height and to 65% at the top of the cavity.

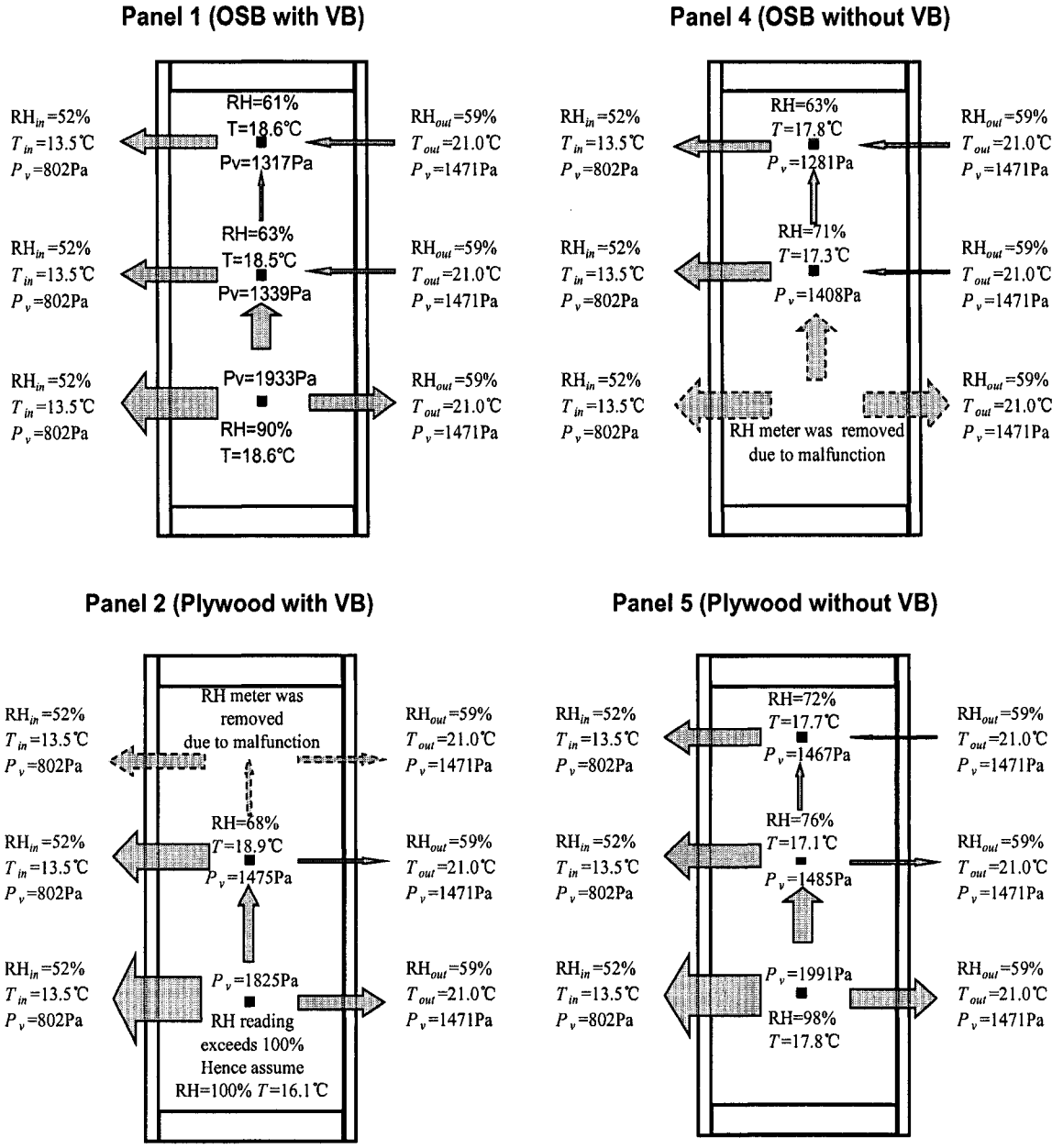

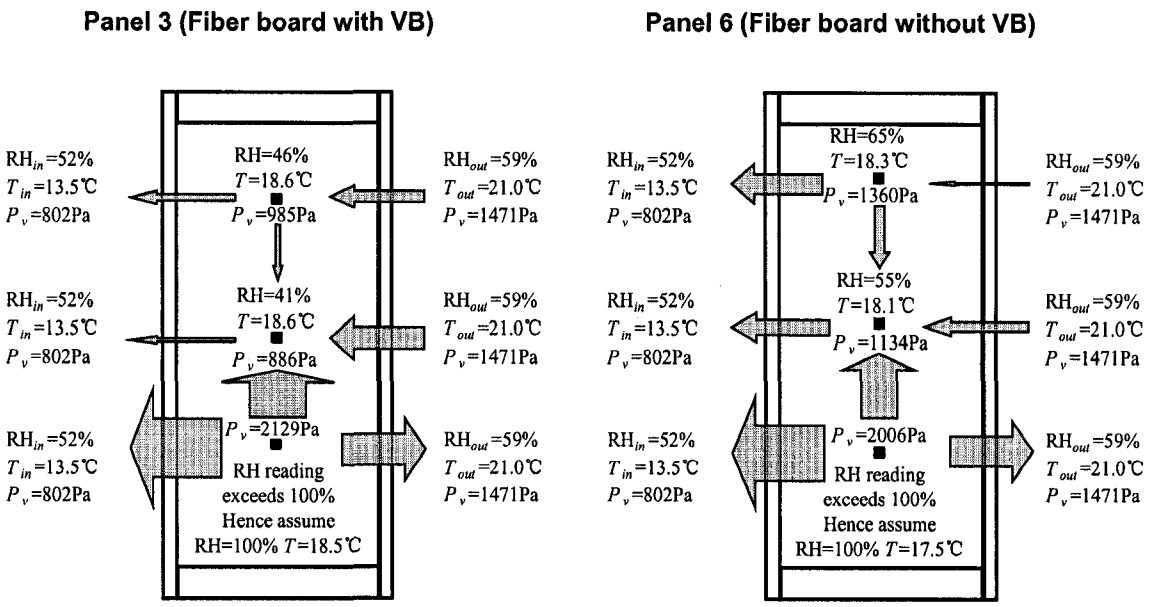

Figure 3.13. Partial vapor pressure, relative humidity, and moisture flow across the wall assemblies

Note: The partial vapor pressure is calculated using temperature and relative humidity recorded during test I

Presence and absence of vapor barriers affected the direction of vapor diffusion in the tested scenarios. The absence of vapor barrier increased the vapor diffusion from the stud cavity to the indoor at the lower part. For the middle and upper part of the cavity, the absence of the vapor barrier increased the vapor diffusion from the indoor to the cavity, which in turn inhibited the evaporation from the water tray to the cavity. The relative humidity values at the upper part of stud cavities with vapor barriers were also generally higher than those without vapor barriers, as observed in Fig. 3.13. For example, the relative humidity at the top level in panel 6 (without VB) was 65% compared to 46% at the top level in panel 3 (with VB). The absence of a vapor barrier was found to have minor impact on the drying rate under the tested condition I, except for panel 5 (plywood

without VB). The recorded evaporation rate for panel 5 was inconsistent with other panels, which may be due to some other unknown factors.

3.5. Variation of daily evaporation rate

Fig. 3.14 shows the daily evaporation rate of the 6 wall specimens under test condition I. All curves follow similar patterns. Those fluctuations of the daily evaporation rates indicate the high sensitivity and responsiveness of the tray system to those inevitable small variations in the loading conditions. The outdoor temperatures were maintained within a standard deviation of 0.3°C. The outdoor and indoor relative humidity was maintained within a standard deviation of 0.9% and 1.4%, respectively.

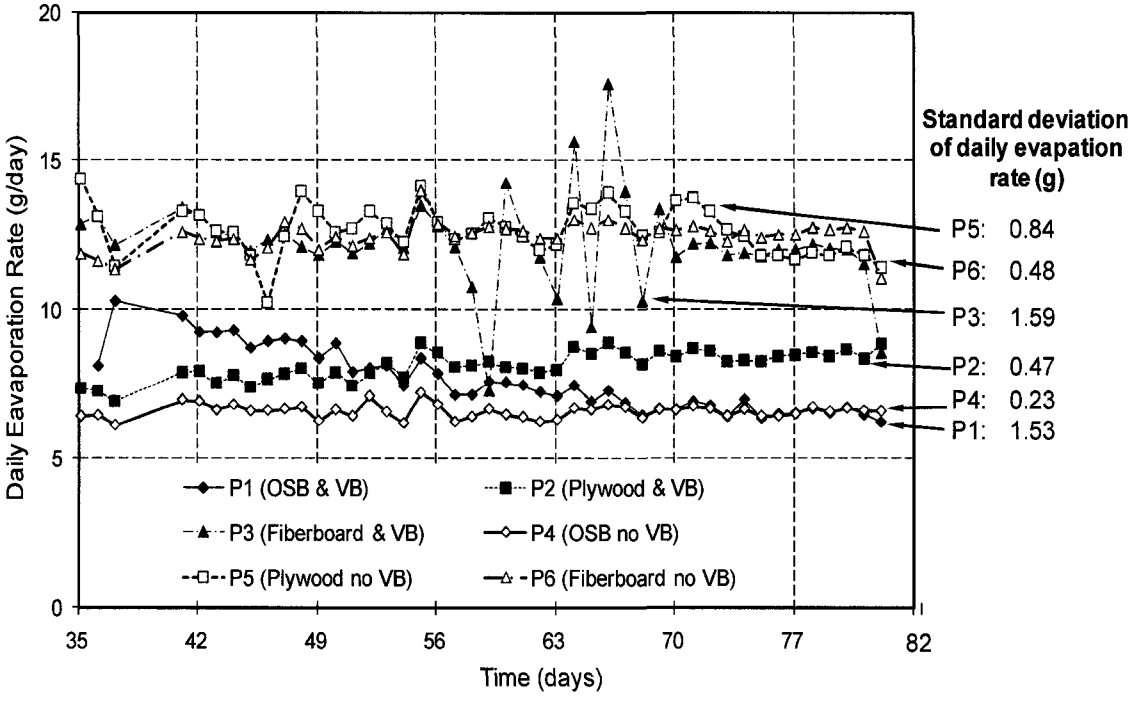

Figure 3.14. Daily average evaporation rate under test conditions I:
(T_{in}=21.0°C, RH_{in}=59%, and T_{out}=13.5°C, RH_{out}= 52%)

Note: Load cell in panel 3 malfunctioned between day 58 to day 70. Condensation was observed on the bottom regions of the OSB sheathing board, especially on panel 1, but not on the plywood board or the fiberboard.

3.6. Effect of test conditions on drying rate

Due to water leakage in the water tray placed inside panel 3, only the data recorded during test period II from day 83 to 114 were used for analysis. Fig. 3.15 plots the cumulative evaporation and Fig. 3.16 shows the daily average evaporation rate.

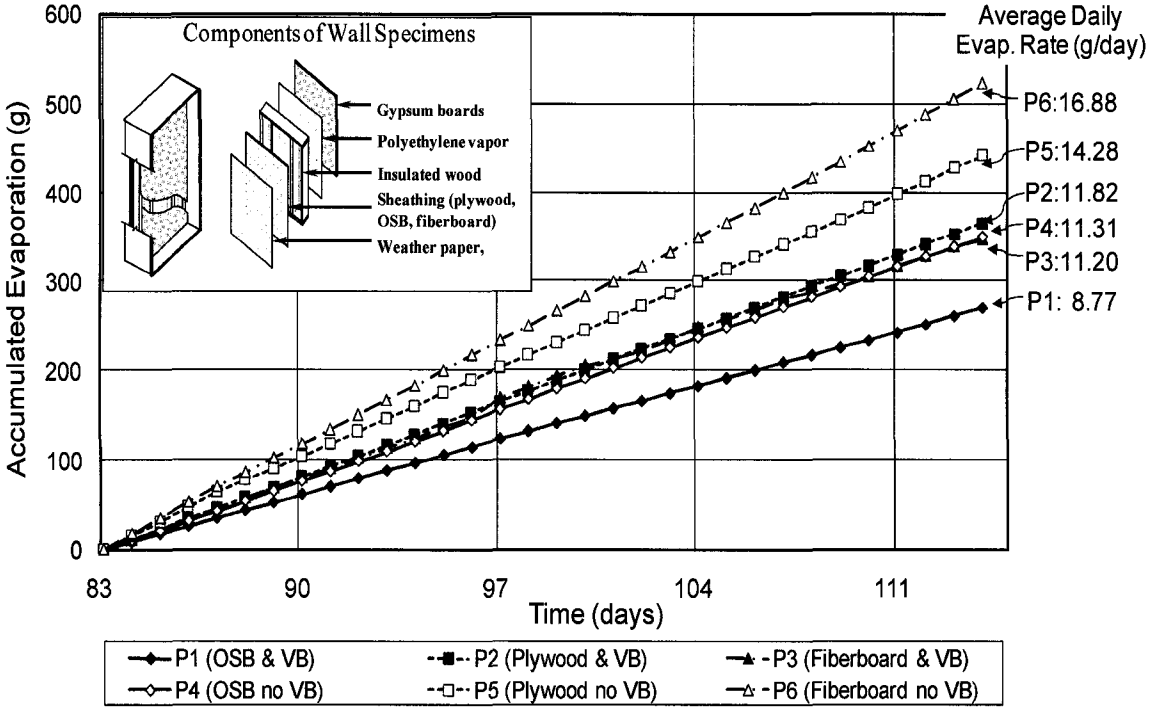

Figure 3.15. Evaporation profiles of different wall assemblies during period II: (T_{in}=21.1°C, RH_{in}=30%, and T_{out}=5.2°C, RH_{out}=69%)

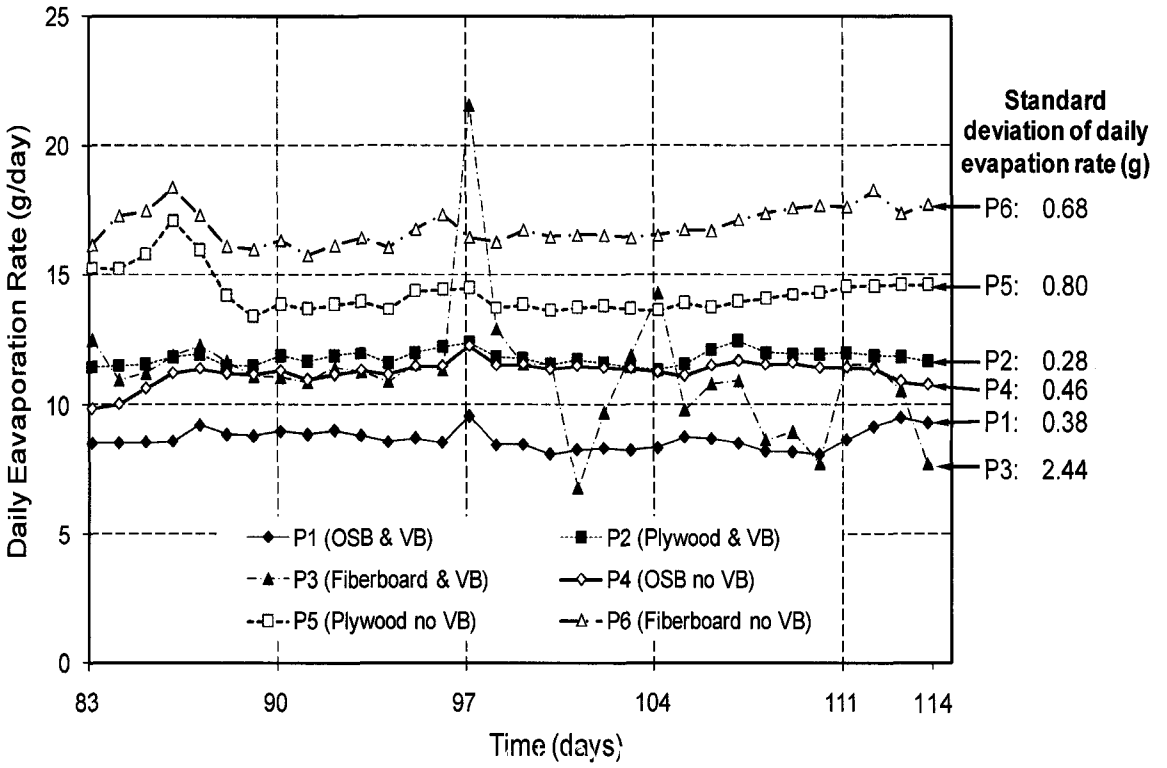

Figure 3.16. Daily average evaporation rate for condition II:
(T_{in}=21.1°C, RH_{in}=30%, and T_{out}=5.2°C, RH_{out}=69%)

Less variations in the daily evaporation rates can be observed under test condition II as compared to test condition I. Similar to the findings from period I, walls with fiberboard sheathing had higher drying rate, followed by plywood and then by OSB. Specimens without the vapor barrier had a higher drying rate (Table 3.4), since more water vapor was transported to indoors in such cases. This observation also confirms the notion that the drying capacity of wall systems could be improved with the use of smart vapor barriers that increase their permeability when exposed to high RH (Kunzel 1998).

Table 3.4. Daily average evaporation rate [g/day] of wall panels under condition II: (T_{in}=21.1°C, RH_{in}=30%, and T_{out}=5.2°C, RH_{out}=69%)

Vapor barrier	OSB	Plywood	Fiberboard
Present	8.77 (Panel 1)	11.82 (Panel 2)	N/A* (Panel 3)
Absent	11.31 (Panel 4)	14.28 (Panel 5)	16.88 (Panel 6)

* The result for panel 3 is not included in this table because water leakage from the tray in this panel was observed.

The moisture distribution in the specimens was monitored by the gravimetric samples located in the sheathing boards. The samples were round discs, about 1/2" (13 mm) thickness and 1 1/2" (38 mm) diameter, and were cut from the same materials as the sheathing boards. In a study on sugar pine, Zarr et al. (1995) found that it took approximately two months for specimens to reach equilibrium moisture content of 9% under 65% RH condition. To accelerate the test and establish this equilibrium moisture content in the gravimetric samples, samples used here were preconditioned in a small environmental chamber with RH set at 85% and temperature at 10°C for one week. At the same time the wall panels were preconditioned in the large environmental chamber with room temperature and 60% RH for two weeks. At the end of this step, the gravimetric samples were installed in their locations and the wall specimens were further conditioned with their gravimetric samples in place for another two weeks. The first day of the fifth week was considered day 0, on which day the gravimetric samples were weighed and water was added to all 6 trays. The changes in the moisture contents were tracked by weighing the gravimetric samples periodically after day 21. These moisture content increments are plotted in Fig. 3.17.

After preconditioning, the initial moisture contents (IMC) of the gravimetric samplers at the start of the test period I were between 7% and 10%. The moisture contents increased gradually from these initial MC values until day 35 when the majority of the samples, except for a few in panel 1, reached steady state. In general, the moisture contents of the gravimetric samples at the bottom (where closest to the water trays) were the highest and they decreased with the increase of distance from the moisture source. This trend also evidenced the moisture diffusion from the water tray to the upper part of the stud cavity. The moisture content of samples at the bottom section (level C and D, Fig. 3.17) of panel 1 kept increasing through test I. This increase indicated the occurrences of condensation, which was visually noted on the surface of the sheathing close to the water tray.

Switching to test conditions II resulted in higher moisture contents in the sheathing and studs, and more noticeable moisture movement towards outdoors since the outdoor vapor pressure was reduced. The increases in moisture contents were found to be more obvious in the assemblies with vapor barriers. The lower outdoor temperature also results in more condensation on the OSB sheathing board; water drops were observed on the gravimetric sample at the bottom of panel 1 and traces of condensation stains were observed on the lower gravimetric samples of panels 2 and 5 (with plywood as sheathing board).

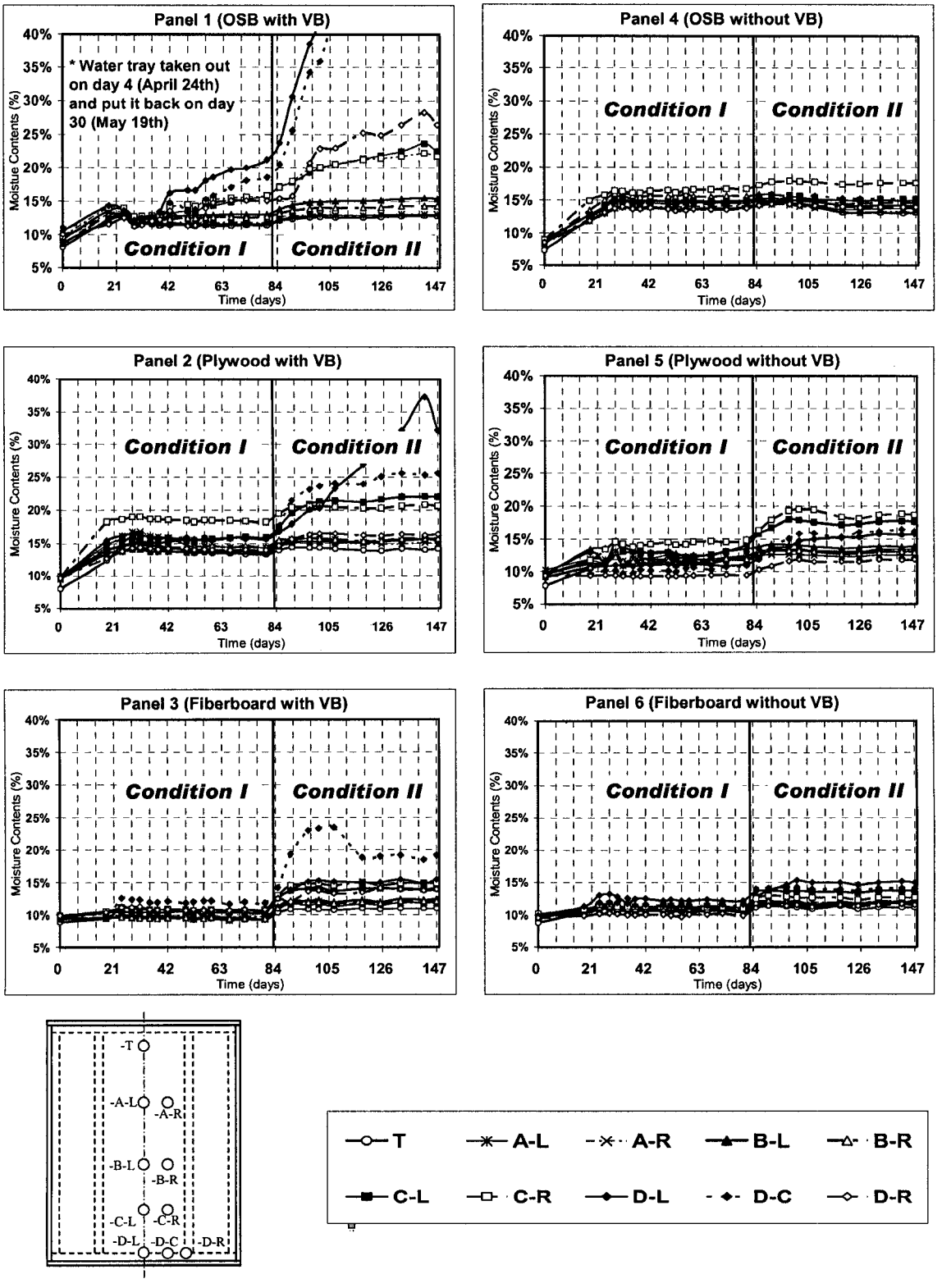

Figure 3.17. Profiles of moisture contents by gravimetric samples for all 6 panels

3.7. Observations, conclusions and lessons learnt

Observations from the preliminary test include:

- The evaporation rates from the water trays are influenced by the properties of materials used in the wall assemblies as well as the indoor/outdoor conditions. The results demonstrate correlations between the evaporation rate from the water tray and the vapor permeability of the sheathing board, the wall configuration, and the indoor/outdoor climatic conditions;
- When the boundary conditions are constant, the daily evaporation rate from the water tray under steady-state conditions represents the drying capacity of the wall assembly before condensation occurs;
- Under uniform loading conditions, the drying capacities of wall assemblies can be related to their performances; and,
- Presence of moisture source at the bottom of the stud cavity results in a typically higher vapor pressure at the bottom of the cavity, and this vapor pressure gradually decreases towards the higher level of the cavity.

The following conclusions can be drawn:

- The water tray method is effective in investigating the drying performance of an envelope system. The source of free water at the bottom of the stud cavity is equivalent to water gathered on the bottom plate due to water penetration. In both cases the evacuation rate of moisture is a function of building envelope characteristics and climatic loading conditions;

- By monitoring the evaporation rate of a free water source placed inside the stud cavity of a wall system, the proposed method can be used to evaluate the relative drying capacity of different envelope systems; and,
- The preliminary test confirms the statement that the drying capacity or Drying by Evaporation Index (DEI) of an envelope system can be increased by increasing the permeability of the sheathing.

Through the design, execution and data analysis of the preliminary test, the test method with water trays can be further improved as follows:

i) *The water tightness of the tray should be ensured through design.*

Several types of silicone caulking compounds were tested by trials before the best one in terms of water tightness was selected. However, leak still happened in one tray during the test. Obviously, the caulking compound does not have sufficient adherence for bonding the acrylic sheets of a tray together. It was not feasible to completely avoid disturbing the water trays during installation and transportation. In addition, silicon's durability after long exposure to water is questionable. A better bonding agent is needed to ensure the water tightness.

ii) *The water tray needs redesign to have adjustable water surface area*

The water tray simulates a moisture sources caused by the water which penetrates the stud cavity and gathers on top of the bottom plate. The evaporation from the water tray would be similar to that from a certain wetted area on the bottom plate. Although the evaporation from the water tray in the preliminary tests demonstrated steady slopes for all tested wall specimens under given boundary conditions, this observation was obtained for a specific area of evaporation. In

real circumstances, the wetted area of the bottom plate can vary. It would be necessary to treat the exposure area of free water as an independent variable that would significantly affect the evaporation rate from the water tray, or in another word, DEI.

iii) *Air leakage through the stud cavity should, if possible, be estimated or minimized.* Based on the analysis in Section 3.2, air leakage through a stud cavity may cause exchange of moisture between the stud cavity and those of the indoor and outdoor air. This exchange can directly affect the vapor pressuring inside the cavity and subsequent the water evaporation from the tray. In addition, air leakage may change local climate of temperature and relative humidity and influence the overall moisture response of the wall assembly. Slight air movement in the stud cavity changes the conditions around the water tray. For an experiment based only on loads and responses analysis, the measurement of air movement is not necessary because its influence has been included in the general responses. For detail tests that focus on the influences of air leakage, estimation of the leakage rate is essential; for future experiments, effects should be made to minimize air leakage of the stud cavity.

Chapter 4
Methodology for Evaluation of Dry Performance of Envelopes

The key elements of the proposed methodology are presented in this chapter. Developing a practical approach for engineering design is one of two ultimate objectives of this research outlined in Section 1.4. To achieve this goal, a common concept and rules related to it in structural engineering are adapted to building envelope performance evaluation. Similar to the concept of strength in structural engineering, the drying capacity is taken as a yardstick to measure and compare the relative performance of different building envelope configurations. A new method of analysis has been developed in this thesis research for evaluating this drying capacity.

The methodology builds on the new test method using a water tray in the stud cavity; and considers that the evaporation from the tray and the moisture accumulation in the sheathing board reflect the drying characteristics of the wall panel. In this chapter, the concepts and techniques of the new methodology are presented.

The new drying capacity indicator will be used to evaluate the performance of wall assemblies according to the limit state design (LSD) criterion. A step-by-step procedure of the application of capacity indicator will be provided in the end of this chapter as well.

4.1. Assumptions and basic concepts

4.1.1. Assumptions

The following assumptions were made in the development of the new test method and in the data analysis:

- The wall systems are subjected to three kinds of moisture loadings. In addition to the moisture loadings of the indoor and outdoor environments, water which has penetrated into the stud cavity is the third type of moisture loading and was named as the in-cavity moisture loading;
- The water tray represents water which has penetrated the stud cavity and gathered at the bottom plate. The evaporation from the water tray is considered equivalent to the evaporation from the water settled at the bottom plate;
- If a wall system outperforms the other systems under the same test boundary condition, say the worst drying potential, it would be expected to also perform better than the others under actual in-service conditions; and,
- Drying occurs along a two-stepped path: evaporating into the stud cavity first and then moving across the outer layers by diffusion or through air leakage. In other words, the major drying path discussed in this study is isolated from other drying paths, such as drainage, capillarity, and liquid diffusion.

4.1.2. New concepts

As synthesized in Chapter 2, three types of indicators have been commonly used for quantifying drying performance. Indicators based on moisture accumulation at a certain location of the surrounding material can indicate the moisture status of the wall system;

the other two types, the effective permeance of the assembly and the evaporation from the bottom plate inside the stud cavity, can reflect the evacuation rate of moisture from the stud cavity. However, none of the above indices can reflect both the evacuation speed and moisture status simultaneously. A more appropriate index should provide a holistic evaluation on the multi-facets of drying process, and is proposed next.

4.1.2.1. Non-Constrained Drying and Constrained Drying

The moisture evacuation from a wall system and the moisture redistribution in wall components are two interrelated processes during the drying process. However, the drying capacity may have different meanings depending on whether it is related to evacuation or accumulation.

In a drying test, if the moisture accumulation at any place of the wall system does not cause any moisture damage, the type of drying process is recognized as non-constrained drying. In this case, the drying capacity should be defined by the maximum drying rate that the test specimen can achieve. However, if the moisture accumulation at any point of the wall system may lead to moisture damage, drying under such a situation is defined as constrained drying. The potential for moisture damage poses a restriction on the drying process.

The effective vapor permeance coefficient $\dot{M}_v$ (belongs to Type I indicator of envelope drying in Chapter 2) and the moisture evaporation rate at the bottom plate $\dot{E}_v^B$, or DEI (belongs to Type II), reflects the drying capacity under non-constrained situation. Both of them indicate the speed of moisture migration. The capacity under constrained drying

should correlate the moisture accumulation in surrounding material (type III in chapter 2) to the amount of water evaporated in stud cavity. Thus, it is necessary to give further consideration to the evaluation of drying capacity.

4.1.2.2. ICEA (In-Cavity Evaporation Allowance)

In this research, the evaporation amount that results in 20% MC (allowable moisture content) in any part of the wall panel is defined as the "In-Cavity Evaporation Allowance[1]" (ICEA). The unit of ICEA is gram, the same as that with the index of cumulative evaporation. ICEA concept is based on the following assumption: if any part of the wall assembly reaches the allowable moisture limit, the whole panel is assumed to have reached the limit.

In essence, ICEA places a limit on the magnitude of water that can evaporate in the stud cavity before the panel reaches the critical moisture state. The higher the ICEA value a panel has, the more water the panel can evacuate from its stud cavity before the allowable moisture state is reached. Therefore, ICEA can be used to indicate the drying capacity of a wall panel. A panel with higher ICEA is deemed to have higher tolerance of moisture within the stud cavity. The ICEA concept facilitates the quantification of resistance to rain penetration into a wall assembly and establishes a link between wetting process and drying process as explained below.

[1] The term "In-Cavity Evaporation Allowance" was suggested by Dr. Yves Fortin in summer of 2006. The cavity here referred to the stud or insulation cavity.

4.2. Procedure to determinate ICEA

4.2.1. Profiles of in-cavity loading and moisture response on sheathing

Generally, two types of profiles can be used to represent the level of evaporation in the stud cavity. One is the *accumulative evaporation profile* with the cumulative evaporation as the vertical axis. When evaporation reaches the steady state, the profile shows a linear pattern with a slope that indicates the evaporation rate (Fig. 4.1a). The other profile, namely the *evaporation rate profile*, takes the evaporation rate directly as the vertical axis. The profile pattern is a horizontal line at a certain height (which is the DEI) when evaporation reaches the steady state (Fig.4.1b).

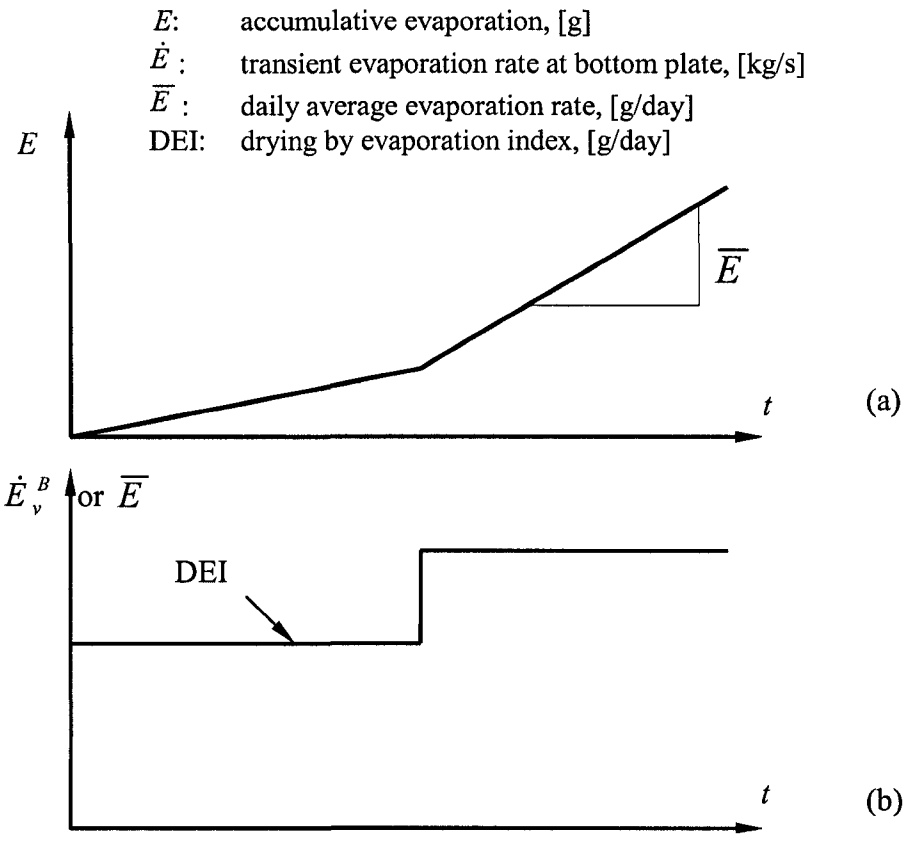

Figure 4.1. Two type of profiles of in-cavity loading

Moisture accumulation at any specific location on the sheathing board could be plotted over time. Fig. 4.2 shows a typical moisture content profile with respect to time.

Figure 4.2. Profile of moisture state in the sheathing board

4.2.2. Establishing load-response relationship

In this experiment, the in-cavity water tray facilitated the measurement and analysis of the in-cavity moisture load. The indoor and outdoor conditions were kept at the steady state during the tests. Therefore, the moisture responses at any point of the assembly were mainly affected by the in-cavity loading and by the configuration of the wall panels being tested. The cumulative evaporation can be considered as the moisture loading and the monitored MC profiles represent the moisture responses.

Normally, the evaporation or moisture contents are plotted versus time. With the intention to establish the load-response relationship, the load-time and response-time profiles are plotted in the same figure. The combination of two figures is illustrated in Fig. 4.3, and the procedure to create load-response curve is the following.

At any time during the experiment, the MC value can be determined from the time-response curve (I) and the corresponding load value can be extracted from the time-load (accumulated evaporation) curve (II). Then on the load-response chart (III), the MC of a point (c) is plotted against the load values, and MC and load are assigned to the vertical axis and the horizontal axis, respectively. This step is repeated for each time point during the experiment. The points obtained on chart III form a continuous trace of dots, which forms the load-response curve for the location where MC is monitored.

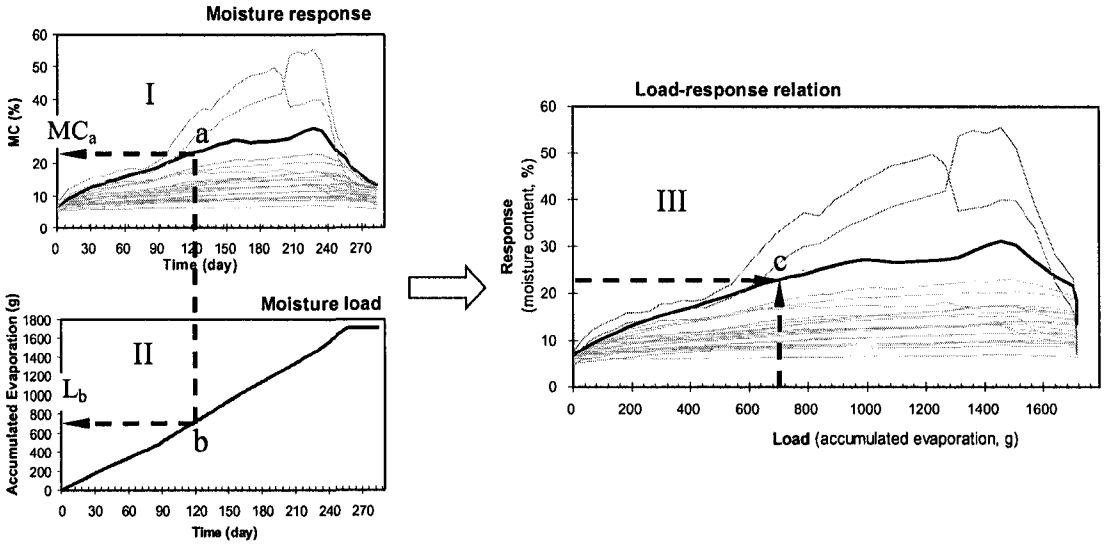

Figure 4.3. Establishing a load-response relation

This Load-Response correlation is shown as the thick line in Fig. 4.3-III. This procedure can be repeated for all the MC measurement locations on the sheathing board and studs. The obtained load-response relations represent the characteristics of a particular wall configuration under a particular in-cavity moisture load.

4.2.3. Determination of ICEA

Notations were made in this study to simplify mathematical calculations and results

presentation. The following symbols were pre-defined:

- E is the cumulative evaporation of water from bottom plate inside the stud cavity [g];
- MC is the moisture content of a material [% by weight];
- σ is the stress in a typical material or structure [kg/m^2]; and
- ε is the strain in a typical material or structure [%].

Accordingly, the moisture load-response relationship for building envelopes can be called the E~MC curve; while the stress-strain relation in structural engineering can be called the σ~ε curve.

One similarity between the E~MC curve and the σ~ε curve is that they both deal with the relation between load and response. In structural engineering, there is a set of well developed theories regarding the stress-strain curve.

In a σ~ε curve, the yield point and the point of ultimate strength deserve close attention. The yield point corresponds to a state that the stress in the material is just tolerable without permanent deformation. Therefore, it can serve as a capacity indicator demonstrating a structure's capability to resist elastic deformation. The ultimate strength represents the limit state of a structure and corresponds to the maximum stress a material can withstand. If the stress in a structure exceeds this limit state, failure would occur. Therefore, ultimate strength is the indicator for evaluating the capacity of a structure for resisting load-induced failures. Usually, ultimate strength represents the nominal capacity, or limit state, in LSD. Due to variations usually unavoidable in resistance of load, ultimate strength should be multiplied by a reduction factor to identify a design oriented

capacity. In LSD the difference between limit state and design allowable state forms a part of the safety margin for a structure (the other part comes from the load factors).

However, some differences can be found between a typical E~MC curve of steel shown in Fig. 4.4 and a typical stress-strain curve shown in Fig. 4.5. First, the coordinate system in E~MC and σ~ε are reversed. The load variable (σ) of the σ~ε curve is the vertical axis, while the load variable E in the E~MC curve lies on the horizontal axis. Secondly, no yield point and ultimate point can be observed along the E~MC curve. Despite these two differences, the philosophy of limit state and design allowable state can be extended and adapted to analyze moisture loading and responses. Table 4.1 matches the limit state concept in structural engineering against that in moisture load-response study. Based on literature review introduced in chapter 2, the allowable state of a wall specimen is set at 20% MC; while the FSP, at about 28% MC, is selected as the ultimate limit state. The corresponding evaporation load at the allowable state is defined as ICEA, which was introduced in last section.

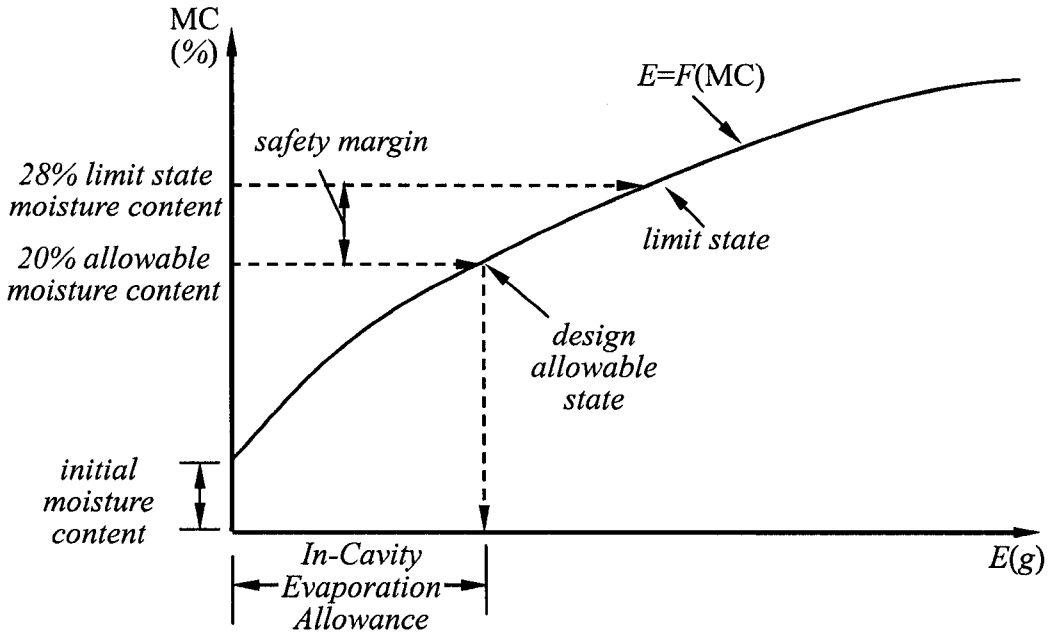

Figure 4.4. Determination of ICEA by typical load-response curve (*E*~MC)

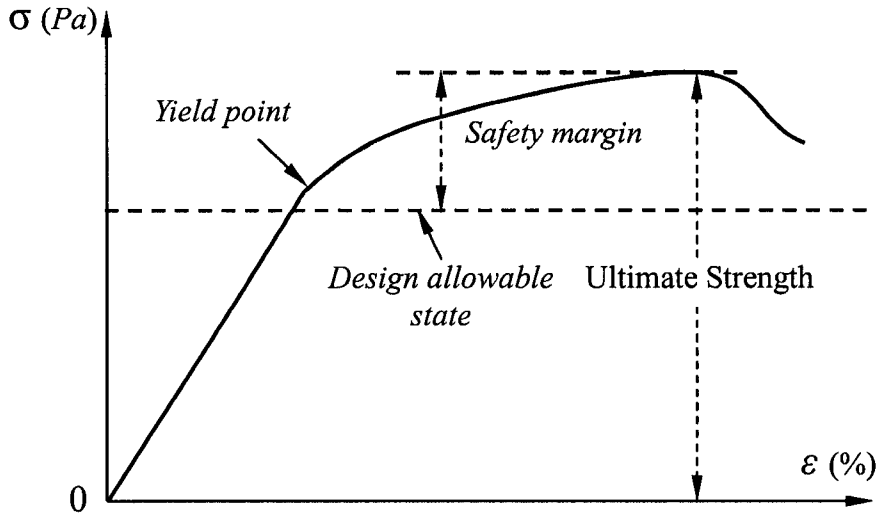

Figure 4.5. Typical stress-strain curve

Table 4.1. Limit state analogy between structural engineering and moisture study

Categories	Structural analysis & design	Moisture analysis & design
Load	Stress σ [Pa]	Cumulative evaporation E [g]
Response	Strain ε [%]	Moisture content [% by weight]
Load-response relationship	σ~ε curve	E~MC curve
Limit state	Ultimate strength Rn , i.e. maximum σ value at σ~ε curve or at ε = 0.35%	FSP, i.e. ultimate moisture content at about 28% MC
Design allowable state	Design capacity-reduction of ultimate strength Rn by multiplying by a factor Φ	ICEA [g] — cumulative evaporation corresponding to 20% MC
Safety margin	The range between design capacity and ultimate strength	The range between 20% MC and 28% MC

Ultimate failure may not occur in most situations of this test. Thus, the cumulative evaporation value corresponding to 28% MC may not serve as an appropriate evaluation index. Neither is there a "yield point" on the E~MC curve. Under such a situation, ICEA may be a reasonable alternative evaluation index. This consideration is based on the fact that ICEA has an explicit physical meaning — it corresponds to the cumulative evaporation that causes any part of the wall system to reach its design allowable moisture content. Thus, ICEA represents a characteristic point on the load-response curve, which can be used for the evaluation of the relative performance of building envelope systems.

The general expression of ICEA is:

$$\text{ICEA} = F(\text{MCL}) = E\big|_{\text{MC=MCL}} \tag{4.1}$$

where MC [% by weight] is the moisture content of the material; MCL is the moisture content limit of wood material (20% MC is used here); F ( ) is the load-response function; the vertical line on the right side of Eq. 4.1 is interpreted as "when"; and the last

term $E\big|_{MC=MCL}$ denotes the amount of evaporation from the water tray when the moisture content at the location of interest in the envelope reaches the allowable state. For the typical curve of E~MC (as shown in Fig. 4.4), ICEA is the amount of cumulative evaporation when a part of the envelope reaches the allowable moisture state at 20% MC.

4.2.4. Minimum ICEA as an auxiliary indicator

Fig. 4.6a shows another possible pattern of E~MC curve: moisture content reaches equilibrium at a level lower than the allowable limit at 20%. In many assemblies, even after increasing the loading potential (i.e. double the evaporation area), the 20%MC is never achieved. In such a case, ICEA could not be determined by using the loading method described in the previous section. As reviewed in Chapter 2, when the moisture accumulation in the wood assembly reaches equilibrium, the net moisture sorption by the material at that moment is equal to zero, and the evaporation rate of the water tray represents the drying rate of the wall assembly. Under such a situation, the amount of total evaporation till a set time point (in this case, till the end of the second test period), is defined as the "minimum ICEA[2]". It is used as an auxiliary indicator instead of the yet-to-be achieved actual ICEA and is denoted as $ICEA_{min}$ (as shown in Fig. 4.6b). The calculation formula can be expressed as:

$$ICEA_{min} = E(t)\big|_{t=\tau} \tag{4.2}$$

where the cumulative evaporation E is a function of elapsed time τ. The value of $ICEA_{min}$ is smaller than the actual value of ICEA since $ICEA_{min}$ indicates that the MC in the wall system has not reached 20%. The longer the time duration the closer the $ICEA_{min}$

[2] The term "minimum ICEA" was suggested by Dr. Paul Morris in reviewing of an intermediate report of the CRD project at the end of 2006.

approaches the actual ICEA. The symbol τ' in Fig. 4.4 corresponds to the end of the first test period.

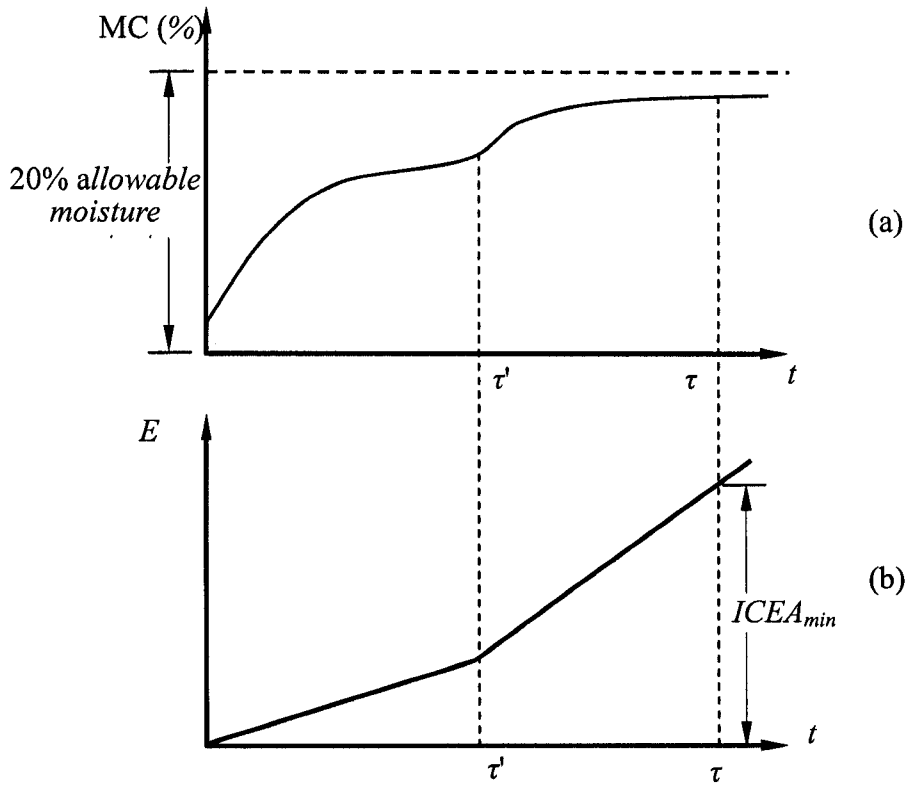

(a) E~MC curves showing moisture equilibrium when MC is lower than 20%
(b) A typical loading profile of E~t

Figure 4.6. Determination of $ICEA_{min}$

4.3. Moisture transport and conservation principle

Generally, the evaporated water from a water tray would be either stored in wall components or evacuated. Therefore, the moisture balance could be expressed as follows:

$$M_E^B = M_E^T + \Delta M_S^T \tag{4.3}$$

where ΔM_S^T is the increase of total mass of moisture stored in the components of the wall system; M_E^B is the mass of water evaporated from the water tray; and M_E^T is the mass of moisture evacuated from the wall system.

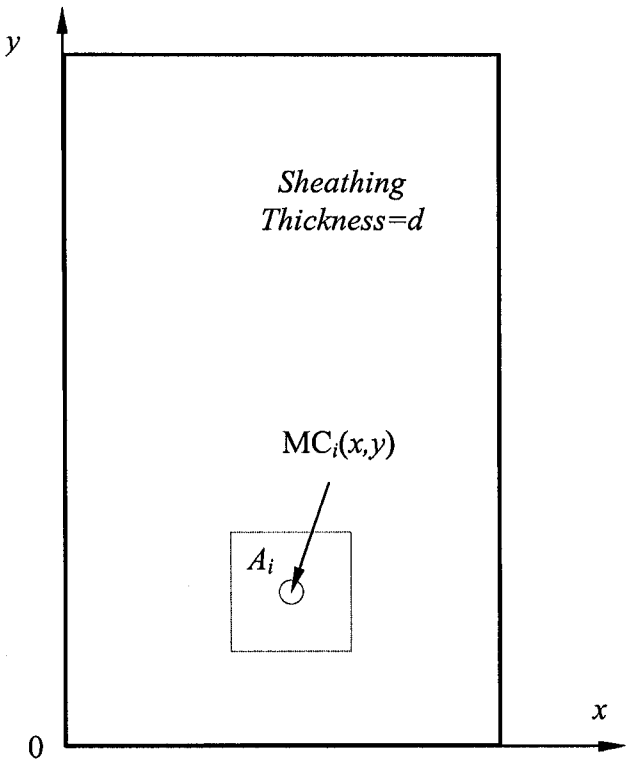

Figure 4.7. Calculation of the total moisture storage/absorption in sheathing

The MC in the sheathing board varies from one measured point to another (Fig. 4.7) (it was assumed that it does not vary along with thickness). Therefore, the total moisture storage in the sheathing board M_S^T can be calculated as following:

$$M_S^T = \iint_A \mathrm{MC} \cdot \rho \cdot d \cdot dxdy \tag{4.4}$$

where ρ is the density of the wood sheathing [kg/m^3]; x and y are the coordinates of the point; d is the thickness of sheathing board. M_S^T can also be obtained by a simplified

method which uses the moisture content at the points monitored instead of using the moisture content in a certain range of sheathing. Therefore, the total moisture storage in the sheathing board is:

$$M_S^T = \sum_{i=1}^{n} \mathrm{MC}_i \cdot A_i \cdot \rho \cdot d \tag{4.5}$$

M_S^T varies with time t, therefore the derivative of M_S^T with respect to t — $\dot{M}_S^T$ represents the total absorption rate of moisture in the sheathing board and studs. According to the preliminary test presented in Chapter 3, a typical MC profile shows a sharp slope at the beginning stage and gradually changes to flat when the equilibrium is approached (Fig. 3.17). Thus, the absorption rate profile should start from a high level and decrease to a lower level or even reach zero when absorption and desorption reach equilibrium. The typical absorption rate profile should be in shape as shown in Fig. 4.8. The total mass of moisture absorption can be calculated from the area under the absorption curve and expressed as a definite integration of the absorption rate in:

$$\Delta M_S^T = \int \dot{M}_S^T(t) \cdot dt \tag{4.5}$$

If during a certain period of time t, the moisture content in all wall components remains constant, it indicates the absorption and desorption have reached equilibrium. In this case, the total moisture absorption rate in sheathing and studs, $\dot{M}_S^T$, is equal to zero, as demonstrated by the dash line in Fig 4.8.

In the preliminary test, the evaporation profiles obtained for all the tested panels were observed to have constant slopes, which indicates that the DEI or the rate of evaporation at the bottom plate ($\dot{E}_v^B$) for each assembly should be a constant. If DEI and $\dot{M}_S^T$ are

plotted in the same figure, as shown in Fig. 4.8, the area between the DEI line and the moisture absorption rate curve represents the mass of moisture that is not absorbed by the sheathing and the studs. Experiments indicated that other components absorb little moisture during the drying process except for the sheathing board. Accordingly, it would be reasonable to consider the moisture not being absorbed by sheathing and studs as the amount of moisture evacuated out of the wall system.

It has been observed that the rate of evaporation from the bottom plate inside the stud cavity is relatively constant. This linear process actually included two non-linear processes: the moisture absorption by the boundary materials (shaded area) and the evacuation of moisture from the wall system (the rest area between DEI line and absorption curve), as shown in Fig. 4.8.

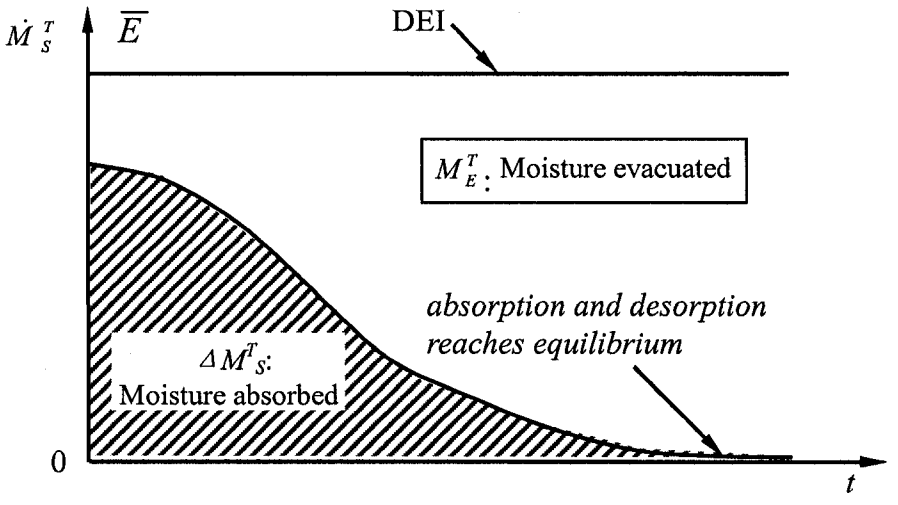

Figure 4.8. Moisture absorption curve and DEI line

4.4. Limit state design (LSD) for building envelope

4.4.1. Essence of LSD method

Ensuring safety, functionality, and economy is the ultimate goal of any engineering design. Usually, the first step of the design processes is to propose a primary plan that includes dimensions of the designed structure as well as the material properties of every component; then, all the participating loads must be estimated; and finally the design draft must be verified through basic requirements/criteria. In LSD, the primary criterion is:

$$\text{Effects of design loads} \leq \text{Design capacity} \tag{4.6}$$

For ULS design, this criterion is expressed as:

$$\sum \gamma_i \cdot L_i \leq \kappa \cdot Rn \tag{4.7}$$

where L_i denotes different types of load; γ_i denotes various kind of load factors; κ is the resistance (reduction) factor; and Rn is the nominal resistance (ultimate strength). These load factors and resistance factor can be determined by statistical reliability analysis.

Applying the LSD method to wood structure design and following the provisions in CSA Standard O86.1-94 of "Engineering design in wood (Limit States Design)", the general requirement equation is formulated as:

$$\alpha_D L_D + \beta \cdot \psi \left(\alpha_L \cdot L_L + \alpha_W \cdot L_W + \alpha_T \cdot L_T\right) \leq \kappa \cdot Rn \tag{4.8}$$

where L_D is the dead load due to weight; L_L is the live load due to static or inertial forces arising from intended use and occupancy (includes vertical loads due to cranes); snow, ice, and rain; earth and hydrostatic pressure; L_W is the load due to wind; L_T is the load due to temperature-caused contraction or expansion; α symbols are the load factors

corresponding to different attributes of loads; β is the load importance factor; ψ is the load combination factor. Most factors in this method are determined based on statistic analysis. Therefore, the LSD method is also known as the LRFD (Load and Resistance Factor Design).

Limit state caused by moisture accumulation in the building envelop belongs to the category of Serviceability Limit State (SLS) because moisture related failure normally does not affect the life safety of residents. Problems caused by moisture accumulation such as fungal growth and decay usually develop slowly and the resident has enough time to fix it. When applying SLS criteria in design, according to CSA Standard O86.1-94, all of the α-type load factors are set to 1.0; 1.0 is also recommended for the importance factor β. Therefore the general verification criterion in Eq. 4.8 becomes:

$$L_D^e + \psi\left(L_L^e + L_W^e + L_T^e\right) \leq \kappa \cdot Rn \tag{4.9}$$

where the superscript "e" indicates that the variable related is an effect of the corresponding load. The combination factor ψ is subjected to the following rule: if only one of L_L, L_W, and L_T acts, ψ is equal to 1.0; if two of L_L, L_W, and L_T act, ψ is equal to 0.7; if all of L_L, L_W, and L_T act, ψ is equal to 0.6. The term on the right side of the inequality, κRn, is the allowable design resistance as specified by corresponding standard clauses, e.g. elastic deflection, permanent deformation, ponding, and vibration (Keenan 1986).

4.4.2. LSD in moisture analysis

In reviewing the mechanisms of moisture movements/redistributions in wall assemblies, moisture evacuation from the wall is found to contain both liquid and vapor phases. Because the design is based on worst drying potential situation, and, in addition, the

amount of water penetrated into the stud cavity of a wood-framed building envelope system is usually small, the moisture evacuation in the liquid form due to drainage and capillary action typically would not occur. Therefore, evacuation in liquid form is considered minor and could be negligible in design unless the wall is leaky and saturated (Fazio 2004). For this reason, evaporation followed by vapor diffusion or air exfiltration is the only path for moisture evacuation from building envelopes.

In the current experiment, the water tray is employed as the in-cavity moisture source where only evaporation occurs. The newly defined concept ICEA places a limit on the amount of water that is allowed to be evaporated from a stud cavity. In addition, ICEA itself includes a certain margin of safety, which is between 20% MC and the FSP at about 28% MC (see Section 2.3). Therefore, the right side of Eq. 4.9, κRn, which sets the capacity for the wall design, can be substituted by ICEA, i.e.

$$\text{ICEA} = \kappa \cdot Rn \tag{4.10}$$

The left side of Eq. 4.9 is the load effects. In the moisture analysis, penetrated water (M_P) is usually introduced by rain penetration, moisture condensation, construction moisture, and accidental water intrusion such as flooding. Among them, construction moisture and accidental water are less common. The impact of condensation is included in the boundary condition of the test. Therefore, rain penetration is the only moisture load that has to be considered in moisture status analysis in the wall system. In addition, the in-cavity loading (evaporation) was introduced continuously because rain penetration may accumulate in the stud cavity and take effect without interruption during the drying process.

The total amount of rain penetration, M_P, can be calculated by introducing a proportionality factor $f(\,)$:

$$M_P = Q \cdot t \cdot \rho_w = \sum_{i=1}^{n} Rw_i \cdot f(\Delta Pw_i) \cdot \rho_w \tag{4.11}$$

where Q [L/hr] is the entering rate (hourly) of rain water into the stud cavity and can be obtained by Eq. 2.15; n is the number of hours when driving rain occurs during a specific period of time; and ρ_w [kg/m^3] is the density of water. Empirical relations in existing studies were available for several wall systems (such as Eqs. 2.16 to 2.19). It should be noted that $f(\,)$ is based on an area of 2,400 mm × 2,400 mm specimen.

If urban topographic features and the orientation of building façade are taken into consideration, local climatic conditions would be considered to obtain the precipitation amount on a building façade, and to further calculate the total mass of rain penetration (Fazio et al. 1995) as:

$$M_P = P_\phi^T \cdot f(\Delta Pw) \cdot \rho_w \tag{4.12}$$

Substitute the total precipitation on the building façade (P_ϕ^T) by Eq. 2.13, then

$$M_P = \frac{2}{9} C_\phi A \rho_w \sum_{i=1}^{n} V_i (R_{i\,hor})^{\frac{8}{9}} \cdot \cos\theta_i \cdot f(\Delta Pw_i) \tag{4.13}$$

Therefore, the design verification criterion Eq. 4.9 can be transformed into:

$$M_P \le \text{ICEA} \tag{4.14}$$

For a design of wood-frame wall assembly by applying of LSD criterion, the major steps can be described as follows:

1. Draft a plan of the wall assembly to be designed;
2. Based on the available weather data, specify the outdoor condition based on the month with the worst drying potential;

3. Specify the indoor air condition corresponding to the specified outdoor condition;
4. Measure ICEA according to the test protocol developed in this research;
5. Calculate the total rain penetration during the design period and under the specified test conditions.
6. Check the compliance of Eq. 4.14. If positive results are obtained, the design is deemed acceptable; otherwise, modification of the original design would be necessary, and after modification, the process starts over from step 1 again.

Chapter 5
Test Setup and Implementation

The main test followed the same principle as the preliminary test in which loading caused by rain penetration was simulated by a water tray at the bottom of the stud cavity of the wall specimens. Compared with the preliminary test, the scope of the main test was extended. The water exposure area became adjustable to three levels. In addition, more components and configurations were included into the testing assemblies, e.g. two different claddings: stucco and wood siding. The dimensions of specimens were changed to represent regular wall segments between two floors (the dimensions of specimens in the preliminary test represented the wall segments under the sill of the windows). Problematic issues found in the preliminary test were addressed and solved. For example, water tightness of the water trays was greatly increased using a better sealing compound. The number of sensors was also increased and all sensors were carefully calibrated and checked to ensure that they would work properly.

5.1. Test hut and wall configurations

The main test employed a two-storey test hut; and consisted of 31 full-size wall specimens, 15 on the 1st floor and 16 on the 2nd. The outer dimension of the hut was 5,442 mm × 2,972 mm × 6,020 mm (37'9 1/2" × 20'7 2/3" × 41'9 2/3"). Figure 5.1 shows

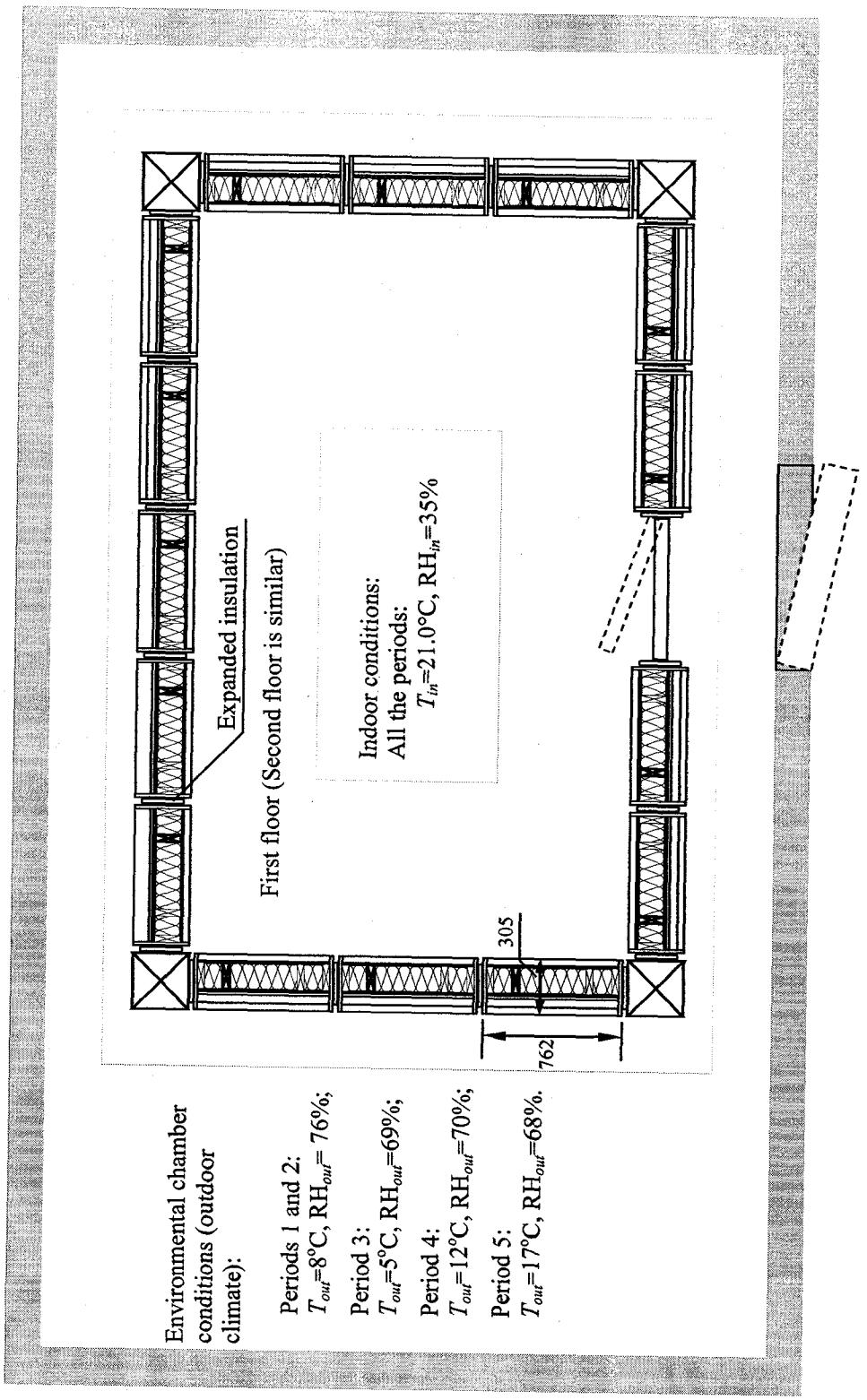

Figure 5.1. Layout of test hut in the environmental chamber

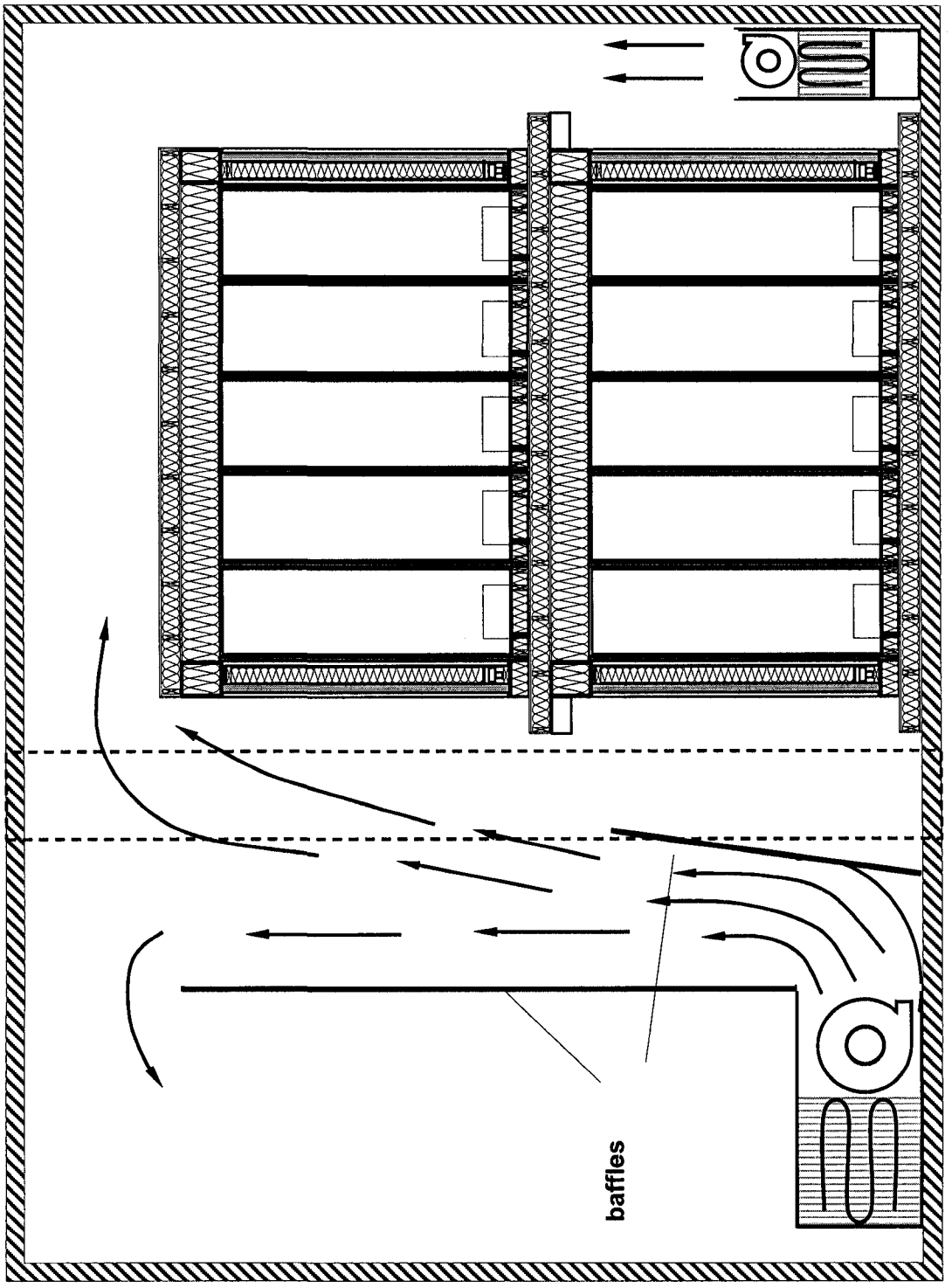

Figure.5.2. Cross-section elevation of test hut in the environmental chamber

the layout of the test hut in the environmental chamber. Figure 5.2 is the cross-section elevation of the test hut in the chamber.

The test plan included the following:

1. Configuring the tested specimens;
2. Maintaining the test schedule and boundary conditions;
3. Installing and calibrating the sensors, gravimetric samples, and data acquisition system (DAS); and
4. Specifying a loading protocol to apply a uniform moisture source in the stud cavity.

The size of an individual specimen was 2,477 mm (8' 1 1/2") in height, 762 mm (2' 6") in width, and 305 mm (1') in thickness. A 19 mm (3/4") thick plywood board frame surrounded the specimen and served as an air and vapor separator. A measuring zone was located at the middle of each specimen, and the effective vapor diffusion area was 406 mm (1' 4") in width and 2,438 mm (8') in height. Two 140 mm (5 1/2") wide buffering zones were located on both sides of the measuring zone to reduce the influence of thermal bridge between specimens. Fig. 5.3 shows the cross section of a specimen.

The wall assemblies were composed of two types of cladding (wood siding and stucco), three types of sheathing (OSB, plywood, and fiberboard), and with or without polyethylene vapor barrier. The fiberglass insulation was used in all specimens inside the stud cavity. The compositions of the 31 test specimens are summarized in Table 5.1. The material properties of these specimen components were the same as those in the preliminary test (see Table 3.2).

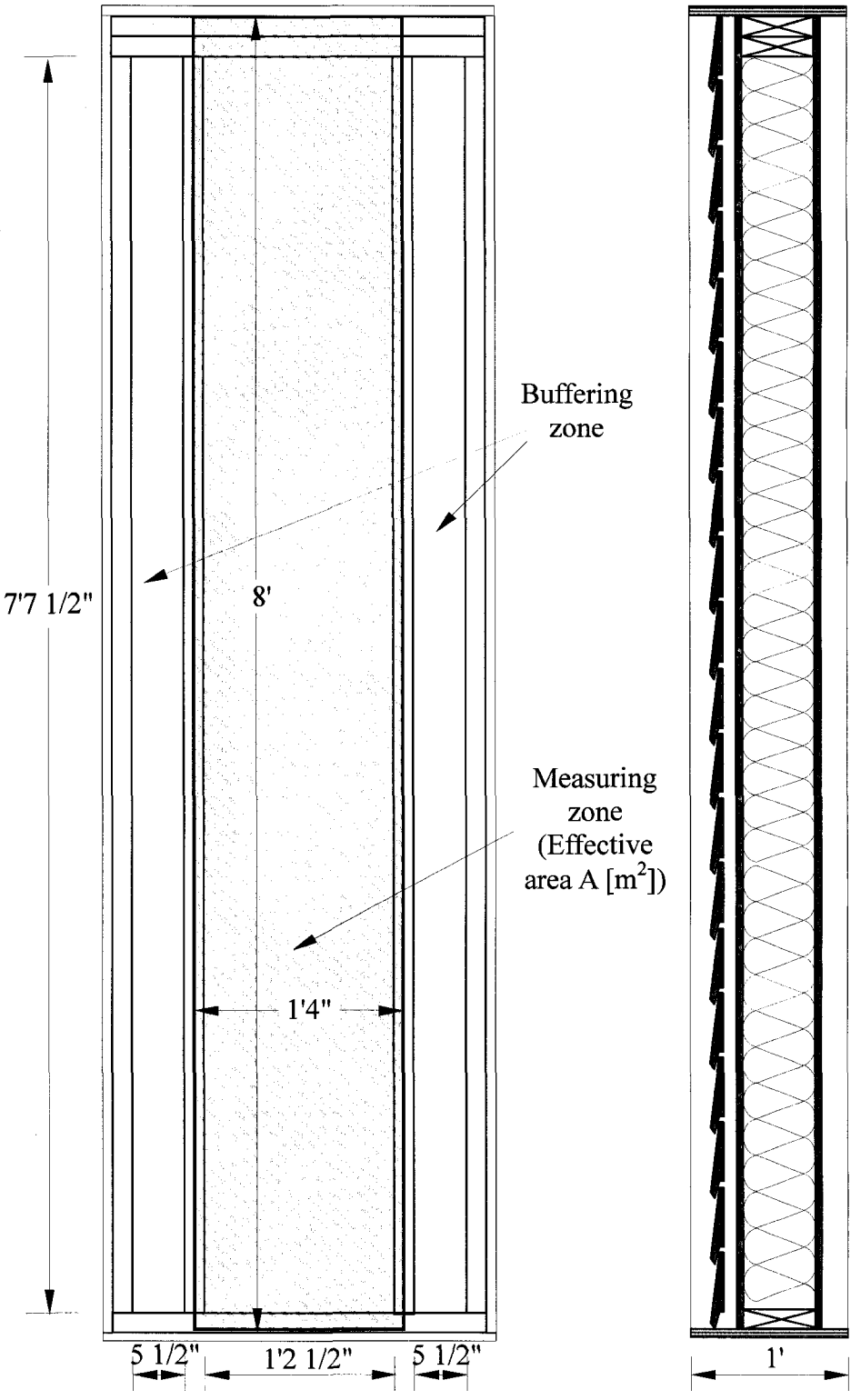

(a) Outside view (b) Cross section

Figure 5.3. Cross section of a typical wood siding cladding specimen

Twenty-four specimens were built in pairs, each pair having identical configuration, but different from the configurations of other pairs. The pairs are indicated by the rows with two wall numbers in Table 5.1. The two specimens in a pair were placed at the same location in the test hut, but one on the first floor and the other on the second floor. The other seven specimens do not have duplicates, P01 to P04 and P29 to P31, were used only once. Fig. 5.4 shows the locations of all the specimens on the two floors of the test hut.

Table 5.1. Configurations of all 31 specimens

No.	Cladding	Air gap	WRB	Sheathing	Insulation	Vapor barrier	Dry wall
01	None		Spun bonded polyolefin (SBPO)	OSB	Fiberglass batt 140mm (5½" thick)	Polyethylene	Painted gypsum board 13mm (1/2" thick)
02				Plywood			
03				Fiberboard			
04				EPS foam			
05 & 17	Wood siding	19mm (3/4")	polyolefin	OSB			
06 & 18	Stucco	None	2-asphalt	OSB			
07 & 19	Wood siding	19mm (3/4")	polyolefin	Plywood			
08 & 20	Stucco	None	2-asphalt	Plywood			
09 & 21	Wood siding	19mm (3/4")	polyolefin	Fiberboard			
10 & 22	Stucco	None	2-asphalt	Fiberboard			
11 & 23	Wood siding	19mm (3/4")	polyolefin	OSB		None	
12 & 24	Stucco	None	2-asphalt	OSB		None	
13 & 25	Wood siding	19mm (3/4")	polyolefin	Plywood		None	
14 & 26	Stucco	None	2-asphalt	Plywood		None	
15 & 27	Wood siding	19mm (3/4")	polyolefin	Fiberboard		None	
16 & 28	Stucco	None	2-asphalt	Fiberboard		None	
29	Wood siding	EPS foam filled	polyolefin	OSB		Polyethylene	
30	Wood siding		polyolefin	Plywood		Polyethylene	
31	Wood siding		polyolefin	Fiberboard		Polyethylene	

Note: 2-asphalt represents two-layer asphalt.

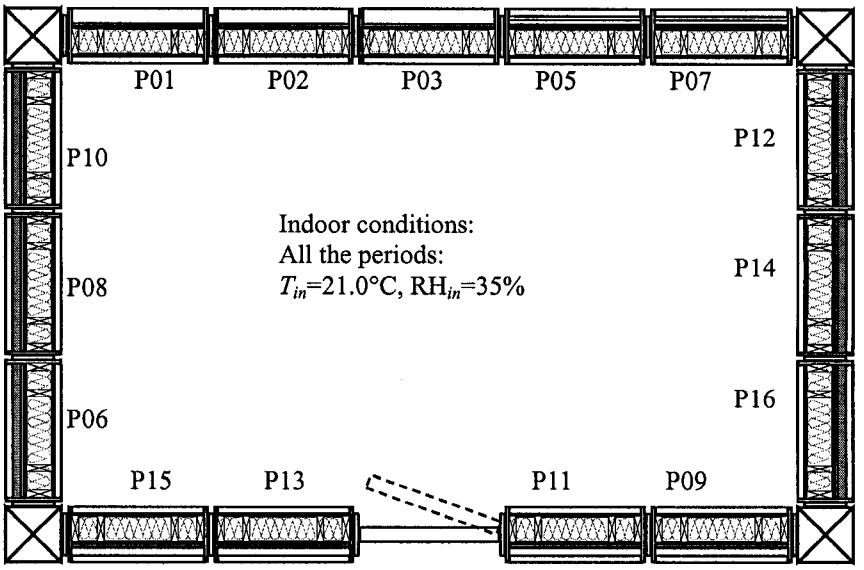

(a) Floor plan for 1st floor

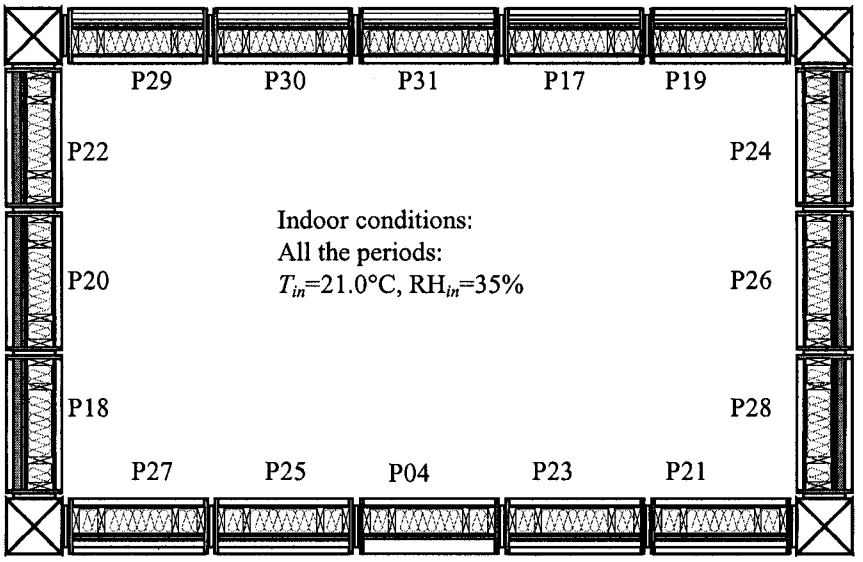

(b) Floor plan for 2nd floor

Figure 5.4. Layouts of specimens in both floors of test hut

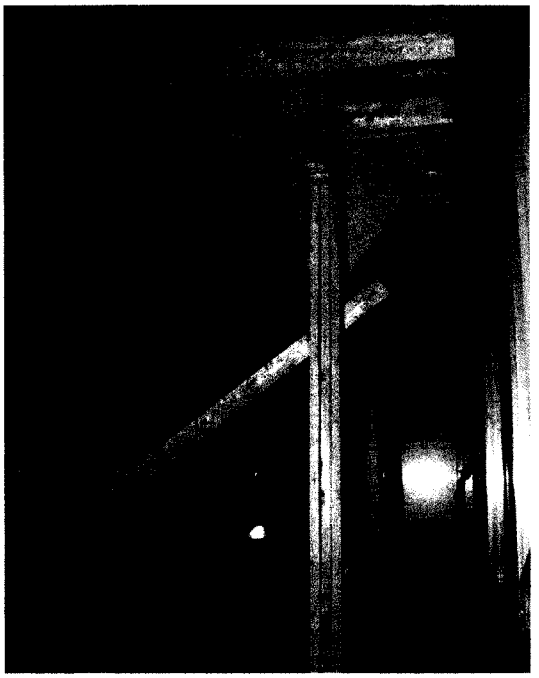

(a) building the frame of test hut

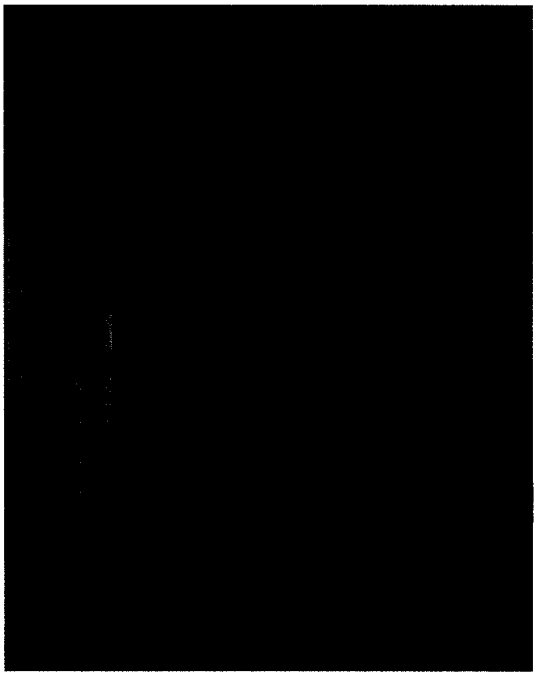

(b) installation of test specimens

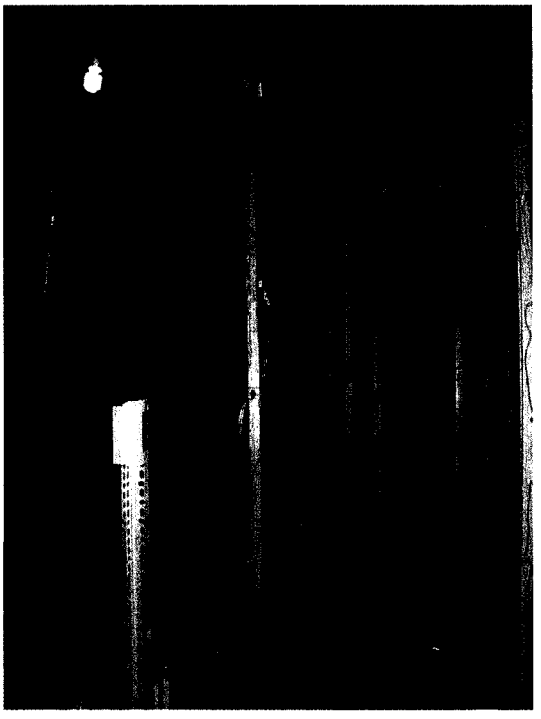

(c) filling of insulation into stud cavity

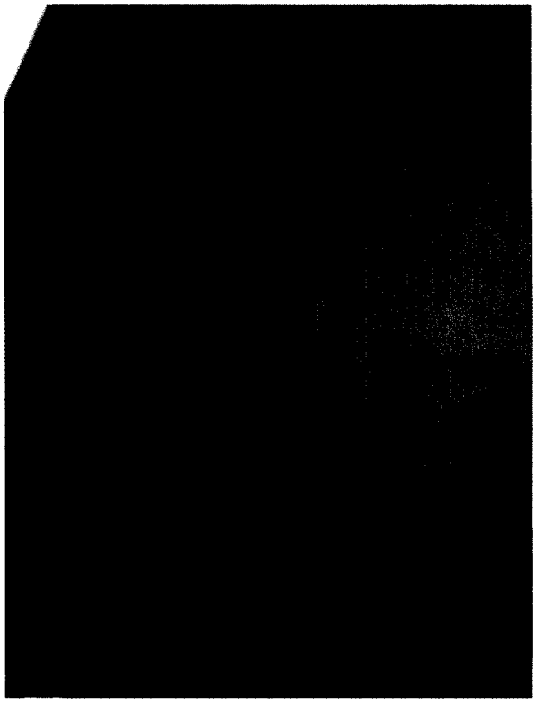

(d) stucco cladding with "access door"

Figure 5.5. Photos taken during test hut construction

Figs. 5.5a through 5.5d show some photos during the construction of test hut and the installation of test specimens.

5.2. Test periods and conditions

The construction of the test setup commenced in January of 2005. The test started on July 28-2005. On this day, the trays were filled with water. The main test consisted of five periods and lasted 283 days until April 30, 2006.

All the specimens were subjected to the same steady-state boundary conditions. Table 5.2 lists the test periods of the main test and the corresponding conditions maintained in the environmental chamber and test hut. The outdoor test conditions for each test period was selected from the weather year that had the 10% worst drying potential based on a monthly average drying index (DI) calculation from actual 31-year weather data of Montreal. The analysis and ranking behind the principle of outdoor condition selection were based on Candanedo et al. (2006). The indoor test conditions were based on a statistical analysis of winter weather conditions in Canada presented by IEA's (International Energy Agency) Annex 24 (Sanders 1996).

Table 5.2. List of test periods

Test periods #	Outdoor condition T [°C], RH [%]	Indoor condition T [°C], RH [%]	10% worst month of	Water exposure area	Duration [day]
Pre-condition 1	20±2 °C, 40%			0	>60
Pre-condition 2	8°C, 76%	21°C, 35%	October	0	20
Period 1				1/3	87
Period 2				2/3	113
Period 3	5°C; 69%		March	2/3	31
Period 4	12°C; 70%		April	1/3	29
Period 5	17°C; 68%		May	0	28

The pre-conditioning included two time periods during which the test hut was built, the specimens were placed at their locations, and instrumentations and equipment were installed. The aim was to allow all the materials to reach their EMCs (Equilibrium Moisture Content) under the same surrounding conditions. During the first period of pre-conditioning, the entire environmental chamber and the test hut was maintained at 20±2°C and 40% RH for about two months (from the middle of April to June 28).

The data acquisition system (DAS) started recording data one month before period 1 started on June 28; water was first introduced into the trays on July 18. During test periods 1 and 2, the test hut was subjected to constant indoor and outdoor conditions while the in-cavity moisture loading increased following 3 steps (no water, 1/3 evaporation area, and 2/3 evaporation area). In the meantime, the 10% worst month of October weather (which was in 1977) was maintained in the environmental chamber with the temperature at 8°C and the RH at 76% for 200 days (see Table 5.2). There was another 20-day short period of pre-conditioning, after completing the construction of test hut, but before adding of water into water tray. This second pre-conditioning period was intended to establish the evaluation baseline. Date analysis started from the day when water was first added into the center compartment of the trays that covered 1/3 of tray area. Period 1 of 87 days elapsed and it was followed by 113-day period 2 during which water covered 2/3 of tray surface area.

During test periods 3, 4, and 5, 10% worst weather for March, April, and May were maintained in the environmental chamber respectively (See Table 5.2), while the in-

cavity moisture loading was 2/3, 1/3 evaporation area and finally no water for the 3 periods respectively. The indoor test conditions remained unchanged at 21°C and 35% RH through test periods 0 to 5.

Only the data collected during periods 1 and 2 are analyzed in this thesis. Test periods 3, 4, and 5 were subjected to different outdoor climatic conditions from those in periods 1 and 2. Inclusion of the last 3 periods in developing an evaluation indicator is not suitable because their boundary conditions are different from the first 2 periods. Exploring the performance under various climate conditions is a large topic that is beyond the purpose and scope of this thesis research. Therefore, data collected during periods 3, 4, and 5 were not analyzed in this thesis. However, all the data were saved properly and can be used in future by others to facilitate their research.

The outdoor condition was controlled by the environmental chamber which was introduced in the preliminary test in Section 3.3.2.

For indoor conditions, there were two identical sets of equipment, one per floor, to maintain constant temperature and relative humidity. Fig. 5.6 shows one of the two sets of equipment for temperature and humidity control, which consisted of a humidifier, a dehumidifier, a heater, and a blower. The controls of the on/off of the equipment were achieved by a dedicated data acquisition system aside from the one used for the data collection.

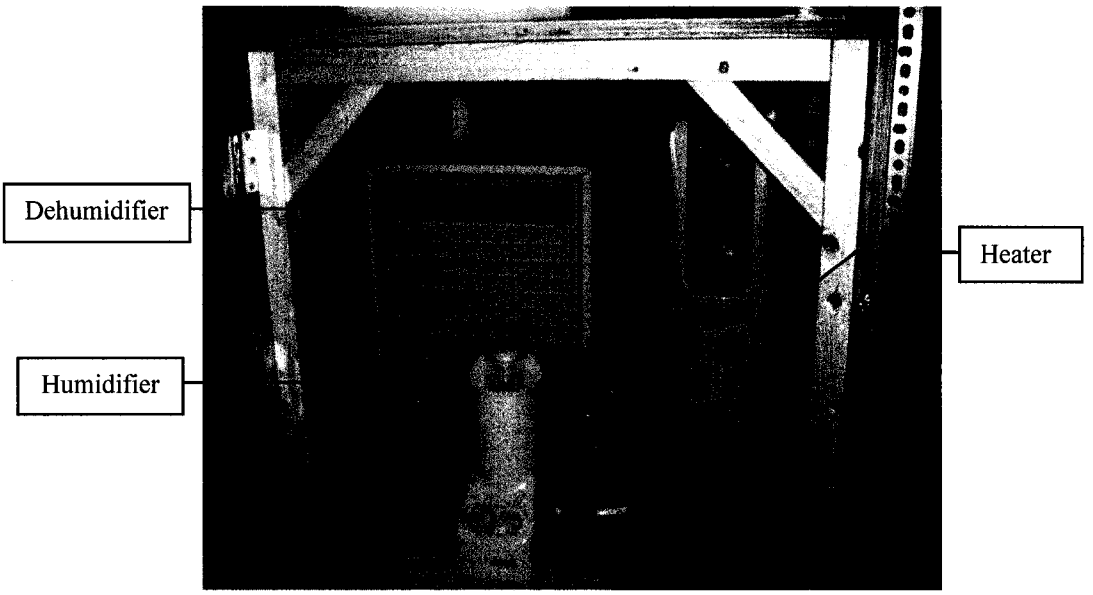

Figure 5.6. Temperature and humidity control system for a test room

5.3. Instrumentation and data collection

The instrumentation process involved the installation and calibration of sensors, the set up of devices, and the connection of DAS. There were a total of 1,007 different types of electronic sensors installed in the wall specimens, including 545 thermocouples, 66 RH sensors, 364 pairs of electric resistance moisture content probes and 32 load cells. Some additional sensors were also installed for monitoring and controlling the test conditions, e.g. chamber temperature and RH. In addition, 757 gravimetric samples were used for measuring the moisture contents at different locations on the sheathing (540) and on the studs (217) of the 31 specimens. Figure 5.7 is the schematic of sensor and gravimetric sample locations in the wall specimens.

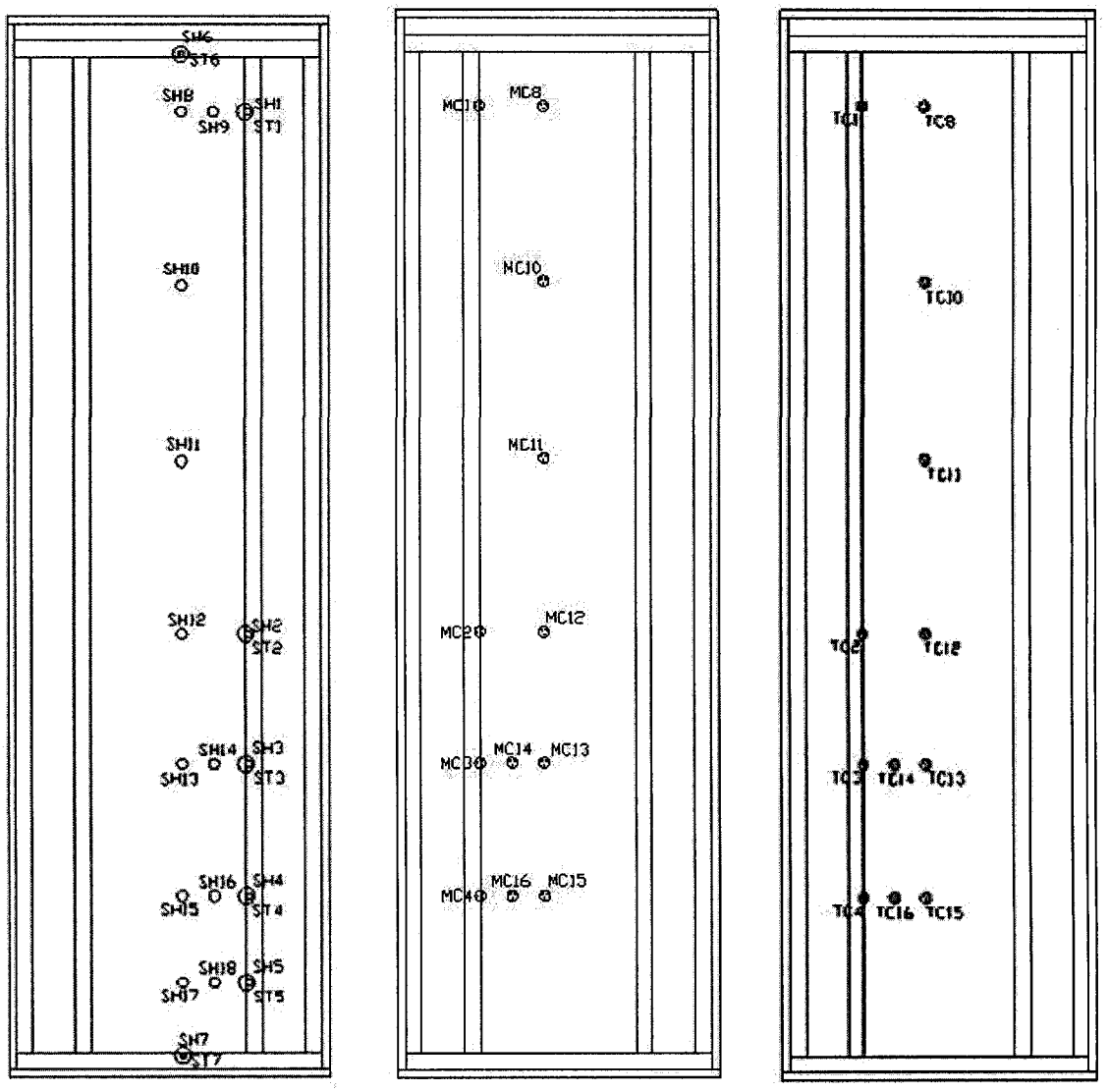

(a) gravimetric samples (b) moisture pins (c) thermocouples

Figure 5.7. Scheme of sensor locations (outside view)

5.3.1. Gravimetric samples

This thesis relied on gravimetric samples to measure the moisture content variations at the locations of interest. Electronic moisture content probes were also used in this study to monitor moisture content changes. There were two advantages associated with electronic moisture content pins: i) less disturbance to the cavity environment and ii) very

short measuring intervals, such as 10 minutes used in this test. However, the electronic resistive moisture content measurement has limitations: it is only suitable for a narrow range of moisture contents between 7% and 28%. Under 7%, the electrical resistance is too high and out of the range of the moisture content transmitters used in this test; above 28% or the FSP, the relation between the electronic resistance and the moisture content in wood becomes unreliable. This research aimed to explore the moisture limit states of wall assemblies, the moisture contents at locations of interests often exceeded the measurable range of the electronic moisture content measurement. Therefore, moisture contents measured by gravimetric samples were employed for the analysis in this thesis.

In the main test, there were two sizes of round gravimetric samples for the sheathing board and one size cubic samples for the stud. The hole for placing of a larger round sample with 38 mm (1 1/2") diameter allowed access to the vertical stud for picking up the cubic samples located on the stud. The smaller round sample was 25 mm (1") in diameter and the size of cubic sample was 13 mm × 13 mm × 13 mm (1/2" × 1/2" × 1/2"). Fig. 5.8 shows some of the gravimetric samples for three different sheathing boards.

The gravimetric samples from 18 locations on the sheathing and 7 locations on the stud for each panel were weighted once per week manually using an analytical balance (LA310S, Sartorius, 310 g capacity and accurate to ±0.1mg). More details concerning the gravimetric samples can be found in publications or reports of the experimental project, e.g. Alturkistani et al. (2008). Photos in Fig. 5.9 showed the process of collecting and weighing gravimetric samples.

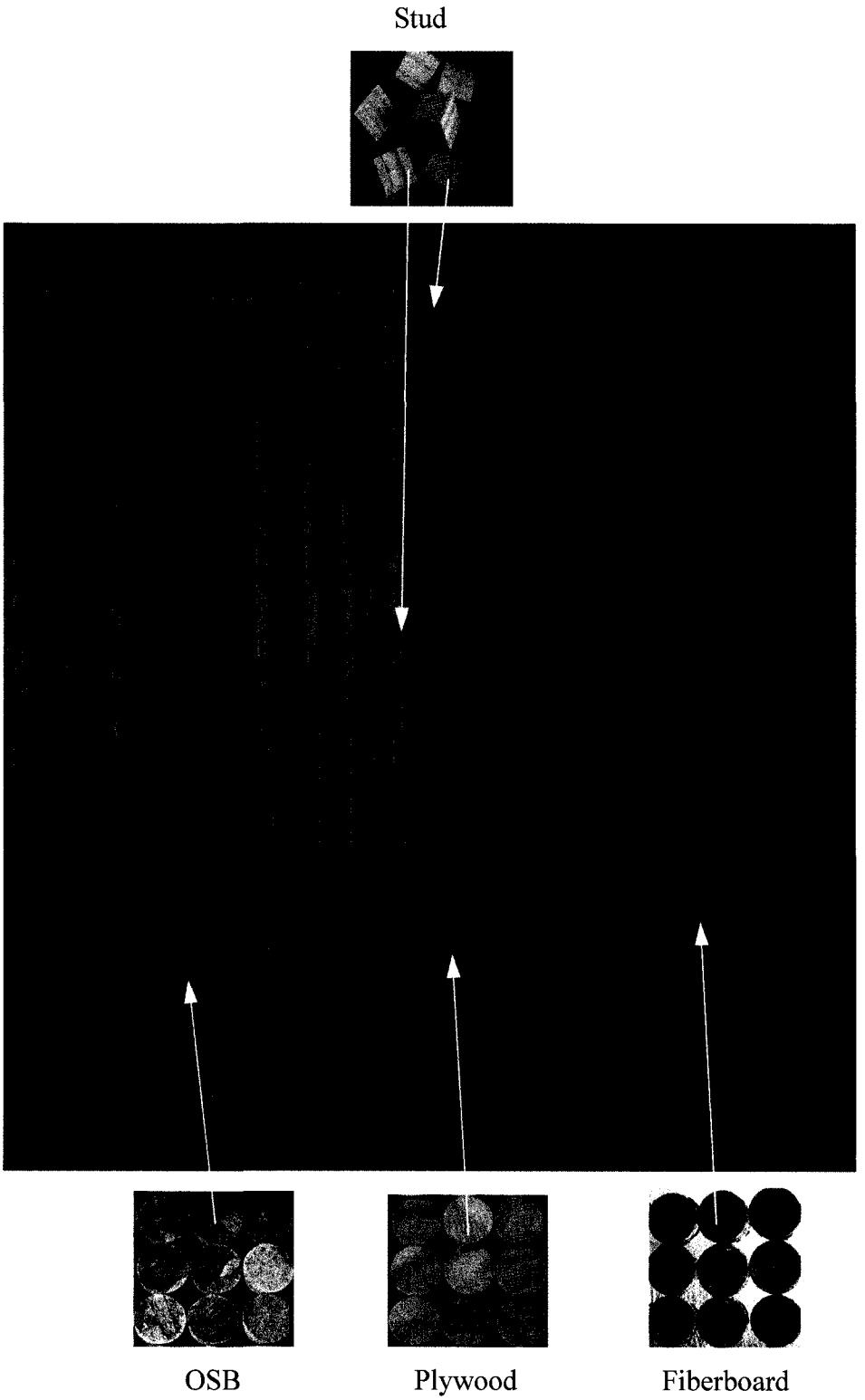

Figure 5.8. Gravimetric samples for different specimens

(a) "door" on the stucco cladding opened

(b) gravimetric sample picked up

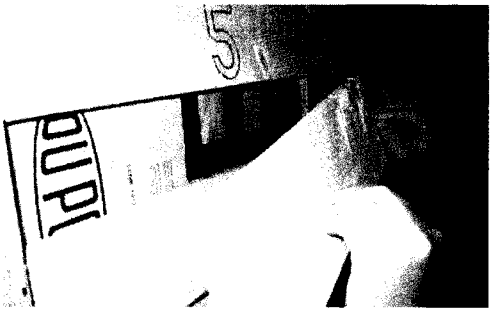

(c) a rung of wood siding was uncovered

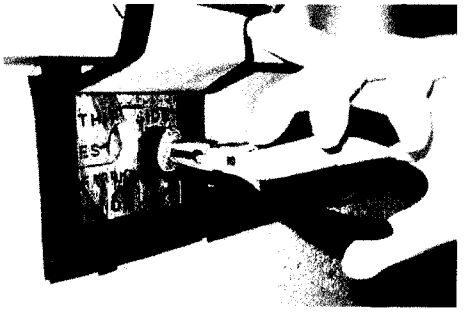

(d) a gravimetric sample was taken out

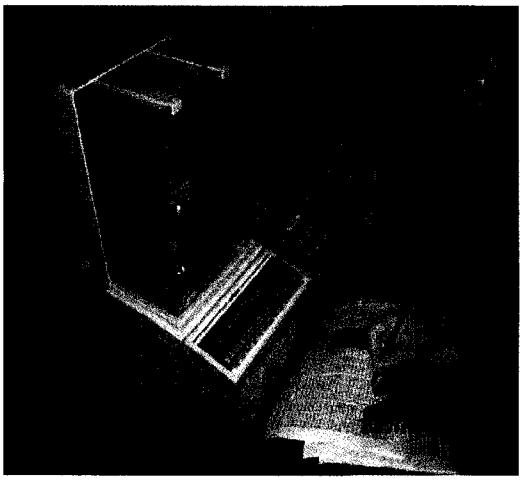

(e) gravimetric samples were weighed

Figure 5.9. Process for measuring of moisture content in gravimetric samples

5.3.2. Measurement of air leakage

Most of the air velocity measurements in previous studies focused on the air space behind the cladding where vent or ventilation was usually installed (Gudum 2003, van Straaten

2003). Measuring air velocity directly in the stud cavity with glass fiber insulation installed is more difficult because the air velocity is much lower. Four commonly used measurement approaches, including thermo anemometer (TA), tracer gas technique (TG), particle image velocimetry (PIV), and Pitot tube, were reviewed and excluded. These methods either do not have enough sensitivity or bring too much change in the testing environment.

Air leakage characteristics of the stud cavity of each wall specimens were estimated with the fan pressurization test. Fig. 5.10 shows the setup for the air leakage test. A pressure difference was maintained between the indoor air and the stud cavity by an air pump. The pressure difference between the stud cavity and exterior of the test hut were maintained at several values between zero and 75 Pa by adjusting the flow rate through a gate valve. The profile of pressurization had been recorded in pairs of data — air flow rate and pressure difference. After that, the reversed process of depressurization was recorded as well. Fig. 5.11 shows a pair of typical pressurization and depressurization profiles of specimen P20.

The equipment and instruments used in the pressurization test included:

- For air flow rate, in-line flow meter (LFE-laminar flow element, Meriam Instrument), range 100 CFM, output range 10" water accuracy ±0.8%;
- Pressure meter to measure LFE output: digital manometer, model HM28, by Nod-Tronic Instruments Ltd., range 10" water, ±0.2% full-scale;
- Pressure meter: pressure transmitter, PX655-0.5DI, range 125 Pa, accuracy ±0.3 Pa; and
- Pump: regenerative blower, Model R3105, Gast Manufacturing, Inc.

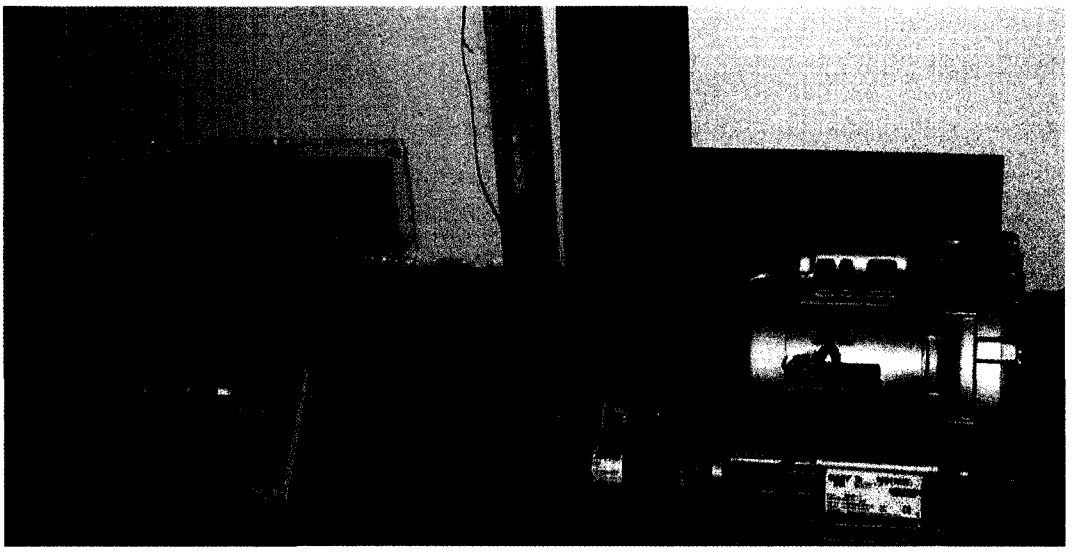

Figure 5.10. Pressurization and depressurization test for stud cavity

An additional procedure were undertaken to further identify the air leakage characteristics of the drywall. First a stud cavity was pressurized to 50 Pa (with respect to the exterior side of the specimen) while the door of the test room was open, an entire test room of the test hut was pressurized to 50 Pa using a blower door. The air flow rates at both the above two settings were measured and were found to be the same. Therefore, it was concluded that there was no measureable air leakage from the drywalls and all air leakage paths were on the exterior sides of the specimens.

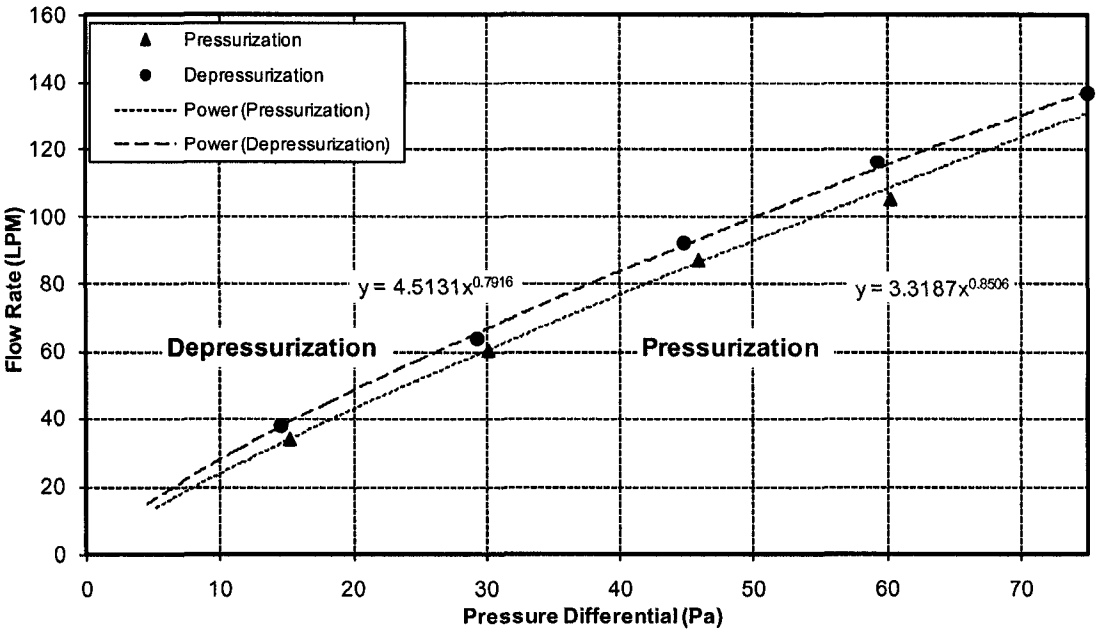

Figure 5.11. Pressurization and depressurization profiles for the stud cavity of P20

5.3.3. Data acquisition system (DAS)

Since extensive data were collected by a large number of sensors, the DAS was upgraded in the main test. The new DAS had more channels for input and output, to a capacity of 1,200 input channels and 22 output channels. The data from different types of sensors were allocated to three individual DACs (Data Acquisition Centers), numbered as DAC 0, DAC 1, and DAC 2. Each DAC had up to 11 slots which could host difference modules for data input or output. When possible, cables were used to facilitate and organize wires leading from sensors to the DACs. DOC 0, as shown in Fig. 5.12a, was placed outside the environmental chamber and was used only to collect data from moisture pins, load cells, and sensors for monitoring the conditions inside the environmental chamber and the test hut. DAC 1 and DAC 2 were in charge of collecting data from all the thermocouples and the relative humidity meters inside the stud cavity. To reduce the length of wires, DACs 1

and 2 were placed inside the test hut, one on each floor. Fig. 5.12b shows DAC 1 located on the first floor of the test hut.

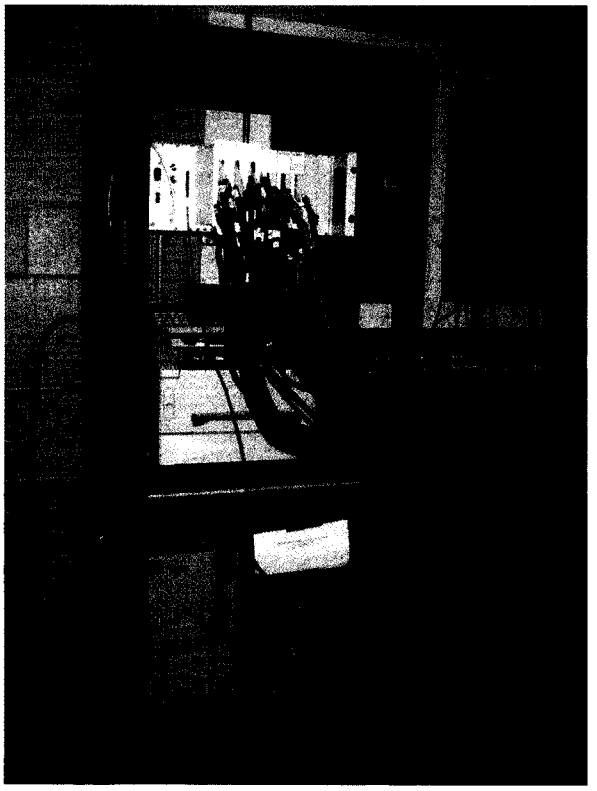

(a)

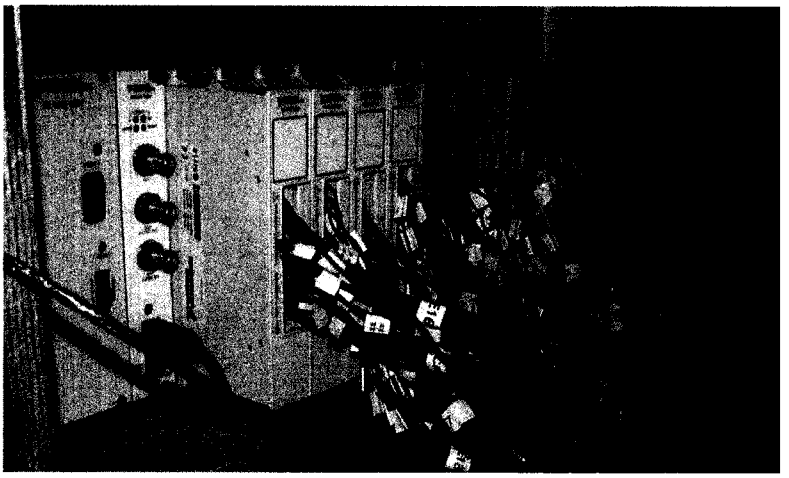

(b)

Figure 5.12. One of the DACs for collecting data from sensors

5.3.4. Sensor calibration

It was necessary to calibrate all the sensors and instruments to ensure the accuracies of the measured data. RH meters and load cells were calibrated before installation. Fig. 5.13 shows the calibration devices for RH meters (Humitter 50Y by Vaisala, ±3% and calibrated to 2% accuracy). Load cells (range 1 kg, accuracy ±0.25g) were calibrated with precision weights and/or against a precision scale (accuracy 1 mg); results indicated that all the sensibilities provided by the manufacturer were precise and did not need any correction. Calibrations of thermocouples (Type T, premium grade, special limits of errors, calibrated to ±0.3°C) were performed with all thermocouples installed in place, and the environmental chamber and the two test floors were maintained at one constant temperature at around 20±0.1°C for over 24 hours. The thermocouple readings were compared to precision RTD probes to obtain the correction factors for all individual thermocouples.

RH calibration chamber with a chilled mirror RH sensor, model RHCL by Omega Engineering, accuracy ±0.6% RH.

Figure 5.13. Calibration setup for RH meters

5.4. Water tray set up provides three levels of uniform moisture loading conditions

The water tray setup was used as in-cavity moisture loading. Fig. 5.14 shows a typical set of the water tray and load cell inside the stud cavity in the main test. The water tray design was similar to and improved upon that of the preliminary test described in Chapter 3. The general approach and layout remained the same. Load cells were placed under the water tray to monitor the moisture released from the water trays; the water tray and load cell set were located on the bottom plate; and a plastic net was employed above the tray to prevent tiny glass fibers drop into the tray (Fig. 5.15).

The improvements and changes over the set up for the preliminary test described in Chapter 3 were: more adhesive agent for gluing water tray, adjustable exposure areas in a water tray, machined parts used for supports of the water tray and load cell, elimination of the wick, more lightweight and robust design of the plastic net, and visible and controllable water refilling procedure. More details of the water tray setup concerning dimensions, compartments, air tightness of specimen, refilling procedure, and installation are presented next. The reliability of the tray system is discussed in the section 5.5.

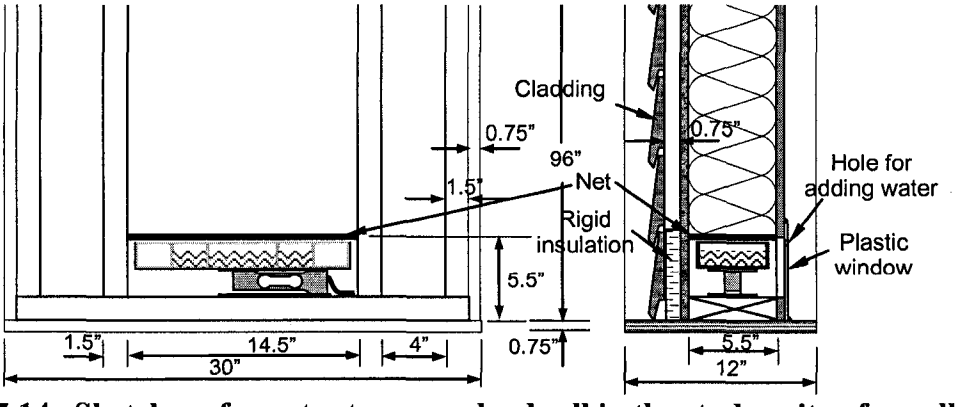

Figure 5.14. Sketches of a water tray on a load cell in the stud cavity of a wall panel

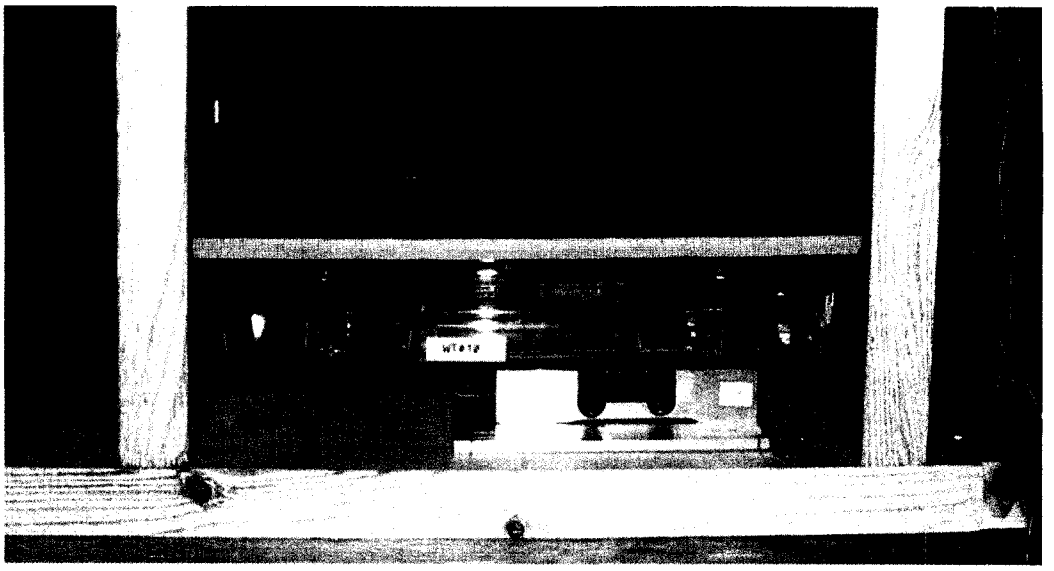

Figure 5.15. Net above the water tray inside panel 10 to prevent particles fall into the tray

5.4.1. Compartment design for water tray

The tray was made of 3 mm (1/8") thick clear acrylic sheets (Fig. 5.16a). The outer dimensions were 343 mm × 114 mm × 38 mm (13 1/2" × 4 1/2" × 1 1/2"), and it fitted well within the stud cavity. Each tray was divided into 5 compartments to provide three different levels of loading by activating 1/3, 2/3 and 3/3 of the tray surface area. Compartments 2 and 4 had half the surface area of compartment 3, and they were joined by a tube (a) to form the 2nd 1/3 area of the tray; similarly, compartments 1 and 5 also had half the surface area of compartment 3, and they were joined by tube (b) to form the 3rd 1/3 surface area of the water tray. With this compartment design, it was feasible to set the water surfaces to three different levels (1/3, 2/3 or full) to meet the requirement of the test. All water trays were pre-checked for water tightness. Fig. 5.16b shows the dimensions and a 3D rendering of the water tray.

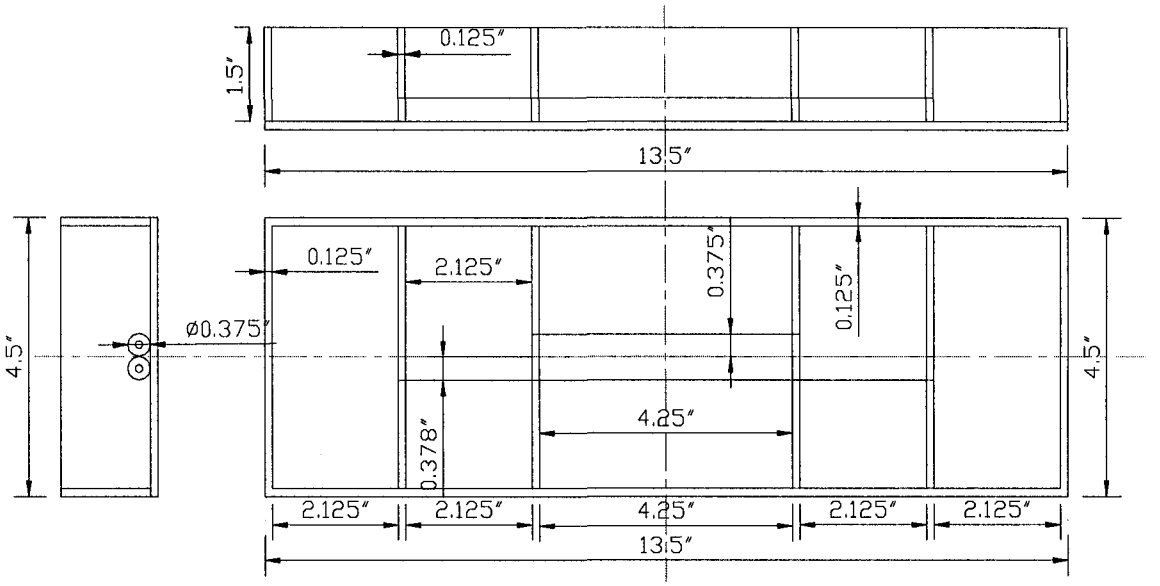

(a)

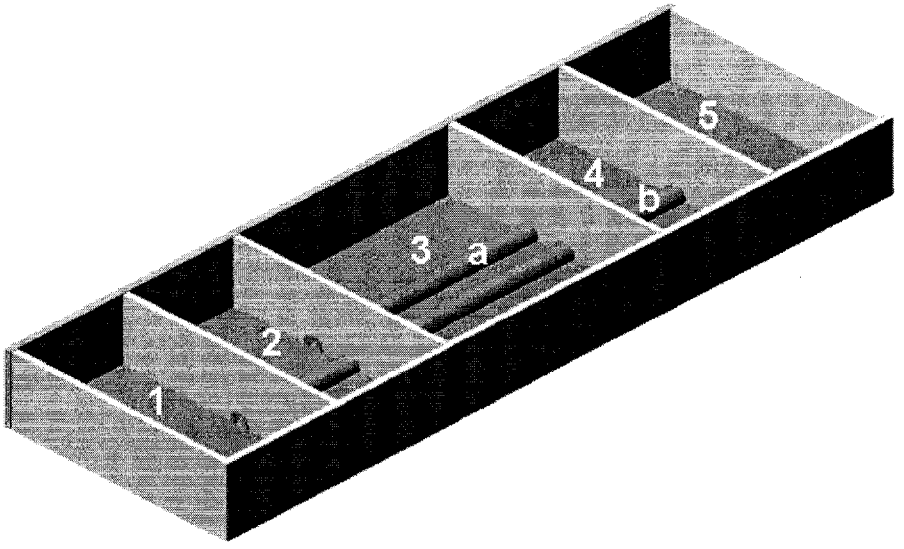

(b)

Figure 5.16. Water tray provides three level moisture loading conditions

(Proposed by P. Fazio, drawn by A. Alturkistani, made by Q. Mao)

5.4.2. Improvement of water tightness

The problem of water leakage, which was experienced in one tray of the preliminary test

presented in Chapter 3, was completely resolved by employing a new sealing compound. Instead of the silicon caulking used in the preliminary test, acrylic powder and acrylic liquid (which are frequently used in the dental repair or surgery) were used. Since the acrylic liquid can melt any acrylic material, the paste made by melting acrylic power in acrylic liquid can bond acrylic sheets very tightly and produce water tight joints. The paste consolidated quickly after the acrylic liquid evaporated. Fig. 5.17a shows a can of acrylic power, a bottle of acrylic liquid, and the tools for applying them. This sealing technique was applied in the main test from the interior side of the water tray. The resulting bonds were found strong enough to prevent any movement of the acrylic tray walls. Fig. 5.17b shows a tray with several acrylic joints. The water tightness of all the trays was thoroughly checked before they were placed into the wall specimens.

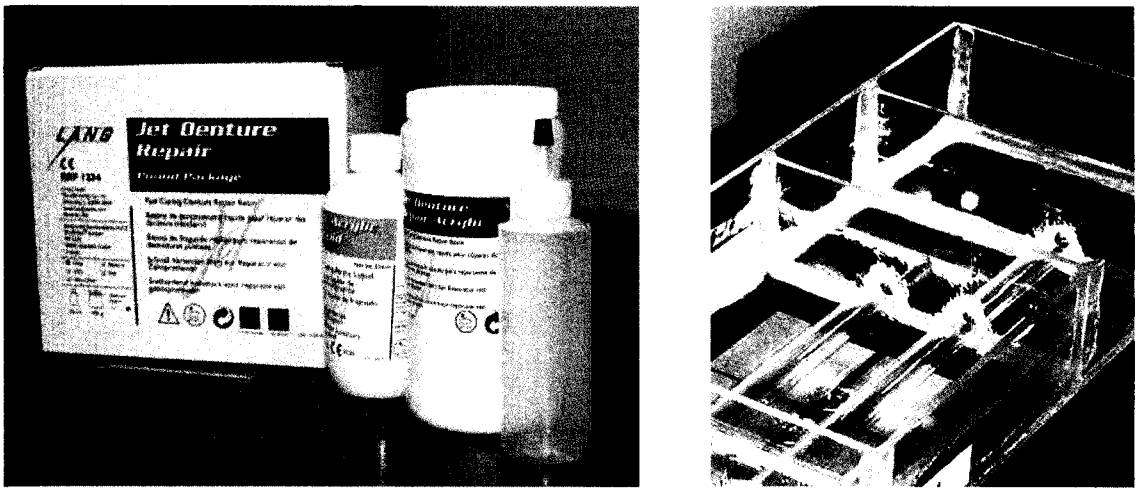

(a) (b)

Figure 5.17. Mixture of acrylic powder and liquid as bonding agent for water trays

5.4.3. Access window on drywall of wall specimens

The water tray and load cell system located in the stud cavity was accessible through an opening on the interior side of the wall. In addition, as the water tray were divided into

different compartments to realize different levels of loading intensity, it was necessary to observe and adjust the water level in each compartment. Therefore, a clear, acrylic sheet was used to cover the access opening and provide a window. The acrylic sheet was tightly fixed on the gypsum board by four sets of stretching bolts, which were anchored to the wood stud at one end and were fastened by wing nuts at the other end. Through the holes in the window, water could be injected into the tray. Fig. 5.18 shows the bottom part of a specimen after the water tray and load cell system was installed inside the cavity.

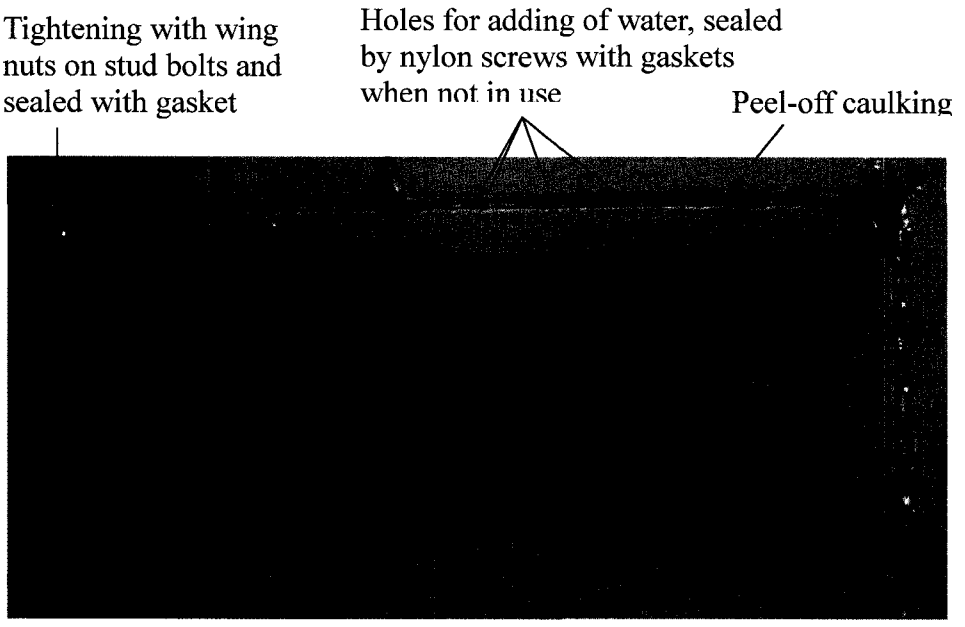

Figure 5.18. Water tray and load cell system on the bottom plate in the stud cavity of the wall panel

To eliminate any disturbance caused by air leakage, care was taken to ensure airtightness around the accessible window. The perimeter of the entire window was sealed with clear, peel-off caulking that could be easily removed to allow the opening of the window when necessary. The inlet holes (for adding water to the compartments of the tray) on the plastic window were sealed by nylon screws with gaskets during the test when not in use.

Airtightness was confirmed by an auxiliary test in which a mock up box contained the bottom portion of a wall specimen including an access window. An air pressure difference around 50Pa was applied across the accessible window, and a smoking source was placed inside the stud cavity. No leak was observed around the perimeter of the acrylic sheet or through the tightening bolts. Fig. 5.19 shows a photo taken during the airtightness check.

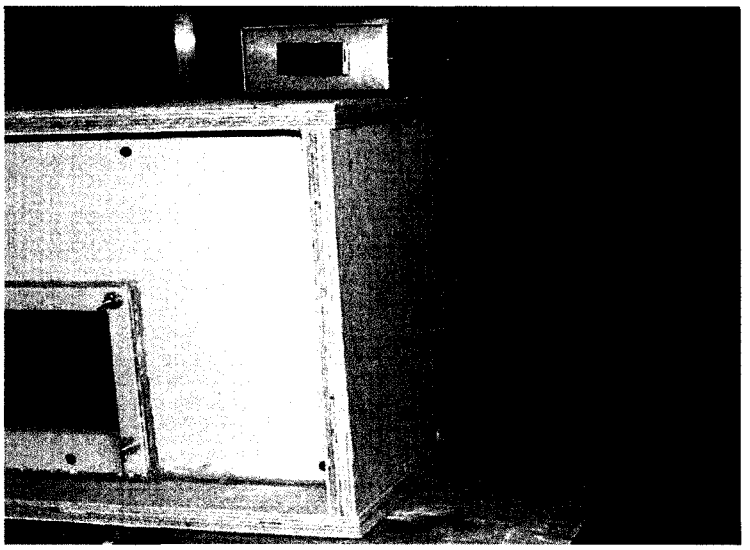

Figure 5.19. Smoke visualization for airtightness of access window

5.4.4. Test procedure for refilling water

Water could be added by several small flexible tubes that were connected to 60-ml syringes. Because these flexible tubes could be removed after water was added, one set could be shared by several neighboring specimens. In total, there were eight sets of refilling devices, four sets for each floor. The syringes were fixed at the mid height of the test specimen from where water could easily flow into the trays under the artesian head. Fig. 5.20a is a photo of the 60-ml syringe. Fig. 5.20b shows the flexible tube as well as the hole in the acrylic sheet window. Fig. 5.21 shows the complete procedure to refill the

trays.

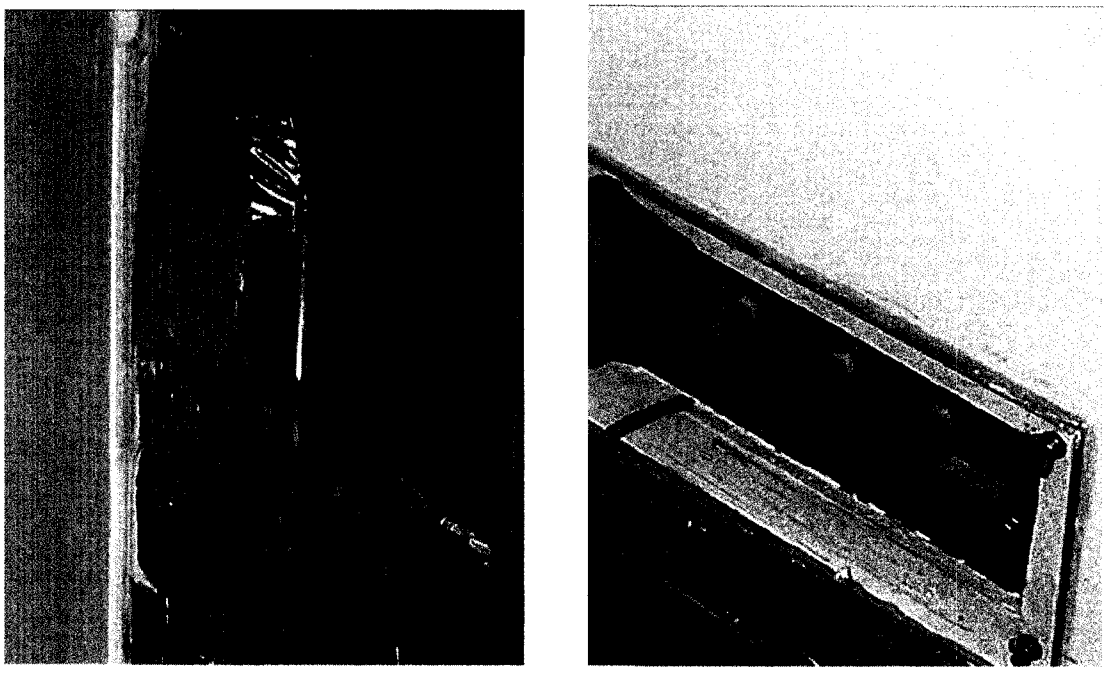

(a) (b)

Figure 5.20. Setup for adding water

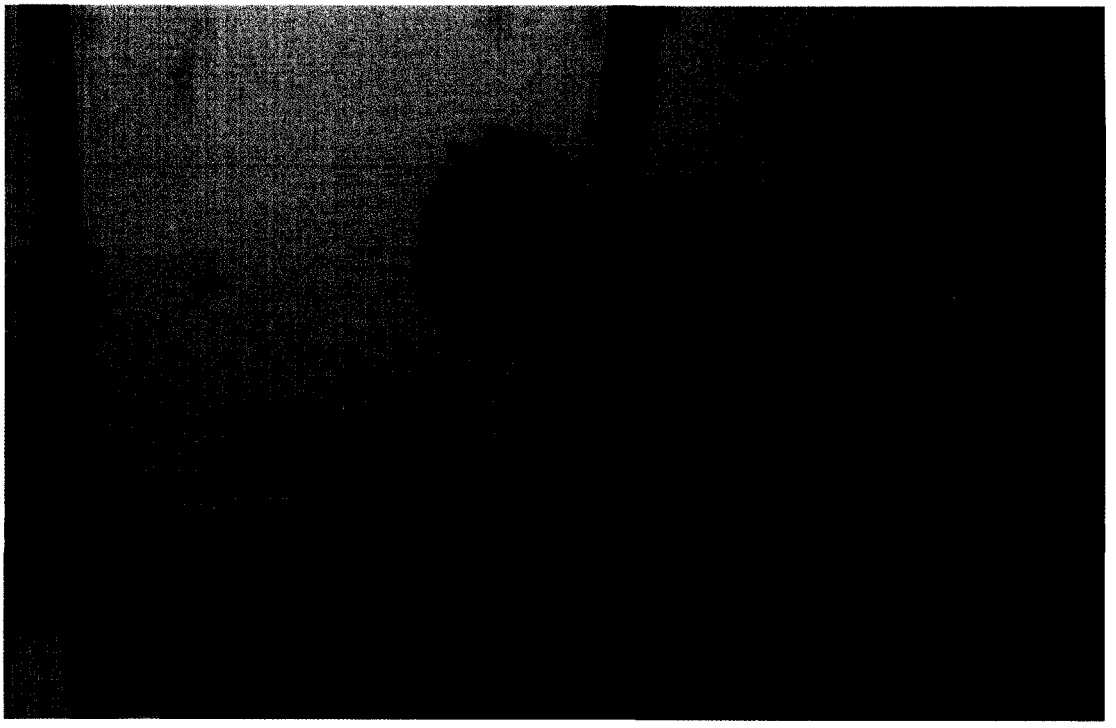

Figure 5.21. Photo taken during water refilling

The water level should be maintained above the height above the interconnecting tubes on the bottom to prevent the change in exposure area, but not too high as to exceed the load capacity of 1000 g of the load cell. Lines in colors were engraved on the side of the tray and were visible through the access window. The green lines indicate the minimum water level for each compartment. The red lines indicate the maximum water level for each compartment when fully evaporation area was applied to keep total weight below 1000 g. The blue lines indicate the maximum water levels when 1/3 or 2/3 evaporation area was applied in the middle compartments of the tray to keep total weight below 1000 g. The blue lines allow more water to be filled into water tray thereby reducing the times of refilling, but they can only be used when two side compartments 1 & 5 are dry.

The total mass of one water tray system included the mass of the dry tray and attachment to the load cell (including metal sheet for supporting, retaining screws and double side sticker) and the water inside the tray. The net mass of each dry tray was less than 350 g and the mass of the plate to support the tray on the load cell was no more than 90 g. Each 1/3 of water evaporation area is 116.5 cm^2 (18.0625 in^2). Table 5.3 demonstrates the

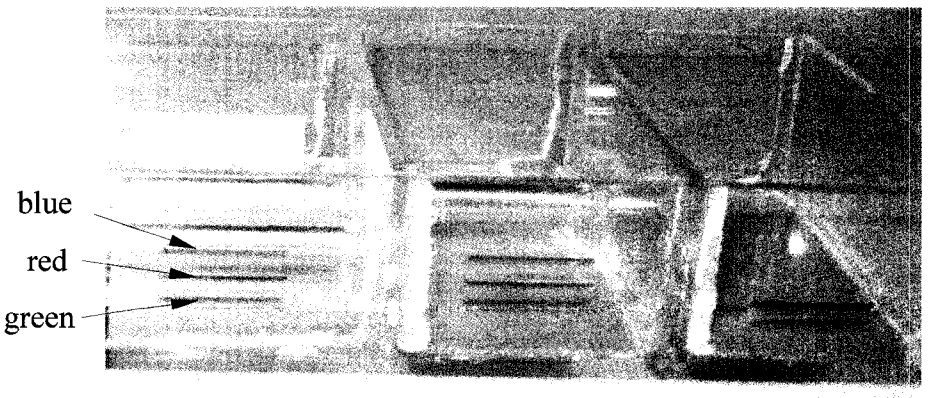

Figure 5.22. Three color lines to indicate maximum and minimum water levels in water tray

verification of the capacity of the load cell when water tray was filled with water. Fig. 5.22 shows the colored lines on the wall of the acrylic tray.

Table 5.3. Verification of load cell capacity

Evaporation area / Components		1/3 area (116.5cm^2)		2/3 area (2×116.5cm^2)		Full area (3×116.5cm^2)	
		Individual	Cumulative	Individual	Cumulative	Individual	Cumulative
Dry tray		350		350		350	
Screws and double side tapes		90	440	90	440	90	440
Water up to min.	Green line (13mm for middle compartments; 10mm for side compartments.)	151	591	2×151	742	2×151 +111	853
Water between max. and min.	Blue line (10mm)	117	708	2×117	976		
	Red line (4mm)					3×47	994

5.5. Reliability of water tray system

The test in the current study used water trays to provide uniform and consistent moisture loading in the stud cavity. The system played two roles; the tray provided the in-cavity moisture source, while the load cell measured the evaporation rate. For such a new wetting method, reliability verification was necessary to guarantee that it would function properly in these two aspects:

Uniformity

The loading should be uniform for all tested wall specimens. Therefore, the water trays subjected to the same microclimatic conditions should have the same evaporation rate.

Ability to distinguish

The evaporation rates should be able to recognize the differences between different specimens.

5.5.1. Free water evaporation process

Water evaporation can be interpreted as a complex interaction between water and its environment. Many studies have focused on the natural evaporation from large open areas of water bodies such as lake, pond, river, etc. (Sartori 2000, Singh and Xu 1997, and Tang and Etzion 2004). Only a few investigations were targeted at the evaporation from a pan or a tray surrounded by still air or low speed air movement (Bansal and Xie 1998, 1999; and Reading and Reiser 1977).

For the case of a water source surrounded by still air, a simplified expression to calculate the water evaporation rate was proposed by (Bansal and Xie 1998) as:

$$\dot{E} = -Dv \cdot Aw \cdot \frac{\rho_{av} - \rho_v}{b} \tag{5.1}$$

where $\dot{E}$ [kg/s] is the rate of water evaporation; Dv [m^2/s] is the diffusivity of water vapor; ρ_{av} [kg/m^3] is the density of water vapor mixed with air; ρ_v [kg/m^3] is the density of saturated water vapor; b [m] is the distance between the water surface and a specific sampling point above it, and Aw [m^2] is the free water surface area. For still air, ρ_{av} depends on both ρ_v and relative humidity, whereas ρ_v is a function of water surface temperature.

Incropera and de Witt (1996) included the effect of air movement around the water source by introducing a mass diffusion coefficient, $\overline{h_D}$ [m/s]:

$$\dot{E} = \overline{h_D} \cdot Aw \cdot (\rho_v - \rho_{av}) \tag{5.2}$$

$$\overline{h_D} = \frac{Dv}{B} \cdot 0.0296 \cdot Re^{4/5} \cdot Sc^{1/3} \tag{5.3}$$

where Re is the Reynolds number, Sc is the Schmidt number, and B [m] is the characteristic length. The mass diffusion coefficient, $\overline{h_D}$, is a comprehensive coefficient that reflects the influence of air movement patterns around the water source; however, there is no easy way to determine its value under unsteady conditions.

Although Eqs. 5.1 and 5.2 cannot be directly applied to the analysis of evaporation from the water trays used in this research, they provide a list of factors that may influence the water evaporation from the trays, such as water temperature, surrounding air flow, temperature and relative humidity inside the stud cavity, and water surface temperature. The influences of most of these factors have been examined by Sartori (2000). For instances, Fig. 5.23 shows the impact of water temperatures on the evaporation. The lines in the figure were calculated based on several well-known empirical correlations or theoretical equations that calculate the evaporation rate from free water surface, given air velocity at 3m/s, temperature difference between water and air at 5°C and RH of 100%. Noticeable variations in evaporation rate can be observed when applying different empirical equations.

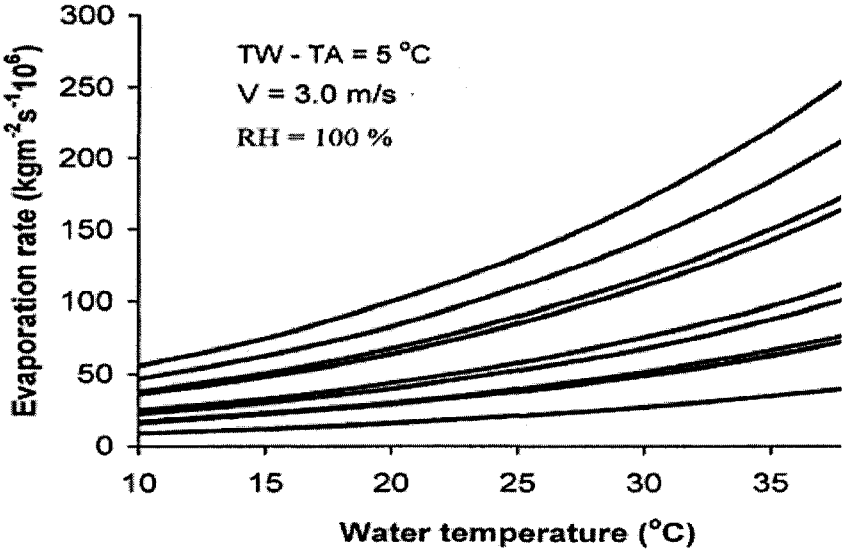

Figure 5.23. Impact of temperature on evaporation rate, based on several empirical correlations and theoretical equations

(Adopted from Sartori 2000)

5.5.2. Auxiliary test for evaluating influential parameters on evaporation

The results from the existing empirical and theoretical studies, however, cannot be applied to the water trays in stud cavities. An auxiliary test was carried out to identify factors affecting the evaporation from the water trays. The trays were placed in the environmental chamber where temperature and RH were controlled to those similar to the working conditions inside wall cavities.

During the test, the air temperature of environmental chamber was controlled between 20 to 24°C and RH between 30 to 35%. Three different sizes of water surfaces were tested namely 1/3, 2/3, and full surface of the water tray. Thirty-eight water trays were arranged on the floor to minimize the impact of air flow. Sensors were placed near the four corners of the region of trays to monitor the air temperature and RH variation in the space (as shown in Fig. 5.24). In order to produce a uniform field of temperature and RH, two fans

were used to create air circulation, whereas the air movement was not directed toward the trays.

A scale (± 0.1g accuracy) was used to manually weigh trays daily. The weighing was not performed at exactly 24 hour intervals. The exact time of the weighing operation for each tray was recorded. The daily evaporation rate can be calculated as following:

$$\overline{E} = \frac{24 \times \Delta W}{\Delta t} = \frac{24 \times (W_2 - W_1)}{t_2 - t_1} \tag{5.4}$$

where $\overline{E}$ is daily evaporation rate [g/day], W_1 is initial weight of the tray with water [g], W_2 is final weight of the tray with water [g], and $\Delta t = t_2 - t_1$ is the time interval between the two weighing operations [hr].

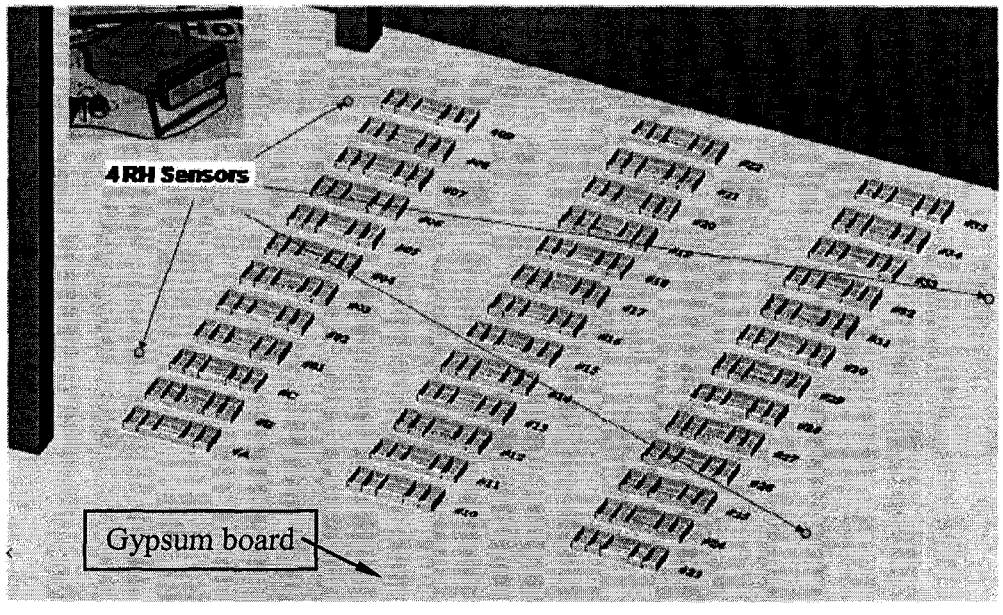

Figure 5.24. Array of trays inside environmental chamber

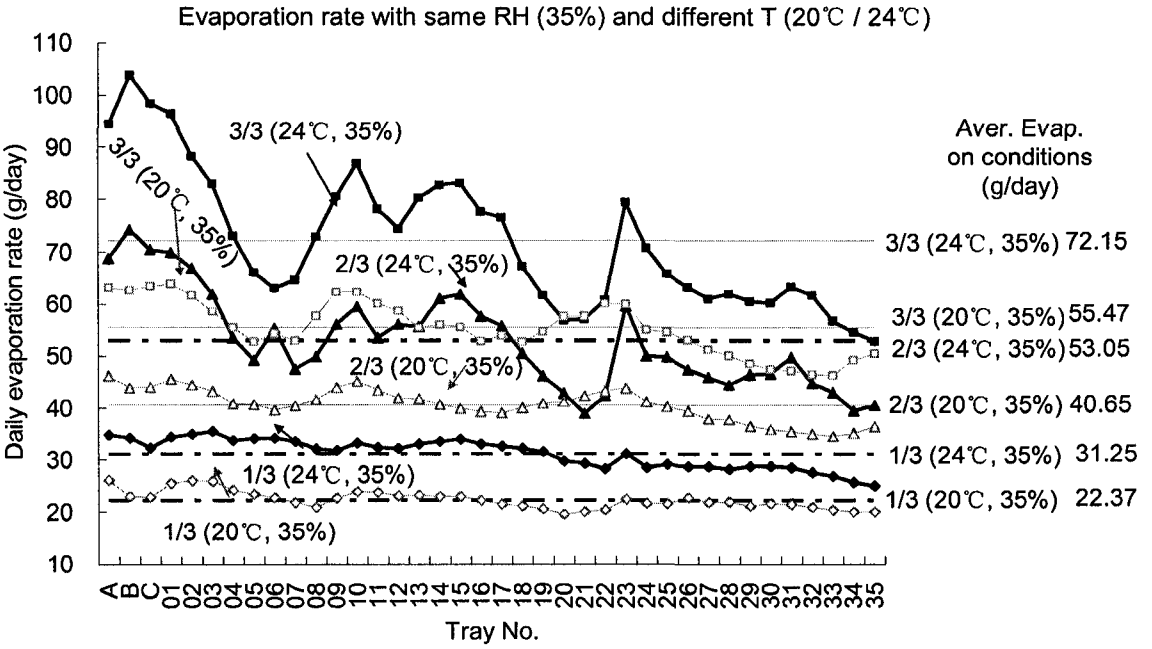

Figure 5.25. Influence of temperature on evaporation rate

(Evaporation rate at different temperature and at a constant RH)

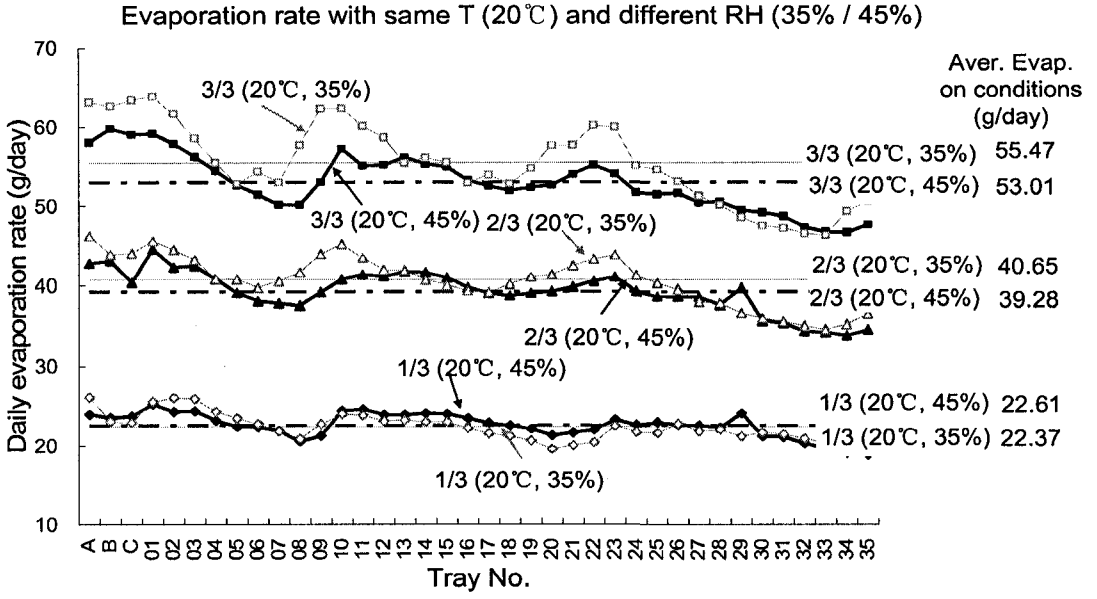

Figure 5.26. Influence of RH on evaporation rate

(Evaporation rate at different RH and at a constant temperature)

The main observations and conclusions from these results are:

- *Air temperature has a greater influence on the evaporation rate than RH.*

  For the same RH at 35%, the daily average evaporation rate at 24°C was higher than that at 20°C by 30.1% for the full surface area of the water tray, by 30.5% for the 2/3 area and by 39.7% for the 1/3 area (see Fig. 5.25). In contrast, at the constant 20°C temperature, the evaporation rate at 35% RH was higher than that at 45% RH by only about 4.6% for the full surface area of the tray, by 3.5% for the 2/3 surface area and by 1.1% in the case of the 1/3 surface area (see Fig. 5.26).

- *Local air movement conditions around trays significantly affect the evaporation rates.*

  The large variations in the evaporation rates among water trays were observed in Fig. 5.26. Since the main differences among trays were airflow patterns and speeds, the observation variations among trays indicate that the location of water trays significantly affected the evaporation rates.

  To maintain a uniformity of both temperature and relative humidity inside the environmental chamber, the air inside chamber was moving between the heating and cooling devices. This air movement generally was location related. Hence, the location related evaporation patterns indicate that the evaporation rate of the water trays was sensitive to air movement.

- *Evaporation rate is not linear to the water surface areas.*

  In all cases, the evaporation rate increased less than 100% when the water surface doubled, which indicates that the increases in evaporation and in the surface area of the water are not proportional to each other. This may due to the fact that, when

the surface area was doubled, the humidity in the air above tray increased and thus became higher than that in the case with less surface area. Such an increase in the ambient air humidity reduced the evaporation potential.

Nevertheless, the evaporation rates did increase greatly with the exposed water surface areas. Therefore, the same water exposure areas of the trays must be maintained throughout a given test to ensure the uniformity in the moisture loads.

5.5.3. Auxiliary test for verifying consistency of water trays

The application of the in-cavity moisture load by the water tray system was based on a basic hypothesis that if the trays are placed under identical conditions, the rate of water evaporated from one tray should be the same as that from another tray. This consistency hypothesis was verified through another auxiliary test which could be seen as a calibration test (Fazio et al. 2006b).

The calibration test was intended to determine whether or not two identical water trays would generate equal evaporation rate when subjected to the same microclimatic conditions. In the test, two trays were placed in a small box as shown by Fig. 5.27. Temperature and RH outside this box ranged from 24°C to 26°C and from 35% to 45%, respectively. A small gap (5 mm or 3/16") at the bottom was located along the perimeter of the box to allow convection and water vapor diffusion. Because the box space was small (16" × 20" × 18"), the temperature and RH in it was assumed to be uniform. Though air velocity was not monitored, it was considered to be very low.

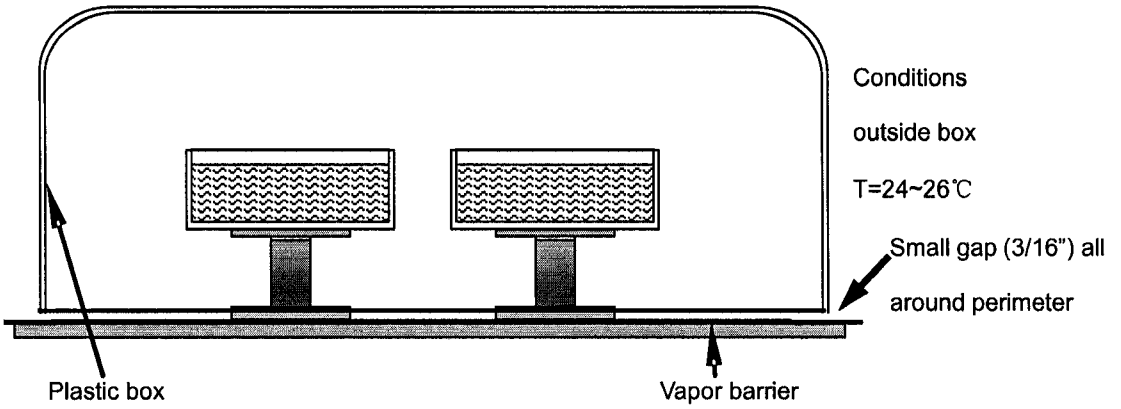

A small box with a low air exchange to the exterior provides the same environmental conditions for two trays with same water surface areas

Figure 5.27. Two trays in the calibration box

Fig. 5.28 shows the cumulative evaporation amounts from the two trays. The slopes of the curves indicate the evaporation rates. The evaporation rates were 1.259 g/hr (30.21 g/day) and 1.342 g/hr (32.21 g/day) for tray 1 and tray 2, respectively. The average value was 31.21 g/day with a deviation of only 3.2%. Repetitions of the test produced similar results. Hence, it could be concluded that, under similar conditions and when air movement is negligible, the evaporation rate of the water tray remains constant and this water tray method can be used as a consistent moisture source.

The preliminary test acquainted the author with the performance of the water tray and load cell system. The measurement results recognize the differences in evaporation between different specimens under the same environmental conditions and with the same water exposure area. More sophisticated verification is presented along with the data analysis in the main test (see next Chapter).

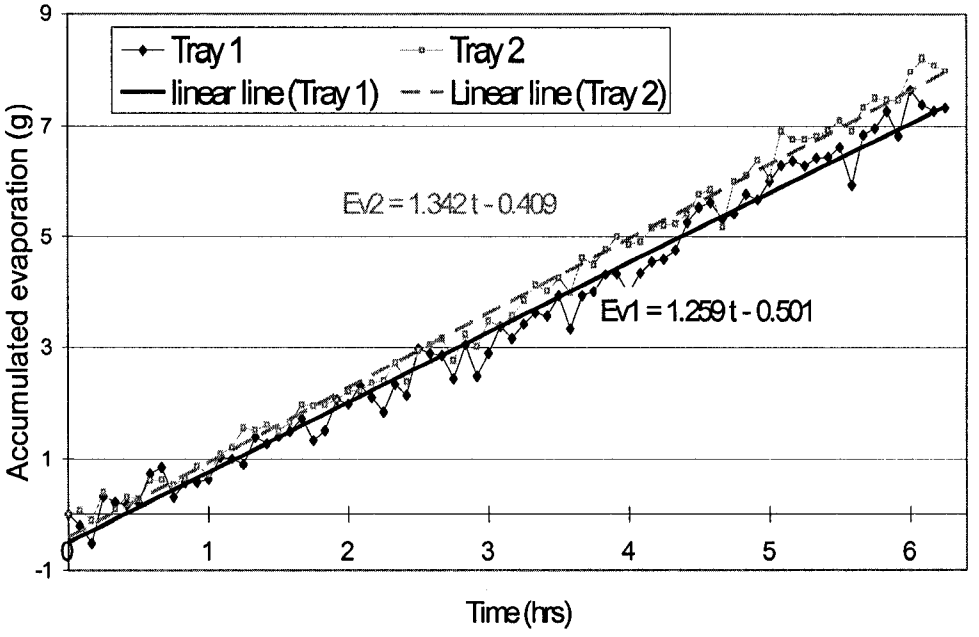

Figure 5.28. Evaporation rates of two trays in a low air velocity environment

Chapter 6
Test Results, Comparative Studies and Limit State Verification

In this chapter, the new methodology proposed in this thesis research and developed in previous chapters is applied to the data obtained from the long-term experiments on 31 full-scale wall assemblies. The application includes the following:

1. Establishing the accumulative evaporation profiles and the Drying by Evaporation Index (DEI) values for all the 31 tested specimens; Further observation of the sensitivity of DEI with respect to different specimens and different wall configurations;
2. Estimating load-response profiles and finding out the similarity and dissimilarity between two duplicate specimens;
3. Determining the newly proposed In-Cavity Evaporation Allowance (ICEA) for all the tested specimens;
4. Comparative studies for different wall configurations by using ICEA as the indicator; and,
5. An example to show how the LSD based verification procedure works.

6.1. Measured moisture loads as DEI

The amount of water evaporation from the water tray is influenced by the characteristics of wall configurations and by the test conditions; and the rates reflect the characteristics and relative drying capacities of the different wall systems that are tested under the same indoor and outdoor conditions. Therefore, the evaporation rate has been defined as the Drying by Evaporation Index (DEI) in Section 3.1.

The profiles of the cumulative evaporation vs. time (E~t) of selected wall assemblies are plotted to depict the behaviors of the in-cavity moisture loading. Fig. 6.1 shows the accumulated evaporation profiles in three panels 17, 19 and 21. These panels, together with the rest of the 31 specimens, were subjected to the same steady-state boundary conditions. During test periods 1 and 2, T=21°C and RH=40% for indoor and T=8°C and RH=76% for outdoor. The water evaporation areas were set at 1/3 of the tray in period 1 and 2/3 in period 2.

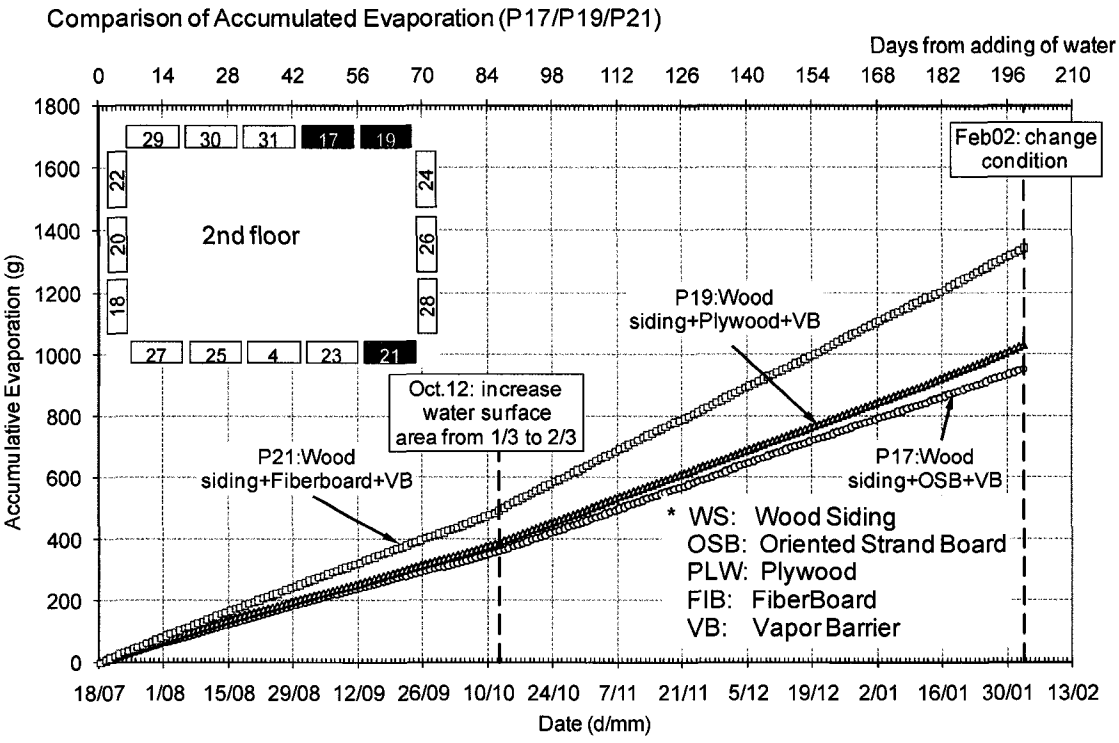

Figure 6.1. Accumulated evaporation rate in periods 1 and 2

DEI, the slopes of these profiles, is determined by curve fitting. The solid lines in Fig. 6.2 are the results of linear fitting of the accumulative evaporation profiles for two duplicate specimens P07 and P19. Furthermore, DEI values estimated for all the 31 tested specimens are listed in Table 6.1.

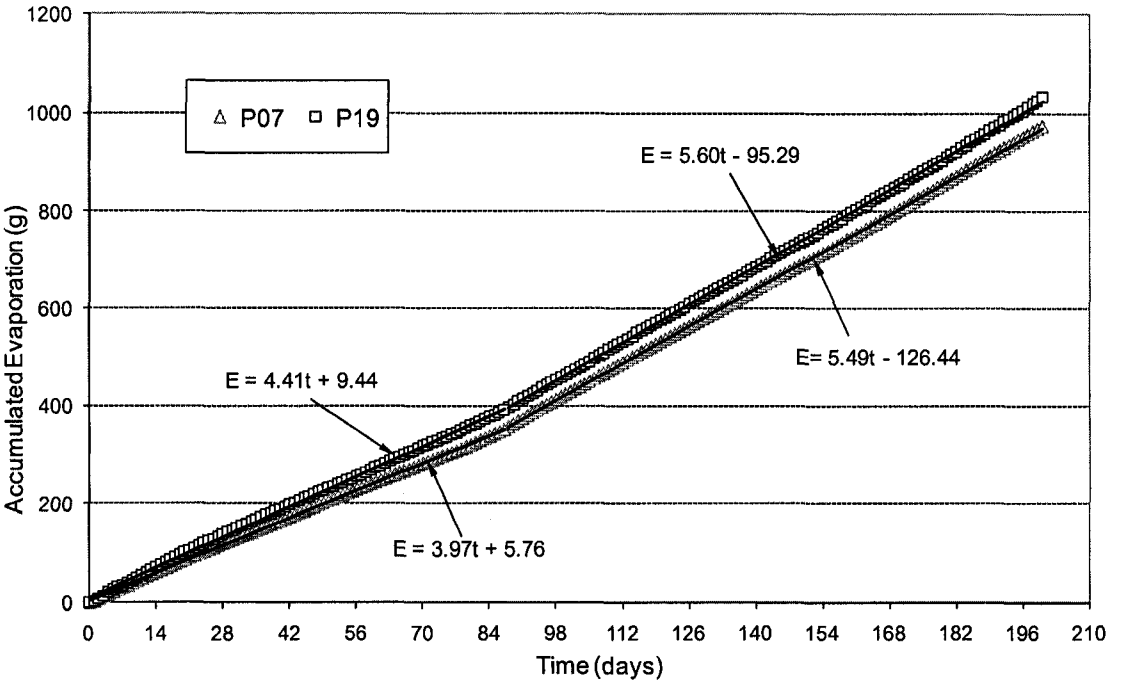

Figure 6.2. Fitting lines of accumulative evaporation profiles for P07 and P19

Table 6.1. Measured DEI for all 31 tested specimens during periods 1 and 2

Wall configurations	Floor #	Panel #	DEI [g/day]		Floor #	Panel #	DEI [g/day]	
			Period 1	Period 2			Period 1	Period 2
WS+OSB+VB	1	P5	4.44	5.65	2	P17	4.12	5.26
WS+PLW+VB		P7	3.93	5.49		P19	4.41	5.6
WS+FIB+VB		P9	6.47	9.07		P21	5.65	7.48
ST+OSB+VB		P6	5.53	6.95		P18	3.71	4.81
ST+PLW+VB		P8	6.1	8.7		P20	3.71	5.36
ST+FIB+VB		P10	5.07	7.35		P22	4.9	6.7
WS+OSB+NVB		P11	4.3	5.78		P23	5.02	6.18
WS+PLW+NVB		P13	4.82	6.51		P25	4.49	6.04
WS+FIB+NVB		P15	4.77	6.22		P27	5.44	7.06
ST+OSB+NVB		P12	4.76	6.51		P24	4.87	6.1
ST+PLW+NVB		P14	5.02	6.52		P26	4.87	6.72
ST+FIB+NVB		P16	5.39	7.89		P28	6.15	8.49

Note: ST=Stucco, WS=Wood siding, OSB= Oriented Strand Board, PLW=plywood, FIB=Fiberboard, VB=vapor barrier, NVB=no vapor barrier.

Based on the E~t profiles and the estimated DEI values, the following observations can be made:

1. When the water exposure area and the boundary conditions remained constant during a period of testing, the evaporation profiles of the specimens obtained from the main test approached straight lines during the period of interest;
2. In the main test, all the evaporation profiles underwent a noticeable shift when the water exposure surfaces were increased from 1/3 to 2/3 of the total water tray area;
3. Large difference can be found between the DEI values obtained from some duplicate specimens. For example, the DEI values of P8 were 6.10 g/day and 8.70 g/day in test periods 1 and 2, respectively; in contrast, the DEI values of P20 (the duplicate specimen of P8) during these two test periods were 3.70 g/day and 5.60 g/day. The relative deviations were found to be 24.4% and 23.8%.

From the above observations, the following conclusions can be drawn:

1. For a wall specimen with a water tray of specific water exposure area and subject to steady-state boundary conditions, DEI remains a constant and reflects the magnitude of the drying performance of the wood-frame wall system;
2. The DEI values obtained directly from the in-cavity moisture loads vary significantly from specimens to specimens of different configurations;
3. DEI is sensitive to the variations in boundary conditions and to the changes in water exposure area;

4. The differences, some quite large, in DEI values between duplicate specimens indicate that there are some unidentified factors affecting the rates of evaporation from the water trays. The unidentified factors may be caused by air leakage, uneven material properties, or airflows in the environmental chamber. Further research is required to address this issue.

6.2. Temporal profiles of moisture contents in sheathing and studs

Moisture content accumulation in the gravimetric samples vs. time (MC~t) is a relationship commonly used to show the moisture status of a wall system. Fig. 6.3 shows a group of MC~t profiles at various locations within wall specimen 19 which had fiberboard sheathing. Comparing the moisture content profiles of samples from different locations, it was observed that the absorption rate is not uniformly distributed throughout the specimen. The distance between a gravimetric sample and the water tray has a major impact on the amount of absorption — the larger the distance from the moisture source is, the lower the moisture absorption rate that can be observed (locations of gravimetric samples are indicated in the Fig. 5.7a). When the moisture contents of various components in the wall specimen reach equilibrium (as shown in Fig 6.3), it may be inferred that additional evaporation from the tray is approximately the amount of water vapor transported out from the entire specimen.

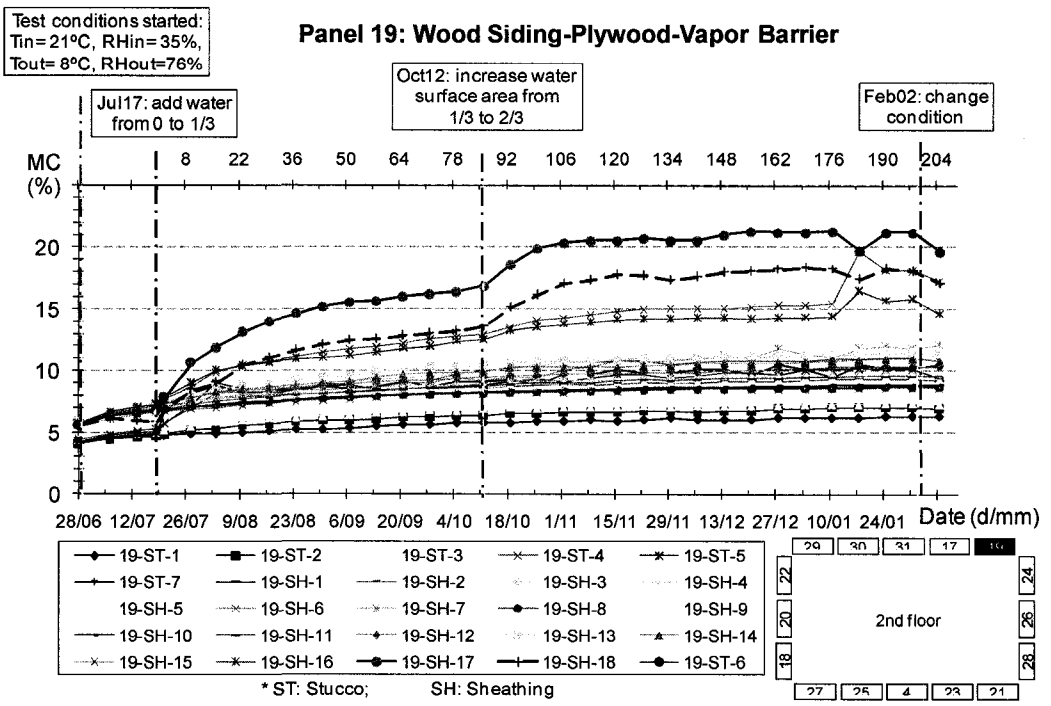

Figure 6.3. Moisture content profiles versus time at different locations on panel 19
(for the locations of the gravimetric samples, please refer to Fig. 5.7a)

The moisture performance of a wall system is determined by its weakest point, where 20% MC limit can be reached the most easily. Theoretically, the moisture content of gravimetric sample SH17 (Fig. 6.3) should increase fastest because it was located closest to the water tray. However, in some wall specimens, the gravimetric sample SH18, which was located at the same horizontal level as SH17 but was off the centre line, had the highest moisture content. An example can be found in Fig. 6.4 for specimen 18. This may be caused by some minor interference, such as variations in material property or uneven distribution of air leakage.

Moisture content profiles versus time of all 31 specimens in the CRD project have been presented by Alturkistani in the Appendix C of his doctoral thesis (Alturkistani 2007).

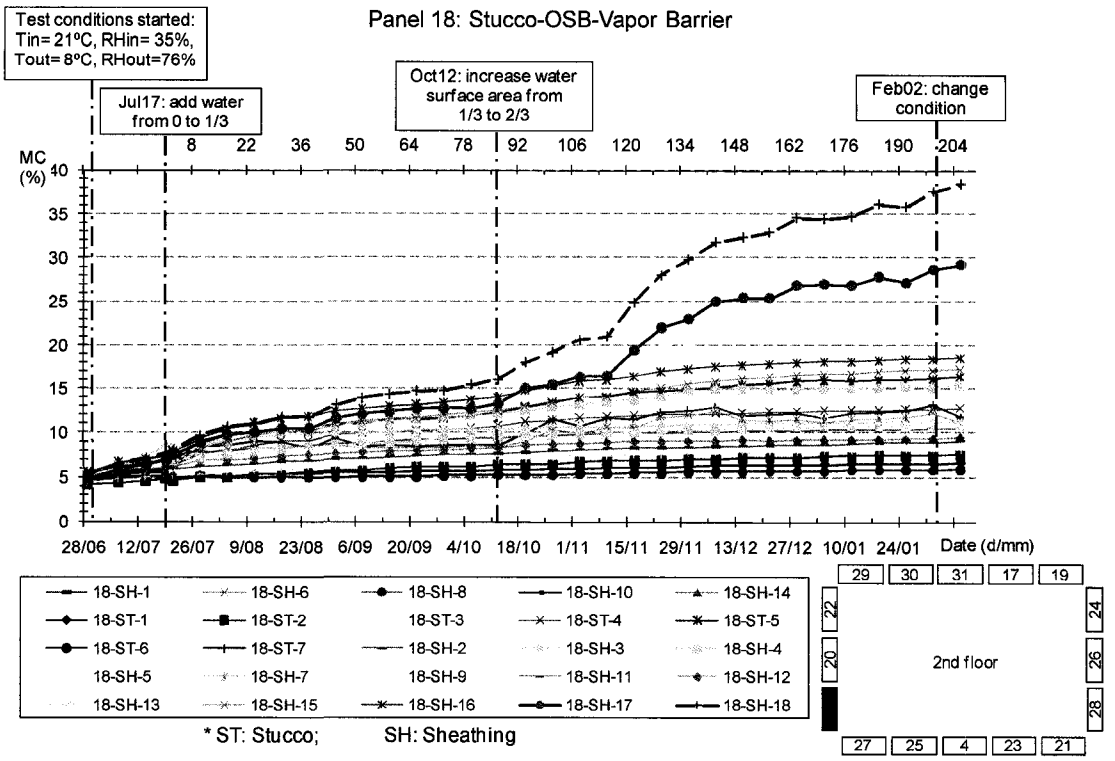

Figure 6.4. Moisture content profiles at different locations on panel 18

6.3. Load-Response Profiles (*E*~MC)

The load-response relations (*E*~MC profiles) described in Section 3.4 correlate the moisture responses on the sheathing board with the in-cavity moisture loading from the water tray. Fig. 6.5 shows two sets of *E*~MC profiles of the duplicate pair of P06 and P18, both with stucco cladding, OSB sheathing and vapor barrier. Fig. 6.6 shows the profiles for another duplicate pair that had wood siding, plywood sheathing, and vapor barrier. In both figures, the test duration was from July 18 to November 23. *E*~MC curves for all the tested specimens in the main test are shown in Appendix A, Figs. from A.1 to A.19.

E~MC curves actually reflect load-response relationship of the underline wall specimens. Some observations on *E*~MC curves are as follows:

- The *E*~MC profiles of the two specimens in duplicate pairs demonstrate similarities in terms of both patterns and magnitudes. For example, when the cumulative evaporation equaled 500 grams, the moisture contents were 21% in P06 (Fig. 6.5a) and 25% in P18 (Fig. 6.5b). Similar trends and patterns can be observed from Figs. 6.6a and 6.6b as well;

- The *E*~MC curves of panels with different wall configurations had differences either in patterns or magnitudes for most of the cases. For example, alternating between different cladding types (Figs. A.1 and A.4; A.2 and A.5; A.3 and A.6; A.7 and A.10; A.8 and A.11; A.9 and A.12) or switching between presence and absence of vapor barrier (A.1 and A.7; A.2 and A.8; A.3 and A.9; A.4 and A.10; A.5 and A.11; A.6 and A.12) had shown significant effects on *E*~MC curves;

- In addition, one conclusion can be made is that the *E*~MC curves are sensitive to different wall configurations and are similar for specimens in duplicate pairs. Thus, the *E*~MC curve can be used for further comparative study of wall systems.

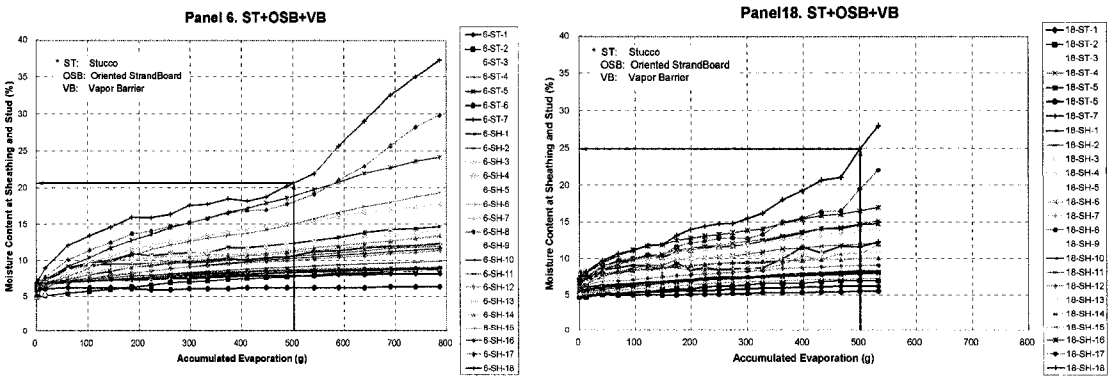

(a) (b)

Figure 6.5. *E*~MC curves for duplicate specimens P06 and P18
(Stucco, OSB, VB)

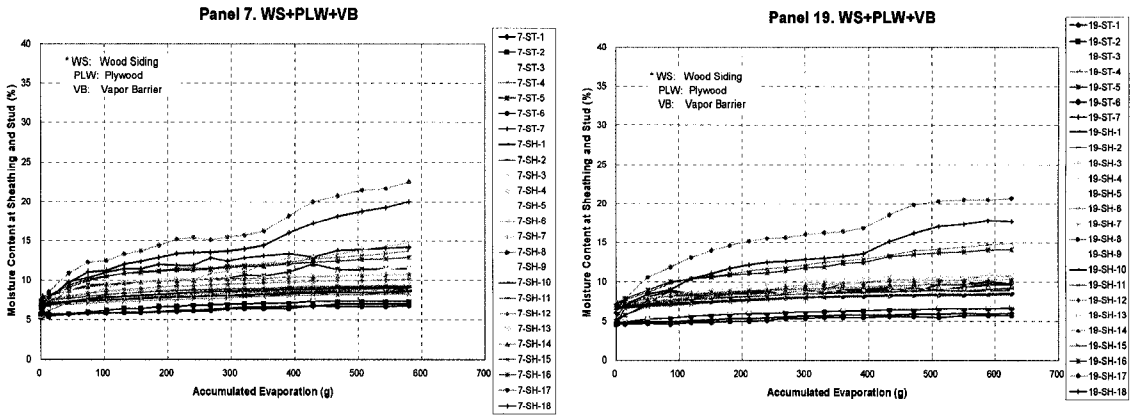

(a) (b)

Figure 6.6. *E*~MC curves for duplicate specimens P07 and P19
(Wood Siding, Plywood, VB)

6.4. Determination of ICEA and $ICEA_{min}$

As defined in Chapter 4, the value of ICEA represents the amount of water evaporated from the water tray when any part of the wall panel reaches the 20% MC. From the load-response chart, ICEA can be identified on the horizontal axis when the corresponding vertical axis of any load-response curves has reached the 20% MC limit. Fig. 6.7 shows the load-response curves and ICEA of wall panel 19.

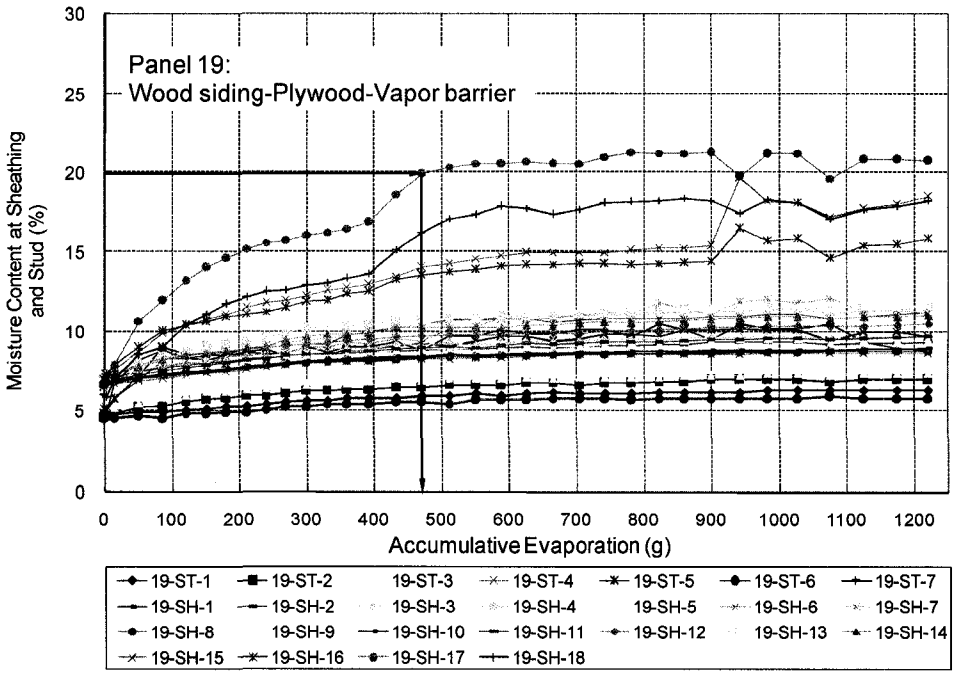

Figure 6.7. Determination of ICEA from load-response profiles for panel 19

As demonstrated by some of the load-response charts of the tested wall specimens, there were cases for which none of the MCs measured in the sheathing and studs reached the set limit state during the test periods 1 and 2 from day 1 to day 200. Fig. 6.8a demonstrates such a case, with MCs of all gravimetric samples under 20%. In such cases, the ICEA could not be determined based on the experimental data available. An $ICEA_{min}$ term was defined instead of the ICEA, as introduced in Chapter 3. Fig. 6.8b shows the cumulative evaporation profile corresponding to Fig. 6.8a and illustrates how to obtain the $ICEA_{min}$ which in this case is $1{,}161g$.

The presence of the $ICEA_{min}$ indicates that the moisture loading was not high enough for the wall component to reach the pre-defined moisture limit state. Had the experiment been extended with higher moisture loading (a larger exposed water surface of the water tray), it is possible for this wall specimen to have reached the moisture limit state so that

an ICEA could have been obtained. It should be noted that no data exist yet to relate the obtained $ICEA_{min}$ value to the actual ICEA value.

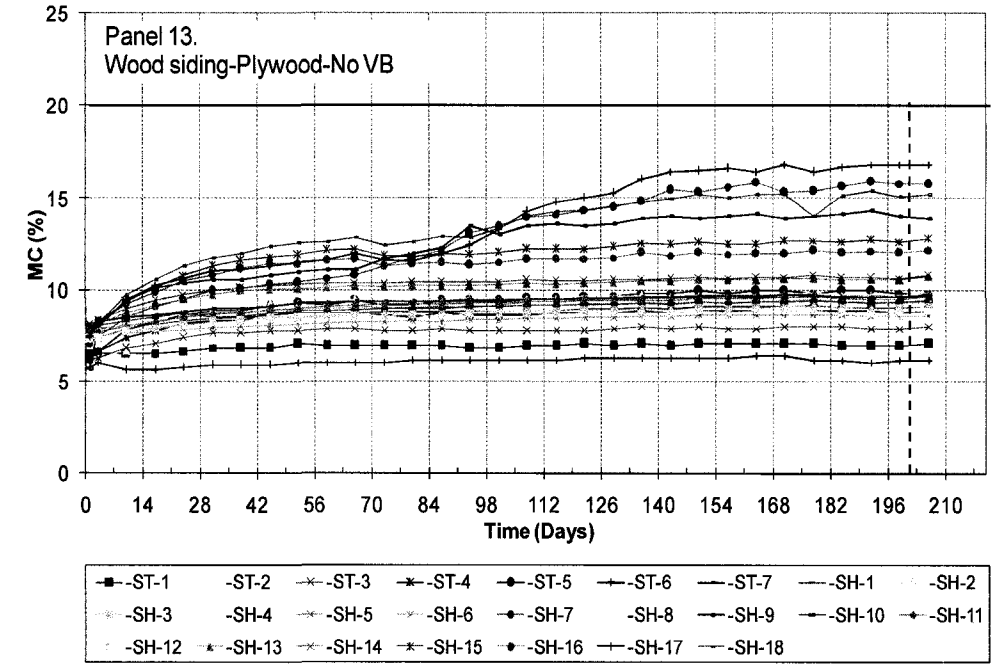

(a)

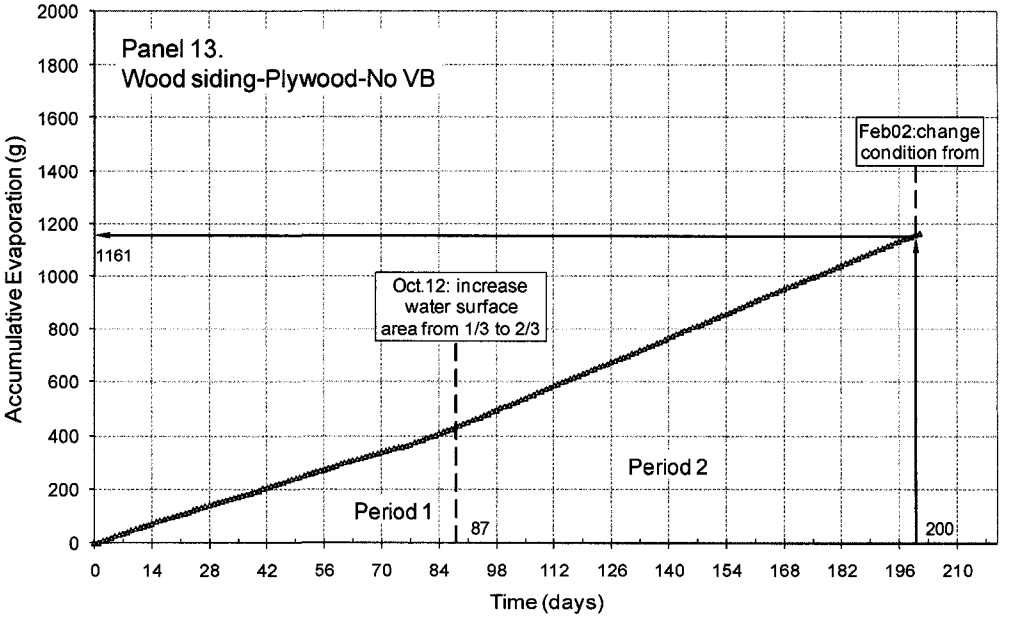

(b)

Figure 6.8. Determining $ICEA_{min}$ when 20% allowable limit could not be reached

Table 6.2 summarizes the obtained ICEA/$ICEA_{min}$ values for all the wall specimens corresponding to the 20% design allowable moisture limit, together with the configurations of the wall systems shown. For those walls in duplicate pairs, the average ICEA values were calculated, which are presented together with both the relative and absolute deviations to the averages.

Table 6.2. ICEA values obtained for all tested wall configurations

Panel No.			Wall configuration	ICEAs of specimens		Average ICEA / $ICEA_{min}$	Relative deviation from average [%]	Absolute deviation from average [g]
1st floor	2nd floor			1st floor	2nd floor			
P05	duplicates	P17	WS+OSB+VB	800	535	668	19.9%	133
P07		P19	WS+PLW+VB	425	475	450	5.6%	25
P09		P21	WS+FIB+VB	>1589	>1344	>1467	8.4%	123
P06		P18	ST+OSB+VB	485	415	450	7.8%	35
P08		P20	ST+PLW+VB	170	95	133	28.3%	38
P10		P22	ST+FIB+VB	50	130	90	44.4%	40
P11		P23	WS+OSB+NVB	>1033	>1141	>1087	5.0%	54
P13		P25	WS+PLW+NVB	>1161	>1075	>1118	3.8%	43
P15		P27	WS+FIB+NVB	>1132	>1270	>1201	5.7%	69
P12		P24	ST+OSB+NVB	770	740	755	2.0%	15
P14		P26	ST+PLW+NVB	480	440	460	4.3%	20
P16		P28	ST+FIB+NVB	>1369	>1492	>1431	4.3%	62
P01			NC+OSB+VB	310		310		
P02			NC+PLW+VB	385		385		
P03			NC+FIB+VB	630		630		
	P04		WSI+OSB+VB	>1441		>1441		
	P29		WSI+PLW+VB		780	780		
	P30		WSI+FIB+VB		>1154	>1154		
	P31		NC+ISH+VB		>1173	>1173		

Note: The "relative deviation to average" is defined by "absolute deviation to average" divided by "average" value.

The deviations from the averages between the specimens in duplicate pairs were generally small. Of the 12 duplicate pairs, there were only three cases with relative deviations from the average larger than 10%, i.e. 19.9% for the WS+OSB+VB pair, 28.3% for the ST+PLW+VB pair, and 44.4% for ST+FIB+VB assembly. There were only two cases where the absolute deviation from the average was larger than 100g, i.e. 133g for the WS+OSB+VB pair and 123g for the WS+FIB+VB pair. The pair with the highest relative deviations had the smallest ICEA values (P10 and P22). Of all the specimen pairs, the maximum absolute deviation was only 133 g and the total range of ICEA (full scale based on the test) was 1,539 g, which resulted in a full scale deviation at only about 8.6%. Although statistically the number of test specimen is not enough to make a solid conclusion, based on the existing data of ICEA measured this indicator seems sensible enough to distinguish one wall configuration from another.

6.5. Comparative Studies by ICEA

ICEA indicates the capacity of a specimen to dry out moisture from the stud cavity. The higher the ICEA value, the more moisture the specimen can evacuate.

Three cases for the application of ICEA are presented in this section. The first case shows good agreement between ICEA and wetness observed from the gravimetric samples on the sheathing, the second case evaluates the impact of different cladding systems (stucco and wood siding), and the third case reveals the influence of the presence or absence of vapor barriers on the drying performance of different wall configurations.

6.5.1. ICEA and moisture accumulation on the sheathing

It has been found that the low values in ICEA obtained from the experimental data coincided with the wetness of the sheathing arising from moisture accumulation. In Fig. 6.9, the wall assemblies listed in Table 6.2 are ranked by the ICEA values in descending order. Seven types of wall assemblies with relatively small ICEAs are highlighted in a darker shade. During the gravimetric sample collection, the bottom regions of the sheathing panels of these seven types of wall panels were found to be noticeably wet due to moisture accumulation, as shown in the photos of Fig. 6.10. In contrast with this, those walls with higher ICEAs were not as wet.

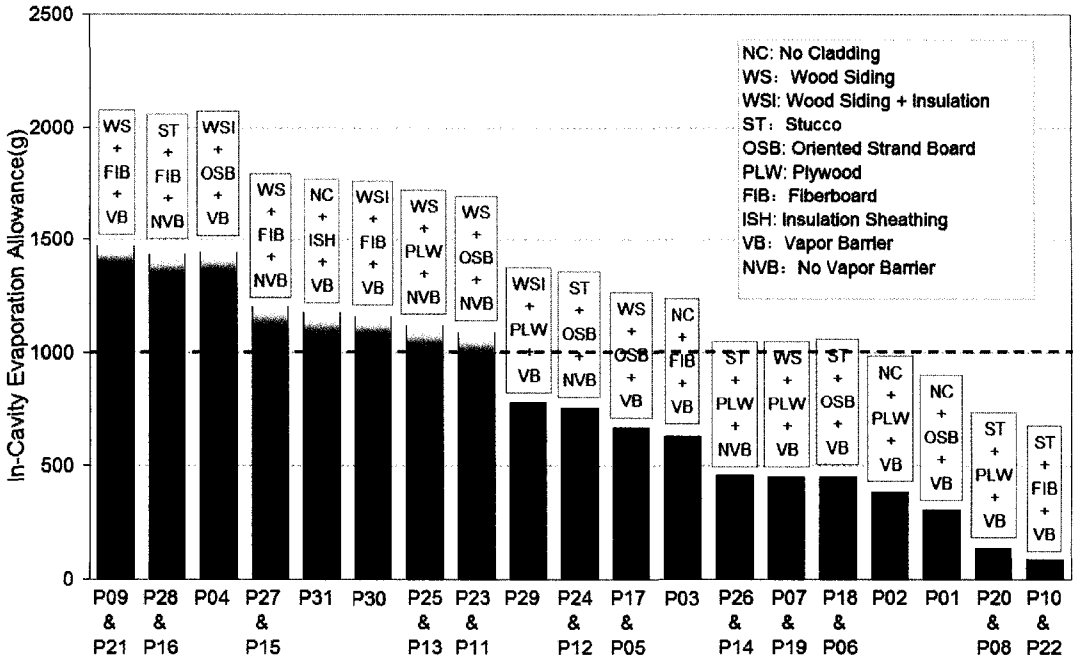

Figure 6.9. Ranking of wall configurations in descending order by ICEA or $ICEA_{min}$

Note: The opening & fading shade at the top of the bar identifies wall configurations with $ICEA_{mins}$

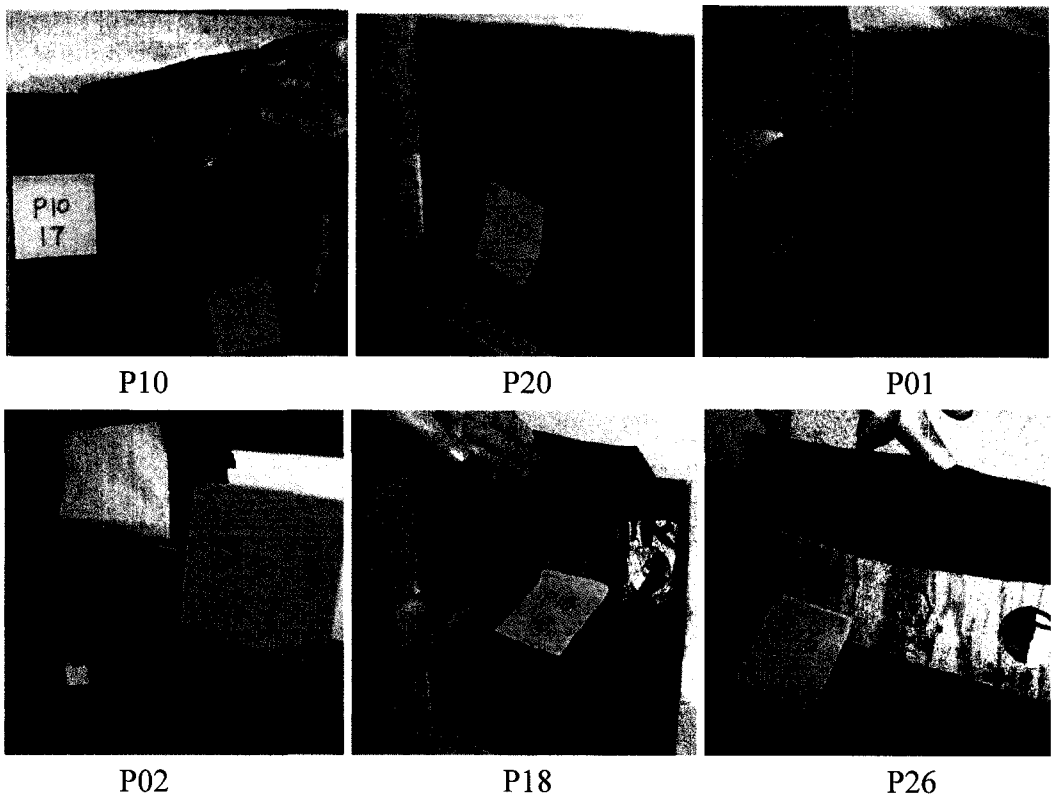

Figure 6.10. Photos of specimens with wet sheathing

6.5.2. Comparison of wall specimens with different claddings

Fig. 6.11 compares the ICEA/ $ICEA_{min}$ values for wall assemblies having wood siding with those having stucco cladding. It can be observed that the walls with stucco claddings exhibited lower ICEA values than those with wood siding do. An exception to this was the comparison between the pair at the extreme right with fiberboard sheathing and no vapor barrier. Here, moisture contents from gravimetric samples in the sheathing of these two assemblies did not reach the moisture limit state at 20% MC and $ICEA_{min}$ values replaced ICEA.

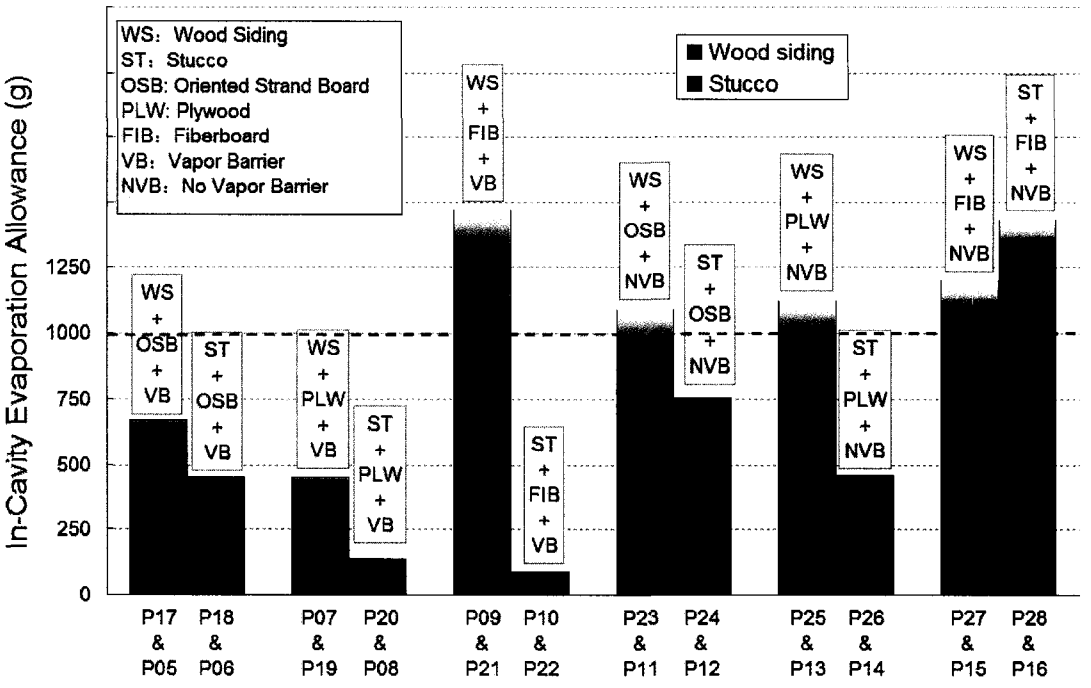

Figure 6.11. Comparisons of wall assemblies clad with stucco and wood siding

Note: The opening & fading shade at top of the bar identifies the walls that have $ICEA_{mins}$

6.5.3. Comparison of wall specimens configured with and without vapor barrier

ICEAs for specimens with vapor barriers and those without vapor barriers are compared in Fig. 6.12. The comparisons indicate that the vapor barrier can significantly reduce the ICEA of a specimen. The effect of the vapor barrier on the drying performance was the most noticeable for walls with stucco cladding on fiberboard sheathing, as demonstrated by the last pair on the right in Fig. 6.12. On the other hand, one exception occurred in walls with wood siding on fiberboard sheathing (3rd pair from left in Fig. 6.12). Similar to the case when different cladding/siding were compared, the two walls of the exception did reach the 20% MC limit during the experiment and $ICEA_{min}$ were used as the values of comparison instead of ICEAs.

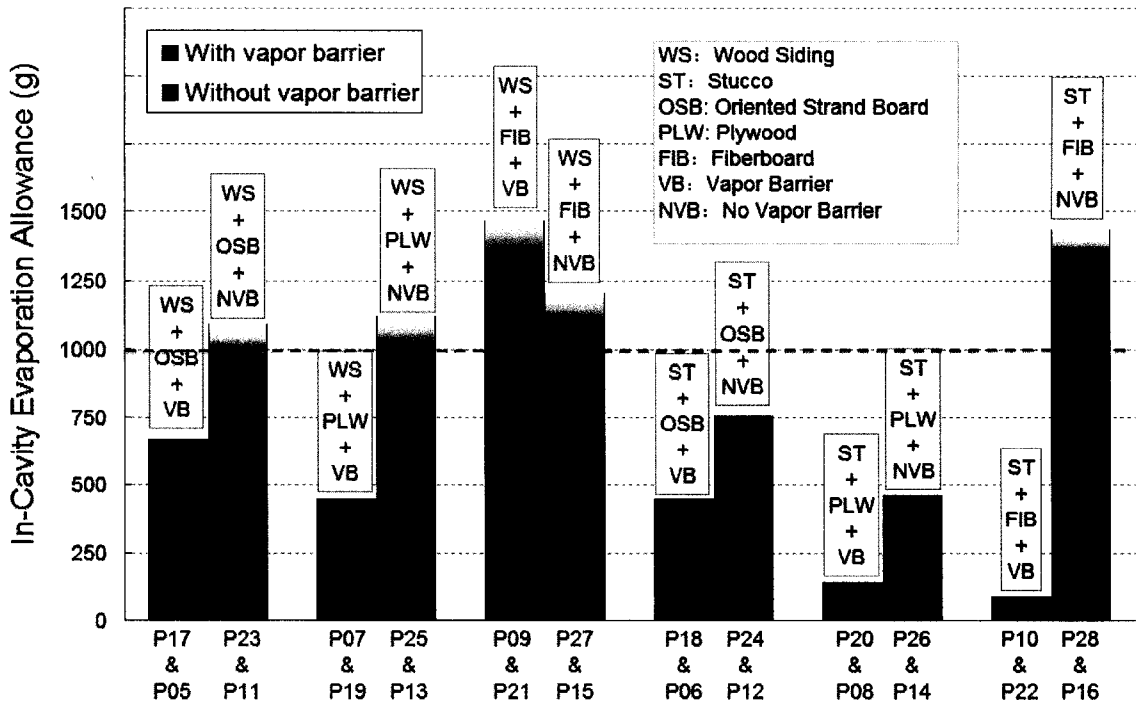

Figure 6.12. Comparisons between wall assemblies with and without vapor barrier

Note: The opening & fading shade at top of the bar identifies the walls that have $ICEA_{mins}$

There are three pairs where one assembly in the pair reached the set moisture limit state (thus ICEAs were calculated) and the other assembly did not (and thus $ICEA_{min}$ was used), as the first two pairs of assemblies from the left (wood siding plus OSB sheathing and wood siding plus plywood sheathing) and the last pair assemblies on the right (stucco plus fiberboard sheathing) in Fig. 6.12. It is apparent that the assembly indicated by $ICEA_{min}$ (the actual value of ICEA is higher than this $ICEA_{min}$) performed better than the other assembly in the same pair that indicated by ICEA.

However, for a pair with two $ICEA_{min}$ values, the comparison cannot be made based on the $ICEA_{min}$ directly. One observation is that the wall with larger $ICEA_{min}$ does not necessarily have a higher ICEA value. That is, had the test duration been extended and/or

the in-cavity loading level been increased, the ICEA of the wall currently with a lower $ICEA_{min}$ might be larger than that of the wall currently with a higher $ICEA_{min}$. Since all the specimens with $ICEA_{min}$ values have very high drying capacity, no further comparisons were made between these specimens. In other words, specimens that have not reached the pre-defined moisture limit state (20% MC) during the experiment were all considered to have excellent drying performance and comparisons between these wall configurations are not necessary.

6.6. Summary on drying performance indicators

Two drying performance indicators, DEI and ICEA, have been presented in this thesis research. Chapter 4 deals with the methodology and this chapter shows the application of these indictors. Table 6.3 shows a comparison of DEI and ICEA with other evaluation methods in performance of drying speed and moisture accumulation. Overall drying speed and drying speed at the bottom plate are chosen for comparison; while moisture responses is compared in three aspects: moisture content variation profile, mold growth potential, and moisture limit state. From Table 6.3, it may be concluded that ICEA is a comprehensive indicator that can quantitatively address many issues related to moisture performance.

The number of test specimen is not enough to make statistic error analysis for the DEI and the ICEA. For such a large scale test, the total error of a wall system may accumulate errors from inconsistency of workmanship, the non-uniformity of material, the air leakage in stud cavity, and the errors of instruments themselves. According to the literature review, most full scale tests do not have duplicate specimens as it was done in the study reported in this thesis; therefore, there is no reference test for comparing.

Conclusions made according to data measured from this project look reasonable and may serve as a reference for later studies.

Table 6.3. Addressed envelope performance issues by DEI and ICEA as compared to existing studies

Literatures	Indicators	Drying performance				
		Evacuation speed		Different aspects/consequences of moisture responses		
		General evaporation	Evaporation at bottom plate	Moisture content variation	Mold growth	Limit state
TenWolde et al. (1995)		√				
Salonvaara et al. (1998)		√				
Hazleden and Morris (2001)		√				
Kumaran et al. (2002) Beaulieu et al. (2002)	RHT			√	√	
Lawton et al. (1999)		√		√		
Ojanen et al. (2002)		√				
van Straaten (2003)		√				
Teasdale-St-Hilaire et al. (2004, 2005)		√	√			
This thesis research	DEI		√			
	ICEA		√	√	√	√

6.7. Evaluating rain penetration and comparing it to ICEA of wall

In this section, a case is presented to show how to evaluate the amount of wind driven rain that would penetrate the stud cavity of 12 wall configurations used in this study, and then compare it to the ICEA value for the respective wall configurations to determine whether each of the configurations is within the limit state.

Assumptions for environmental conditions of the evaluated wall assemblies

The following environmental conditions are assumed at the location of the wall assemblies:

- The two types of wall assemblies with wood siding and stucco are considered to have the same proportionality factor functions as that used in the MEWS project (see the $f(\Delta Pw)$ factor in Section 2.2.3).
- The evaluated wall assemblies are assumed located on a façade of a building in Montreal at 5 meters above the "average roof-top level" (see Fig 2.8). The topography of the building belongs to a largely urbanized area of a large city with the height of the zero plane displace at z_0=2.5m. The building façade (the normal plane of the façade) is oriented at an angle of 40° from the true North;
- As the wind speed included in weather data package is the reference wind speed, a pressure coefficient of 0.7 is assumed when calculating the maximum dynamic wind pressure over the building façade.
- The penetrated water could stay in the stud cavity for a long time if a wall system does not have enough drying ability. To take into account the lag between rain incursion and drying, the months before the time of testing, during which weather data from October of 1977 were used for deriving test conditions, should also be considered. Therefore, the rainfall and wind data of the weather record from June 1 to December 18 of 1977 is used for calculating rain penetration. The selected period has the same length (200 days) as the testing of drying capacity; and it has the heaviest rainfall during the year of 1977. The monthly rainfall values are listed

in Table 6.4.

Table.6.4 . Monthly rainfall data in 1977

Month	Jan	Feb	Mar	Apr	May	Jun	Jul	Aug	Sep	Oct	Nov	Dec
Rainfall (mm)	0	0	59	43	25	108	72	82	145	114	50	9

Calculating rain penetration

The amount of rain penetration into the stud cavity depends on the defects on the walls, the available rain water reaching the wall surface, and wind-induced pressure on the wall. The available water (total precipitation on the building façade) can be calculated from the hourly weather data, the urban topography and the orientation of the building façade. The total water load for the stud cavity can be calculated according to Eq.4.11:

$$M_P = \frac{2}{9} C_\phi \rho_w \sum_{i=1}^{n} V_i \left(R_{i\,hor}\right)^{\frac{8}{9}} \cdot \cos\theta_i \cdot f(\Delta P w_i) \cdot \left(\frac{A}{A_{ref}}\right) \tag{6.1}$$

The attenuation coefficient C_ϕ is 0.347 according to Table 2.2. The ratio A/A_{ref} is added to account for the difference in specimen sizes. The area A (406 mm × 2,438 mm, 0.99 m^2) is the actual dimension of the specimen, while A_{ref} (2,400 mm × 2,400 mm), as a reference, is the area of the specimen that was used in the rain penetration test to obtain the proportional factor $f(\,)$.

The calculation of the hourly rain penetration through the wood siding assembly over the selected weather month (October 1977) is shown in Table 6.5. The actual numerical calculations were performed in an Excel spreadsheet.

Table 6.5. Calculation of total mass of rain penetration for wood siding assemblies

Month	Date	Hour	C_ϕ	A (m^2)	ϕ	V_i (km/hr)	$R_{i\ hor}$ (mm/hr)	θ	ΔPw (Pa)	$f(\Delta Pw)$	M_{Pi} (g)
Jun.	1	1	0.347	0.991	40 °	7	0	100 °	1.71	0.042	0
Jun.	1	2	0.347	0.991	40 °	9	0	110 °	2.83	0.042	0
Jun.	1	3	0.347	0.991	40 °	7	0	120 °	1.71	0.042	0
⋮	⋮	⋮	⋮	⋮	⋮	⋮	⋮	⋮	⋮	⋮	⋮
Oct.	17	9	0.347	0.991	40 °	39	6.6	-20 °	53.1	0.043	31.1
Oct.	17	10	0.347	0.991	40 °	39	5.3	-20 °	42.8	0.043	22.9
⋮	⋮	⋮	⋮	⋮	⋮	⋮	⋮	⋮	⋮	⋮	⋮
Dec.	18	22	0.347	0.991	40 °	19	0	10 °	12.61	0.042	0
Dec.	18	23	0.347	0.991	40 °	22	0	10 °	16.90	0.042	0
Dec.	18	24	0.347	0.991	40 °	22	0	20 °	16.90	0.042	0
										Σ	563.9

Verification of envelope systems by LSD criterion

Table 6.6 lists the ICEAs measured from 12 types of wall assemblies and compares them with the rain penetrations calculated above. It can be easily observed that three wall assemblies are marked with "X" in the verification result column and they do not meet the requirement on drying performance; therefore, these wall assemblies should be replaced by other wall systems or be redesigned.

Table 6.6. Verification wall assemblies by LSD criterion

Assemblies			M_P (g)	Comparison	ICEA (g)	Verification result
Cladding	**Sheathing**	**Vapor barrier**				
Wood siding	OSB	With	563.9	<	668	√
	Plywood			>	450	**X**
	Fiberboard			<	〉1467	√
	OSB	Without		<	〉1087	√
	Plywood			<	〉1118	√
	Fiberboard			<	〉1201	√
Stucco	OSB	With	441.2	<	450	√
	Plywood			>	133	**X**
	Fiberboard			>	90	**X**
	OSB	Without		<	755	√
	Plywood			<	460	√
	Fiberboard			<	〉1431	√

Generalization

The evaluation of the envelope systems presented in the above case has been carried out for conditions generated in the lab. However, the calculation presented above can be extended to site conditions by taking measurements of the ICEA under prevailing conditions.

Chapter 7
Conclusions and Contributions

7.1. Conclusions

The major conclusions of this thesis research include:

1. As a new loading method, the water tray method has exhibited its advantages in the following aspects.
   i) This loading method is capable of creating a moisture source which has uniform evaporation area for all tested specimens, which can greatly benefit further comparative studies on the performances of different wall systems;
   ii) This loading method isolates the evaporation from the other drying mechanisms, drainage and capillarity, to make possible the comparison of the relevant drying performance across different wall systems.
   iii) This loading method can effectively excite the specimens to reach their limit state, which further identifies the relative performance of the wall systems;
   iv) The load intensity can be varied by increasing the evaporation area from 1/3 to 2/3 and 3/3 of the tray;
   v) The moisture loading from the water tray system can be monitored continuously and real-time data can be collected.

In summary, the tray method is applicable, efficient, adjustable (controllable), and convenient for collecting the data required to carry out the relative drying performance of wall systems. Experiments using the tray method provide repeatable results with limited deviations.

2. For a given wall assembly under certain boundary conditions with a given evaporation area, the cumulative evaporation profile from the water tray was found to be linear. The slope of the E~t profile has been named as DEI (Drying by Evaporation Index) and can be used to represent the severity of moisture loading being applied to the stud cavity;
3. It was observed that the moisture accumulation on sheathing board varied in response to the water evaporation from the tray located inside the stud cavity. The profiles of moisture loading (cumulative evaporation) versus moisture response (moisture content variation on sheathing board) have some similarity to the stress-strain curves used for limit state design in structural engineering;
4. As a newly proposed concept and indictor of in-cavity evaporation allowance, ICEA, exhibited the following characteristics:
    i) The ICEA expresses well the constraint of moisture load in relation to the moisture accumulation in the sheathing board;
    ii) The ICEA can serve as an indicator for the evaluation of the relative drying capacity of wood-frame wall systems, since it has been proven effective in comparing the drying performances between different wall assemblies;
    iii) As a new concept, the ICEA identifies critical points in the wall system susceptible to moisture damage.

7.2. Contributions

This thesis research has advanced the drying capacity measurements through a full-scale experiment on a large number of wall assemblies. Based on the literature reviewed, a lot of moisture related knowledge was not well organized. For example, the moisture failure criteria of wood material and moisture safety margin have been discussed for a long time, and this is also the case for the topics such as moisture induced loading protocol and rain penetration calculation. In addition, the idea to correlate the moisture load with the moisture response has been in discussion for years, but no attention was paid to the limit state identification for the entire wall system. Work elaborated in this thesis represents the first effort to merges all of above knowledge together and to provide an integrated engineering solution for the design of wood-frame wall system.

The contributions can be summarized as follows:

1. A literature review on the state-of-the-art knowledge related to moisture loading and performance of building envelope systems has been presented. The structure of the literature review implicates the engineering solution for design of wood-frame wall systems with consideration of climatic loading and moisture performance on building envelope;
2. A preliminary test was carried out to confirm the feasibility of the current test method for CRD project, to expose problems and to improve the water tray technique;

3. Based on the constraint placed by moisture accumulation in sheathing board during the process of moisture drying from stud cavity, the new concept of ICEA was developed in this research;
4. Moisture load-response relationship was established by correlating the in-cavity moisture loading with the moisture response of the sheathing board;
5. A practical theory for identifying the value of ICEA was developed, in which the widely accepted 20% MC rule was applied to the moisture failure criterion for wood products;
6. The reliability of the water tray and load cell system was verified;
7. The measured ICEAs in the CRD project were employed to compare the drying performances of different wall systems;
8. A method has been presented which compares the amount of water penetrating into the stud cavity, to that indicated by the ICEA for the respective wall configuration; this comparison is made to verify whether each of the wall configurations is within the limit state.
9. Extensive data have been collected in the experiment, which are relevant to a wide range of studies on moisture performance in wood-frame wall systems. The data analysis in this thesis study covered only periods 1 and 2 at the beginning of the measurement and only the moisture contents from gravimetric samples. The data measured from moisture pins and collected during the last three periods were still available and left for further studies. The measured air leakage characteristics based on pressurization and depressurization tests can be valuable for further

studies focusing on the impacts of air leakage on moisture transfer through building envelops.

7.3. Recommendations for Future Work

This thesis research has proposed a set of principles to quantitatively evaluate moisture performance of wall systems. Similar to any other theory, there are limitations on the method used in this thesis research. Recommendations for additional research are made below to overcome some of these limitations in future work:

1. The impact of air leakage, in terms of both airflow rate and airflow pattern, on the cumulative evaporation from the water tray and the moisture responses on the sheathing has yet to be fully explored. Identification of the impact of air leakage may help explain the deviations in the current DEI and ICEA data. If an air leakage adjustment is applied to these indicators, better agreement between the experimental data can be expected. This area is worthy of further experimental measurements and/or computer simulations;
2. The current experiment can be standardized; further consideration is needed, for example: i) to generalize the verification method to determine whether a wall assembly is within the limit state, the measurement of the ICEA of a wall assembly under a natural weather profile can be performed; ii) to obtain ICEA values for specimens that did not achieve the 20% MC limit, further test periods with full water exposure area of the tray can be conducted; iii) to clarify the exact influence of the load intensity (exposure area) to the value of ICEA; and

3. The experiment in current study for measuring drying capacity is carried out under the cold climate of Montreal. The test can be adapted to test building envelope systems in hot and humid weather.

In addition, several aspects of the proposed methodology could be improved, for example:

1. Criteria for judging moisture failure and safety margin deserve further exploration. The new criteria could be based on the mold growth potential indicator RHT that was developed during the MEWS project; and,
2. A wider range of envelope assemblies can be tested. It would also be beneficial to include more climate types.

7.4. Related Publications

Mao, Q., Fazio, P., and Rao, J. (2009), "Test Method and Analysis to Establish Relative Building Envelope Capacity to Cope with Moisture in the Stud Cavity Using Limit of 20% Moisture Content in the Materials", Accepted by 4th International Conference in Building Physics (IBPC4), Istanbul, Turkey, Jun 15-18.

Alturkistani, A., Fazio, P., Rao, J., and Mao, Q. (2008), "A New Test Method to Determine the Relative Drying Capacity of Building Envelope Panels of Various Configurations", Building and Environment, 43(12): 2203-2215.

Fazio, P., Mao, Q., Ge, H., Alturkistani, A., and Rao, J. (2007), "A Test Method to Measure the Relative Capacity of Wall Panels to Evacuate Moisture from Their Stud Cavity", Journal of Architectural Engineering, American Society of Civil Engineers (ASCE), 13(4): 194-204.

Fazio, P., Mao, Q., Alturkistani, A., Vera, S., and Rao, J. (2006), "Establishing a Uniform and Measurable Moisture Source to Evaluate the Drying Capacity of Building Envelope Systems", Proceedings of the 3rd International Conference in Building Physics (IBPC3), Montreal, QC, Canada, Aug 27-31, pp. 369-377.

Mao, Q., Rao, J., and Fazio, P. (2004), "Effect of Capillarity on Rainwater Penetration in the Building Envelope", Proceedings of the World Building Congress 2004, International Council for Building Research (CIB), Toronto, ON, Canada, May 2-7, pp. 369-377.

References

AAMA (1994a), AAMA 501.1: Standard Test Method for Metal Curtain Walls for Water Penetration Using Dynamic Pressure, American Society for Testing and Materials, Philadelphia, PA, USA.

AAMA (1994b), AAMA 501.2: Field Check of Metal Shop Fronts, Curtain Walls and Sloped Glazing Systems for Water Leakage, American Society for Testing and Materials, Philadelphia, PA, USA.

AAMA (1994c), AAMA 501.3: Field Check of Water and Air Leakage through Installed Exterior Windows, Curtain Walls and Doors by Uniform Air Pressure Difference, American Society for Testing and Materials, Philadelphia, PA, USA.

Alturkistani, A. (2007), "Large Scale Experimental Investigation of the Relative Drying Capacity of Building Envelope Panels of Various Configurations", PhD thesis, Concordia University, Montreal, QC, Canada.

Alturkistani, A., Fazio, P., Rao, J. and Mao, Q. (2008), "A New Test Method to Determine the Relative Drying Capacity of Building Envelope Panels of Various Configurations", Building and Environment, 43(12): 2203-2215.

Argiriou, A., Lykoudis, S., Kontoyiannnidis, S., Balaras, C.A., Asimakopooulos, D., Petrakis, M. and Kassomenos, P. (1999), "Comparison of Methodologies for TMY Generation Using 20 Years Data for Athens, Greece", Solar Energy, 66(1): 33-45.

ASHRAE (1993), Standard 55-1993: Thermal Comfort for Human Occupancy, American Society of Heating, Refrigerating, and Air-conditioning Engineers, Inc., Atlanta, GA, USA.

ASHRAE (2001), ASHRAE Handbook of Fundamentals, American Society of Heating, Refrigerating and Air-Conditioning Engineers, Atlanta, GA, USA.

ASTM (2004), E241-04: Standard Guide for Limiting Water-Induced Damage to Buildings, Annual Book of ASTM Standards, vol.04.11.

ASTM (1996a), E331-96: Standard Test Method for Water Penetration of Exterior Windows, Curtain Walls, and Doors by Uniform Static Air Pressure Difference, Annual Book of ASTM Standards, vol.04.07.

ASTM (1996b), E514-96: Standard Test Method for Water Penetration and Leakage through Masonry, Annual Book of ASTM Standards, vol.04.07.

ASTM (1996c), E547-96: Standard Test Method for Water Penetration of Exterior Windows, Curtain Walls, and Doors by Cyclic Static Air Pressure Differential, Annual Book of ASTM Standards, vol.04.07.

ASTM (1996d), E1105-96: Standard Test Method for Field Determination of Water Penetration of Installed Exterior Windows, Curtain Walls, and Doors by Uniform or Cyclic Static Air Pressure Difference, Annual Book of ASTM Standards, vol. 04.07.

Bansal, P.K. and Xie, G. (1998), "A Unified Empirical Correlation for Evaporation of Water at Low Air Velocities", International Communications in Heat and Mass Transfer, 25(2): 183-190.

Bansal, P.K. and Xie, G. (1999), "A Simulation Model for Evaporation of Defrosted Water in Household Refrigerators", International Journal of Refrigeration, 22(4): 319-333.

Beaulieu, P., Bomberg, M., Cornick, S., Dalgliesh, A., Desmarais, G., Djebbar, R., Kumaran, K., Lacasse, M., Lackey, J., Maref, W., Mukhopadhyaya, P., Nofal, M., Normandin, N., Nicholls, M., O'Connor, T., Quirt, D., Rousseau, M., Said, N., Swinton, M., Tariku, F., and van Reenen, D. (2002), "Hygrothermal Response of Exterior Wall Systems to Climate Loading: Methodology and Interpretation of Results for Stucco, EIFS, Masonry and Siding Clad Wood-Frame Walls", Final Report from Task 8 of MEWS Project (T8-03), IRC-RR-112, Institute for Research in Construction, National Research Council Canada, Ottawa, ON, Canada.

Bomberg, M. and Allen, D. (1996), "Use of Generalized Limit States Method for Design of Building Envelopes for Durability" Journal of Building Physics, 20(1): 18-39.

Brown, W., Adams, P., Tonyan, T., and Ullett, J. (1997), "Water Management in Exterior Wall Claddings", Journal of Thermal Envelope and Building Science, 21(7): 23-43.

Brown, W., Chouinard, K., Lawton, M., Patenaude, A., Vlooswyk, J. (2003), "Field Experience with Moisture Management – Putting Principles into Practice", BSI 2003 Proceedings of the Seminar Series, 15 Locations across Canada, Oct 2003-Jan 2004, pp. 1-21.

Brundrett, G.W. (1990), Criteria for moisture control, Butterworths, London, UK.

Canadian Wood Council (2000a), Fire Safety in Residential Buildings, Building Performance Series No. 2, Canadian Wood Council (CWC), Ottawa, ON, Canada.

Canadian Wood Council (2000b), Moisture and Wood-Frame Buildings, Building Performance Series No. 1, Canadian Wood Council (CWC), Ottawa, ON, Canada.

Candanedo, L., Derome, D., and Fazio, P. (2006), "Analysis of Montreal 30-year Weather Data to Select Loading Conditions for Large-Scale Tests on Wall Panel Systems", Proceedings of the 3rd International Conference in Building Physics (IBPC3). Montreal, QC, Canada, Aug 27-31, pp. 959-966.

Carll, C. and Highley, T.L. (1999), "Decay of Wood and Wood-Based Products above Ground in Buildings", Journal of Testing and Evaluation, JTEVA, 27(2): 150-158.

Carll, C. (2000) "Rainwater Intrusion in Light-Frame Building Walls", Proceedings of the 2nd Annual Conference on Durability and Disaster Mitigation in Wood-Frame Housing, Madison, WI, USA, Nov 6-8, pp. 33-40.

Chouinard, K.L. and Lawton, M.D. (2001), "Rotting Wood Framed Apartments – Not Just a Vancouver Problem", 8th Conference on Building Science and Technology: Solutions to Moisture Problems in Building Enclosures Toronto, ON, Canada, Feb 22-23.

Cornick, S.M., Chown, G.A., Dalgliesh, W.A., Djebbar, R., Lacasse, M.A., Nofal, M., Said, M.N., Swinton, M.C., and Tariku, F. (2001), "Defining Climate Regions as a Basis for Specifying Requirements for Precipitation Protection for Walls", Canadian Commission on Building and Fire Codes, National Research Council of Canada, Apr 12, pp. 36.

Cornick, S., Dalgliesh, A., Said, N., Djebbar, R., Rariku, F., and Kumaran, M.K. (2002), "Environmental Conditions Final Report", Report from Task 4 of MEWS Project,

IRC-RR-113, Institute for Research in Construction, National Research Council Canada, Ottawa, ON, Canada.

CSA (1986), CSA O86.1-94 Engineering Design in Wood (Limit States Design), Canadian Standards Association Publication.

Desjarlais, A.O., Karagiozis, A.N., and Aoki-Kramer, M. (2001), "Wall Moisture Problems in Seattle", Proceedings for Performance of Exterior Envelopes of Whole Buildings VIII: Integration of Building Envelopes, Clearwater Beach, FL, USA, Dec 2-7.

Djebbar, R., van Reenen, D., and Kumaran, M.K. (2001), "Environmental Boundary Conditions for Long-Term Hygrothermal Calculations", Proceedings for Performance of Exterior Envelopes of Whole Buildings VIII: Integration of Building Envelopes, Clearwater Beach, FL, USA, Dec 2-7.

Fazio, P., Athienitis, A., Marsh, C., and Rao, J. (1997), "Environmental Chamber for Investigation of Building Envelope Performance", Journal of Architectural Engineering, 3(2): 97-103.

Fazio, P., Mallidi, S.R., and Zhu, D. (1995), "A Quantitative Study for the Measurement of Driving Rain Exposure in the Montreal Region", Building and Environment, 30(1): 1-11.

Fazio, P. (2004), "Protocol on Loading for the Project: to Develop Data on the Relationship between Measurable, Physical Building Envelope Parameters and Movement, Accumulation and Evacuation of Moisture in Wood-Based Building Envelope Systems", funded by an NSERC Collaborative Research & Development (CRD) grant and the wood industry, Mar.

Fazio, P., Rao, J., Alturkistani, A., and Ge, H. (2006a), "Large Scale Experimental Investigation of the Relative Drying Capacity of Building Envelope Panels of Various Configurations", Proceedings of the 3rd International Conference in Building Physics (IBPC3), Montreal, QC, Canada, Aug 27-31, pp. 361-368.

Fazio, P., Mao, Q., Alturkistani, A., Vera, S., and Rao, J. (2006b), "Establishing a Uniform and Measurable Moisture Source to Evaluate the Drying Capacity of

Building Envelope Systems", Proceedings of 3rd International Conference in Building Physics (IBPC3), Montreal, QC, Canada, Aug 27-31, pp. 369-377.

Fazio, P., Mao, Q. Ge, H., Alturkistani, A., and Rao, J. (2007), "A Test Method to Measure the Relative Capacity of Wall Panels to Evacuate Moisture from their Stud Cavity", Journal of Architectural Engineering, American Society of Civil Engineers (ASCE), 13(4): 194-204.

Forest Products Laboratory (1999), Wood Handbook: Wood as an Engineering Material, General Technical Report FPL-GTR-113, Department of Agriculture, Forest Products Laboratory, Madison, WI, USA, 463p.

Ge, H. and Fazio, P. (2004), "Experimental Evaluation of Thermal Response and Condensation Performance of Metal Curtain Walls Subjected to Air Leakage", Journal of Architectural Engineering, American Society of Civil Engineers (ASCE), 10(2): 61-68

Geving, S. (2000), "Hygrothermal Analysis of Building Structures Using Computer Models", Journal of Thermal Envelope and Building Science, 23(3): 224-243.

Griffin, D.M. (1977), "Water Potential and Wood Decay Fungi", Annual Review of Phytopathology, vol.15: 319-329.

Gudum, C. (2003), "Moisture Transport and Convection in Building Envelopes Ventilation in Light Weight Outer Walls", PhD thesis, R-047, TUD (Technical University of Denmark), Lyngby, Denmark, February.

Hansen, M.H., Nicolajsen, A., Stang, B.D. (2002), "On the Influence of Cavity Ventilation on Moisture Content in Timber Frame Walls", 6th Nordic Symposium, Trondheim, Norway, Jun 17, vol.2: 603-610.

Hazleden, D.G. and Morris, P.I. (1999), "Designing for Durable Wood Construction: the 4 Ds", 8th International Conference on Durability of Building Materials and Components, Vancouver, BC, Canada, May 30-Jun 3.

Hazleden, D.G. and Morris, P.I. (2001), "The Influence of Design on Drying Rates in Wood-Frame Walls under Controlled Conditions", Proceedings for Performance of Exterior Envelopes of Whole Buildings VIII: Integration of Building Envelopes,

Clearwater Beach, FL, USA, Dec 2-7.

Hensen, I.J. (1999), "Simulation of Building Energy and Indoor Environmental Quality - Some Weather Data Issues", Proceeding of International Workshop on Climate Data and their Applications in Engineering, Czech Hydrometeorological Institute, Prague, Czech.

Hoppestad, S. (1955), "Slagregn i Norge (in Norwegian)", Norwegian Building Research Institute, rapport Nr. 13, Oslo.

Hutcheon, N.B. and Handegord, G.O. (1995), Building Science for a Cold Climate, National Research Council of Canada, Ottawa, ON, Canada.

Hunt, G. and Garratt, G. (1938), Wood Preservation, McGraw-Hill, NY, USA.

Incropera, F.P. and de Witt, D.P. (1996), Fundamentals of Heat and Mass Transfer, 4th Edition, John Wiley & Sons, NY, USA, pp.315, 355.

Karagiozis, A.N. and Salonvaara, M. (1995), "Influence of Material Properties on the Hygrothermal Performance of a High-Rise Residential Wall", ASHRAE Transactions, 101(1): 647-655.

Keenan, F.J. (1986), Limit States Design of Wood Structures, Morrison Hershfield Limited.

Kragh, M.K. (1998), "Microclimatic Conditions at the External Surface of Building Envelopes", IBE, Department of Buildings and Energy, Technical University of Denmark.

Krus, M., Sedlbauer, K., Zillig, W., and Kunzel, H.M. (2001), "A New Model for Mould Prediction and Its Application on a Test Roof", 2nd Internal Scientific Conference on "the Current Problems of Building Physics in the Rural Building", Cracow, Poland, OR, USA.

Kumaran, M.K., Mukhopadhyaya, P., Cornick, S.M., Lacasse, M.A., Maref, W., Rousseau, M., Nofal, M., Quirt, J.D., and Dalgliesh, W.A. (2002), "A Methodology to Develop Moisture Management Strategies for Wood-Frame Walls in North America: Application to Stucco-Clad Walls", 6th Nordic Symposium, Session 15:

Effects of Moisture 2, pp. 651-658.

Kumaran, M.K., Mukhopadhyaya, P., Cornick, S.M., Lacasse, M.A., Rousseau, M.Z., Maref, W., Nofal, M., Quirt, J.D., Dalgliesh, W.A. (2003), "An Integrated Methodology to Develop Moisture Management Strategies for Exterior Wall Systems," 9th Canadian Conference on Building Science and Technology, Vancouver, BC, Canada, February, pp. 45-62.

Kunzel, H.M. (1998), "Smart Vapor Retarder: An Innovation Inspired by Computer Simulations", ASHRAE Transactions, 104(2): 903-907.

Lacasse, M.A., O'Connor, T.J., Nunes, S., and Beaulieu, P. (2003), "Experimental Assessment of Water Penetration and Entry into Wood-Frame Wall Specimens", Final Report from Task 6 of MEWS Project, IRC-RR-133, Institute for Research in Construction, National Research Council Canada, Ottawa, ON, Canada.

Lacy, R.E. (1962), "An Index of Exposure to Driving Rain", Building Research Institute, Digest 23(2).

Lacy, R.E. (1965), "Driving-Rain Maps and the Onslaught of Rain on Buildings", Proceedings of RILEM/CIB Symposium on Moisture Problems in Buildings, Helsinki.

Lawton, M.D., Brown, W.C., and Lang, A.M. (1999), "Stucco-Clad Wall Drying Experiment", CHMC Research Report, No. 5972204.00, Vancouver, BC, Canada.

Lstiburek, J. (2001), Builder's Guide — Climate Specific Series Including Cold, Mixed-Humid, Hot-Dry, Mixed-Dry, and Hot-Humid Climates, Building Science Corporation and the Energy Efficient Builders Association.

Lstiburek, J. (2002), "Moisture Control for Buildings", ASHRAE Journal, 44(2): 36-41.

Mao, Q., Rao, J., and Fazio, P. (2004), "Effect of Capillarity on Rainwater Penetration in the Building Envelope", Proceedings of the World Building Congress 2004, (CIB), Toronto, ON, Canada, May 2-7, pp. 369-377.

Maref, W., Booth, D.G., Lacasse, M., and Nicholls, M. (2002), "Drying Experiment of Wood-Frame Wall Assemblies Performed in the Climatic Chamber EEEF:

Specification of Equipment Used in EEEF-Environmental Exposure Envelope Facility", IRC-RR-105, Institute for Research in Construction, National Research Council Canada, Ottawa, ON, Canada.

Moon, H.J. and Augenbroe, G.L.M. (2004), "Towards a Practical Mould Growth Risk Indicator", Building Services Engineering, Research & Technology, 25(4): 317-326.

Morris, P.I. and Winandy, J.E. (2002), "Limiting Conditions for Decay in Wood Systems", 33rd Annual Meeting of the International Research Group on Wood Preservation, Cardiff, South Wales, UK, May 12-17.

Morrison Hershfield Limited (1996), "Survey of Building Envelope Failures in the Coastal Climate of British Columbia", Canadian Mortgage and Housing Corporation, Vancouver, BC, Canada.

Morrison Hershfield Limited (1999), "Comparative Analysis of Residential Construction in Seattle", Technical Series 99-111, CMHC, Ottawa, ON, Canada.

Morrison Hershfield Limited (2000), "Wall Moisture Problems in Alberta Dwellings", Technical Series 00-112, CMHC, Ottawa, ON, Canada.

NRC (1995), National Building Code of Canada (NBCC), National Research Council of Canada, Ottawa, ON, Canada.

Nofal, M. and Morris, P. (2003), "Criteria for Unacceptable Damage on Wood Systems", Proceedings of the Japan-Canada Conference on Building Envelope, Vancouver, BC, Canada, Jun 4-5, pp. 1-14.

Ojanen, T. (1998), "Improving the Drying Efficiency of Timber Frame Walls in Cold Climates by Using Exterior Insulation", Thermal Performance of the Exterior Envelopes of Building VII, Clearwater Beach, FL, USA, Dec 6-10, pp. 155-164.

Ojanen, T., Salonvaara, M., and Simonson, C.J. (2002), "Integration of Simplified Drying Tests and Numerical Simulation in Moisture Performance Analysis of the Building Envelope", 6th Symposium on Building Physics in the Nordic Countries, Trondheim, Norway, Jun 17.

Pel, L. (1995), "Moisture Transport in Porous Building Materials", PhD thesis in

Eindhoven University of Technology, Netherland.

Prior, M.J. (1985), "Directional Driving Rain Indices for the United Kingdom — Computation and Mapping", Building Research Establishment Report, Department of the Environment, Building Research Establishment, Building Research Station, Garston.

Reading C.A. and Reiser A. (1977), "A Calorimeter for Measuring Liquid Evaporation Rates", Journal of Physics E: Scientific Instruments, 10(10): 1069-1071.

Salonvaara, M.H., Ojanen, T., Kokko, E., and Karagiozis, A.N. (1998), "Drying Capabilities of Wood Frame Walls with Wood Siding", Thermal Performance of the Exterior Envelopes of Buildings VII, Clearwater Beach, FL, USA, pp. 165-177.

Sanders, C. (1996), "ICEA-Annex 24", Final Report Volume 2, Task 2, Environmental Conditions, Leuven, Belgium.

Sartori, E. (2000), "A Critical Review on Equations Employed for the Calculation of the Evaporation Rate from Free Water Surfaces", Solar Energy, 68(1): 77-89.

Sedlbauer, K., Krus, M., Zillig, W., and Kunzel, H.M. (2001), "Mold Growth Prediction by Computational Simulation", Proceedings IAQ (Indoor Air Quality) 2001, Moisture, Microbes, and Heath Effects-Indoor Air Quality and Moisture in Buildings, San Francisco, CA, ASHRAE, USA, Nov 4-7.

Singh, V.P. and Xu, C.-Y. (1997), "Evaluation and Generalization of 13 Mass-Transfer Equations for Determining Free Water Evaporation", Hydrological Processes, 11(3): 311-323.

Straube, J.F. and Burnett, E.F.P. (2000), "Simplified Prediction of Driving Rain on Buildings", Proceedings of the International Building Physics Conference, Eindhoven University of Technology, Einhoven, Netherland, pp. 375-382.

Straube, J.F. and Burnett, E.F.P. (2005), "Building Science for Building Enclosures", Building Science Press, Westford, MA, USA, 549 p.

Tang, R. and Etzion, Y. (2004), "Comparative Studies on the Water Evaporation Rate from a Wetted Surface and that from a Free Water Surface", Building and

Environment, 39(1): 77-86

Teasdale-St-Hilaire, A., Derome, D., and Fazio, P. (2003), "Development of an Experimental Methodology for the Simulation of Wetting due to Rain Infiltration for Building Envelope Testing", Proceedings of the 9th Canadian Conference on Building Science and Technology, Vancouver, BC, Canada, Feb 27-28, pp. 459-474.

Teasdale-St-Hilaire, A., Derome, D., and Fazio, P. (2004), "Behavior of Wall Assemblies with Different Wood Sheathings Wetted by Simulated Rain Infiltration", Performance of the Exterior Envelopes of Whole Buildings IX, Conference Proceedings, ASHRAE, Clearwater Beach, FL, USA, Dec 5-10, 15 p.

Teasdale-St-Hilaire, A., Derome, D. and Fazio, P. (2005), "Investigating the Role of the Vapor Retarder in the Drying Response of Wood-Frame Walls Wetted by Simulated Rain Infiltration", Proceedings of the 10th Canadian Conference on Building Science and Technology, Ottawa, ON, Canada, May 12-13, 13 p.

TenWolde A. and Carll, C. (1992), "Effect of Cavity Ventilation on Moisture in Walls and Roofs", Proceedings of the Thermal Performance of the Exterior Envelopes of Buildings V, Clearwater Beach, FL, USA, Dec 7-10, pp. 555-562.

TenWolde, A., Carll, C., and Malinauskas, V. (1995), "Airflows and Moisture Conditions in Walls of Manufactured Homes", Airflow Performance of Building Envelopes, Components, and Systems, ASTM STP 1255 Mark P. Modera and Andrew K. Persily, Eds., American Society for Testing and Materials, Philadelphia, PA, USA, pp. 137-155.

TenWolde, A., Carll, C.G., and Malinauskas, V. (1998), "Air Pressures in Wood Frame Walls", Thermal Performance of the Exterior Envelopes of Buildings VII, Clearwater Beach, FL, USA, pp. 665-675.

TenWolde, A. and Walker, I.S. (2001), "Interior Moisture Design Loads for Residences", Proceedings for Performance of Exterior Envelopes of Whole Buildings VIII: Integration of Building Envelopes, Clearwater Beach, FL, USA, Dec 2-7.

Trechsel, H.R. (1994), Manual on Moisture Control in Buildings (Manual on Moisture Analysis in Buildings), ASTM manual series: MNL 18.

Tsongas, G.A., Govan, D.P., and McGillis, J.A. (1998), "Field Observations and Laboratory Tests of Water Migration in Walls with Shiplap Hardboard Siding", Thermal Performance of the Exterior Envelopes of Buildings VII, Clearwater Beach, FL, USA, pp. 469-483.

Urban Development Institute (2000), "Submission to the Second Commission of Inquiry into the Quality of Condominium Construction", Urban Development Institute, http://www.udi.bc.ca/Publications/UDI/UDI SubmissionCondoConstruction2000.pdf.

van Straaten, R. (2003), "Measurement of Ventilation and Drying of Vinyl Siding and Brick Clad Wall Assemblies", Master thesis in University of Waterloo, ON, Canada.

Viitanen, H. and Salonvaara, M. (2001), "Chapter 4: Failure Criteria", Moisture Analysis and Condensation Control in Building Envelopes (Manual on Moisture Analysis in Buildings), ASTM manual series: MNL40, pp. 66-80.

Wang, M.L., Sakamoto, I., and Bassler, B.L. (1992), Cladding, Council on Tall Buildings and Urban Habitat Committee 12A, McGraw-Hill, Inc.

Wu, Y., Kumaran, M.K., and Fazio, P. (2008), "Moisture Buffering Capacities of Five North American Building Materials", Journal of Testing and Evaluation, 36(1): 7p.

Zabel, R.A. and Morrell J.J. (1992), Wood Microbiology: Decay and Its Prevention, Academic Press, San Diego, CA, USA.

Zarr, R.R., Burch, D.M., and Fanney, A.H. (1995), "Heat and Moisture Transfer in Wood-Based Wall Construction: Measured Versus Predicted", NIST Building Science Series 173, National Institute of Standards and Technology.

Zhu, D., Mallidi, S.R., and Fazio, P. (1995a), "Approach for Urban Driving Rain Index by Using Climatological Data Recorded at Suburban Metrological Station", Building and Environment, 30(2): 229-236.

Zhu, D., Mallidi, S.R., and Fazio, P. (1995b), "A Quantitative Driving Rain Exposure on a Vertical Wall at Various Canadian Cities", Building and Environment, 30(4): 533-544.

Appendix
E~MC profiles for all specimens

List of the figures and corresponding configurations

1st floor		Wall configurations	2nd floor	
Figure No.	Panel No.		Panel No.	Figure No.
Figure A.1a.	P05	WS+OSB+VB	P17	Figure A.1b.
Figure A.2a.	P07	WS+PLW+VB	P19	Figure A.2b.
Figure A.3a.	P09	WS+FIB+VB	P21	Figure A.3b.
Figure A.4a.	P06	ST+OSB+VB	P18	Figure A.4b.
Figure A.5a.	P08	ST+PLW+VB	P20	Figure A.5b.
Figure A.6a.	P10	ST+FIB+VB	P22	Figure A.6b.
Figure A.7a.	P11	WS+OSB+NVB	P23	Figure A.7b.
Figure A.8a.	P13	WS+PLW+NVB	P25	Figure A.8b.
Figure A.9a.	P15	WS+FIB+NVB	P27	Figure A.9b.
Figure A.10a.	P12	ST+OSB+NVB	P24	Figure A.10b.
Figure A.11a.	P14	ST+PLW+NVB	P26	Figure A.11b.
Figure A.12a.	P16	ST+FIB+NVB	P28	Figure A.12b.
Figure A.13.	P01	NC+OSB+VB		
Figure A.14.	P02	NC+PLW+VB		
Figure A.15.	P03	NC+FIB+VB		
		WSI+OSB+VB	P04	Figure A.16.
		WSI+PLW+VB	P29	Figure A.17.
		WSI+FIB+VB	P30	Figure A.18.
		NC+ISH+VB	P31	Figure A.19.

Note: ST=Stucco, WS=Wood Siding, OSB= Oriented Strand Board, PLW=Plywood, FIB=Fiberboard, VB=Vapor Barrier, NVB=No Vapor Barrier.

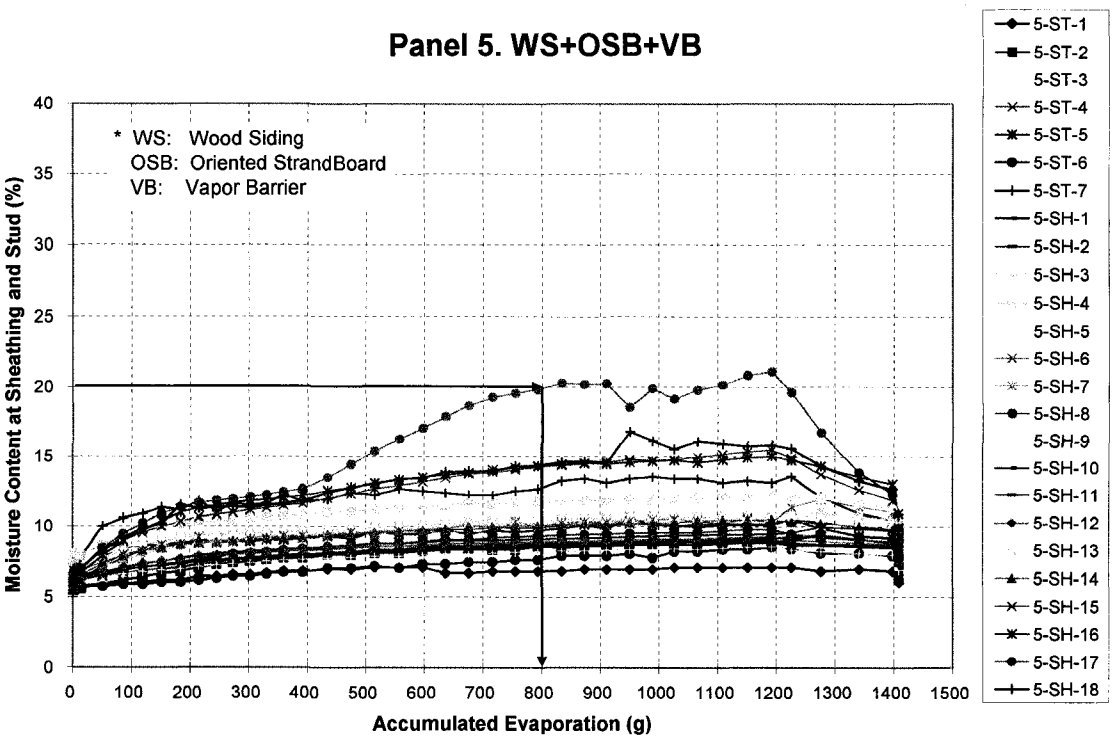

Figure A.1a. Wall specimen #5, with WS, OSB & VB

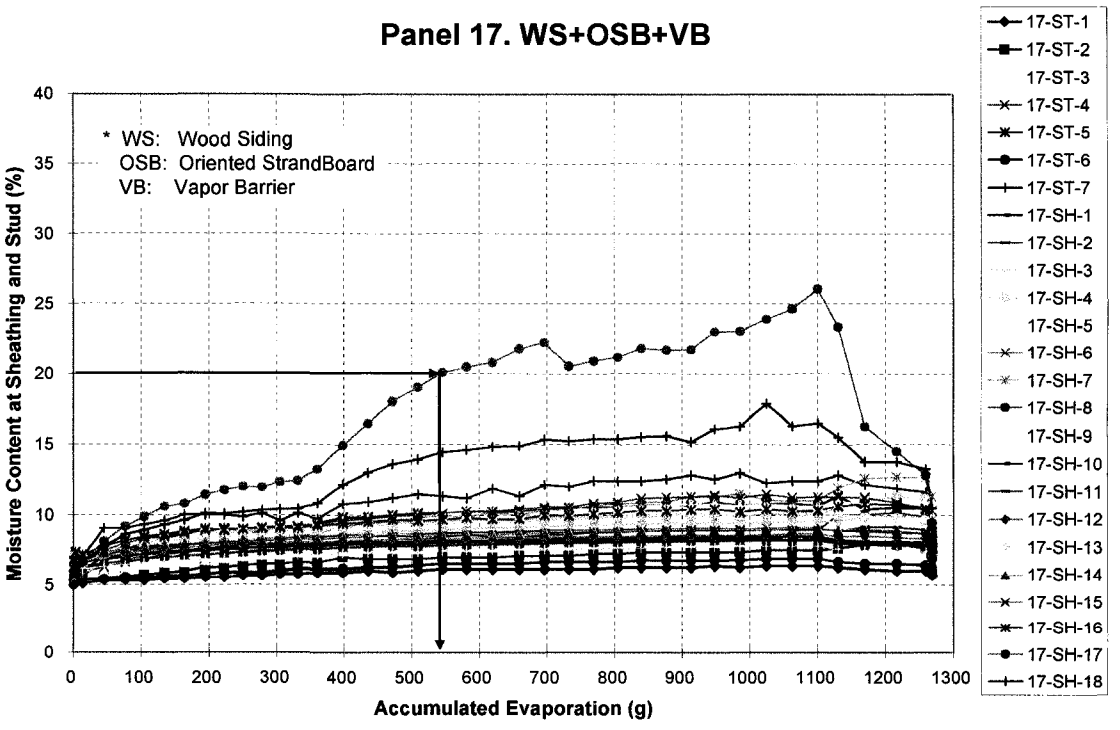

Figure A.1b. Wall specimen #17, with WS, OSB & VB

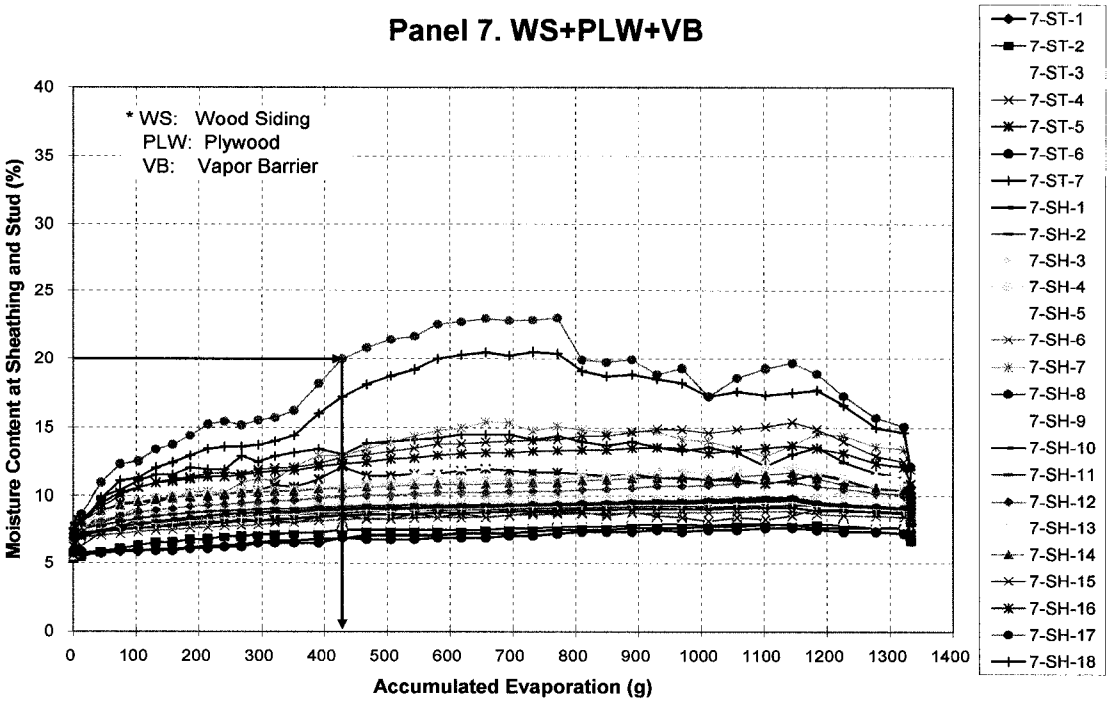

Figure A.2a. Wall specimen #7, with WS, PLW & VB

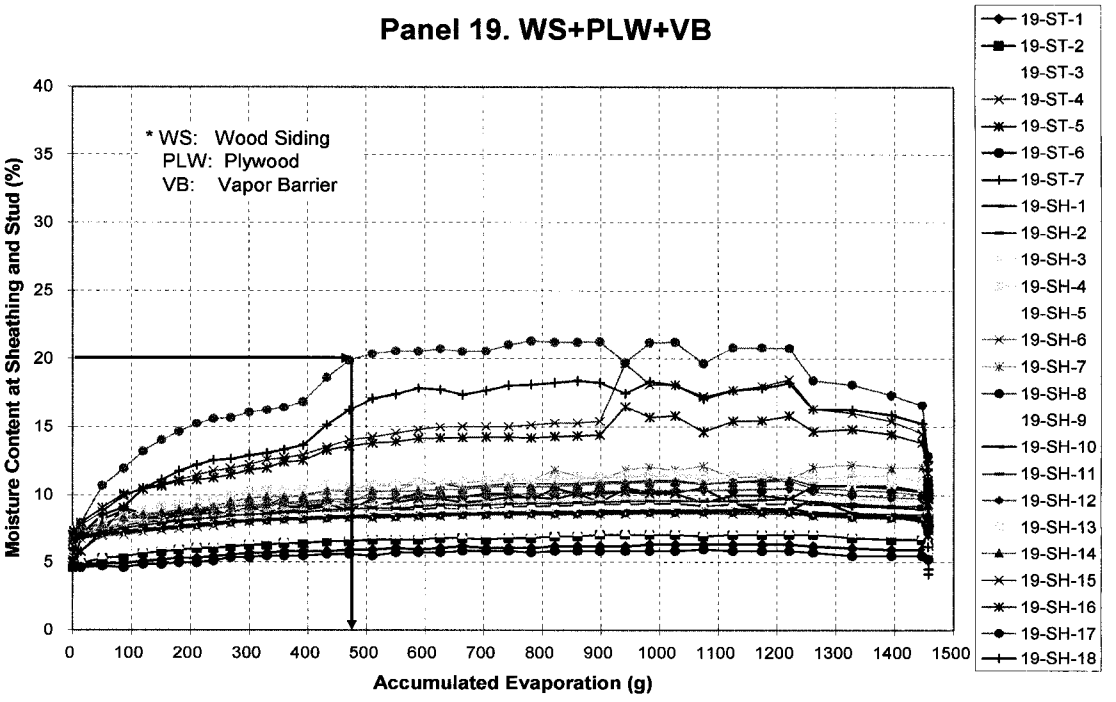

Figure A.2b. Wall specimen #19, with WS, PLW & VB

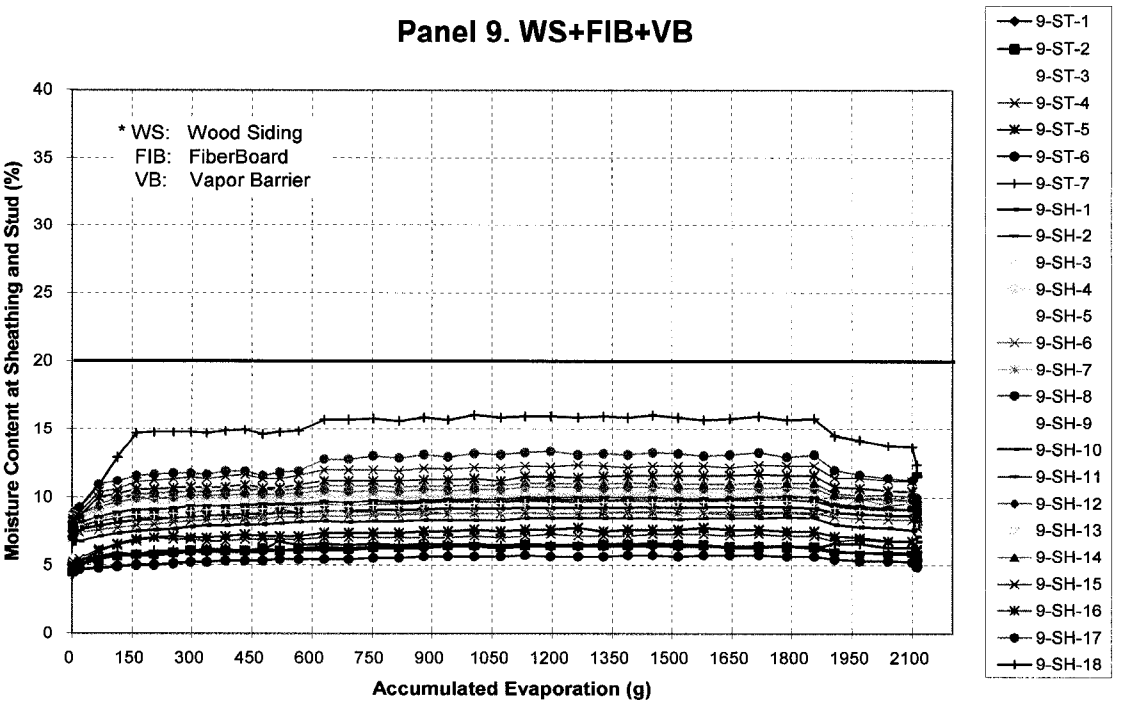

Figure A.3a. Wall specimen #9, with WS, FIB & VB

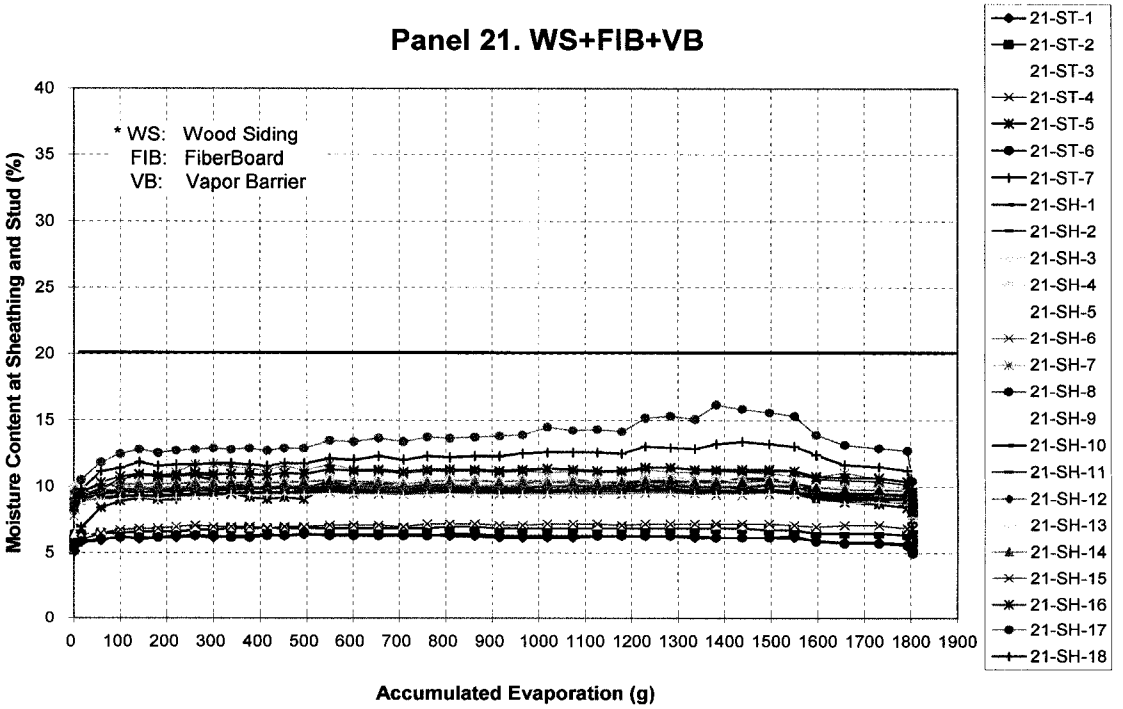

Figure A.3b. Wall specimen #21, with WS, FIB & VB

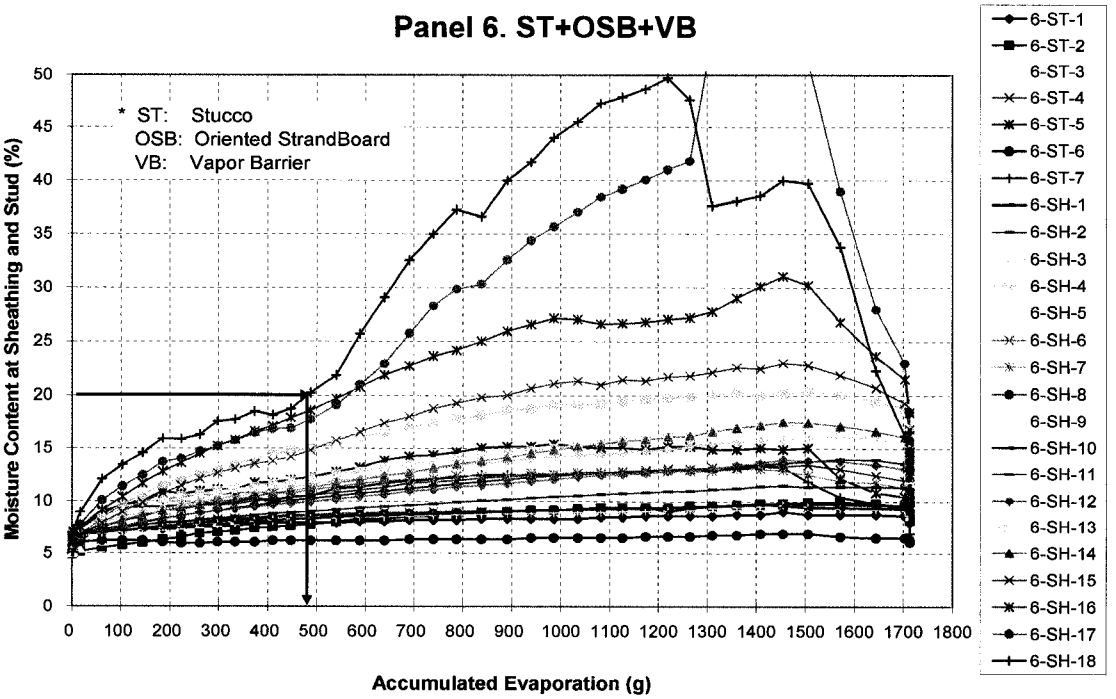

Figure A.4a. Wall specimen #6, with ST, OSB & VB

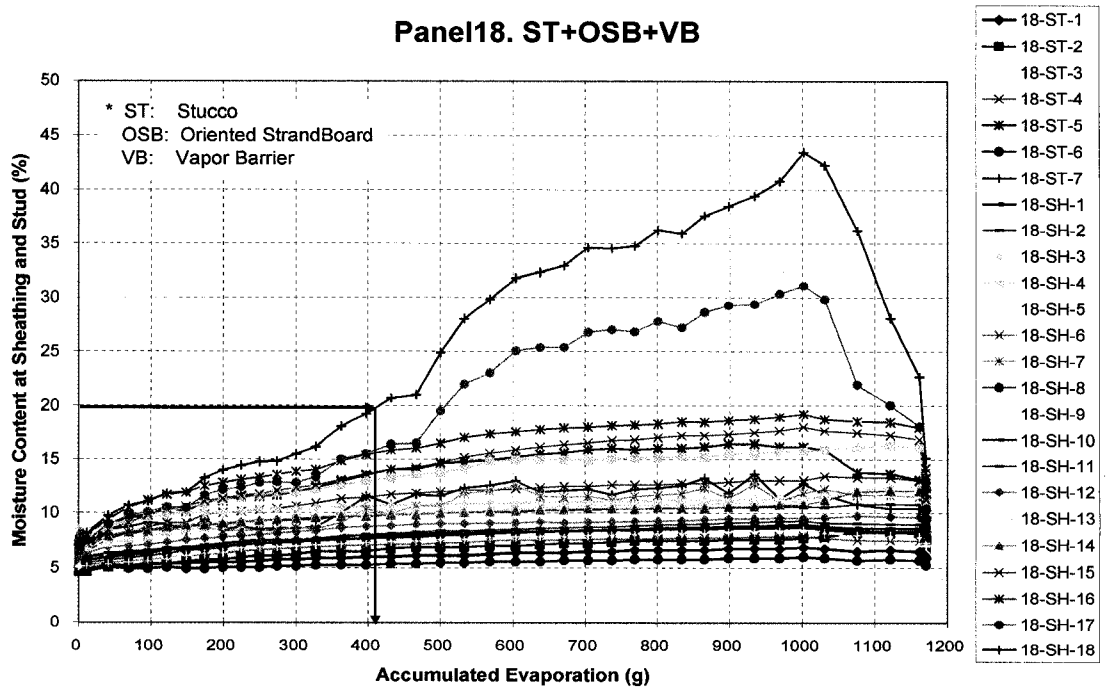

Figure A.4b. Wall specimen #18, with ST, OSB & VB

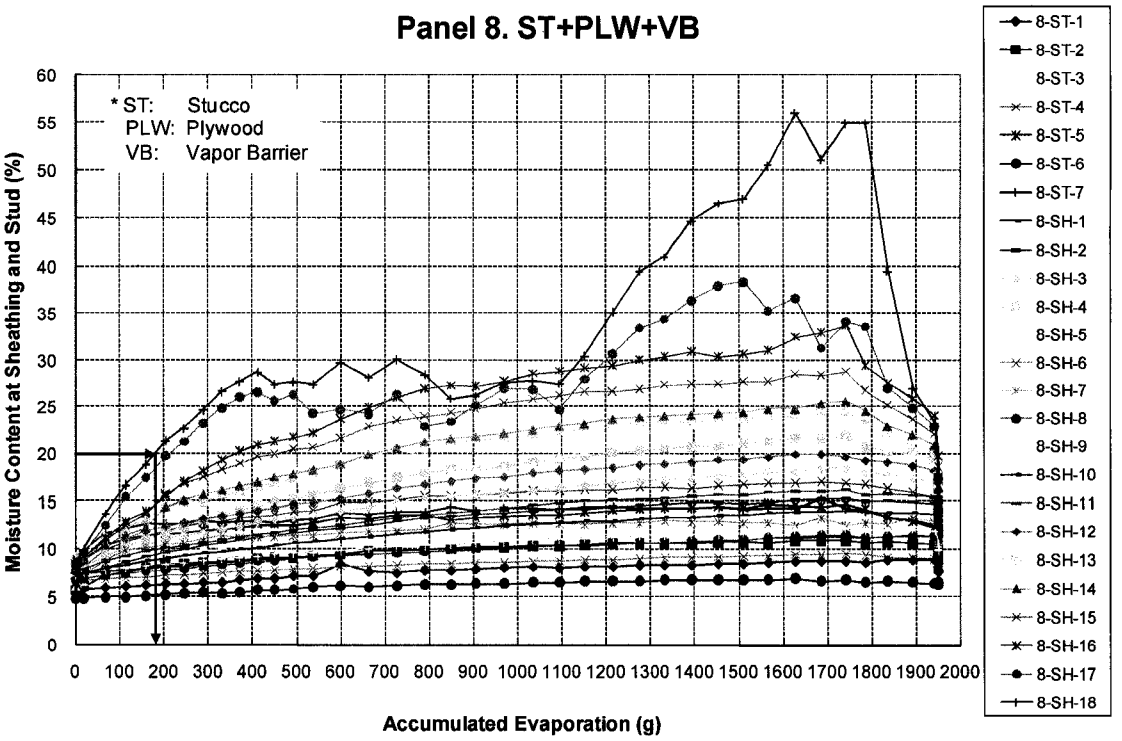

Figure A.5a. Wall specimen #8, with ST, PLW & VB

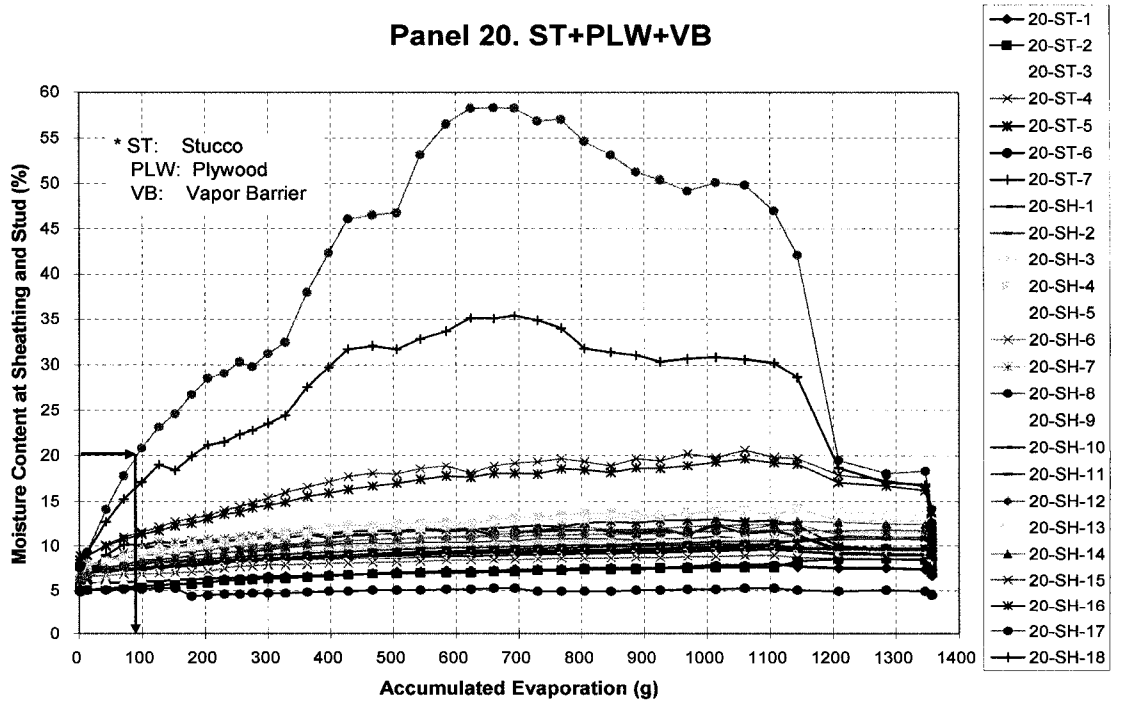

Figure A.5b. Wall specimen #20, with ST, PLW & VB

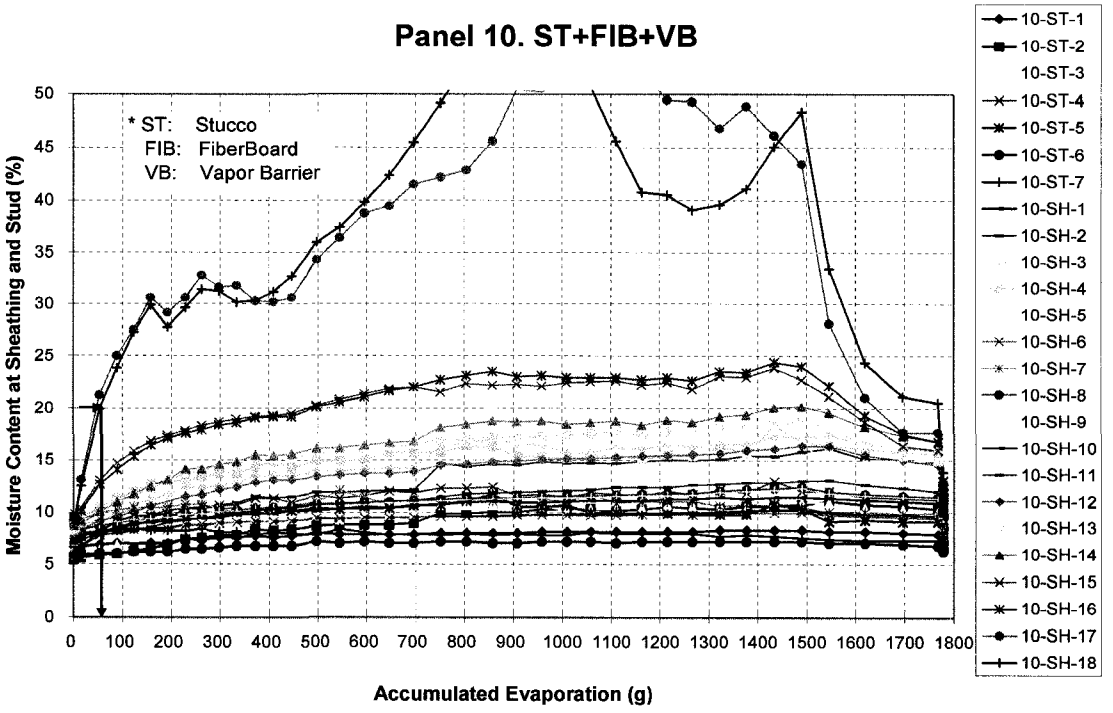

Figure A.6a. Wall specimen #10, with ST, FIB & VB

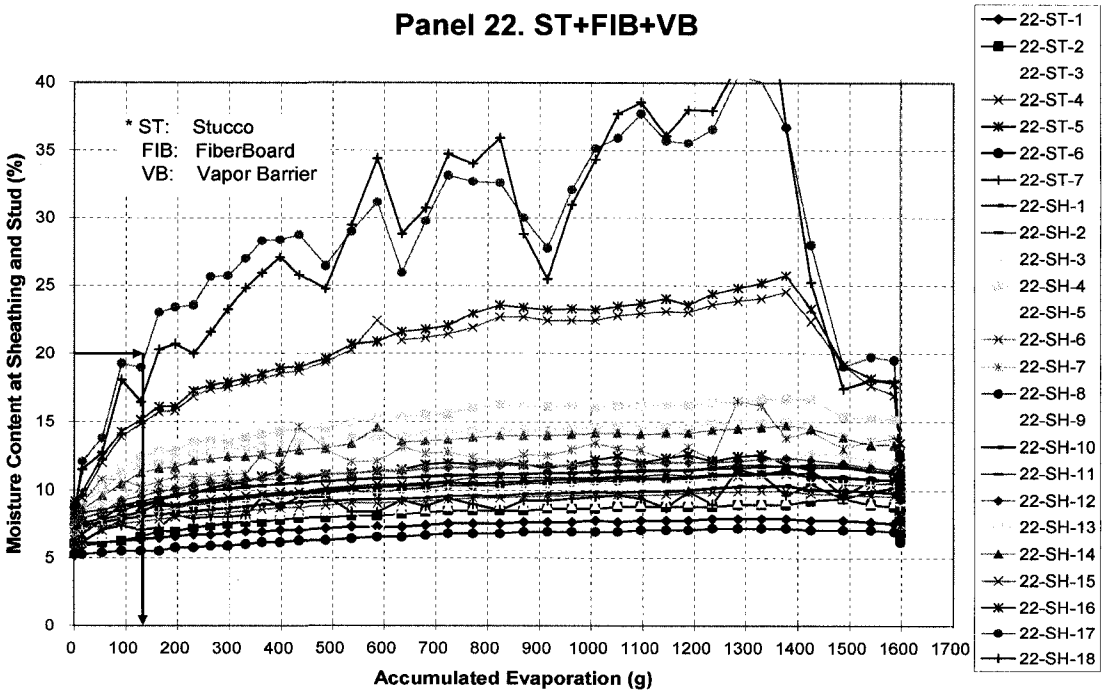

Figure A.6b. Wall specimen #22, with ST, FIB & VB

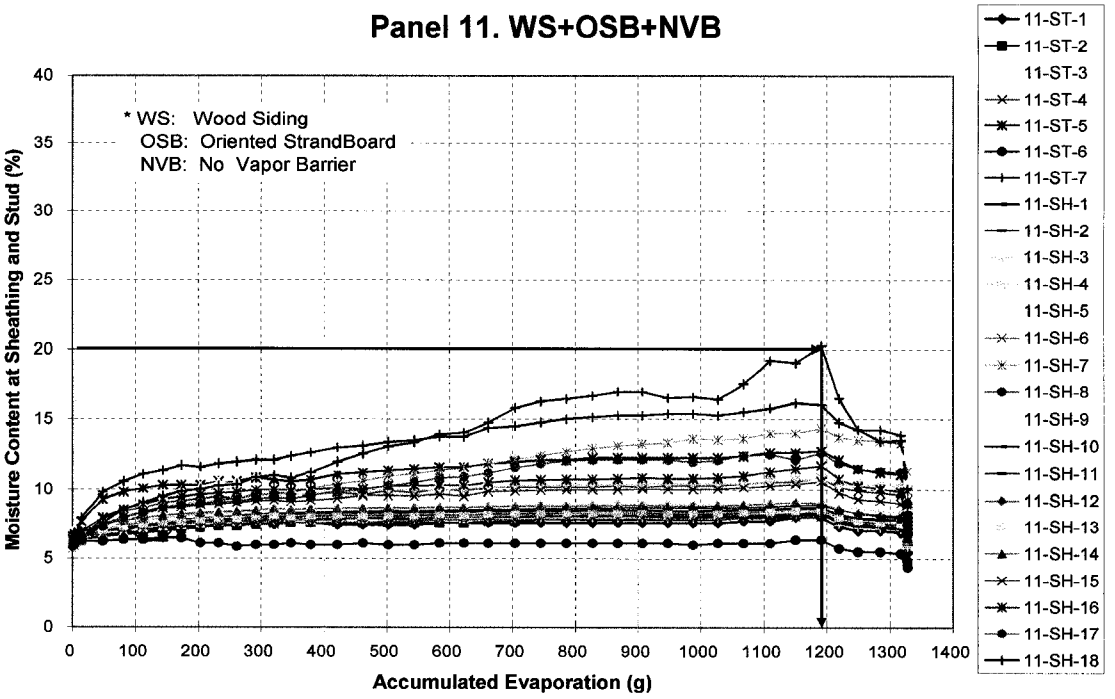

Figure A.7a. Wall specimen #11, with WS, OSB & NVB

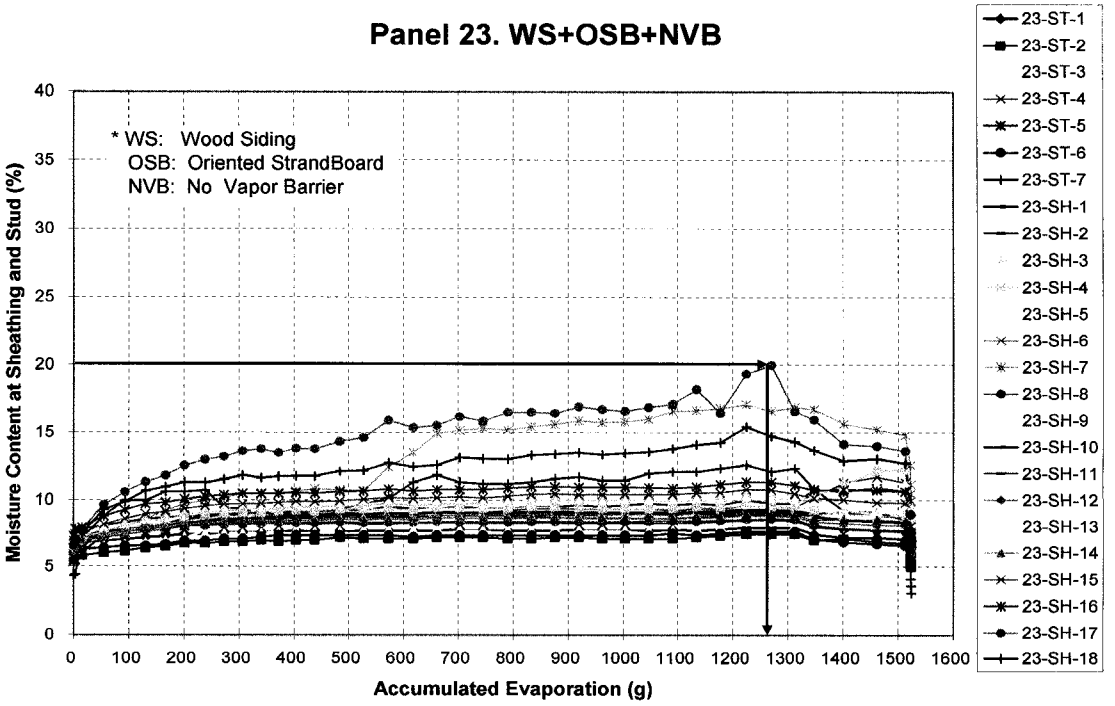

Figure A.7b. Wall specimen #23, with WS, OSB & NVB

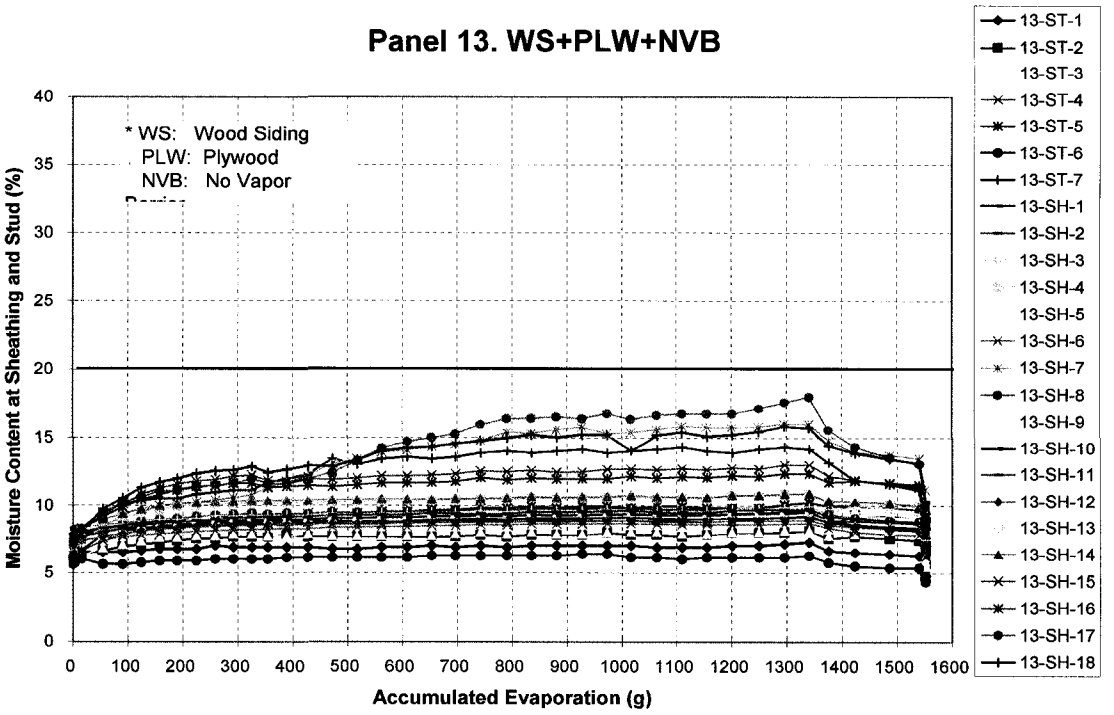

Figure A.8a. Wall specimen #13, with WS, PLB & NVB

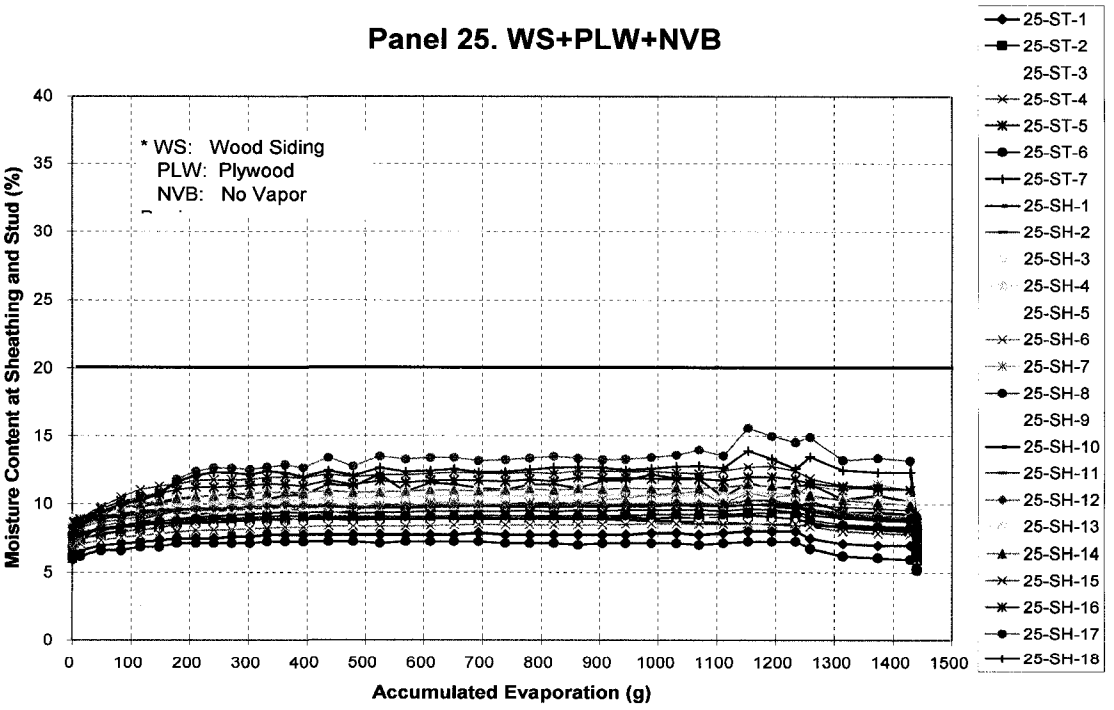

Figure A.8b. Wall specimen #25, with WS, PLB & NVB

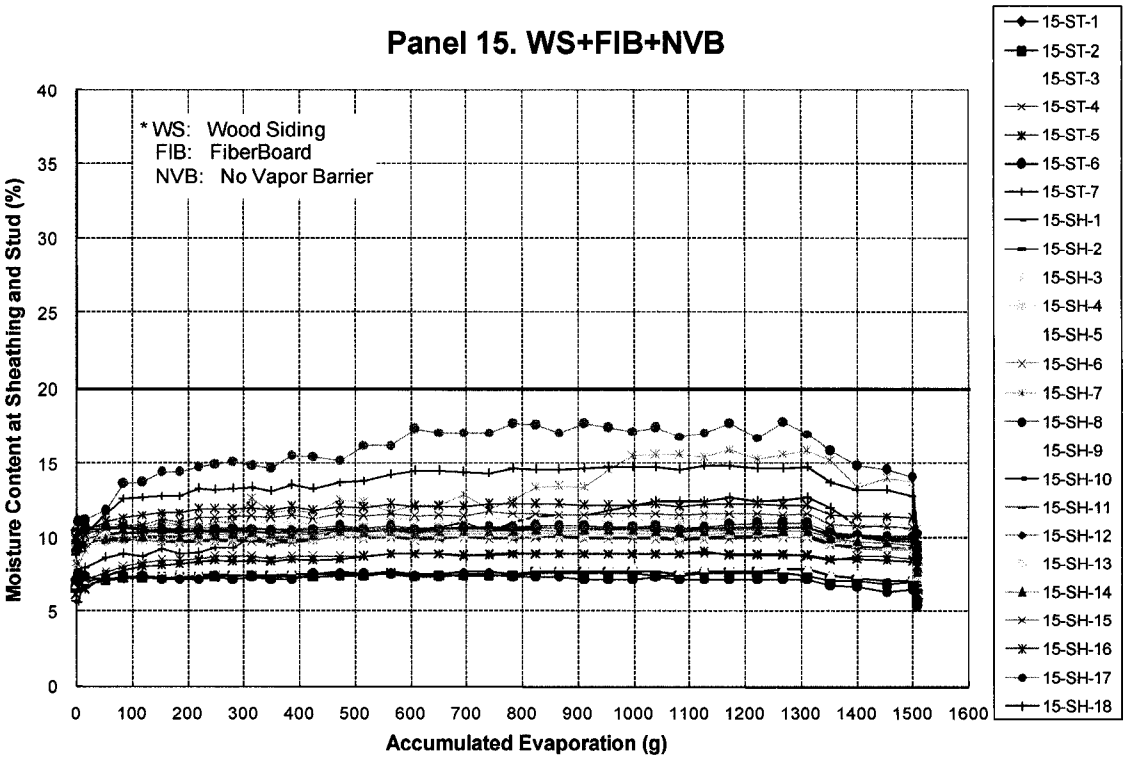

Figure A.9a. Wall specimen #15, with WS, FIB & NVB

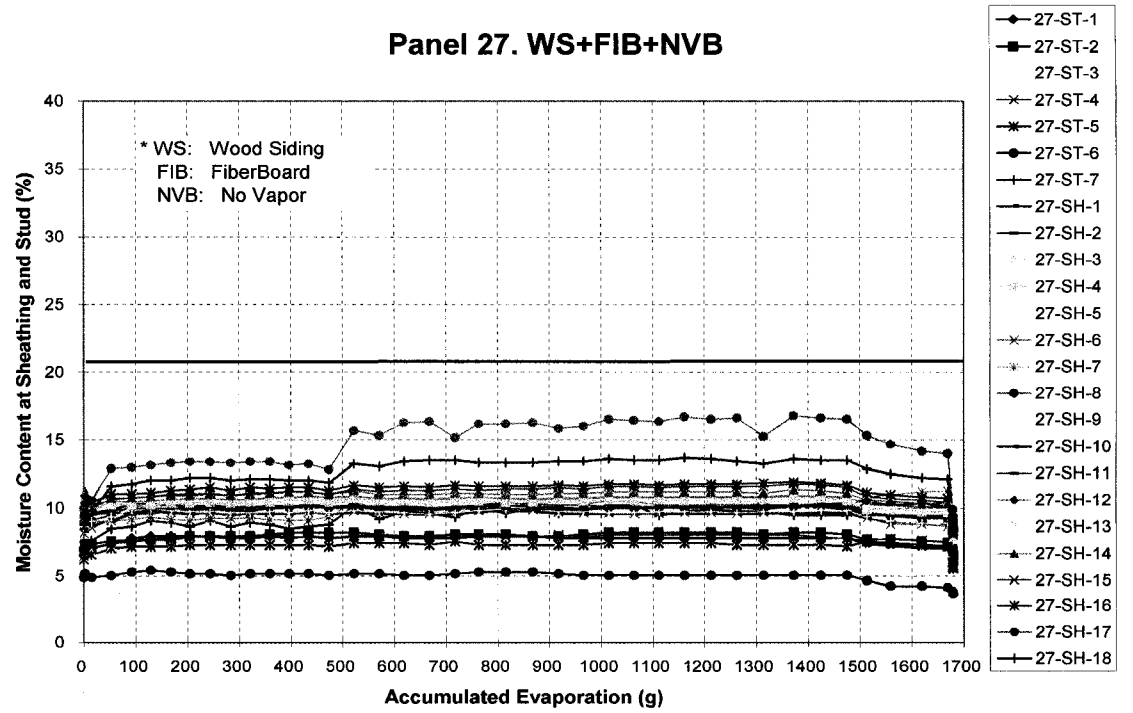

Figure A.9b. Wall specimen #27, with WS, FIB & NVB

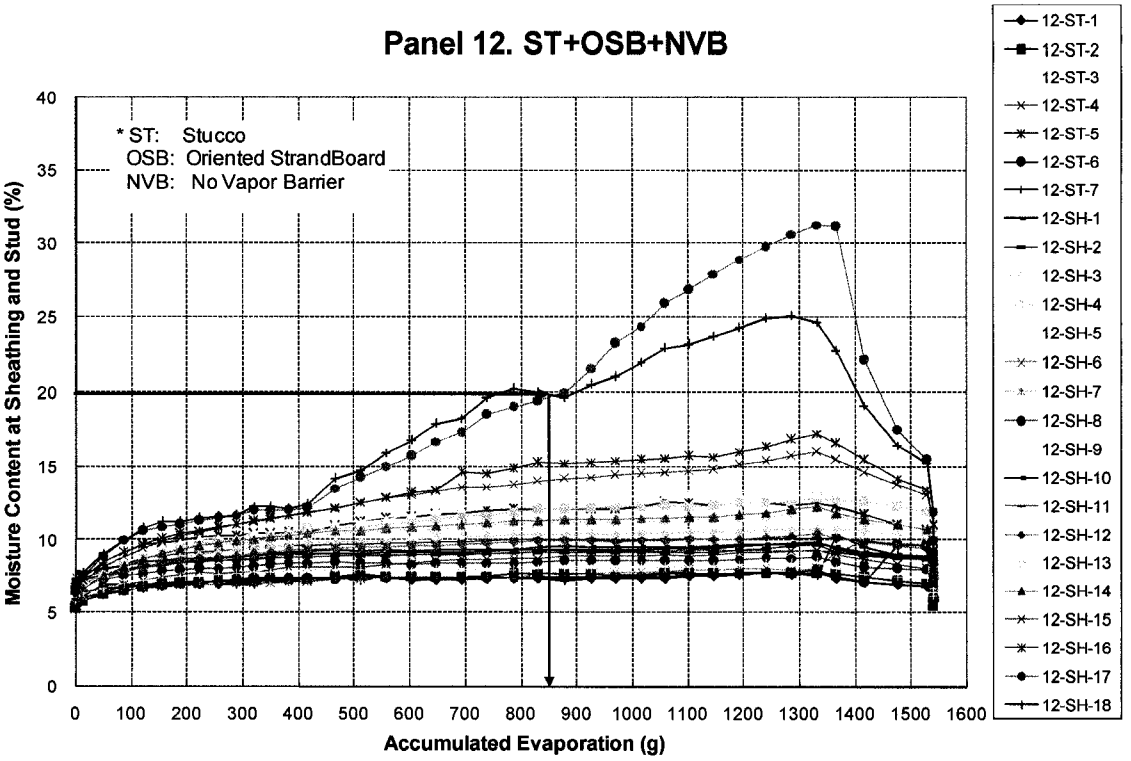

Figure A.10a. Wall specimen #12, with ST, OSB & NVB

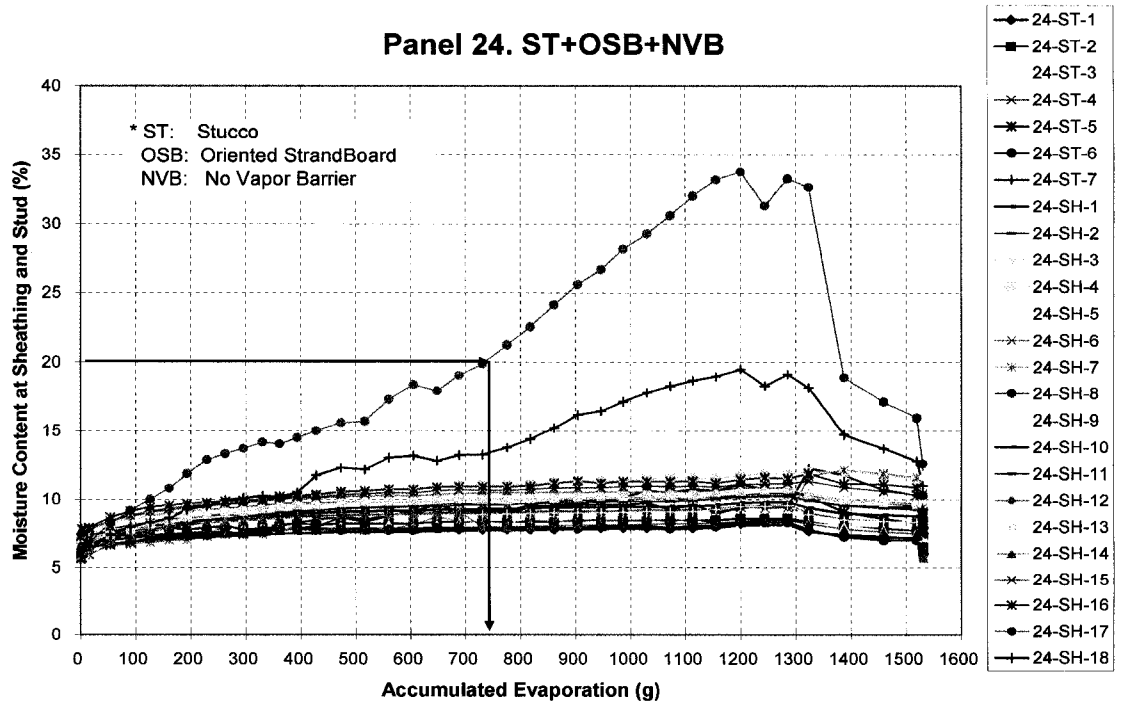

Figure A.10b. Wall specimen #24, with ST, OSB & NVB

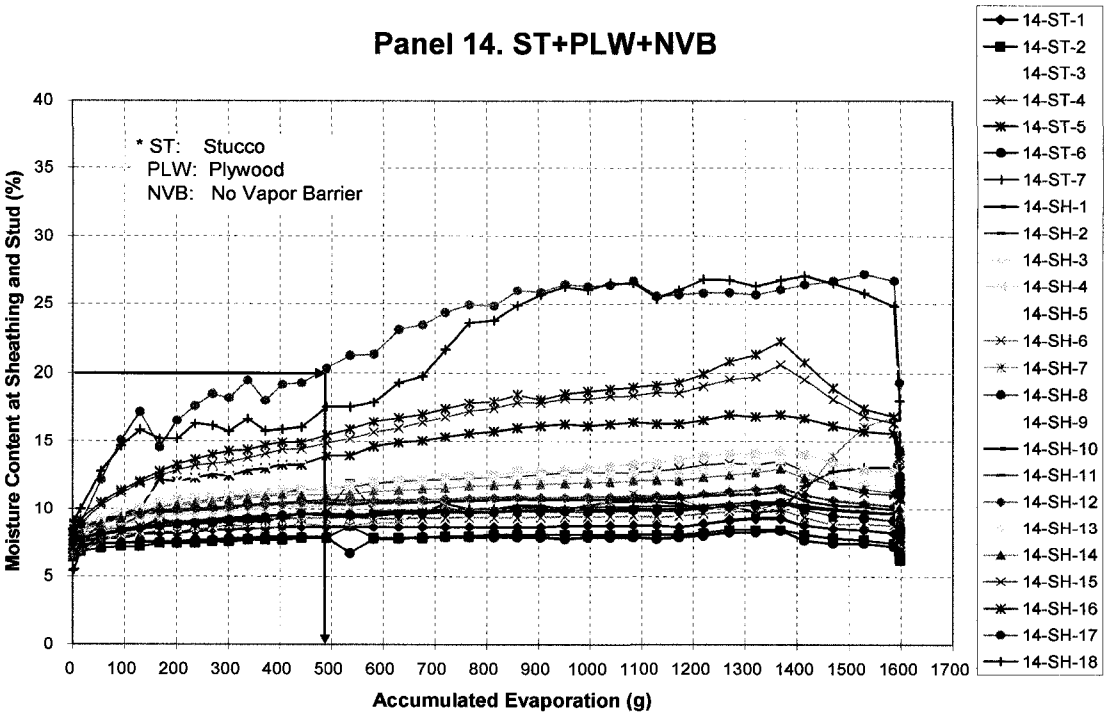

Figure A.11a. Wall specimen #14, with ST, PLB & NVB

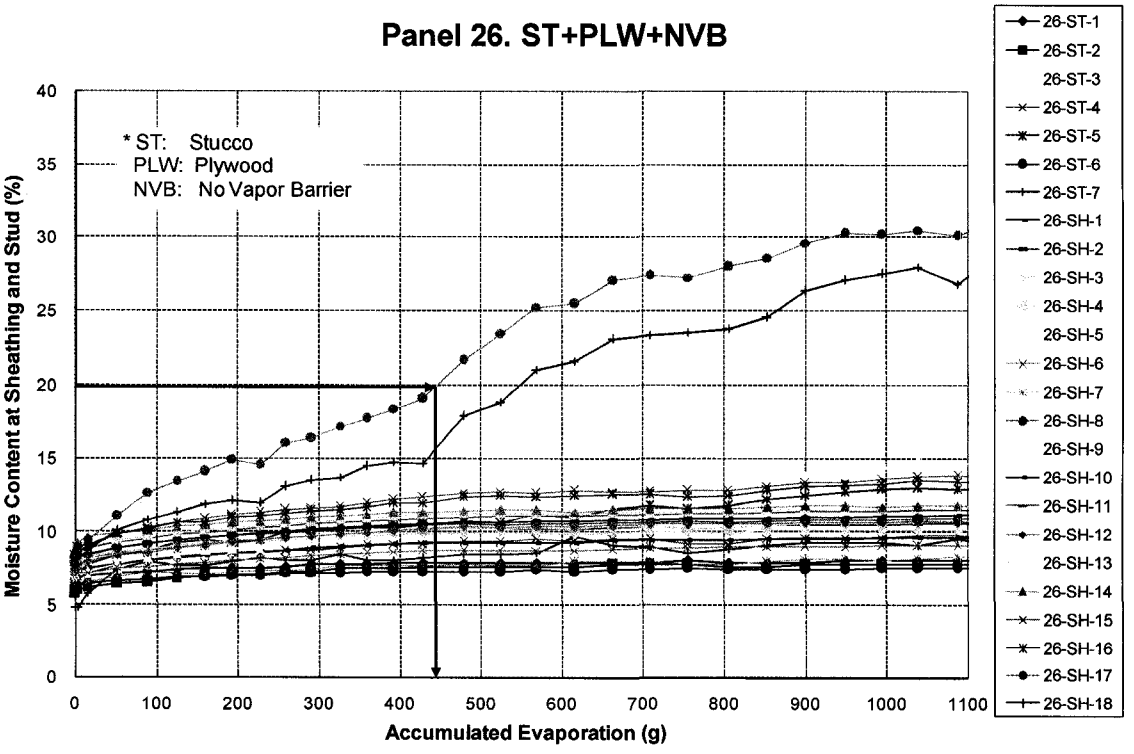

Figure A.11b. Wall specimen #26, with ST, PLW & NVB

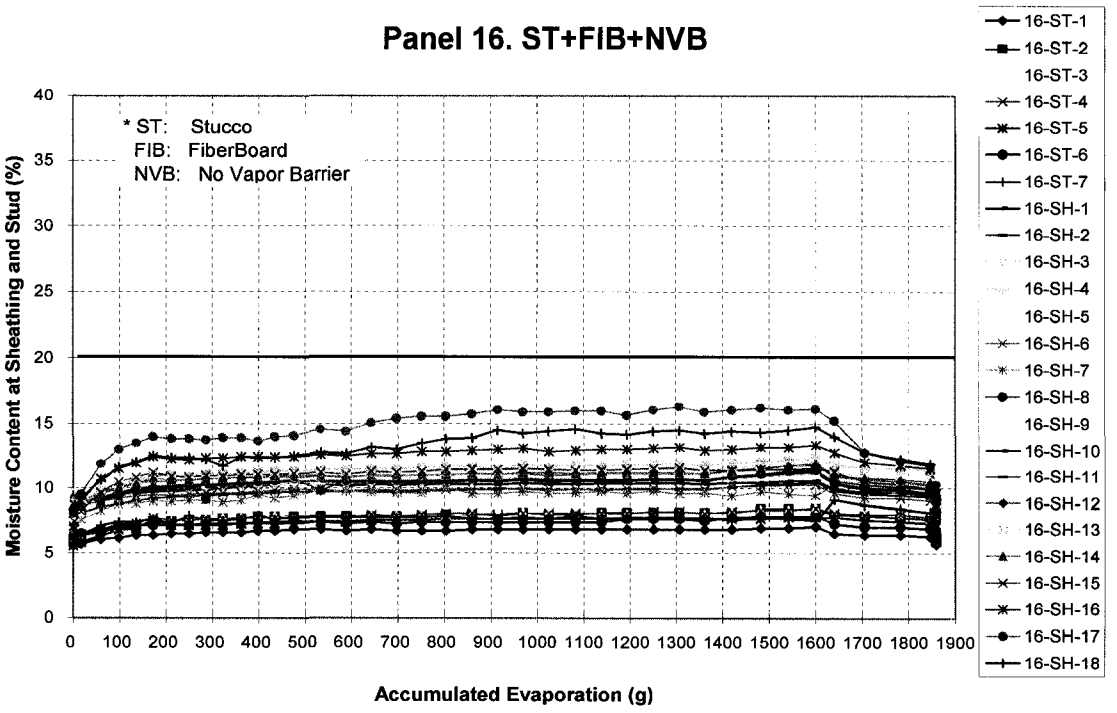

Figure A.12a. Wall specimen #16, with ST, FIB & NVB

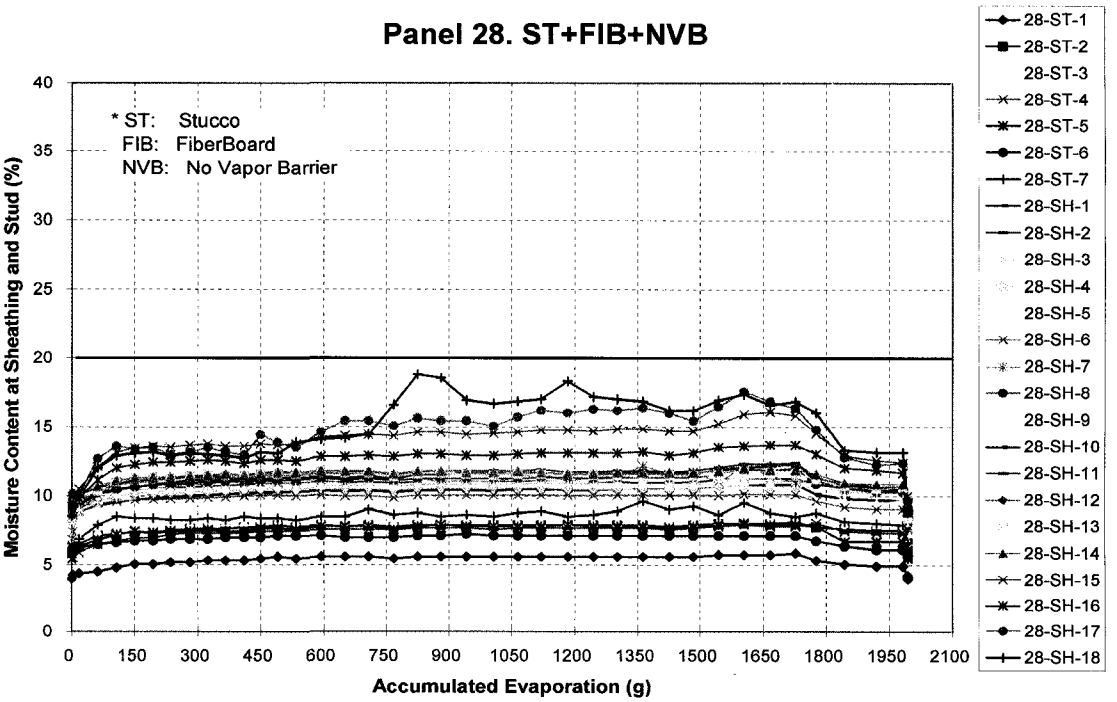

Figure A.12b. Wall specimen #28, with ST, FIB & NVB

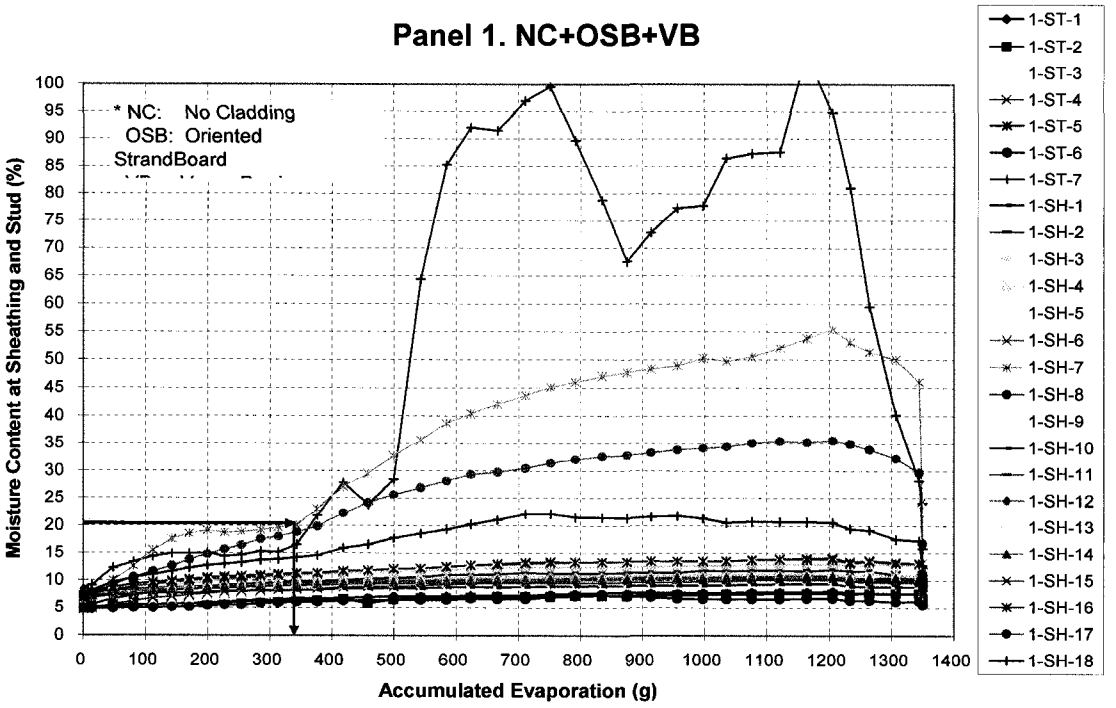

Figure A.13. Wall specimen #1, with NC, OSB & VB

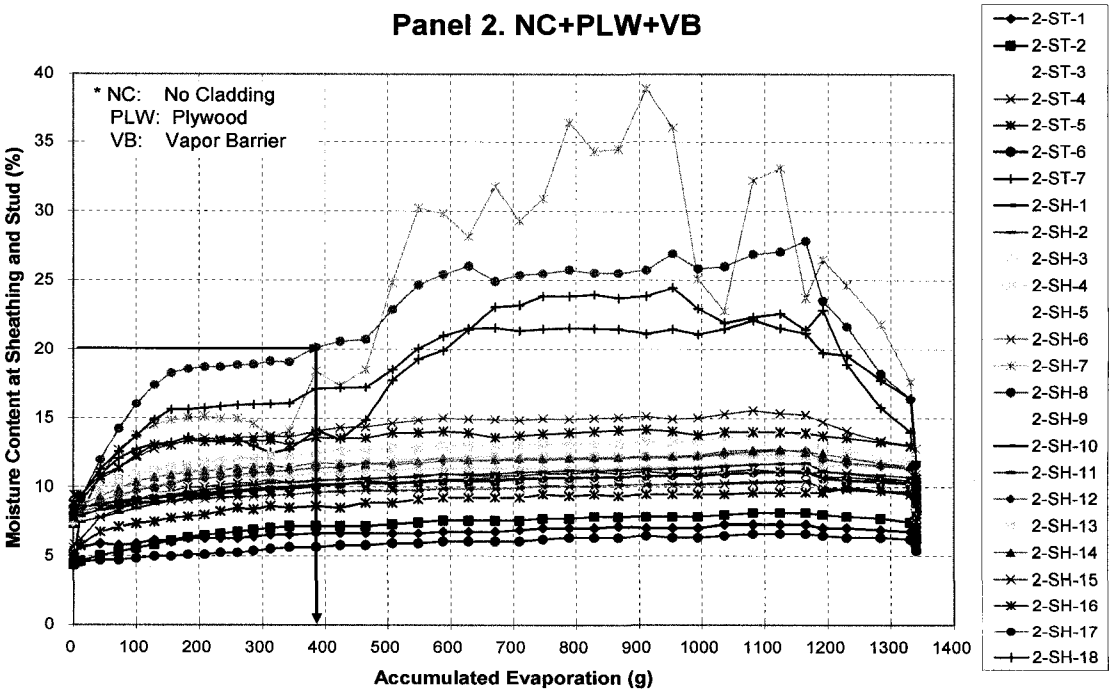

Figure A.14. Wall specimen #2, with ST, PLB & VB

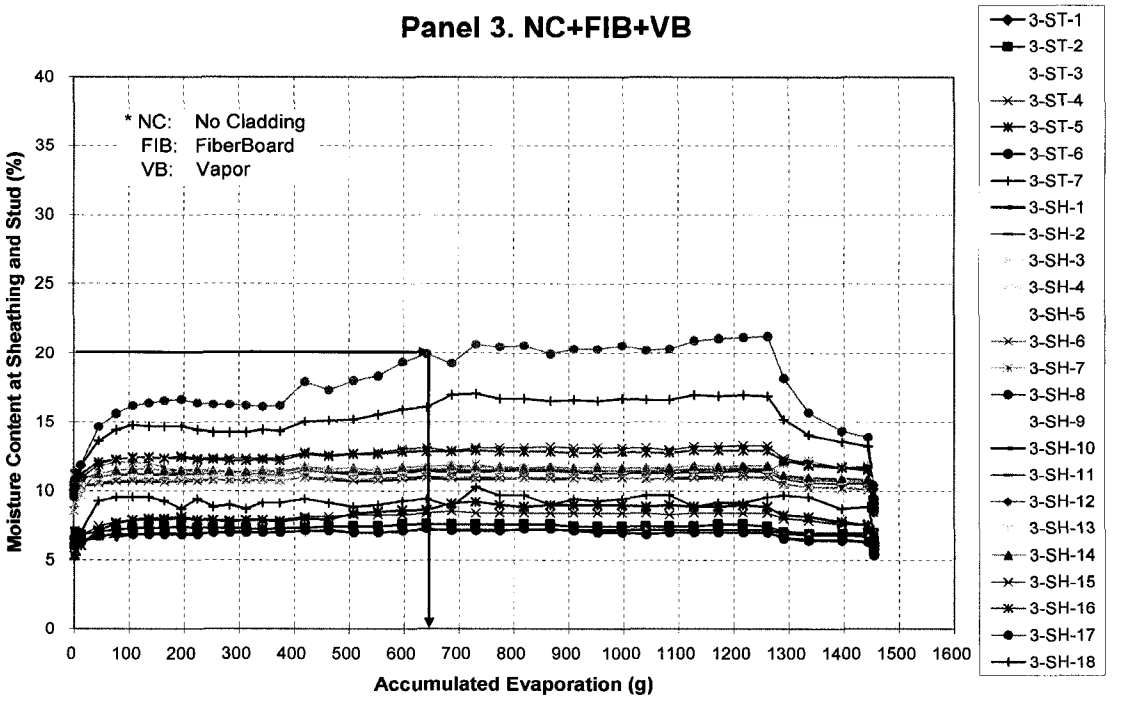

Figure A.15. Wall specimen #3, with NC, FIB & VB

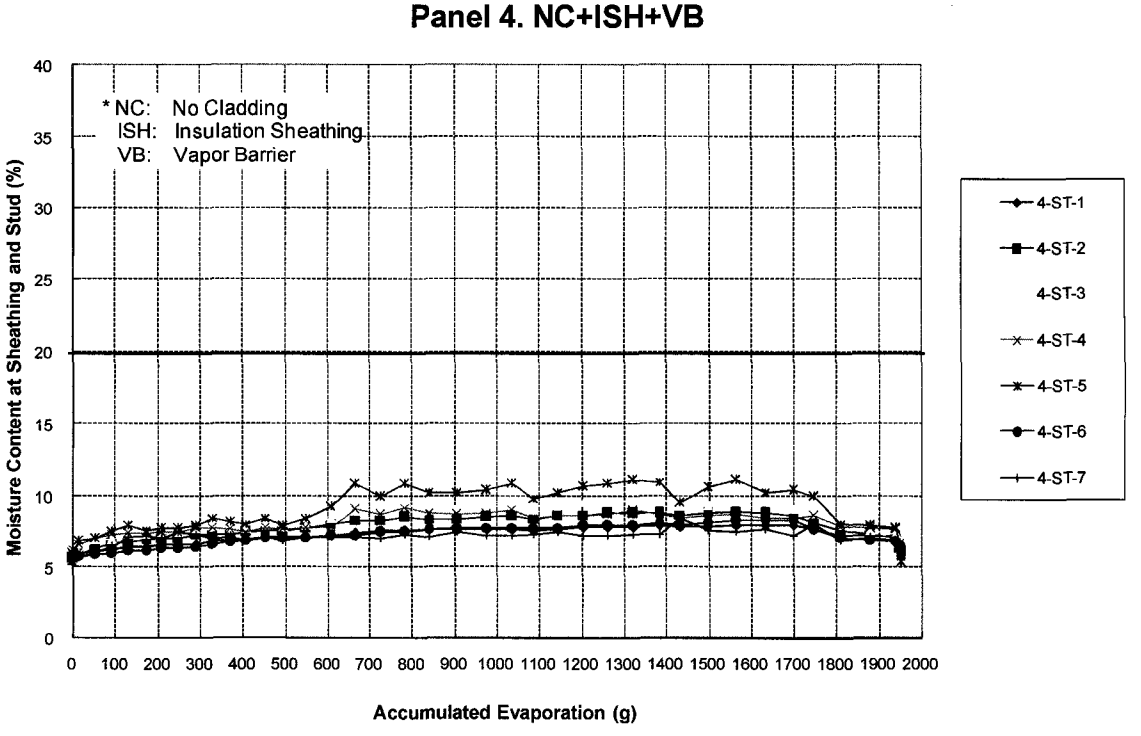

Figure A.16. Wall specimen #4, with NC, ISH & VB

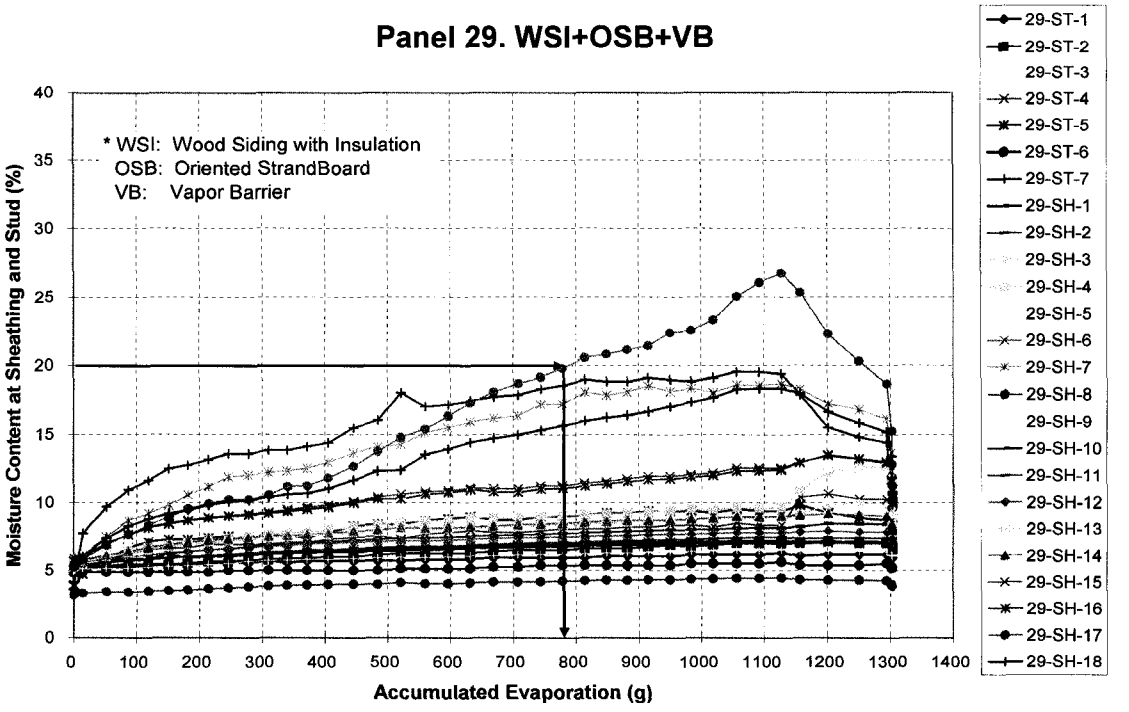

Figure A.17. Wall specimen #29, with WSI, OSB & VB

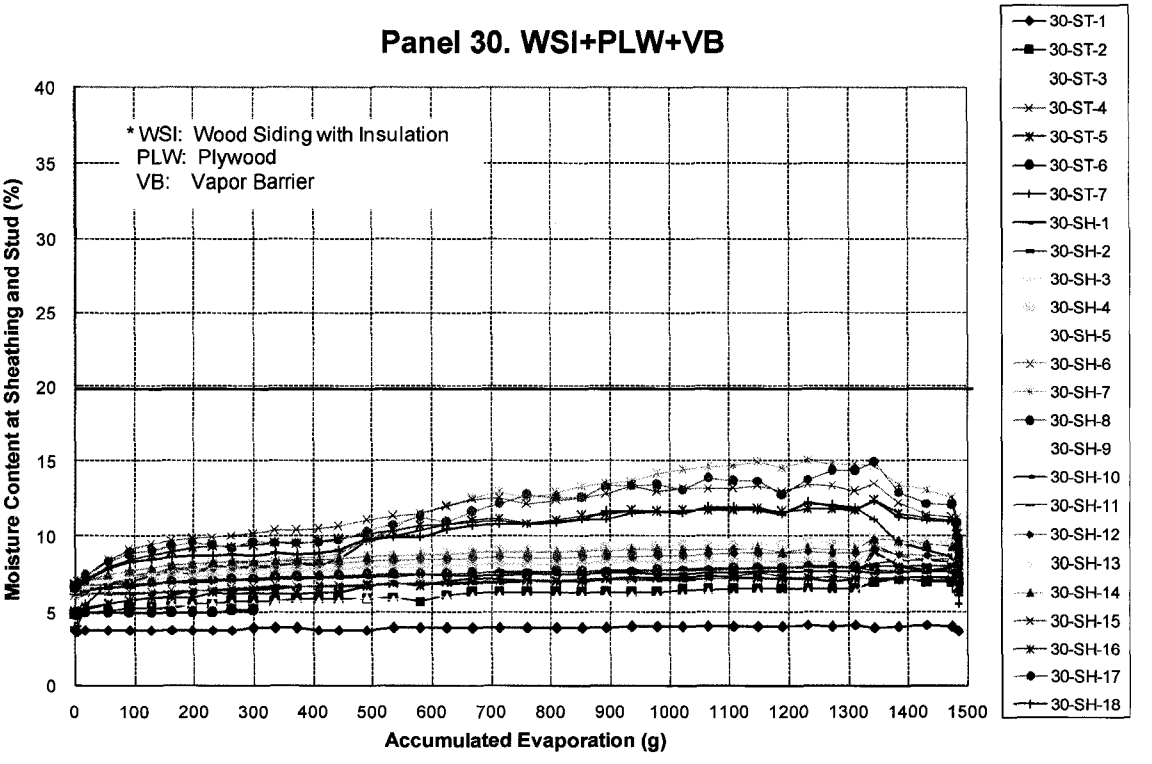

Figure A.18. Wall specimen #30, with WSI, PLW & VB

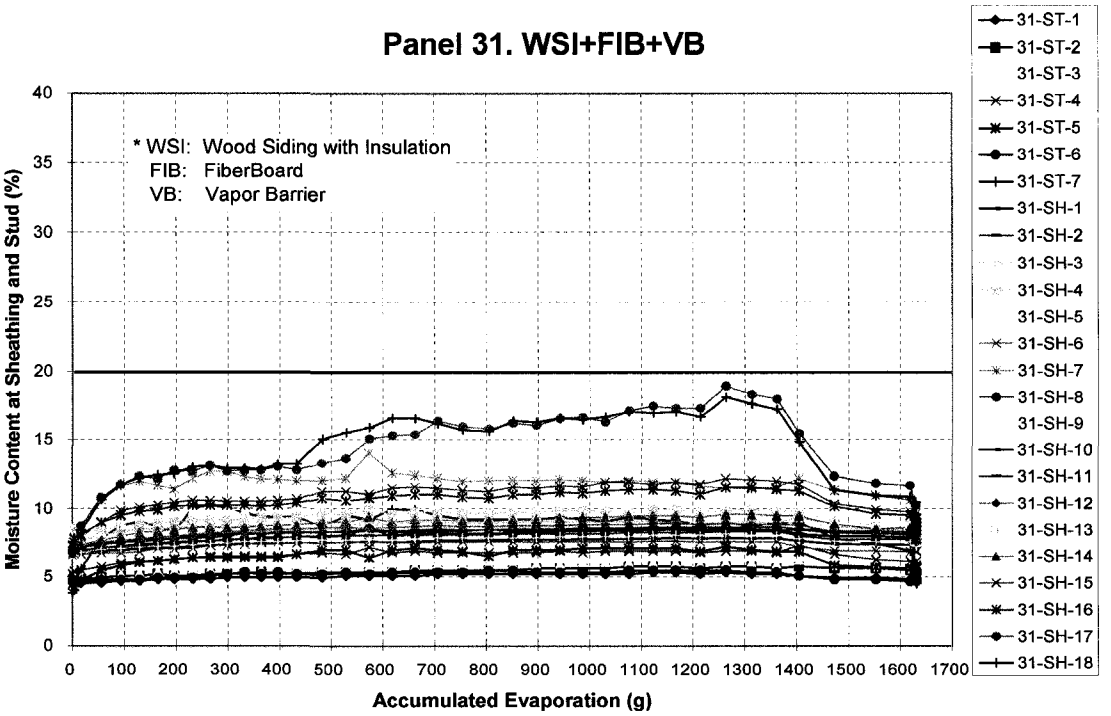

Figure A.19. Wall specimen #31, with WSI, FIB & VB